UNIVERSITY OF SOUTHAMPTON

FACULTY OF ENGINEERING AND APPLIED SCIENCE

DEPARTMENT OF ELECTRICAL ENGINEERING

THE RESOLUTION OF WATER-IN-OIL EMULSIONS BY THE APPLICATION OF AN EXTERNAL ELECTRIC FIELD

by

TREVOR JAMES WILLIAMS

A Thesis Submitted for the Degree
of
Doctor of Philosophy

January 1989

UNIVERSITY OF SOUTHAMPTON

ABSTRACT

FACULTY OF ENGINEERING AND APPLIED SCIENCE

ELECTRICAL ENGINEERING DEPARTMENT

Doctor of Philosophy

THE RESOLUTION OF WATER-IN-OIL EMULSIONS BY THE APPLICATION OF AN EXTERNAL ELECTRIC FIELD

by Trevor James Williams

Over the years, the electrical treatment of W/O emulsions has established itself as the most important method of separation, though the process is usually enhanced by heating and chemical addition. It is practised at the oil field, in the refinery, and on site by the user.

Water becomes mixed with the oil in several ways, e.g. it may be produced with the oil or contamination during shipping may occur. Emulsification of the two immiscible liquids results from the agitation induced by pumping.

Application of an electric field induces droplet coalescence leading to increased size and settling rate. Electrophoretic and dielectrophoretic forces may be established by the field, which induce droplet coagulation by migratory coalescence and dipole coalescence respectively. These processes may be modelled using a mechanistic approach or by considering their coagulation kinetics. They are investigated experimentally using turbidimetric, laser diffraction and microscopic techniques.

The effects of different electric excitations are considered, as is the use of insulated electrodes. Interfacial polarization is important in the latter case and time-varying electric fields are required for efficient phase separation.

Though separation efficiency initially increases with electric field intensity, a limit is eventually reached when droplet dispersion occurs; the various electrostatic and hydrodynamic dispersion mechanisms are therefore examined.

The design of electric treaters (electro-coalescers) has continued to improve since they were first used commercially in 1909. However, as oil supplies diminish, user specifications become increasingly stringent, and more sensitive refinery processes are introduced, the requirement to improve their efficiency will persist.

ACKNOWLEDGEMENTS

I should like to express my gratitute to the following parties:

Plenty Bescon Limited and subsequently GKN Birwelco for their financial support during this study.

Professor A G Bailey for his help, support and encouragement during the study.

Mr D White and Mr K Frampton for their assistance in constructing apparatus.

Mr C Parker, of the Hartley Library, for his assistance in performing computer searches for patents and literature.

Mrs D Mogg, for her efficient and accurate typing of the thesis.

My wife Frances and daughter Charlotte for their patience, understanding and selflessness during the write-up.

PRINCIPAL NOMENCLATURE

A = electrode area (m^2), interfacial area (m^2)

a = particle or droplet radius (m)

B = mobility ($m^2V^{-1}s^{-1}$), Bernoulli number (when subscripted)

b = distance between origin and centre of sphere in the bispherical co-ordinate system (m)

C = capacitance (F), Euler's constant (0.57722)

c = concentration of solute (mol dm^{-3}), length scale factor in the bispherical co-ordinate system (m)

D = dielectric displacement (Cm^{-2})

d = droplet diameter (m), separation (m)

E = electric field (Vm^{-1})

e = magnitude of charge carried by electron ($1.6021 \times 10^{-19}C$), eccentricity of ellipsoidal droplet

F = force (N), flow speed of emulsion (ms^{-1})

f = cyclical frequency (Hz)

G = conductance (S)

g = acceleration due to gravity (ms^{-2})

H = height of emulsion (m)

h = film thickness, that is min imum separation between opposed surfaces (m), Lamé coefficient (when subscripted with co-ordinate variable)(m)

I = viscosity group function

i = current (A)

J = current density (Am^{-2})

j = $\sqrt{-1}$

K = coagulation rate constant (when double subscripted or within <<>>)(m^3s^{-1})

k = Boltzmann's constant ($1.38054 \times 10^{-23}JK^{-1}$)

ℓ = length (m), length of dipole (m)

M = molecular weight

N = number of particles per unit volume (m^{-3})

n = number of counter ions per unit volume (m^{-3}), number density of particles per unit volume (when a function) (m^{-6})

P = Legendre polynomial (when subscripted by integer), conical function (when subscripted by $\frac{1}{2}$)

p = charge per unit length (Cm^{-1})

Q = rate of energy dissipation per unit mass (m^2s^{-3})

q = charge (C)

R = resistance (Ω), Reynolds number

r = radial distance (m), radius of ion or particle (m)

S = maximum velocity gradient in external flow field (s^{-1}), surface area (m^2)

T = absolute temperature (K), turbidity (NTU)

t = time (s)

U = energy (J)

u = speed of particle or flow speed (ms^{-1})

V = potential difference (V)

W = Weber group

w = speed in vertical direction (ms^{-1})

X = maximum displacement in migratory coalescence (m)

x = cartesian co-ordinate displacement (m)

y = cartesian co-ordinate displacement (m)

z = cartesian co-ordinate displacement (m)

α = polarisation per unit volume (Fm^{-1}), semi-angle of Taylor cone (rad)

β = geometric factor in coagulation rate constant

Γ = surface or interfacial excess of solute (mol m^{-2})

γ = surface or interfacial tension (Nm^{-1})

Δ = diffusion coefficient (m^2s^{-1})

δ = length scale of turbulent eddy (m), Kronecker delta ($\delta_{ij} = 1$ when $i = j$, $\delta_{ij} = 0$ when $i \neq j$)

ϵ = permittivity (Fm^{-1})

ζ = electrokinetic or zeta potential (V), Riemann zeta function

η = bulk viscosity (Pas), bispherical co-ordinate angular variable (rad)

θ = angular variable (rad)

K = dielectric constant, Debye parameter (multiplicative inverse of the electric double layer thickness) (m^{-1})

Λ = separation between the centres of a pair of droplets (m)

λ = bispherical co-ordinate variable (azimuthal angle) (rad)

μ = dipole moment (Cm), bispherical co-ordinate variable

ν = valency (number of electronic units per ion)

ξ = function defining the surface shape of a droplet in close proximity to a plane or another droplet (m)

ρ = density (kgm^{-3}), volume charge density (Cm^{-3})

$\sum$ = viscosity group

σ = electrical conductivity (Sm^{-1}), surface charge density (Cm^{-2})

τ = electrical charge relaxation time (s), emulsion resolution time (s)

Φ = function in coagulation rate constant

φ = volume fraction of dispersed phase

Ψ = surface stress due to viscous forces (Pa)

ψ = potential difference of electric double layer (V)

Ω = volume (m^3), droplet volume (m^3)

ω = angular frequency (rad s^{-1})

PRINCIPAL SUBSCRIPTS

c	= continuous phase
d	= dispersed phase, deformable droplet
h	= high frequency
ℓ	= low frequency
u	= undeformable droplet
1,2,3	= phase 1,2,3
n	= subscript of coefficient (n = 0,1,2,....)

It should be noted that many of the English and Greek characters are also used as constants, subscripts and subscripted coefficients not described above. When this occurs a local definition is made. Some of the characters are used to define more than one variable; ambiguity should not arise however.

The superscript * is used to denote a complex quantity, the real and imaginary parts of which are specified by Re and Im respectively (e.g. $z^* = x + jy$ where $Re(z^*) = x$ and $Im(z^*) = y$).

GLOSSARY OF TERMS

ADSORPTION: The accumulation of substance at an interface between two phases which increases the concentration there, above that in the bulk (reducing interfacial tension).

AGGLOMERATION: See Flocculation.

AMPHIPHILIC: An emulsifying agent of the polar–non–polar type which has balanced affinity for aqueous and organic solvents.

ANAPHORESIS: Electrophoretic motion towards the anode.

ANIONIC EMULSIFIER: An ionic emulsifier in which the anion dictates the emulsifier properties.

BREAKING OF AN EMULSION: See Resolution of an Emulsion.

CATAPHORESIS: Electrophoretic motion towards the cathode.

CATIONIC EMULSIFIER: An ionic emulsifier in which the cation dictates the emulsifier properties.

COAGULATION: See Coalescence.

COALESCENCE: The merging of droplets of the same phase, in an emulsion, thereby forming a larger one.

CONTINUOUS PHASE: See External Phase.

CREAMING: The accumulation of dispersed phase droplets at the top or bottom of the continuous phase (depending on density difference of the phases) by sedimentation, where droplets touch but do not coalesce.

DEMULSIFIER: A surface–active agent which destabilizes an emulsion by neutralizing the effect of the emulsifier, and promoting flocculation and coalescence of dispersed phase droplets.

DIELECTRIC DISPERSION: The difference in dielectric constant (or conductivity) when measured at low and high frequencies (arising from interfacial polarization).

DIELECTROPHORESIS: The translational movement of an uncharged particle in a non-uniform electric field.

DISCONTINUOUS PHASE: See Internal Phase.

DISPERSED PHASE: See Internal Phase.

DUAL EMULSION: An emulsion in which the internal phase droplets contain droplets of the external phase.

ELECTRIC DOUBLE LAYER: A system comprising a layer of ions, preferentially adsorbed at an interface, and in excess of neutralizing ions dispersed by diffusion.

ELECTROPHORESIS: The migration of dispersed, charged particles, towards an electrode, under the action of an electric field.

ELECTROSTRICTION: The volume force acting on a dielectric material in a non-uniform electric field.

EMULSIFIER: See Emulsifying Agent.

EMULSIFYING AGENT: A surface-active agent which promotes emulsification by reducing interfacial tension, and stabilizes the emulsion by oriented adsorption.

EMULSION: A system comprising two immiscible liquids, one of which is dispersed in the other in the form of droplets (regarded as having diameters in the range 0.1-100μm), which may be stabilized by an emulsifying agent.

EXTERNAL PHASE: The continuous phase of an emulsion which encloses the dispersed droplets.

FLOCCULATION: The clustering of droplets without coalescence.

HYDROPHILIC: Having an affinity for water.

HYDROPHOBIC: Having an aversion to water.

INTERNAL PHASE: The phase of an emulsion which is dispersed into droplets.

INVERSION OF EMULSION: A reversal of rôles of the liquid phases in which the dispersed phase becomes the continuous phase and vice versa.

IONIC EMULSIFIER: An emulsifying agent which acts by dissociation.

LIPOPHILIC: See Hydrophobic.

LIPOPHOBIC: See Hydrophilic.

MERCAPTANS: Organic compounds with the general formula R.SH where R represents a hydrocarbon chain.

MICELLE: An aggregate of amphiphilic molecules having colloidal dimensions ($10^{-3} - 10^{-1}\mu m$).

MULTIPLE EMULSION: An extension of the Dual Emulsion in which the external phase droplets, dispersed in the internal phase droplets, themselves contain droplets of the internal phase.

NEGATIVE ADSORPTION: The movement of a substance away from an interface towards the interior of the bulk liquid phase (increasing interfacial tension).

NON-IONIC EMULSIFIER: An emulsifier which does not dissociate in aqueous solution.

NON-POLAR MOLECULE: A molecule of symmetric structure which is electrically neutral in that it does not exhibit an electric dipole.

OLEOPHILIC: See Hydrophobic.

OLEOPHOBIC: See Hydrophilic.

ORIENTED ADSORPTION: The adsorption of long particles at an interface such that they are oriented normal to it.

O/W EMULSION: An oil-in-water emulsion in which the internal phase is oil and the external phase water.

PEARL-CHAIN: A row of dispersed phase droplets, of varying size, apparently in contact with one another, which aligns itself with the electric lines of force within

an electrified emulsion.

PHENOLS: A class of organic compounds containing one or more hydroxyl groups attached directly to the benzene ring.

POLAR MOLECULE: A molecule of asymmetric structure which possesses an electric dipole.

RESOLUTION OF AN EMULSION: The irreversible separation of an emulsion into distinct bulk phases.

SECONDARY RECOVERY: The extraction of oil from a formerly uneconomic well by pumping water or steam down the well.

SEDIMENTATION: The downward or upward movement of particles in a dispersion due to gravity.

STABILITY OF AN EMULSION: The characteristic of an emulsion which dictates its resolution time under the conditions pertaining; the greater the stability of an emulsion the longer its resolution time.

SURFACE-ACTIVE AGENT: A substance which is adsorbed at a liquid surface or interface between liquid phases and thereby reduces the surface tension or interfacial tension.

SURFACTANT: See Surface-Active Agent.

TREE: A branched Pearl-Chain which quite often consists of multiply-branched collections of dispersed phase droplets.

VOLUME FRACTION: The ratio of the volume of the internal phase of an emulsion to the total emulsion volume.

W/O EMULSION: A water-in-oil emulsion in which the internal phase is water and the external phase oil.

ABBREVIATIONS

AC (ac):	Alternating Current.
ASA-3:	Anti-Static Additive 3.
BBL(bbl):	Barrel (1bbl ≈ 159ℓ).
BPD (bpd):	Barrels per Day.
BPSD (bpsd):	Barrels per Stream Day.
BS&W:	Basic Sediment and Water.
DC (dc):	Direct Current.
HLB:	Hydrophile-Lipophile Balance.
O/W:	Oil-in-Water (emulsion)
ppm:	parts per million.
PTB (ptb):	Pounds per Thousand Barrels.
RMS:	Root Mean Square.
TBO:	Time Between Overhauls.
W/O:	Water-in-Oil (emulsion).

PLATES

PLATE 1 : See Chapter 10, Section 3.

PLATE 2 : See Chapter 10, Section 3.

PLATE 3 : See Chapter 10, Section 3.

PLATE 4 : See Chapter 9, Sections 9.11 and 9.12.

PLATE 5 : See Chapter 9, Section 9.12.

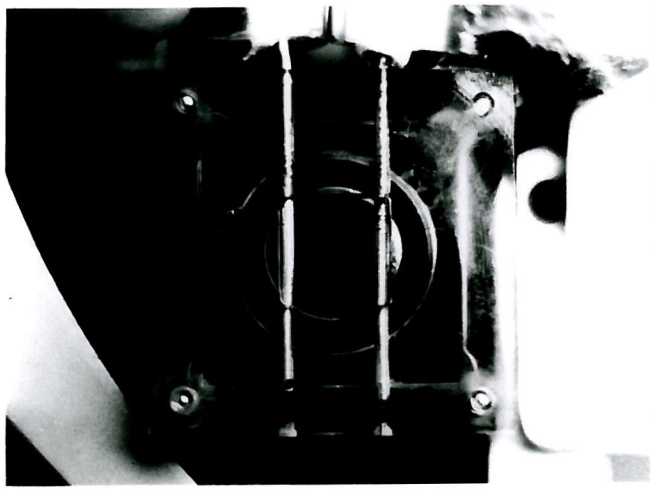

a. Microscopic electrode cell showing the parallel rod electrodes of diameter 1mm.

b. Pearl chain bouncing at the negative electrode (magnification x 130).

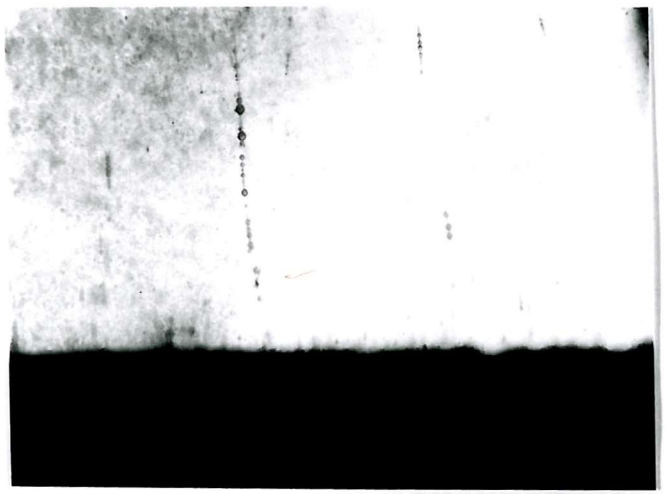

c. Six pearl chains aligned and almost forming a droplet bridge between the electrodes (magnification x 27).

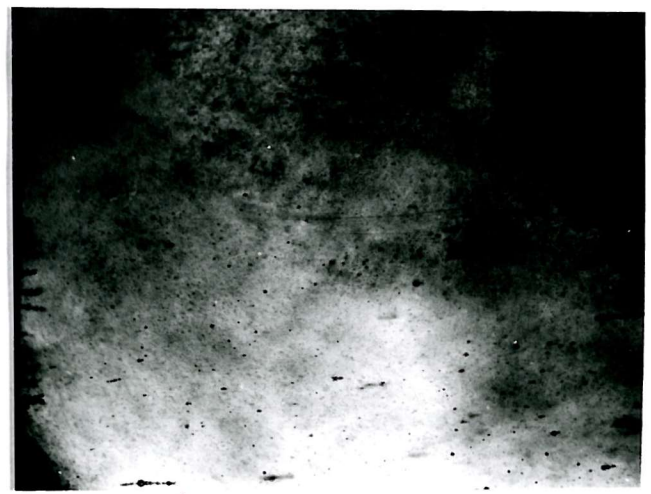

d. Pearl chains in transit between the electrodes (magnification x 27).

PLATE 1

e. Pearl chains and trees attached to the negative electrode (magnification x 130).

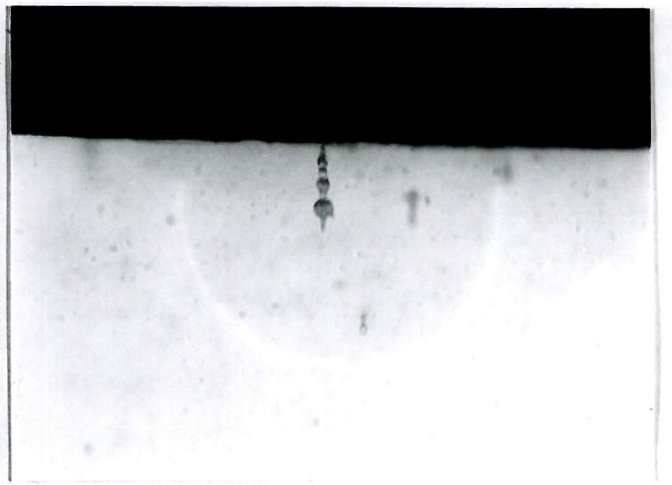

f. A solitary pearl chain attached to the positive electrode - an unusual event (magnification x 130).

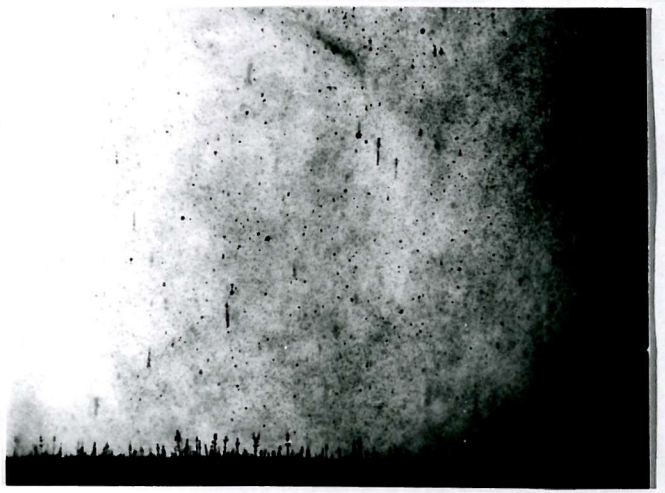

g. Pearl chains and trees attached to the negative electrode (see h.) (magnification x 27).

h. Positive electrode (just after g.) devoid of pearl chains and trees (magnification x 27).

PLATE 2

i. Pearl chains and trees attached to the negative electrode - diameter of largest droplet ~ 45μm (magnification x 130).

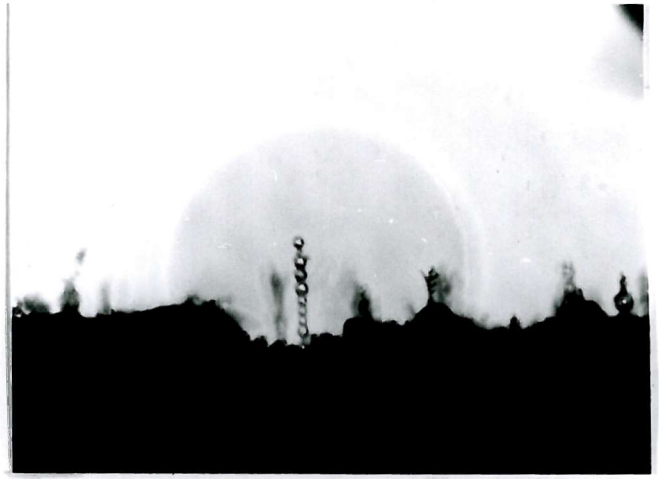

j. Pearl chain attached to the negative electrode - length of pearl chain ~ 150μm (magnification x 130).

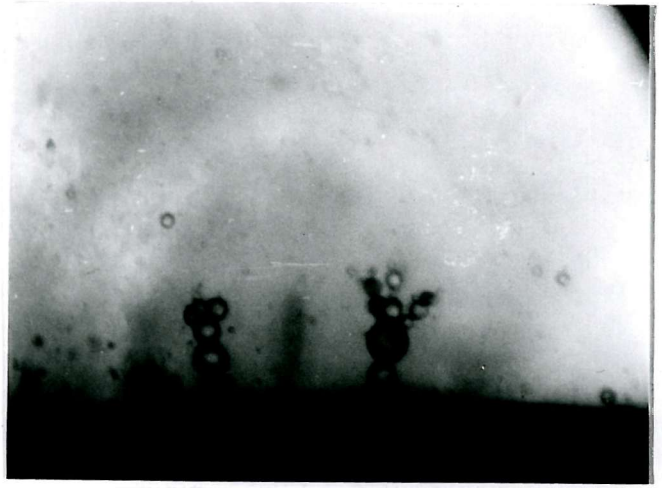

k. Trees attached to the negative electrode - largest water droplet has diameter ~ 50μm (magnification x 130).

l. Pearl chains aligned with the curving electric lines of force in the corner of the cell (magnification x 27).

PLATE 3

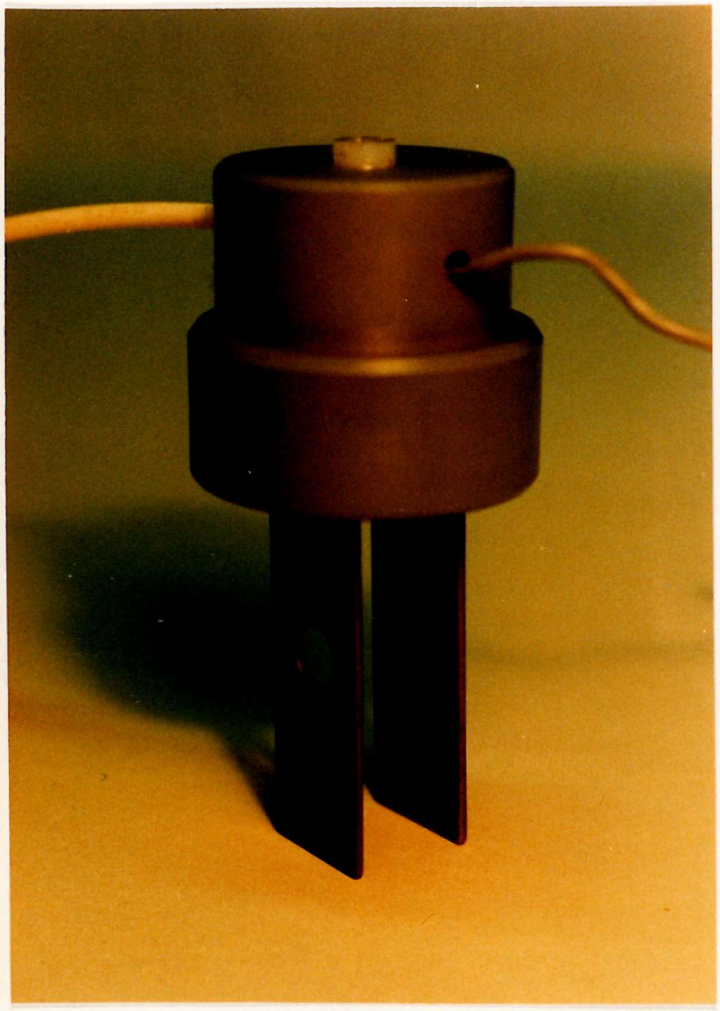

a. Curvette electrodes for use with the nephelometer - incident light beam passes between electrodes - scattered light passes through hole in electrode.

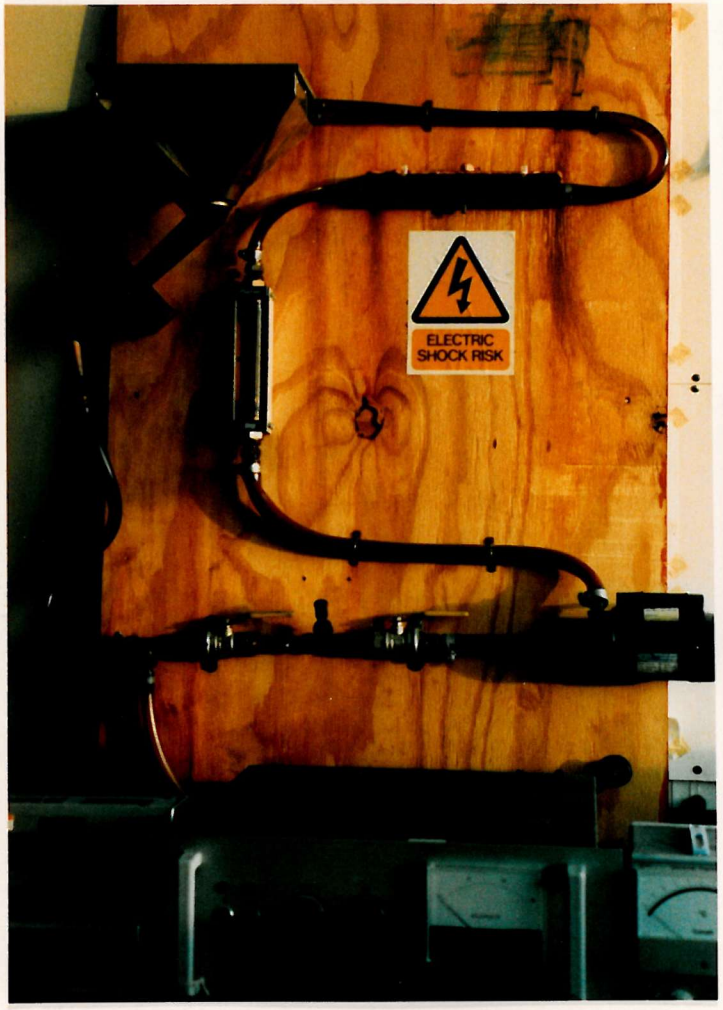

b. Closed circuit emulsion system comprising reservoir, centrifugal pump (providing emulsification), and horizontal electro-coalescer.

PLATE 4

PLATE 5

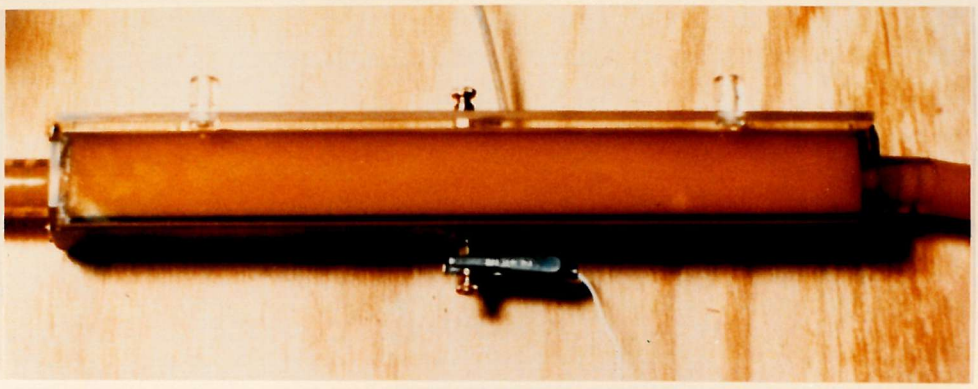

a. W/O emulsion in electro-coalescer after cessation of flow and just prior to applying the electric field (potential difference ~ 5 kV RMS, electrode spacing 25.4mm).

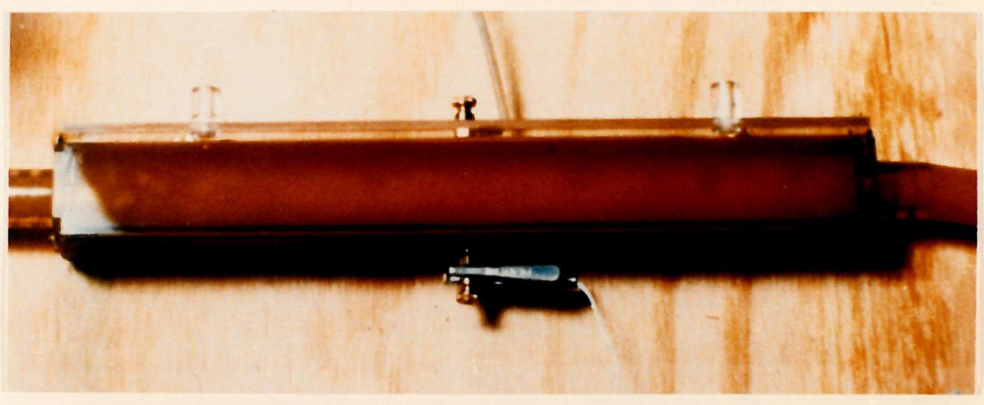

b. Phase separation underway, the water droplets are coalescing rapidly and settling out - the situation ~3s after a. above.

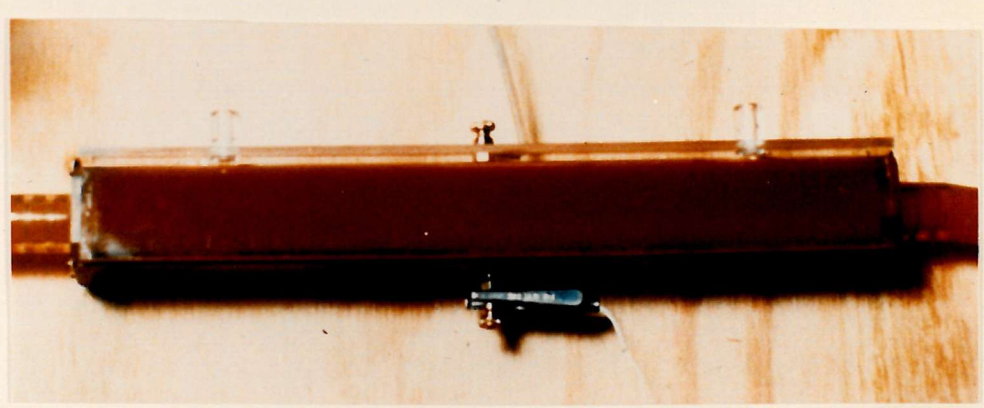

c. The W/O emulsion has effectively been resolved into its constituent phases, water at the bottom and oil at the top - the situation ~ 3s after b. above.

CONTENTS

1. INTRODUCTION

This study is concerned with the resolution of W/O emulsions experienced in the petroleum industry, particularly by the application of an external electric field. However, it should be borne in mind that the theory and techniques described may be applicable in other areas such as solvent extraction.

Although water and oil are immiscible liquids, it is possible for them to form an intimate mixture, namely an emulsion, which is quite stable and takes days to resolve under the action of gravity alone.

In the oil field, emulsions are formed, from the distinct water and oil phases present, due to the agitation induced by pumping. The type of emulsion formed (W/O or O/W) generally depends on the amounts of water and oil present before mixing, the dispersed phase usually being formed from the phase of least volume. However, the presence of emulsifying agent, which can occur naturally in the oil phase, is also of importance. The petroleum industry usually has to deal with W/O emulsions though O/W emulsions do occur.

There are various ways in which water can become mixed with oil. For example, brines are associated with crude oil because salt water generally underlies the oil in the geological formations from which it is drawn. Though it is possible, using careful completion and production methods, to sink wells which initially produce no brine, increasing amounts are produced, with the oil, as the productive life of a well is extended. Water entering oil during shipping is another source of contamination. In refineries, water is routinely mixed with oil, then separated out, in the desalting process, which is undertaken to reduce corrosion in refinery equipment and to meet user specifications.

Besides reducing the effects of corrosion, there are other reasons why it is desirable to remove dispersed free water droplets from oil. Their presence in pipelines and refinery equipment increases pumping costs and reduces oil throughput. Hazardous situations can arise when pumping distillates since the build up of static electricity is known to be enhanced by the presence of dispersed water (Klinkenberg and van der Minne, 1958).

Various methods, and combinations of methods, can be used to remove water from oil with which it has become mixed. These include: gravitational settling, centrifugation, heat treatment, the addition of chemical demulsifiers, and the application of an electric field.

1.1 Origin and Development of Electric Treatment

The origin of the electrical treatment of W/O emulsions can be traced back to an article by Buckner Speed (Speed, 1919) entitled: "An Appreciation of Dr Cottrell". Dr Frederick G Cottrell, it will be recalled, perfected a method of precipitating solids from flue gases using an intensive electric field. The second paragraph of Speed's article reads as follows:

This is the way the man's mind works: I recall some twelve years ago, when he was working on the precipitation of smelter smoke, I asked him for help on what seemed to be scarcely an allied problem, the freeing of California crude oil from its emulsified water. Instantly his mind worked with a snap. "Why," he said, "it's the same problem. For air put oil; for smoke particles, the minute water particles," and then his favorite form of expression: *"What will happen* if we put a high electrostatic stress on the oil?" Then in his characteristic quick manner, in a few minutes there were thrown together a beaker of oil, a spark coil, and two pieces of copper, and lo, the de-emulsification of the California oil had been solved. Within a few minutes, on a block of paraffin under the microscope there was spread out a drop of the emulsified oil, with two electric wires touching its edges. When the spark coil was put in operation the water drops were seen to arrange themselves in the field of the microscope like the iron filings between the poles of the magnet, to dance about and jiggle themselves into larger drops; and in these few minutes of experimentation the problem was solved by which millions of barrels of unmerchantable California oil were rendered fit both for refining and for fuel purposes.

The first commercial electric treater installation was established at the Lucille Oil Company at Coalinga, California in 1909.

Approximately two years later, in 1911, the pioneering patents (US 987114/5/6/7) on the subject were granted. Since then many hundreds of patents have appeared on the electrical treatment of W/O emulsions.

In 1935, the techniques of electrical treatment were modified to facilitate the removal of sediment and corrosion-causing inorganic contaminants from crude oil charged to refineries. Subsequently, in 1950, the method was extended to encompass the removal of organic impurities from petroleum distillates.

The technique of electrical treatment is the major method used for separating W/O emulsions. It is a necessary, efficient and cost-effective procedure. Electric treaters have no moving parts, require little maintenance and can be operated for long periods (sometimes years) without a shutdown. They are used, in the oil field, for dewatering purposes, and at the refinery they are employed for desalting crude oil charge and for scrubbing in the treatment of distillate fuel. Users (e.g. gas turbine operators) also may desalt fuel which has become contaminated with brine during transportation, prior to combustion.

1.2 The Nature of Electrical Separation

In principle, the electrical separation of a W/O emulsion is easy to conceive; the electric field simply acts to enlarge dispersed phase droplets, by inducing coalescence, after which they settle out under gravity at an increased rate. However, as the technique is investigated further it becomes more complex. Firstly, there are two types of electrical coalescence to consider, namely dipole and migratory coalescence, both of which may be present simultaneously. These depend, amongst other things, on: the dielectric properties (permittivity and conductivity) of both emulsion phases (continuous and dispersed), dispersed phase volume fraction and size distribution, electrode geometry (uniform or non-uniform electric field), electric field intensity, electrode excitation (ac, dc, pulsed, unidirectional, etc.), electrode insulation and so on. Coalescence due to sedimentation and Brownian motion confuses the issue. Another complicating factor is the possibility of dispersed phase droplet disruption if the electric field intensity is too great.

As the interfacial area of an emulsion is large, in comparison with its volume, factors associated with it such as interfacial polarisation, interfacial tension and chemical adsorption, may be important. The presence of surface-active agents (which can occur naturally in oils) at the interface is of considerable importance since they can reduce interfacial tension and confer stability to an emulsion.

A further complication is the nature of the oil itself, which can vary widely dependent on where it originated from. The density and viscosity of crudes are diverse and sometimes flow is only possible at elevated temperatures. Similarly, the contamination of oil by water, organic and inorganic substances, and solids is likely to differ markedly from one oil to another.

It can be appreciated, therefore, that the subject is complicated, interdisciplinary in nature and requires knowlegde in the areas of electrostatics,

surface and colloid chemistry, physics, fluid mechanics, and mathematics (to cope with the theoretical aspects which can be most complex).

1.3 Experimental Background

It would appear that experimentation, relevant to the electrical separation of W/O emulsions, has been somewhat sporadic since its inception in 1907 with perhaps more emphasis since about 1950.

The earliest experiments, performed by Cottrell in 1907 (mentioned by Speed, 1919), were mainly qualitative in nature. In them, a drop of W/O emulsion was subjected to an electric field and examined microscopically. The dispersed phase water droplets were observed to align themselves with the electric field lines and to coalesce. Similar experiments, in which particles or droplets formed chains, have been performed over the years by such workers as Muth (1927), Kuczynski (1929), Hollmann (1950), Putilova et al. (1950) and Pearce (1954). The formation of pearl chains has also been considered theoretically by Krasny-Ergen (1936), Saito an Schwan (1961) and Pohl (1978).

The coalescence of pairs of droplets is the fundamental process which occurs in an electro-coalescer. Owe Berg et al. (1963), working with droplet pairs in air, suggested that coalescence was the switching of intermolecular bonds from within the droplets to across their common interface. Two mechanisms were proposed for this, whereby the bonds were either gradually re-arranged, or broken and reformed by the supply of energy (e.g. electrostatic discharge).

Charles and Mason (1960a) investigated the coalescence of a droplet at a plane interface under the influence of gravity and an electric field. They also observed rupture of the intervening film and tried to correlate a theoretical expression for rupture velocity with experimental values.

Allan and Mason (1962) considered the behaviour of suspended droplet pairs undergoing shear flow, with special emphasis on the effect of electric fields and charge on coalescence.

Various workers have considered coalescence in terms of coagulation kinetics. Sadek and Hendricks (1974), for example, suggested that the droplet size distribution of a W/O emulsion, undergoing migratory coalescence in an electric field, was of self-preserving type. Similarly, Volkov and Krylov (1972a,b) investigated dipole coalescence in an alternating electric field. They were able to

specify the integral properties (e.g. mean size and variance) of a W/O emulsion, without solving the coagulation–kinetics equations of the size distribution function itself.

The separation of W/O emulsions can also be considered using a mechanistic approach, in which resolution time (or residence time) is determined from a droplet growth expression based on the coalescence of a pair of droplets. Williams and Bailey (1983) and Zeef and Visser (1987) developed such models to investigate dipole coalescence and migratory coalescence respectively.

Laser light scattering techniques have also been used to study W/O emulsions. For example, Williams and Bailey (1984) monitored the change in size distribution of a W/O emulsion, subjected to a steady electric field, as a function of time. Joos, Snaddon and Johnson (1984) performed a similar investigation and developed an expression for droplet growth in terms of an average coalescence time.

The separation of flowing W/O emulsions, using insulated electrodes, has been investigated by Bailes and Larkai (1981, 1982, 1984) and Galvin (1984). In both cases, the insulating material used was perspex and a pulsed, unidirectional electric field was applied to the emulsions. Bailes and Larkai found that optimum phase separation occurred at a particular frequency and deduced a relationship between the collision frequency of droplets and the electrical current supplied. Galvin established that phase separation increased with excitation frequency until constrained by power supply limitations.

As well as inducing coalescence, electric fields can also promote droplet disruption, if the field strength is sufficiently large. This may occur directly due to electrostatic stresses or indirectly as a result of hydrodynamic stresses which are caused by droplets being driven by the electric field (electrophoretically for example). The electrostatic stress, at the surface of a droplet, may be due to the applied electric field or the presence of charge on the droplet. Rayleigh (1882) developed an expression for the maximum charge a droplet can hold before disrupting (the Rayleigh limit). Many workers have investigated the elongation and disruption of droplets in an intense electric field, including: Zeleny (1917), Wilson and Taylor (1925), Nolan (1926), Macky (1931), Panchenkov and Tsabek (1968b), and Rosenkilde (1969). Taylor (1964) analysed the situation where an intense electric field stresses a conducting droplet so much that it develops a conical protruberance (Taylor cone) which oscillates and ejects a jet of charged droplets from its apex. Taylor (1934) and Hinze (1955) investigated the dispersion of

droplets under well-defined flow conditions (e.g. Couette flow and plane hyperbolic flow). Anisimov and Emel'yanchenko (1976) studied a coalescence-inhibiting mechanism called contact-separation charging. It is believed to result when charge exchange occurs between two droplets undergoing dipole coalescence while suspended in a low-conductivity dielectric liquid; droplet repulsion results following the exchange of charge. The phenomenon has been observed by other workers, notably Sartor (1954) and Allan and Mason (1962).

The experimental investigations outlined above and many others are described in more detail within the body of the thesis.

1.4 Layout of Thesis

The commercial and industrial aspects concerned with the electrical separation of W/O emulsions, in the recovery and refining of oil, are discussed in Chapter 2. This covers: the contamination of crude oil by water, organic and inorganic materials, and solids; the problems contamination can cause to pipeline authorities, refiners and users such as corrosion, abrasion, erosion, scaling, and plugging; electrical treatment including the dewatering and desalting of crude oil and the scrubbing of distillate fuels; the cost, history and scope of the electrical treatment technique.

Chapter 3 describes the surface chemistry, and physical and electrical properties of emulsions. It covers most of the properties of emulsions which should be considered in order to understand the various aspects of emulsion behaviour. The surface chemistry of emulsions is discussed since a small amount of surface-active agent can have a profound effect on emulsion stability and interfacial tension. Interfacial tension is important since it governs the ease with which droplets can be dispersed. Another important physical property of an emulsion is its effective viscosity which depends on the dispersed phase volume fraction and size distribution; this governs the ease with which the emulsion flows and can be pumped. The electrical properties of importance are effective dielectric constant and conductivity which also depend on the dispersed phase volume fraction. Interfacial polarisation is of concern since it can render the dielectric constant and conductivity of an emulsion frequency dependent.

The electric double layer and its relation to emulsions is discussed in Chapter 4. This phenomenon is of interest since it is concerned with the eletrophoretic transport of dispersed phase droplets. It can also act to stabilise O/W emulsions. Some rudimentary double layer experiments performed with W/O

emulsions are described.

Chapter 5 discusses the principal forces associated with the coalescence of dispersed phase droplets and the formation of pearl chains. A bispherical co-ordinate analysis is presented for the interaction of two equally-sized conducting spheres, aligned with the applied electric field. This yields a description of the potential difference and electric field at all points in space, and also the force of interaction between the spheres. The dipole method of determining the radial and transverse force components is also presented, and the zones of attraction and repulsion defined. A comparison is made between dielectrophoretic and electrophoretic forces which is relevant to the action of the forces in W/O emulsions.

In Chapter 6, the theory concerned with the drainage of the intervening film between two droplets in close proximity is examined. In one case the droplets are assumed to be undeformable and in the other case deformable. The driving force is taken as the electrostatic force of attraction between two polarized spheres, almost in contact with one another. The analysis shows that droplets become more stable as they coalesce and grow in the applied electric field.

Droplet dispersion mechanisms, caused directly or indirectly by the application of an electric field, are examined in Chapter 7. These include disruption due to the application of an intense electric field or possession of charge, and also hydrodynamic breakup. The formation of Taylor cones is discussed, as is a coalescence-inhibiting mechanism termed contact-separation charging.

Chapter 8 covers the various techniques of emulsification and describes four methods which were tried experimentally. One of these, ultrasonic agitation using magnetostriction, was adopted as the standard method of emulsification, in view of its convenience.

Chapter 9 is the heart of the thesis and it discusses the coalescence of W/O emulsions in depth. In its broadest sense, coalescence is considered to be: long-range flocculation, film thinning, droplet collision, film rupture, and unification of droplets. Coalescence involving electrostatic forces (dipole and migratory coalescence) is discussed, as is that due to sedimentation, Brownian motion and shear forces. The phenomena of partial coalescence and limited coalescence are described. The use of mechanistic and statistical emulsion models is discussed. In the mechanistic approach, the coalescence of an average pair of dispersed water

droplets is considered, which leads to a growth rate equation. This yields the resolution time of a W/O emulsion after solving the sedimtation equation. In the statistical approach, the coagulation kinetics of the dispersed water droplets are considered. It is possible to determine the integral emulsion characteristics without solving the coagulation-kinetics equations of the droplet size distribution itself. Experimentation is described in which a turbidimetric technique is used to monitor the water content of an emulsion, subjected to a steady electric field, from which the emulsion resolution time can be determined. The theoretical model correctly predicts the manner in which the measured resolution time descreases as the electric field strength is increased. Qualitative experiments are described in which a closed-loop emulsification system and electro-coalescer with insulated electrodes are used. Time varying electric fields are required to produce effective coalescence in the W/O emulsions (a high-voltage, mains-frequency transformer was found to be a suitable power supply). Phase separation can be achieved in stationary or slow-flowing emulsions. A laser light scattering technique is used to monitor the size distribution of dispersed phase droplets, in a W/O emulsion, subjected to a steady electric field. The size distribution is found to broaden and its peak moves to larger sizes, with the passage of time, which demonstrates water droplet coalescence in the applied field.

The formation of particle chains is investigated in Chapter 10. In the case of W/O emulsions droplets coalesce readily at first. Subsequently, however, they become more stable and pearl chains form. A microscopic study of pearl chain formation in W/O emulsions, subjected to a steady electric field is described. Photographs taken during the experimentation are presented (see Plates 1-3).

Chapter 11 describes the use of insulated electrodes for resolving W/O emulsions. In order to model the system it is necessary, firstly, to consider the effects of interfacial polarisation at the water/oil interface and subsequently at the emulsion/insulator interface. The potential difference established across the emulsion is low unless the applied frequency exceeds the characteristic frequency of the system. Power supplies, however, serve as a constraint on frequency, since it is difficult to achieve high output voltages at high frequency. This relates to the ability of the power supply to provide current and therefore also serves to constrain electro-coalescer dimensions.

Finally, Chapter 12 deals with patents associated with the electrical treatment of W/O emulsions. The use of computer search techniques to locate relevant patents, in various data bases and using various search strategies, is described. A list of such patents is presented in Appendices B, C and D.

1.5 The Author's Contribution to the Theoretical and Experimental Techniques Pertaining to the Electrical Resolution of W/O Emulsions

The author's contributions to the subject are presented here in the order of the chapters in which they occur.

The effect of charged droplet migration on the effective conductivity of an emulsion is examined in Chapter 3 (3.6.3), which does not appear to have been discussed in the literature. An expression is derived for the component of conductivity in a parallel plate electrode system, due to this mechanism, assuming the droplets to be conducting. The conductivity component turns out to be proportional to the square of the continuous phase dielectric constant, the square of the applied electric field strength, the dispersed phase volume fraction, and inversely proportional to the continuous phase viscosity.

Chapter 5 (5.1) presents a relatively complete and detailed analysis of the interactive force between two uncharged conducting spheres, of equal size, whose line of centres is aligned with the applied electric field; the bispherical co-ordinate system is adopted for this purpose. Papers on the subject tend to be more helpful than books, though they are somewhat brief by necessity. The paper by Panchenkov and Tsabek (1968a), for example, is good but it does not present a derivation of (or even give an expression for) the interactive force. The paper by Davis (1961) omits most of the steps in the derivations but does give an expression for the interactive force. Unfortunately it is littered with errors which does not instil confidence in the reader. Davis also integrated over the surface of one of the spheres, rather than the median plane, which leads to more involved expressions. His paper is, however, more general since it accounts for droplet pairs of unequal size, which may possess charge, and whose line of centres need not be aligned with the applied electric field. The author of this thesis has taken two limits of the force expression derived; firstly, as the droplets become very far apart and, secondly, as they become very close together. The first limit yields the conventional dipole force expression which, apparently, has not been derived in this manner before. The second limit yields an expression which, apparently, has not been derived by any other author. It can be used in conjunction with film thinning equations (see Chapter 6), to specify the rate of approach of droplets in the final stages which precede coalescence of the droplet pair. The limiting force expression is convenient to use in view of its simple formulation.

Chapter 5 (5.4) also presents a comparison of electrophoretic and dielectrophoretic forces, believed to be unique, which relates to the rôle of the

forces in inducing dispersed phase droplet coalescence in W/O emulsions. In order to do so, use has been made of Lebeder and Skal'skaya's (1962) expression for the charge acquired by a conducting sphere on contacting a charge electrode. This allows a useful expression to be derived for the electrophoretic force which can then be compared with the dielectrophoretic force expression.

Lastly, in Chapter 5 (5.5), a derivation (believed to be unique) is presented of the dipole moment of a lossy dielectric sphere in a lossy dielectric liquid. In the derivation, the surface charge density of the sphere (due to interfacial polarisation) is defined in terms of Legendre polynomials, as are the potential functions inside and outside the sphere. A sinusoidal excitation is assumed to be applied, at some moment in time, which yields a solution with transient and steady-state components. The dipole moment is found to change as a function of time and frequency of excitation, due to interfacial polarisation.

Film thinning theory is discussed in Chapter 6. The force driving the droplets together is assumed to be the electrostatic force discussed in Chapter 5 (5.1), in the limit as the droplets become very close together. Two film thinning equations are considered, one corresponding to deformable droplets the other to undeformable droplets. In each case the rate of film thinning is different. The equations can be integrated to determine the time taken by droplets in approaching one another between specified distance limits. The results suggest that small droplets coalesce readily, being undeformable, and that once they have reached a critical size, a longer time elapses before coalescence can take place, since the droplets flatten off and their relative speed reduces.

Chapter 7 examines all the known mechanisms which lead to droplet dispersion or inhibit droplet coalescence, due to the application of an electric field to a W/O emulsion. Two of these mechanisms (dispersion in a strong electric field (7.1) and contact-separation charging (7.1.2)) can be presented straightforwardly in graphical terms, by plotting the critical electric field strength as a function of droplet radius. By considering the charge acquired by a conducting sphere on contacting a charged electrode (Lebder and Skal'skaya, 1962), it is possible to present two other mechanisms (dispersion due to possession of charge (7.1.3) and hydrodynamic dispersion (7.2.1)) in the same way. In the case of dispersion by possession of excessive charge (i.e. the Rayleight limit), the charge limit is identified as that charge a conducting sphere acquires on contacting an electrode. In the case of hydrodynamic dispersion, the droplet is assumed to be driven electrophoretically by the applied electric field; the droplet charge is again taken as the charge acquired by a conducting sphere on contacting an electrode.

It is necessary, however, to equate the electrostatic driving force to the drag on the droplet (assumed to remain spherical) which requires that the drag coefficient (a function of the Reynolds number) be considered. The overall graph may be used to assess the likelihood of droplet disruption, or the inhibition of droplet coalescence, at any particular level of applied electric field.

In Chapter 9 (9.10.2) a dipole coalescence model is presented which is mechanistic in form. That is, the coalescence of an average pair of conducting dispersed phase droplets is considered, under the action of the conventional dipole force. The rate of change of separation of the droplets is used, in conjunction with the equation defining volume fraction, to obtain a differential equation which, when solved, leads to an exponential droplet growth expression. The droplet growth expression can then be used, in the gravitational sedimentation equation, to obtain the time required by a growing droplet to fall from the emulsion surface to the rising free-water interface. This time is identified as the emulsion resolution time. The technique can easily be extended to flowing emulsions and this has been done, in Section 9.10.3 for an upwardly-flowing emulsion. In this case, however, the droplets rise with the emulsion flow until they reach the upper electrode, by which time they have grown sufficiently to start to fall against the flow. An expression is given which relates the electrode separation to the potential difference applied.

Chapter 9 also describes the use of turbidity to monitor the water content of a W/O emulsion (see Sections 9.10.1, 9.11, 9.11.1, 9.11.2 and 9.11.3). The technique used is applicable to low water content ($< 0.1\%$ by volume) W/O emulsions having a transparent oil phase. The turbidity is found to be roughly proportional to water content and the technique is capable of monitoring water concentrations down to about 1ppm ($\simeq$ 1NTU). The techniques of monitoring water content by measuring turbidity is believed not to have been used before.

Lastly, Chapter 9 (9.13) investigates the use of a laser diffraction technique for determining the size distribution of a W/O emulsion. A commercial instrument, the Malvern Particle and Droplet Size Analyser (HSD 2600), is used for this purpose. It allows a sequence of up to 24 droplet size distribution measurements to be made automatically. This enables the changes brought about by electric-field-induced coalescence to be studied as a function of time. The dispersed phase droplet size distributions are determined while the electric field is in action and so, once an experimental sequence has been initiated, it runs automatically without the need for manual sampling.

1.6 Aims of the Study

The aims of the study are to establish a more scientific footing for electric treater design and to lay down guidelines for the development of an improved electrostatic separator. By improving separation efficiency it should be possible to increase oil throughput, reduce operating costs and save space (particularly important in offshore applications). As the World's supply of oil diminishes, leading to the more frequent use of secondary recovery techniques, user specifications become more stringent, and refinery practices become more complicated, there will be a continuing demand to improve the effectiveness of separators.

2. W/O EMULSIONS IN THE RECOVERY AND REFINING OF OIL

Water generally underlies the crude oil in the geological formations from which the oil is drawn. This is why water is often produced with oil. As the production life of a well is extended, the proportion of water increases. Indeed, if secondary recovery techniques are used, water or steam may be pumped down a well, in order to extract the oil.

Being immiscible liquids, the water and oil retain their separate identities when combined. However, the high shear forces created by pumping the mixture through pipes, valves and other equipment lead to the formation of an emulsion, usually of W/O type. The emulsification process may be aided by emulsifying agents, which can occur naturally in an oil, leading to the production of relatively stable W/O emulsions.

The presence of water droplets in the crude oil produced from oil fields (on-shore and off-shore) is undesirable for a number of reasons. Firstly, it increases pumping costs since the viscosity of the emulsion is greater than that of the oil alone (see Section 3.5), and the bulk of the water itself must be moved. Secondly, the water contains salts which lead to the corrosion of pipelines and other equipment. Lastly, solid materials such as silt, clay and drilling mud tend to accumulate at the water/oil interface where they can act as a stabilizers. The salt, solids and water content of crude oil must, therefore, be reduced (at the oil field) to meet shipping and pipeline specifications (normally 0.5 to 2% brine).

The presence of water, and contaminants, in oil are also undesirable at the oil refinery, for similar reasons. Severe corrosion to distillation equipment can result too, from the presence of salts. Further, energy is wasted in heating the water component of the oil, which has more demanding heat transfer requirements. For these reasons, reduction of the salt and water content of crude oils, before distillation, is practised at oil refineries. Besides, it is usually necessary to do so, in any case, to satisfy user specifications.

Contamination of fuel, with salt water, can also occur during transportation. For example, one utility (Florida Power) on the East coast of the United States occasionally experienced levels of up to 4ppm sodium in their distillate fuel, which normally averaged 0.8ppm sodium (General Electric publication c. 1973).

Gas turbines can suffer severe corrosion to turbine blades and stators if the fuel burnt has an excessive sodium content. Users are keen not to incur un-scheduled shutdowns and expensive overhauls, and so their specifications may be stringent.

It can be seen, therefore, that there is a need for de-watering and de-salting equipment at each stage : during production at the oil field, during refining at the oil refinery, and on-site prior to consumption by the user.

2.1 Oil Contaminants

The composition of brines, produced with crude oil, is influenced by the geological formations (e.g. sands, gypsum, limestone, dolomite) from which the oil originates. For a particular crude, the salt content is likely to vary according to the amount of basic sediment and water (B S &W) it contains. It is meaningless, therefore, to make generalisations regarding the water, chloride, sediment and acid/alkaline content of crudes; these must be evaluated occasionally at the oil refinery. Broadly, crude oil, as received at the refinery, contains 0.2 to 2% residual water which cannot economically be removed at the oil field (Fisher et al., 1962). Its salt content varies from about 3 to 200 ptb (pounds per thousand barrels, where 0.3ptb ≡ 1ppm) (Waterman, 1965a). Fluctuations are common and seasonal variations the rule, due to less efficient de-watering in the oil field, during cold weather.

2.1.1 Chloride Content and its Relevance to Corrosion

The content of chloride ions is generally measured in refinery salt analyses. In brines, the metal ion content of salts may vary widely, though common averages are 75% sodium, 15% magnesium and 10% calcium (Waterman, 1965a). Chlorides are responsible for hydrogen chloride (HCl) evolution during the distillation process; the chloride content is used as an index of the corrosion potential of a crude oil, and also of mechanical fouling. The most prolific producer of HCl is magnesium, followed by calcium and sodium in descending order. The evolution rate of HCl diminishes as the chloride concentration decreases, however, the proportion (of available chloride) converted increases. The presence of organic acidity and other impurities can increase the proportion of chloride converted. For a chloride content of about 5ptb, virtually all of it is converted into HCl.

The conversion of chloride into HCl, which occurs in distillation columns, is called hydrolysis. Hydrolysis starts to become appreciable at a temperature of around 120°C (Fisher et al., 1962). The hydrochloric acid produced begins to attack metals, in refinery equipment, where the temperature exceeds this value. Hydrolysis continues to increase as the distillation temperature is raised up to about 350°C. The hydrochloric acid liberated, which may be substantial at high temperatures, is then carried overhead in the flash and fractionating towers, where it leads to corrosion. Not only is hydrochloric acid extremely corrosive itself, but the experience of refiners indicates that corrosion due to hydrogen sulphide is increased in its presence. This has been explained by a mechanism in which hydrogen sulphide (H_2S) and hydrochloric acid (HCl) enter a cyclic oxidation-reduction reaction† with the metals in fractionating equipment, in which the normally protective iron sulphide layer is continually removed by the hydrochloric acid. Metal surfaces are thereby exposed to simultaneous and continuous attack by the two corrosive agents (Davis et al., 1938). The units most susceptible to corrosion by HCl are those where moisture is present; condensers, exchangers, fractionater top trays, transfer lines, and receivers are particularly vulnerable.

According to Wilten (1962) chloride ions and caustic lead to stress corrosion (caustic embrittlement) in stainless steel at refineries. The life of metals may therefore be prolonged (in a two-fold way) by reducing the chloride content, since less caustic is then required for neutralizing hydrochloric acid (which is produced by the hydrolysis of chlorides).

2.1.2 Sulphates and Carbonates

Sulphates and carbonates may be present in crude oils in significant quantities. In some crudes the sulphate content may be in excess of the chloride content, which can be troublesome. The solubility of calcuim sulphate decreases with temperature above 40°C and undergoes a change in hydration at 100°C. It follows that sulphate scale formation can occur without the need for brine evaporation. Scaling, due to solubility changes, is a problem in the primary exchnagers, and care must be exercised to minimise it. Such scale can be flint hard and may necessitate the premature replacement of tubes in exchangers and furnances.

---

† $2HCl + Fe = Fe\,Cl_2 + H_2\uparrow$
$FeCl_2 + H_2S = 2HCl + FeS$

2.1.3 Sediment

In addition to salts, most crude oils contain highly-dispersed solid materials, generally referred to as sediment. Sediment may contain fine particles of sand, clay, volcanic ash, drilling mud, rust, iron sulphide, metal and scale. Typically, a crude oil will contain 10 - 200ptb of sediment. The amount of sediment is likely to increase as the quantity of connate water produced rises, however, there does not appear to be any correlation with salt content. It is obvious that such materials should be removed from an oil, before it is refined, otherwise they will have damaging effects on equipment due to plugging, abrasion and erosion.

Sediments, hydrolysis products and salts find there way into residual products such as fuel oil and asphalt. Solids and salts are also carried into distillate fractions by entrainment, which can lead to fouling of exchangers and poisoning of catalysts in subsequent refinery processes. Solids in residual fuel oil tend to plug burners and form deposits on furnance pipes and brick-work. The coke formed by burning salty crudes is usually flint hard and difficult to remove, in contrast to the softer coke resulting when salt-free oil is burned.

Sediment is a passive nuisance in that it can occupy expensive storage space, lodge in quiescent parts of refinery equipment and settle out on exchanger surfaces. It also contributes to waste and pollution since emulsion may be stabilized in the form of oil-wetted soilds, which carries a significant amount of oil into the waste-oil recovery system at a refinery.

2.1.4 Organo-Metal Compounds

These comprise hydrocarbon combinations with vanadium, nickel, copper and iron principally, and many others in trace amounts. Arsenic may be included in this group since it has a similar effect with regard to poisoning platinum catalysts (used in the reconstitution of petroleum distillates). These materials are unwelcome in that they produce undesirable reactions in refinery equipment. Further, their presence is cumulative as is their damaging effect.

The levels of arsenic and iron (and to a lesser extent the other metals) can effectively be reduced, by the desalting operation, to acceptable values.

2.2 Corrosion in Gas Turbines

Sodium, potassium and vanadium are constituents of oils which can lead to corrosion in gas turbines. The vanadium content of petroleum is mainly in oil-soluble forms such as vanadium porphyrins. These are usually inhibited by the injection of magnesium compounds after desalting. Vanadium reacts during the combustion of fuel, to produce metal oxides which, on their own or in combination with other ash ingredients, lead to the corrosion of metal surfaces in the path of the hot combustion products.

Inorganic contaminants, such as salts, are of prime importance in relation to corrosion and ash deposition problems, arising from the combustion of distillate fuels. The deposits are largely metal oxides and sulphates which are formed, during combustion, from metal-containing impurities. When oxides of sodium and potassium react with sulphur and vanadium oxides (also combustion products) molten ash deposits are produced, which are corrosive by one or more mechanisms (Greenlee and Lucas, 1972).

If there is sufficient sodium in the fuel, the corrosive compounds formed during combustion can severly damage the first-stage buckets, of a gas turbine, leading to an unscheduled shutdown and expensive re-blading work.

Once deposits form they continue to corrode the underlying metal. Water washing can help but it is never completely successful in removing all the deposits, especially those in inaccessible regions. Any salt in the atmosphere tends to continue the corrosion initiated by the sodium deposits.

Operating experience shows that maintenance costs increase in an almost-exponential fashion once the sodium/potassium content exceeds 0.5ppm. If the level doubles to 1ppm, the maintenance costs for overhaul and repair increase by a factor of 3 or 4 (General Electric publication, c. 1973).

Gas turbine manufacturers have warned that fuel concentrations of more than a few ppm by weight can reduce TBO's (Time Between Overhauls) from several thousand to hundreds of hours and increase the cost of overhaul and repair by a factor of 2.5 to 3 (General Electric publication, c. 1973).

Some users believe that manufacturers have underestimated the problem and that the corrosive damage to turbine blades and stators may be more severe than recognised. They suggest a 0.5ppm sodium/potassium limit instead of the

5ppm value accepted by many specifications.

2.3 Desalting

Desalting basically involves the addition of about 3 to 5% fresh water to crude oil, mixing them together thoroughly, then separating the aqueous and oil phases. The best results are obtained by emulsifying the fresh water into small droplets; this increases the probability of it contacting and coalescing with the dispersed brine droplets. However, the degree of fresh-water dispersion required renders coalescence and phase separation difficult by simple gravitational methods. Besides, crude oil contains materials such as asphalt, asphaltines, resins, oxygenated sulphur and nitrogen compounds. These materials gather at the water/oil interfaces and hamper coalescence; they are called stabilizers because they confer stability to an emulsion.

The stability of an emulsion can be reduced by subjecting it to heat, chemical treatment, and electrical treatment (the subject of this thesis). In the refinery, heat is available, at no additional cost, in the primary heat exchanger of the crude distillation system. The temperature in desalting systems is usually in the range 100 to 200°C, and the pressure sufficient to suppress evaporation of higher fractions. Heat increases the solubility of the oil phase for the stabilizer and also increases the rate of diffusion of stabilizer into the oil. The viscosity and cohesion of the interfacial film are reduced by heating, as is the viscosity of the oil. Nevertheless, the force of impact, brought about by random collision of water droplets, is still insufficient to rupture the interfacial film and allow coalescence.

The interfacial film can be further modified by the use of chemical destabilizers. These materials, also called demulsifiers, are surface-active agents which displace the stabilizer from the water/oil interface. The nature of the demulsifier molecule is such as to reduce the thickness of the interfacial film and render it susceptible to rupture. Selection of treating chemicals, from the many hundreds available, is empirical and requires a skilful specialist.

Perhaps the most commonly used emulsion separation technique relies on the application of an electric field. It is a powerful technique for overcoming the resistance of stabilizing interfacial films. The collision and coalescence of dispersed phase droplets is accomplished by induced dipole attraction between them (see Section 9.10). This holds for the complete range of oils, from crudes to distillates, no matter what kind of electrical excitation is used (ac, dc, pulsed, etc.). In the case of low-conductivity oils, such as distillates, droplet collision and

coalescence also result from electrophoresis (migratory coalescence, see Section 9.8), if a unidirectional electric field is applied. After electrical coalescence, the separation of the water and oil phases results from gravitational sedimentation.

Coalescence by electrical means is eventually limited by the reduction in number density of dispersed phase droplets. As the dispersed phase volume fraction reduces to about 0.1%, the efficiency of electrical separation falls off (Waterman, 1965a), since the droplets are then about eight droplet-diameters apart, on average, and the dipole coalescence force is very weak. If a further reduction in the level of contaminantion is desired, it is necessary either to resort to electrophoresis (ac dipole forces are normally used initially) or to increase the number density of the dispersed phase by introducing additional material (usually water) to coalesce with the residual impurities. Conventionally, the former process is used in treating petroleum distillates whereas the latter is employed for crude oil desalting (see Figure 2.1). The latter process is also used in on-site installations

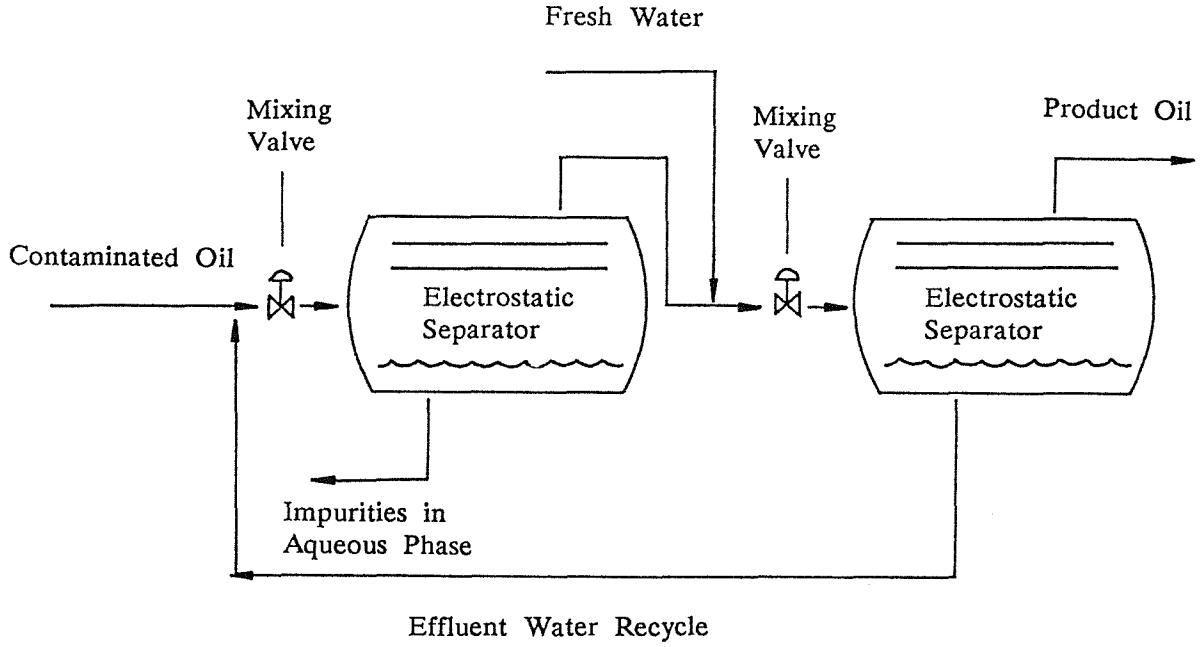

FIGURE 2.1 Schematic diagram of two-stage desalting system.

for removing impurities from fuels which have become contaminated during transportation.

The effectiveness of the desalting process depends on the nature of the crude charge and dispersed brine, and also on the extent to which the refiner can provide suitable wash water and optimum operating temperatures. Modern desalting plants are capable of reducing the salt content by 90 to 98% in most cases, the average reduction being greater than 95% (Fisher et al., 1962). According to Greenlee and Lucas (1972), current refinery operations reduce the sodium content of crude oil to the 3ppm level in a single stage, and below 1ppm (sometimes down to 0.1ppm) in two stages of electrically-assisted separation.

Solid particles are also removed during the desalting process, though the efficiency of deposition, usually between 50 and 75%, is less than that of droplets (due, in part, to the hydrophobic nature of some of the solids involved) (Fisher et al., 1962). However, solid particles are removed in significant quantities.

The amount of water which can be removed by electrical separation would appear to depend on the type of oil being processed. Thus crude oil can be dehydrated down to a level of about 0.1% (Waterman, 1965a, Greenlee and Lucas, 1972), whereas for a distillate the limit can be as low as 10ppm (Greenlee and Lucas, 1972). The difference in limits is probably attributable to the difference in conductivities between crude oil and distillate, and also to the different electric field excitations applied. Crudes, of high electrical conductivity ($> 10nSm^{-1}$, Waterman, 1965b), are typically processed using ac fields, for which there is no electrophoretic coalescence (the use of dc field would not help much as charge would quickly relax from the droplets). Distillates, however, are usually processed with dc fields, and so advantage can be taken of electrophoretic (migratory) coalescence (since the charge relaxation time of the continuous oil phase is large).

The addition of small amounts of alkaline material (such as caustic or soda ash) to the system, prior to desalting, is beneficial for two reasons. Firstly, excessive emulsion stability is avoided. Secondly, when crude oils having acidic brines are treated, the decomposition of salts into chlorides, and the subsequent formation of the corrosive HCl, is reduced. However, the use of excessive quantities of caustic, to reduce sulphur and organic acidity, can lead to highly stable emulsions and caustic embrittlement of the equipment (Fisher, et al., 1962).

As the complexity of refinery operations increases, with the advent of new processes, so has their sensitivity to contaminants in the crude oil charge. When this is considered, in conjunction with the ever-increasing demands of user specifications, it can be seen why refiners require increasing efficiencies of their desalting equipment.

2.4 Distillate Treating

Electrical separation techniques are used in the elimination/conversion of oleophilic contaminants from distillates (as well as the dehydration and desalting of crude oils) in the processes described below.

Sulphuric acid is used to reduce the sulphur content of distillates, to extract the stability-promoting components of certain fuels, and for removing nitrogen and metal-containing compounds from process feedstocks. Trace amounts of acidic products can be removed by an alkaline neutralization process.

Dilute caustic (NaOH or KOH in solution) is used for the extraction of acidic components such as hydrogen sulphide, naphthenic acids and the more acidic mercaptans from distillates. More concentrated caustic solutions are necessary for the extraction of organic materials, of less acidity, such a phenols (e.g. cresylic acid); water is also effectively removed.

In other processes, mercaptans of low acidity are converted to disulphides, which may be removed by sulphuric acid. Water is used as a reagent for removing low levels of metallic contamination, from previous treatment processes, particularly trace metals and caustic materials.

In these distillate treating processes, the separation technique is similar to single-stage desalting. The chemical reagent is added to the distillate, dispersed using a mixing device to ensure good contact with the distillate impurity, then separated by electrical treatment which enhances coalescence of the dispersed droplets of reagent.

2.5 Advantages of Desalting

The benefits of electrical desalting may be summarised as follows (according to Waterman, 1965a):

Increased crude throughput due to:

i. Longer runs
ii. Running at maximum capacity
iii. Less down time for maintenance
iv. Less water charged to the crude unit
v. Uniform crude charge without slugs of water during tank switching

Reduced labour costs due to:

i. Frequent turnarounds
ii. Worn or corroded equipment
iii. Fouled exchangers
iv. Furnace tube hot spots

Less plugging, scaling, coking and slagging of:

i. Exchangers
ii. Furnaces

Relief from catalyst poisoning by:

i. Arsenic in platformers
ii. Sodium, iron and other metals in crackers

Less corrosion due to sulphur, salts and organic acidity in:

i. Exchangers
ii. Fractionaters
iii. Receivers and lines

Savings in chemical cost for:

i. Ammonia
ii. Inhibitors

Less erosion by solids in:

i. Control valves
ii. Exchangers and furnaces
iii. Pumps

Pollution abatement by:

i. Clarifying condensate water
ii. Phenol extraction from catalytic process water

Savings or recovery of oil from:

i. Slops from waste oil recovery system

ii. Cleanout of storage tank bottoms

iii. Oil in process water (sour vacuum tower condensate)

iv. Less dumping of oil to sewer for maintenance

v. Less slopping of off-specification products

Improved products because of:

i. Better operational control

ii. Removal of catalyst poisons

iii. Less salt and solids in residual fuel

iv. Cleaner coke for specialities such as electrodes

v. Improved oleinsis, and ductility in asphalts.

The refinery advantages of single-stage desalting can be seen from Figure 2.2 which shows average data based on figures from 43 refineries.

A good example of the improved efficiency of general refinery operations, after the removal of salts and solids, is shown in Figure 2.3. This corresponds to conditions in a Gulf Coast refinery, processing crude oil in which the salt content was reduced from 45 to 4 ptb (Fisher et al., 1962). Illustrated is the drastic effect of solids accumulation in the heaters and exchangers which led to a reduction in the transfer line temperature from 832°F to 814°F. In this case crude runs were extended from 800-hours to over 1600-hours, the latter being a voluntary rather than forced shutdown.

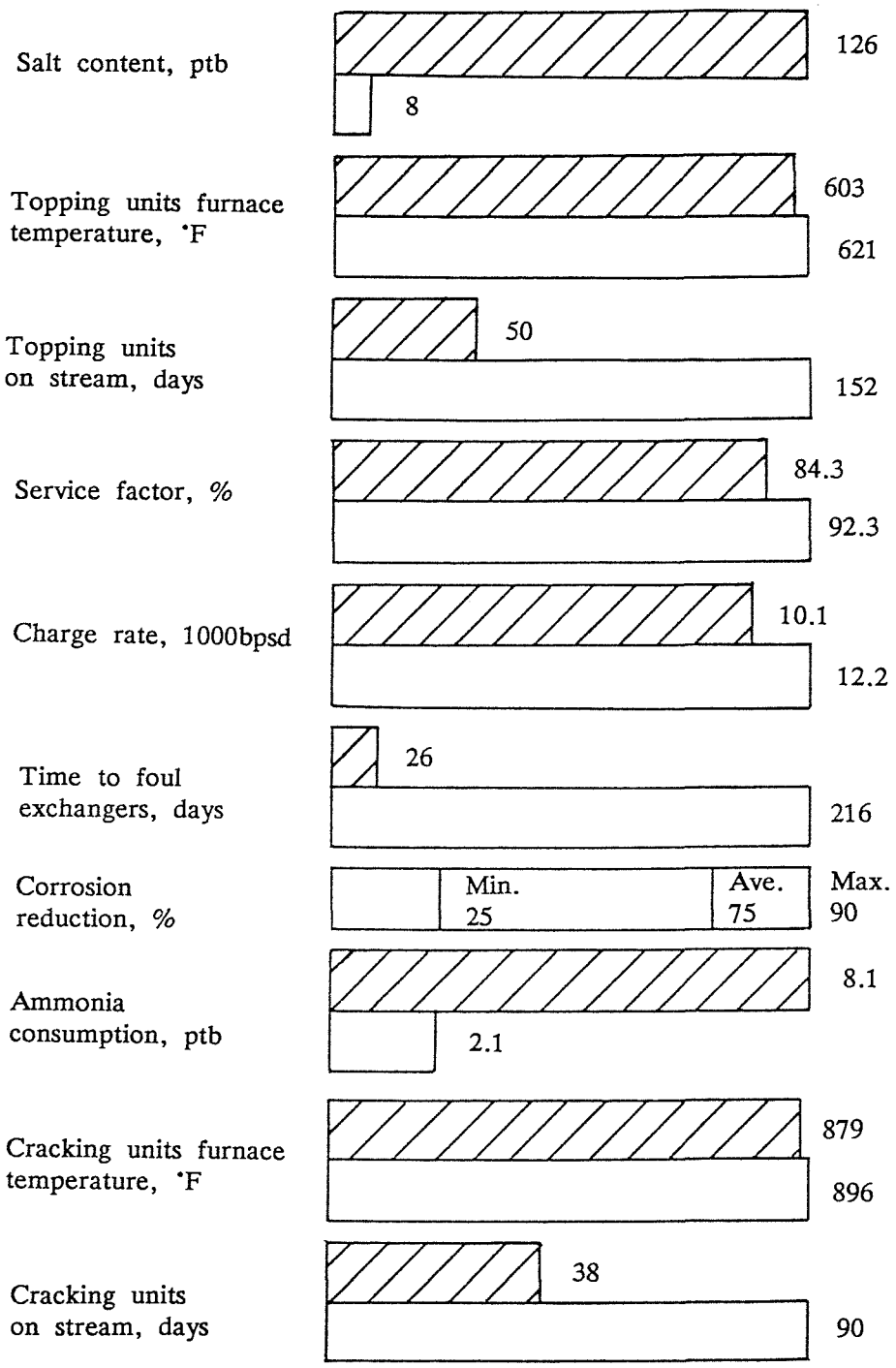

FIGURE 2.2 The advantages of single-stage desalting in the refinery: before - shaded, after - unshaded (Waterman, 1965a).

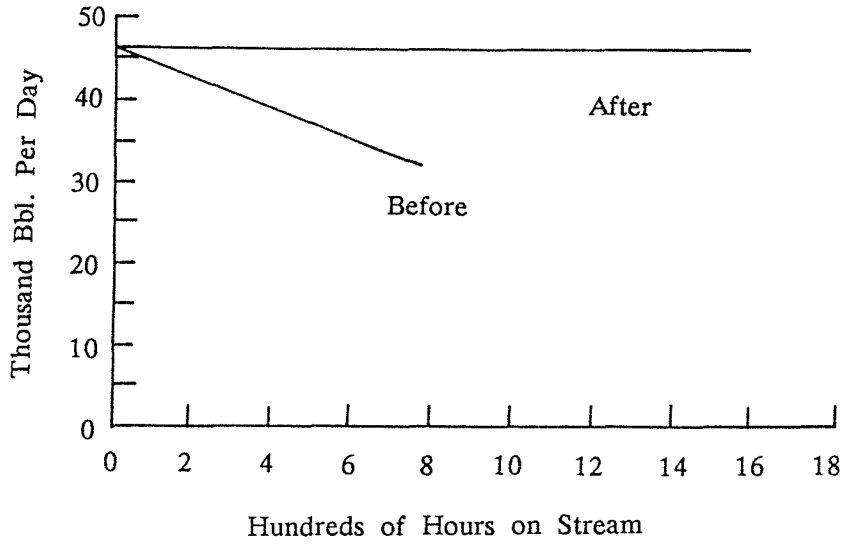

FIGURE 2.3 The effect of desalting on the throughput rate of crude oil at a refinery (Fisher et al., 1962).

2.6 The Cost of Electrical Treatment

The cost of electrical treatment can be split up into the installation cost of the equipment and its subsequent operating costs. Both of these are affected by an economy of scale in that the cost increases approximately as the cube root of the capacity ratio (or equivalently capacity rate ratio). Thus going from 10,000 to 100,000bpd (barrels per day) little more than doubles the price (see Figure 2.4). The installation cost can also vary by a factor of 2 to 3, depending on the type of fuel to be desalted and its sodium content. This depends on whether single or double-desalting is necessary, and the nature of ancillary equipment (rectified systems being more expensive presumably).

The operating costs of a desalter depend, amongst other considerations, on the amount of wash water and electricity consumed during processing. These are related to the type of oil being processed, the throughput rate and the temperature of operation. The power consumption, when desalting crude oils electrically, ranges from about 12kWhr/1,000bbl for light crudes to 36kWhr/1,000bbl for heavy crudes (which have higher electrical conductivities) (Waterman and Pettefer, 1969). In the case of distillates (which have very low conductivities), the power consumption is typically 0.2kWhr/1,000bbl, in the electrofining process (Waterman, 1965b).

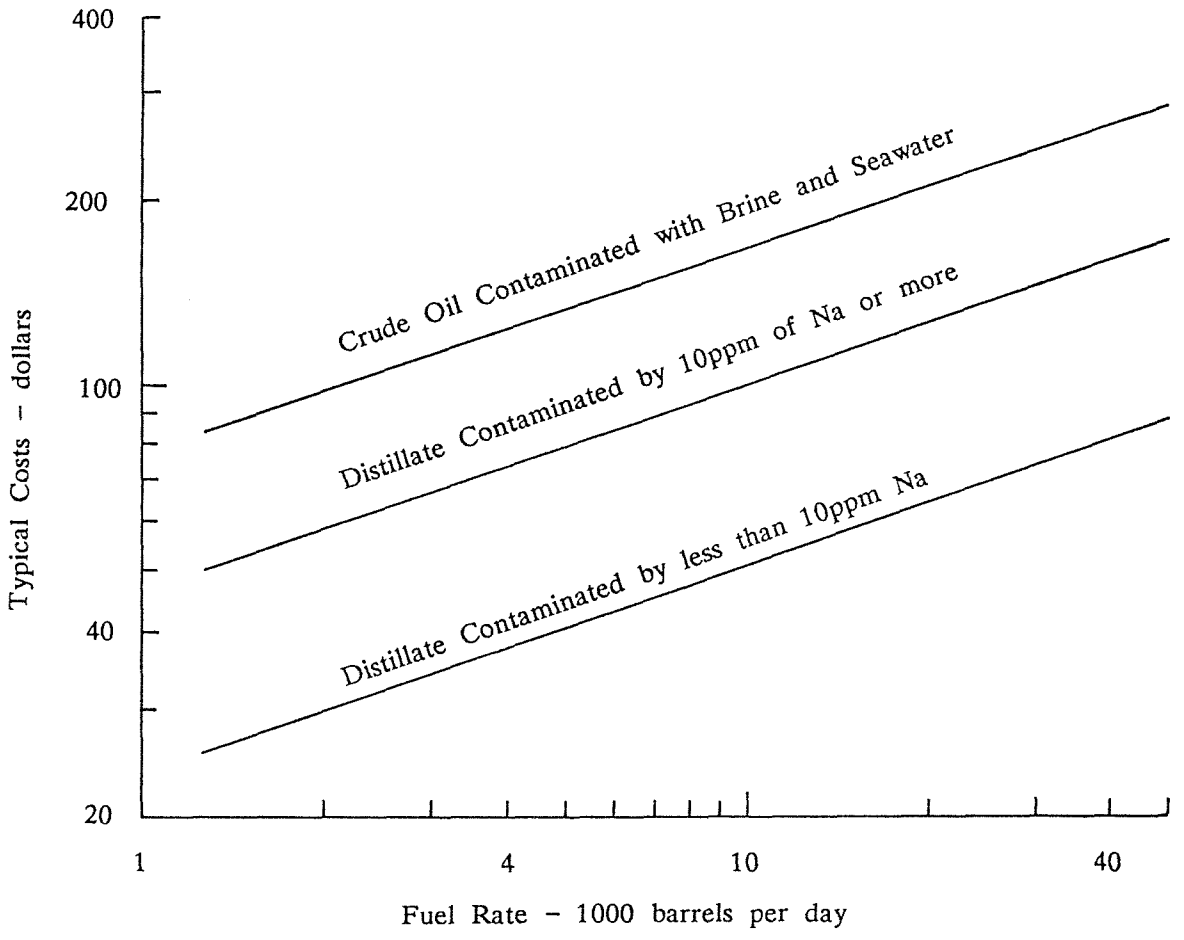

FIGURE 2.4 Cost–capacity relationships for electrostatic fuel purification systems (Greenlee and Lucas, 1972).

The cost of desalting is minimal as can be seen from Table 2.1. Double desalting is approximately twice the cost of single desalting. In fact, the desalting

crude unit capacity, bpd	desalting cost cents/bbl	
	single unit	double unit
10,000	0.3	0.5
40,000	0.2	0.3
100,000	0.1	0.2

TABLE 2.1 Approximate cost of desalting crudes in 1965 (Waterman, 1965a,b)

costs are outweighed by the savings that can be made from increased throughput, savings in chemicals, reduction of corrosion, and reduction of labour costs.

2.7 History and Scope of the Electrical Treatment of W/O Emulsions

Following an extensive series of tests, into the use of an electric field for breaking emulsions (as suggested by F G Cottrell, who is famous for pioneering a method for precipitating solids from flue gases using an intense electric field), the first commercial installation was set up at the Lucille Oil Company at Coalinga, California in 1909. The plant successfully reduced an emulsion of 14% water to less than 2%, at the rate of 1000 barrels per day. The techniques were subsequently (1935) modified to facilitate the removal of sediment and corrosion-causing inorganic contaminants (primarily sodium salts), from crude oils charged to refineries. Additional modifications (1950) extended the refinery application of electrostatic techniques to the removal of organic impurities (such as compounds of sulphur, nitrogen and oxygen) from petroleum distillates.

The electrical treament of W/O emulsions is practised at the oil field, in petroleum refineries, and on-site prior to combustion by the user. The major portion of produced water (and associated inorganic impurities) is separated from the crude oil in an oil-field operation called dehydration (or dewatering); the water content of the oil after electrical treatment is usually in the range of 0.2 to 2%. The remaining water-soluble impurities (principally sodium chloride) and some sediment are washed from the crude oil in a refinery operation called desalting (which may be single or double-staged). During distillation, organic impurities (such as sulphur compounds) and small quantities of water are fractionated into various fuel products. These are removed in a refinery operation, called scrubbing, in which reactive chemicals are employed. After scrubbing, the aqueous phase is separated from the distillate by electrical treatment.

World-wide there are more than 500 electric desalters in operation, capable of processing around 25 million barrels per day of crude oil. The throughput rate of electric treaters usually ranges from 20,000 to 200,000 bpd, a value of 100,000bpd being typical (Greenlee and Lucas, 1972).

Around 350 electric distillate treaters are in operation, which are capable of processing about 3.5 million barrels per day of distillate fuel. The throughput rate of these units is generally in the range 2,000 to 40,000bpd (Greenlee and Lucas, 1972).

The electrical treatment of oils is very attractive since it is inexpensive, the units have no moving parts and run periods measured in years can be obtained (with the occasional shutdown for removal of sediment and cleaning).

3. BACKGROUND TO THE SURFACE CHEMISTRY, PHYSICAL PROPERTIES AND ELECTRICAL PROPERTIES OF EMULSIONS

An emulsion is a heterogeneous system comprising two essentially immiscible liquids, one of which is dispersed in the other in the form of droplets which may be stabilised by a relatively small amount of emulsifying agent. That the word essentially appears in the above definition, acknowledges the fact that all liquids are soluble in one another to some extent, which is temperature dependent; the level of mutual solubility being low for two liquids regarded as being immiscible. For example, water and oil are immiscible liquids but the oil phase may contain typically 100ppm water in soluble form (Zaky and Hawley, 1973).

The two liquid constituents involved are called the phases of the emulsion. After emulsification, one liquid is dispersed in the other in the form of fine droplets.

In pure systems, where there is no emulsifying agent present, the phases quickly separate gravitationally, with the less dense phase at the top and the denser phase at the bottom. However, when emulsifying agent is present, stability is conferred to the emulsion which takes very much longer to separate gravitationally.

In an emulsion, the liquid which is dispersed into droplets is termed the internal phase (dispersed phase or discontinuous phase) whereas the other is termed the external phase (continuous phase).

Most types of emulsion have an aqueous phase which may contain dissolved salts, organic material or colloidal substances. This is referred to as the water phase. The other phase, though not necessarily an oil, is called the oil phase; it behaves towards water like an oil. Such liquids include: hydrocarbons, waxes, resins, nitrocellulose solutions, etc. (Sutheim, 1946).

Other substances to be found in emulsions, can be classified according to their affinity for one or other of the two emulsion phases. Those which are water soluble or have an affinity for water are called hydrophilic (oleophobic or lipophobic). Those which have an affinity for oil-like liquids are called hydrophobic (oleophilic or lipophilic). Hydrophilic and hydrophobic substances have very different molecular structures which account for their behaviour when in contact with aqueous or oil-like liquids. Examples of hydrophilic substances are: water soluble compounds, many water-insoluble salts and oxides, and organic substances in which the oxy, hydroxyl or polar groups are predominant. Typical

hydrophobic substances are: oils, fats, waxes and generally those inorganic substances which contain many carbon atoms and few or no polar groups.

When an emulsion is made, it is possible for either of the phases to form the continuous phase or the dispersed phase. When oil forms the dispersed phase, O/W (oil–in–water) emulsions result. However, when water forms the dispersed phase, W/O (water–in–oil) emulsions are produced. The kind of emulsion resulting depends on a number of factors including: the type (if any) of emulsifying agent, phase–volume ratio (i.e. volume fraction), method of emulsification, and various additional factors such as the types of solid material present in the mixing vessel (e.g. impellers or the vessel itself) (Dvoretskaya, 1949, Davies, 1961).

It was pointed out by Cobb (1946) that emulsions may be made by brute force or persuasion. In the persuasive approach, the presence of emulsifying agent reduces the need for vigorous mixing. Briggs (1920) demonstrated that with some systems, emulsification is more efficient if an intermittent shaking technique is used rather than a vigorous mixing process. Indeed, with some systems, spontaneous emulsification has been observed (McBain and Woo, 1937). However, in most practical cases, emulsions are made by the brute force approach. The higher the shear forces established during emulsification the smaller the droplet size produced (Rodger et al., 1956).

In general, emulsions will have polydisperse size distributions. It is widely accepted that emulsion droplets typically have diameters in the range 0.1–10μm (Becher, 1977). However, there may be some droplets of diameter less than 0.1μm or greater than 10μm in any emulsion. If the diameters of droplets are in the neighbourhood of 1μm it is said to be a fine emulsion, whereas if they are in the range 5–10μm it is said to be rather coarse (Sutheim, 1946).

Of considerable importance in the study of emulsions are surface tension and interfacial tension since they govern the ease with which new free surface or interface is formed during emulsification.

3.1 Surface Tension

The properties of a liquid at its surface, where it is in equilibrium with a gas, are different from those in the bulk. This can be explained in terms of van der Waals' forces which exist between liquid molecules. The molecules of a liquid exert short–range attractive (cohesive) forces which prevent the liquid from breaking up. Within the bulk of the liquid these cohesive forces balance. However, this is

not so at the surface where molecules are attracted more strongly towards the bulk, giving rise to surface tension. Particles in the surface of a liquid have a higher potential energy than those in the bulk; the increase in energy per unit area is called the surface free energy, which is identical to surface tension. Thus, the free surface of a liquid possesses a contractile skin which acts to minimise its potential energy. This accounts for the spherical shape of a free droplet, which has the least surface area for a given volume contained.

3.1.1 Interfacial Tension

When a liquid is in contact with another liquid, or a solid, a boundary tension is established which is similar to the surface tension of the liquid. In this case, however, the phenomenon is called interfacial tension.

The net force acting on a liquid molecule near the interface is less than it would be in the case of a free surface, since van der Waals' forces attract it to the surface molecules of the other medium. For this reason, the interfacial tension between two liquids is expected to be intermediate their respective surface tensions. Based on a thermodynamic argument, Girifalco and Good (1957) suggested the following relationship:

$$\gamma_{WO} = \gamma_W + \gamma_O - 2\Phi(\gamma_W\gamma_O)^{\frac{1}{2}} \qquad (3.1)$$

For a given system, Φ is constant and can be related to the molar volumes V_W and V_O of the individual liquids as follows:

$$\Phi = \frac{4V_W^{1/3}V_O^{1/3}}{\left[V_W^{1/3}+V_O^{1/3}\right]^2} \qquad (3.2)$$

For all liquids incapable of forming hydrogen bonds with water Φ is found to lie in the range 0.51 - 0.78 whereas for all liquids capable of forming hydrogen bonds Φ lies in the range 1.00 to 1.15. This expression gives satisfactory results for a large number of liquids with respect to water.

Fowkes (1962) suggested a modification to this approach which considers the surface tension of a liquid to be the superposition of two independent phenomena, namely hydrogen bonding (h) and van der Waals' forces (v). Both terms make a contribution to the surface tension of water ($\gamma_W = \gamma_W^h + \gamma_W^v$).

However, if the other liquid is a saturated hydrocarbon, there is no hydrogen bonding component in the surface tension ($\gamma_O = \gamma_O^V$). The attractive forces between molecules of water and saturated hydrocarbon, at an interface, are mainly attributable to van der Waals' forces. Eqn. (3.1) therefore takes on the following form, where $\gamma_W^V = 21.8 \pm 0.7$ dyne cm^{-1} at 20°C for water.

$$\gamma_{WO} = \gamma_W + \gamma_O - 2\left[\gamma_W^V \gamma_O\right]^{\frac{1}{2}} \qquad (3.3)$$

Both eqns. (3.1) and (3.3) have met with some success in predicting the interfacial tension of liquid systems containing emulsifying agent. In such systems, the interfacial tension is found to be mainly dependent on the hydrogen bonding term.

3.1.2 Surface Tension as a Function of Temperature

The surface tension of most liquids decreases as temperature increases. As temperature increases, so does the kinetic energy of the surface molecules which reduces their net attraction to the bulk liquid. On nearing the critical temperature of a liquid, the cohesive forces between its molecules tend to vanish and so the surface tension approaches zero.

Various expressions have been proposed to show the behaviour of surface tension as a function of temperature, two of which are shown below.

Ferguson's equation for normal organic liquids may be expressed as follows (Ferguson, 1915):

$$\gamma = k\,(T_c - T)^n \qquad (3.4)$$

γ = surface tension at temperature T
k = constant for liquid under consideration
T = temperature
T_c = critical temperature
n = 1.2 in the case of organic liquids but generally $1 \leq n \leq 2$.

The Ramsay–Shields–Eötvös equation, shown below, is a semi-empirical expression based on kinetic theory. It was originally proposed by Eötvös (1886) without the d term which was subsequently introduced by Ramsay and Shields (1893).

$$\gamma = \frac{k}{(M\nu)^{2/3}} \left[T_c - T - d\right] \qquad (3.5)$$

M = molecular weight of liquid

ν = specific volume of liquid (reciprocal of density)

d = constant having an approximate value 6

k = a universal constant having an approximate value of 2.2 for a large number of liquids

(other terms are defined as above).

3.1.3 Gibbs' Adsorption Isotherm

The surface (or interfacial) tension of a liquid varies according to the concentration of solute. Such variation may be described in terms of Gibbs' equation, stated below, which can be derived using thermodynamic arguments. For simple, non-ionic compounds in dilute solution it has the following form (Gibbs, 1876):

$$\Gamma = \frac{-c}{RT} \left[\frac{\partial\gamma}{\partial c}\right]_T \qquad (3.6)$$

Γ = surface (or interfacial) excess of solute

c = concentration of solute in bulk solution

γ = surface (or interfacial) tension

T = absolute temperature

R = universal gas constant ($8.3143 JK^{-1}mol^{-1}$)

The surface (or interfacial) excess Γ is a measure of the excess of solute adsorbed at the surface (interface) over that contained in the bulk solution. It was originally defined as the difference between the quantity of solute contained in a given volume of solution having unit area of free surface (interface) and that in an equal volume of bulk solution.

Surface (or interfacial) tension can be explained in terms of cohesive forces between liquid molecules; the approach may be used to consider solutions as well as pure liquids. An interaction energy can be defined in relation to the cohesive force. Molecules for which the interaction energy is lower than average will tend to accumulate at the surface (interface) of the solution, in order to reduce the free energy of the system to a minimum. Consequently, if solute molecules are positively adsorbed at the surface (interface) of a solution (that is,

the surface or interfacial excess Γ is positive), its surface (interfacial) tension will be reduced below that of the pure solvent. Similarly, if solute molecules are negatively adsorbed (that is, the surface or interfacial excess Γ is negative), the surface (interfacial) tension of the solution will be increased above that of the pure solvent.

3.1.4 Surface Tension as a Function of Solute Concentration

In view of the molecular processes which give rise to surface tension it is perhaps not surprising that the presence of solute should affect its value. McBain et al. (1937) classified the three main types of surface-tension curve which are shown schematically, for water, in Figure 3.1.

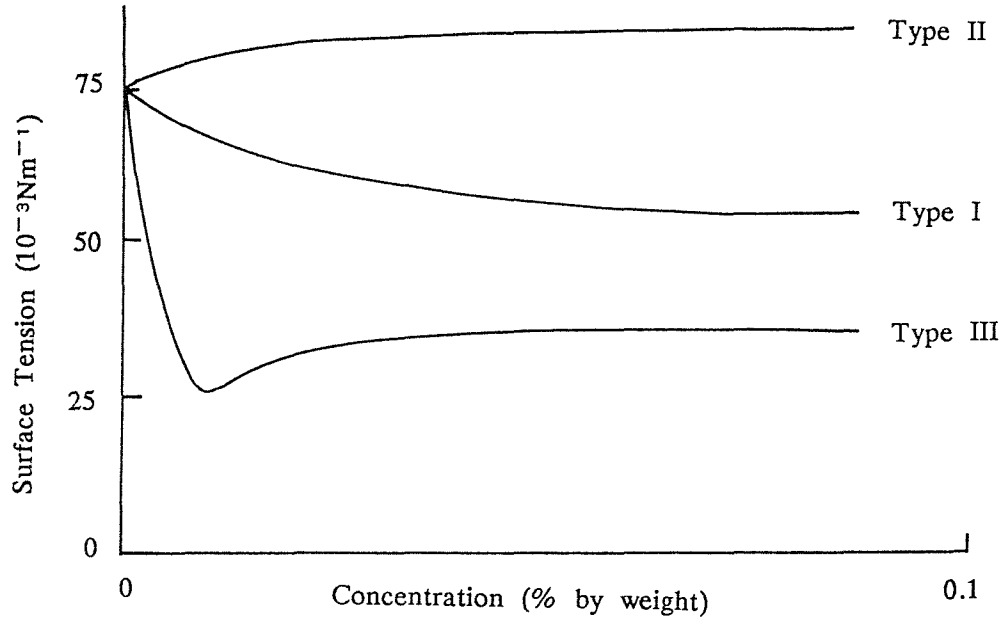

FIGURE 3.1 Principal types of surface tension v concentration curve for water.

For the Type I curve, surface tension falls monotonically, as concentration increases, quickly at first and then gradually. This corresponds to positive adsorption of the solute according to Gibbs' equation. In the case of the Type II curve, surface tension rapidly rises above the value for pure water. This corresponds to negative adsorption, according to Gibbs' equation, which indicates a decrease in concentration of solute at the surface . The Type III curve is the one of most significance. Initially, for very dilute solutions, surface tension reduces very rapidly to a minimum, then increases to a value considerably less than that of pure water. This type of behaviour is not completely in accord with Gibbs' eqn.

(3.6) since in the region of the minimum, a change from strong positive to strong negative adsorption is predicted, which is physically unreasonable.

The minimum is thought to occur when more than one surface-active species is present in solution. Alexander (1941) explained the anomaly in terms of the formation of micelles at concentrations close to that corresponding to the surface-tension minimum. It is accepted that the micelle (to be described shortly), due to its structure, cannot exist at the free surface where the solvent molecule is the single surface-active species. In the bulk solution, however, there are dispersed solvent molecules and molecular aggregates (micelles). It is not surprising, therefore, that Gibbs' equation should break down in this case.

According to McBain (1944), molecular aggregates of an amphiphilic substance (i.e. having Type III behaviour), of colloidal dimension (10^{-3} - $10^{-1}\mu m$), form in the bulk solution. These clusters, known as micelles, are thermodynamically stable constituents of the solution. The formation of micelles can be explained in terms of the molecular structure of the amphiphilic substance. A molecule of such a substance is of polar-non-polar type, that is, part of the molecule is polar in nature and the other part non-polar. In general, the non-polar component comprises a long hydrocarbon chain which exhibits no external dipole and has an affinity for organic solvents (i.e. it is hydrophobic). The polar component comprises one or more polar groups, exhibits an external dipole and has an affinity for aqueous solvents (i.e. it is hydrophilic). As an example consider sodium palmitate, a soap having the chemical formula $C_{16}H_{31}O_2Na$. Using X-ray techniques, the molecular structure of this soap may be established (see Figure 3.2) (Sutheim, 1946).

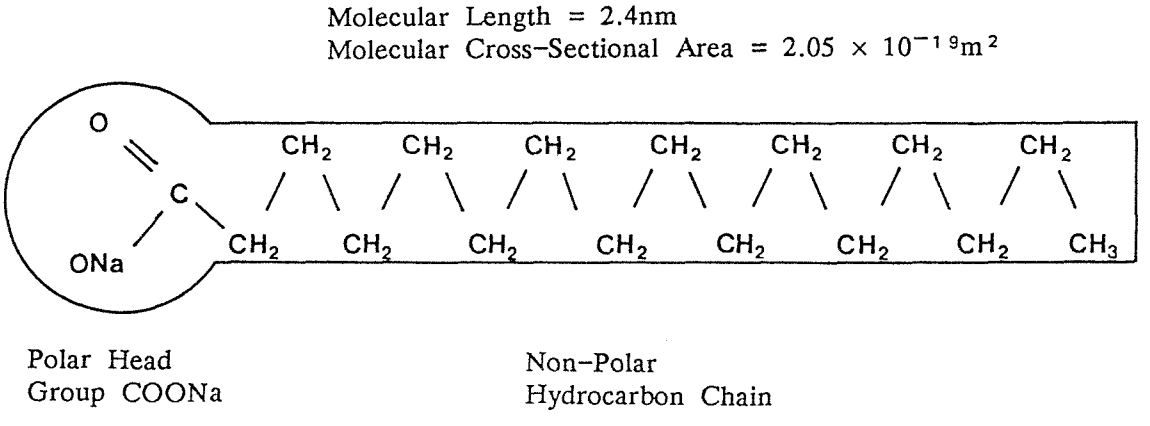

FIGURE 3.2 Molecular structure of sodium palmitate showing polar-non-polar architecture.

For a polar–non–polar molecule to be amphiphilic (having an affinity for both aqueous and organic solvents) there must be a balance between the effects of the polar and non–polar parts, otherwise it would only be soluble in one or other of the solvents. If the concentration of such molecules in an aqueous continuous phase is sufficiently large, there is a tendency for them to form clusters, with the non–polar tails sticking together to form the hydrophobic interiors of the micelles, and the polar heads sticking together to form the hydrophilic outer surfaces. It is also possible for micelles to form in non–aqueous solvents (Debye and Prins, 1958).

The interfacial tensions (with respect to water) of solutions containing an amphiphilic compound are, in general, in the range 1–10 dyne cm^{-1} (for concentrations greater than about 0.2% by weight) (Becher, 1977). By addition of an electrolyte to the solution the interfacial tension can be further reduced, generally. For example, the interfacial tension of a paraffin oil, with respect to water, was 40.6 dyne cm^{-1}. By adding 0.001M oleic acid to the aqueous phase, it reduced to 31.05 dyne cm^{-1}. The system was neutralised using sodium hydroxide, forming the soap sodium oleate ($C_{17}H_{33}COONa$), after which the interfacial tension reduced to 7.2 dyne cm^{-1}. By adding 0.001M sodium chloride to the aqueous phase, the interfacial tension was further reduced to less than 0.01 dyne cm^{-1} (Becher, 1977).

3.1.5 Surface (Interfacial) Tension as a Function of Time

The surface tension of a freshly–created surface of pure liquid or solution changes with time, as the surface strives to attain equilibrium. This time is very short for pure liquids, less than 3ms in most cases; the surface tension being measured by the vibrating–jet technique (Becher, 1977).

With regard to solutions, the migration of solute molecules towards (positive adsorption) or away from (negative adsorption) a surface, according to Gibbs' equation (3.6), must take a finite time. For example, an aqueous solution (M/4000) of sodium oleate had an initial surface tension of 71.0 dyne cm^{-1}, which reduced to 61.0 dyne cm^{-1} in 5 minutes and 42.4 dyne cm^{-1} in 570 minutes (Clayton, 1943).

Surface tension increases with time for some solutions, notably aqueous solutions of volatile liquids, since solute evaporates from the surface more quickly than it can be replenished by diffusion from the bulk (Clayton, 1943).

Time-dependent effects occur in the case of interfacial tension, as well, the literature having been reviewed by Sutherland, 1951. This phenomenon has been found to exist in non-aqueous solvents, by Signer and Berneis (1957) which may be of significance regarding the dynamics of emulsions.

3.1.6 Surface Elasticity

Surface elasticity is a phenomenon caused by non-uniformity of surface or interfacial tension and can only arise in solutions in which solute molecules are subject to adsorption. It occurs when a fresh surface is created or an existing surface is enlarged, due to the dynamic lag in the adsorption process which supplies solute to the surface. As surface area is increased the surface tension value rises to that of the pure solvent, since the surface excess of solute is reduced. Conversely, if surface area is reduced, the surface tension is reduced below the equilibrium value, since time is required for solute to desorb from the surface and diffuse into the bulk solution. Such differences between static and dynamic surface or interfacial tension are termed the Marangoni effect.

The Gibbs' effect (Sherman, 1968) gives rise to a second contribution to surface elasticity in a liquid lamella (such as the thin film of liquid between two colliding droplets of another, immiscible, liquid). It arises due to the fact that a lamella of solution becomes depleted of solute as it thins down, causing interfacial tension to increase.

A thinning lamella of solution will tend to have uniform thickness due to the Marangoni and Gibbs effects. This is because interfacial tension is increased, at any point where the lamella is thinned down by external forces, which opposes the thining process. The gradient of interfacial tension causes not only the interfacial monolayer to be moved but also the underlying liquid, by viscous effects. Ewers and Sutherland (1952) termed this tendency to heal points of potential rupture, surface transport.

3.2 Some Simple Calculations on Emulsions

It is instructive to perform some simple calculations to determine the number of dispersed droplets and the interfacial area between the phases of an emulsion. This is, of course, dependent on the size distribution of the droplets and their total volume. For the sake of simplicity, assume the emulsion to be monodisperse and made from $1cm^3$ of water and $1cm^3$ of oil, contained in a vessel such that the interfacial area is $1cm^2$ prior to emulsification. Assume also

that the diameters of the droplets are 1μm and 5μm in two separate cases. The results are summarized in Table 3.1.

TABLE 3.1 Emulsion characteristics

Droplet Diameter (μm)	Droplet Volume (cm^3)	Number of Dispersed Droplets	Surface Area of Droplet (cm^3)	Total Interfacial Area of Phases (cm^2)
Prior to Emulsification	-	-	-	1
5	6.54×10^{-11}	1.53×10^{10}	7.85×10^{-7}	1.2×10^{4}
1	5.24×10^{-13}	1.91×10^{12}	3.14×10^{-8}	6.0×10^{4}

It can be seen that a vast number of droplets is produced and that the interfacial area between the two phases becomes extremely large in relation to its original value. Any phenomenon which depends on interfacial area, such as interfacial tension or adsorption, will vary proportionately. Interfacial phenomena are crucial to the study of emulsions since interfacial area is large in comparison with volume.

Though a 1μm diameter droplet may seem very small, it is enormous with regard to molecular dimensions. For comparison purposes, a 1μm diameter droplet has a volume of $5.24 \times 10^{-13} cm^3$ whereas a water molecule has a volume of about $3 \times 10^{-23} cm^3$ and a typical oil molecule has a volume of about $1.6 \times 10^{-21} cm^3$ (Sutheim, 1946). Thus a 1μm diameter droplet of water contains about 1.75×10^{10} water molecules and a 1μm diameter droplet of oil contains about 3.28×10^{8} oil molecules.

Consider, now, the adsorption of emulsifying agent at the interface of a 1μm diameter droplet, and the number of surface-active molecules involved. Suppose the emulsifying agent is sodium palmitate (see Section 3.1.4), a molecule of which has a cross-sectional area of $2.05 \times 10^{-15} cm^2$, length of $2.4 \times 10^{-7} cm$ (~ 1/417th droplet diameter) and volume of $4.92 \times 10^{-22} cm^3$. For simplicity, assume the emulsifying agent molecules form a close-packed monolayer orientated with their tails normal to the local droplet surface. Since a 1μm diameter droplet

has a surface area of $3.14 \times 10^{-8}cm^2$ it follows that about 1.53×10^7 soap molecules are required. This corresponds to a total volume of $7.54 \times 10^{-15}cm^3$ of emulsifying agent per $1\mu m$ diameter dispersed phase droplet, that is 1/70th its volume. This explains how a small quantity of emulsifying agent can have such a profound effect.

3.3 Factors Affecting Emulsion Type

If an emulsifying agent is involved in the preparation of an emulsion, it is probably the most important condition relating to the type of emulsion produced (Sutheim, 1946). Hydrophilic agents are known to promote the formation of O/W emulsions whereas hydrophobic agents promote the formation of W/O emulsions (Sutheim, 1946). This is equivalent to Bancroft's rule, of considerable general validity, which states that: the phase in which the emulsifying agent is more soluble will be the continous one (Bancroft, 1926).

A semi-empirical procedure, developed by Griffin (1949), is reminiscent of Bancroft's rule. It is called the HLB method, the initials standing for hydrophile-lipophile balance. Any surface-active agent possesses hydrophilic and hydrophobic groups and can be assigned an HLB number. Agents with HLB numbers in the range 4-6 promote W/O emulsions whereas those in the range 8-18 promote O/W emulsions. The HLB number can be determined by an experimental procedure and even by mathematical formula in the case of some surface-active agents.

Also of importance, with regard to the type of emulsion produced, is the phase-volume ratio (volume fraction). This is defined as the volume of one phase divided by the total emulsion volume. The ambiguity involved with this definition is removed by specifying which of the two phases involved is referred to in the definition of the phase-volume ratio (usually the dispersed phase).

If the phase-volume ratio is close to 50%, there is no *prima facie* reason why a W/O rather than an O/W emulsion should result (Sutheim, 1946). The actual type formed will depend on the other determining factors. However, if one phase is considerably in excess of the other, it is likely to form the continuous phase. This is because such a system is inherently more stable and involves less work of emulsification.

There are exceptions to this rule. For example, Becher (1977) was able to produce an O/W emulsion containing only 4% water, using non-ionic

surface-active agent.

The method of emulsification is also important in relation to the type of emulsion produced. For example, the phase intended to become the dispersed phase should be added gradually to the continuous phase (Sutheim, 1946). By using this technique, the continuous phase is always in excess of the added, dispersed phase and the conditions for stability are favourable.

Other factors, such as viscosity and density of the phases are likely to have some effect in determining emulsion type. For example, heavy-bodied oils are known to form W/O emulsions preferentially (Sutheim, 1946).

The presence of solid material can influence the emulsion type. Finely dispersed solids, such as carbon black and colloidal clay, can behave like emulsifying agents at interfaces (Sutheim, 1946). This relates to the ability of the two phases to wet the particles, carbon black being hydrophobic and colloidal clay hydrophilic.

Finally, the materials involved in emulsification equipment are also known to have an effect on emulsion type. For example, Dvoretskaya (1949) obtained an O/W emulsion by bubbling air through equal volumes of water and oil, contained in a glass vessel which was well wetted with the water. However, a W/O emulsion resulted when a plastic vessel, not wetted by the water, was used.

3.3.1 Determination of Emulsion Type

Various methods exist for determining emulsion type (W/O or O/W) but, since they are not always reliable, it is advisable to use more than one technique before making any deduction.

Probably the simplest test is called the phase dilution method, devised by Briggs (1914). A drop of emulsion is introduced to one of the phases in bulk. If the droplet spreads and disperses, with gentle shaking, the continuous phase of the emulsion can be identified as the bulk liquid. However, if the emulsion drop retains its separate identity the converse is true. The test works best for dilute emulsions.

Another method, attributable independently to Robertson (1910) and Newmann (1914), relies on dyes which are soluble in one of the emulsion phases but not the other. If the colour of a dye spreads throughout the entire emulsion,

when the dye is stirred into it then the phase in which the dye is soluble can be identified as the continuous one. Alternatively, if tiny spots of colour appear, the converse is true.

Should the continuous phase not stain, it is good practice to repeat the test using a dye soluble in the other phase. Water soluble dyes, suitable for use are "Brilliant Blue FCF" and "Methylene Orange", whereas oil soluble dyes include "Oil Red OX", "Red Sudan III" and "Fuchsin". This test is not recommended for concentrated emulsions.

An emulsion can be classified according to its conductivity, a method originally proposed by Bhatnagar (1920). This technique relies on the aqueous phase being a good conductor and the oil phase being a poor conductor, which is usually a reasonable assumption. The continuous phase provides the main path for the electrical current and so, if it is aqueous in nature, its conductivity will be high and vice versa. In some situations the test is unreliable. For example, O/W emulsions stabilised by non-ionic emulsifying agent may have unusually low conductivity. Conversely, W/O emulsions, containing a large amount of aqueous droplets, can exhibit relatively high conductivities; this is because the droplets tend to travel to and fro between the electrodes exchanging charge (see Section 3.6.3).

Since most oils fluoresce when exposed to ultraviolet radiation, this can be used as a test for emulsion type (Becher, 1977). If the entire emulsion field fluoresces the continuous phase is oil whereas if there are only fluorescent spots the continuous phase is aqueous.

An emulsion can also be classified according to its creaming behaviour. If the dispersed phase droplets cream upwards the continuous phase must be aqueous, and if they cream downwards it must be oil (Becher, 1977). The technique is unreliable if the emulsions are complex in nature or highly viscous liquids are involved.

3.4 Stability and Instability of Emulsions

It is difficult to define the stability of an emulsion precisely since it is an inherently subjective concept. However, an emulsion which undergoes little change, in the course of a relatively long period of time, can be considered stable. No emulsion can be completely stable because surface free energy is stored at the interface between its phases; changes in the system act to reduce this energy. Coalescence of dispersed phase droplets, therefore, is a thermodynamically

favourable process whereas the reverse, droplet disruption, (which requires the expenditure of energy) is not.

The instability of an emulsion is manifest in terms of creaming, sedimentation, floculation, coalescence and inversion.

Creaming occurs as a consequence of the two emulsion phases having different densities. If the dispersed phase is of greater density than the continuous phase, sedimentation of the dispersed droplets results. Otherwise, the dispersed phase droplets rise towards the free surface. Should the droplets not coalesce, when they reach close proximity at the top or bottom of the emulsion, creaming results. Stratified layers of dispersed phase droplets are produced during creaming. The process is reversible, unlike coalescence, since the emulsion can be restored by gentle stirring or shaking.

The speed of sedimentation can be used to gauge emulsion stability. According to Stokes' law (Stokes, 1851) the rate of sedimentation of a spherical particle is given by:

$$u = \frac{d^2 g}{18\eta_c} (\rho_d - \rho_c) \qquad (3.7)$$

u = sedimentation rate
d = particle diameter
g = acceleration due to gravity
η_c = continuous phase viscosity
ρ_d, ρ_c = dispersed and continuous phase densities

This is applicable to particles of diameter greater than about 3μm (for which Brownian motion is negligible) (Exner, 1900). Stokes' equation invokes a non-slip boundary condition, applicable to solid particles for example. In the case of emulsions, the particles are liquid droplets, amenable to internal circulation. The Rybczynski (1911) - Hadamard (1911) equation, shown below, should be applicable in this situation.

$$u = \frac{d^2 g}{6\eta_c} \left[\rho_d - \rho_c\right] \frac{(\eta_d + \eta_c)}{(3\eta_d + 2\eta_c)} \qquad (3.8)$$

η_d = dispersed phase viscosity.

It predicts faster sedimentation speeds than eqn. (3.7) (up to 50% faster when $\eta_c >> \eta_d$) and reduces to Stokes' equation (3.7) when $\eta_c << \eta_d$. However, this relation does not appear to accord with experimental findings (Sherman, 1968, Becher, 1977). Even droplets as large as 1mm diameter have been observed to possess non-circulating surfaces in the presence of emulsifying agent. The adsorbed interfacial film acts to immobilize the surface of the droplet. This may be due to the development of interfacial tension gradients (Marangoni effect) or the creation of surface viscosity, as considered by Frumpkin and Levich (1947). In consequence, it is reasonable to use Stokes' equation (3.7) to determine sedimentation speed.

It can be seen from eqn. 3.7 that sedimentation speed is proportional to droplet diameter squared, acceleration due to gravity and density difference of the phases, and is inversely proportional to the continuous phase viscosity. The emulsion can therefore be destabilised by: decreasing the continuous phase viscosity (by increasing temperature for example); increasing the density difference (which can sometimes be achieved by increasing temperature); increasing acceleration by appealing to centrifugal effects (centrifuges and cyclones); inducing droplet coalescence, which is of most importance since a squared term is involved.

Flocculation is the process by which dispersed phase droplets form three-dimensional clusters, without coalescence, in the bulk continuous phase. It is similar to the creaming process in that the droplets do not coalesce. Flocculation can result from the oriented adsorption of emulsifying agent at the interface; the interfacial film formed prevents coalescence and tends to be self mending when ruptured (Sutheim, 1946).

Coalescence is the flowing together of the liquid contained in two dispersed phase droplets, which touch one another, so forming a single, larger droplet. It can arise naturally when droplets are brought together by Brownian motion or differential sedimentation. Coalescence can also be induced by instituting appropriate mechanical or electrical forces within an emulsion (see Chapter 9). Dispersed phase droplet coalescence is a thermodynamically favourable process which ultimately leads to the separation of an emulsion into its constituent bulk phases.

The final manifestation of emulsion instability to be considered is phase inversion. This results when the continuous and dispersed phases reverse their rôles, and must be regarded as a major instability. The inverted emulsion is likely

to have characteristics very much different from the original emulsion, especially with regard to bulk properties such as viscosity and conductivity (e.g. see Section 3.5).

The mechanism of phase inversion, in its initial stages, is quite similar to the coalescence process which leads to emulsion resolution (Sutheim, 1946). The dispersed phase droplets contact one another and flow together but, instead of forming larger droplets, the liquid occludes regions of the formerly continuous phase. Under the action of interfacial tension, the occluded regions assume spherical form and so create the new dispersed phase. The new continuous phase is, of course, formed by coalescence of the original dispersed phase droplets.

Phase inversion can be understood in terms of the delicate state of equilibrium existing at the interface, especially in relation to adsorbed emulsifying agent. This equilibrium can be disturbed by mechanical means, temperature change and chemical action (Sutheim, 1946, Wellman and Tartar, 1930).

Phase inversion can also be achieved by the addition of more liquid from which the dispersed phase is formed. The probability of phase inversion increases as more dispersed phase liquid is added. Ostwald (1910) proposed a phase volume theory based on stereometric considerations. He considered a monodisperse emulsion in which the spheres of dispersed phase liquid were most densely packed. In solid geometry there are two ways of doing this, the methods being described as (i) hexagonal close packing, and (ii) face – centred cubic. In both cases the spheres occupy 74.05% of the available space. Ostwald's conclusion was that when the dispersed phase occupied more than about 74% of the emulsion volume, phase inversion would occur. There is a reasonable amount of justification for this (Becher, 1977). However, the amount of dispersed phase liquid required for inversion depends on the concentration of emulsifying agent present. Similarly, if the emulsion is polydisperse, a greater amount of dispersed phase liquid can be accommodated, since the smaller droplets are able to fit into the interstices between the larger ones. Consequently, an emulsion will not necessarily invert when its dispersed phase volume reaches 74% of the emulsion volume.

Surface–active agents are known to stabilise emulsions by reducing interfacial tension and hence surface free energy. Interfacial tension is lowered by the positive adsorption of molecules of emulsifying agent at the interface. Large reductions in interfacial tension result should the surface–active agents be of the polar–non–polar type since oriented adsorption occurs. Fine solids, such as carbon black and colloidal clay, can act as emulsifying agents to stabilise emulsions. The

process is related to the surface wetting properties of the particles. Electrolytes, in low concentrations are able to stabilise W/O emulsions (Cheesman and King, 1940). Emulsions can also be stabilised by electrical effects, brought about by the repulsion of dispersed phase droplets carrying charges of the same polarity. Alexander and Johnson (1949) postulated that particles in colloidal systems acquire charge by ionisation, adsorption or frictional contact. The difference between the first two mechanisms is unclear in the case of emulsions. The polarity and magnitude of droplet charge is likely to depend on the type of emulsifying agent present. With regard to frictional charging, an empirical rule due to Coehn (1898) states that: a substance having a high dielectric constant acquires positive charge when contacting a substance of lower dielectric constant. The oil droplets in an O/W emulsion, therefore, should be negatively charged whereas water droplets in a W/O emulsion should be positively charged.

According to Gouy (1910) - Chapman (1913) theory, the preferential adsorption of potential-determining ions, at the surface of a droplet, gives rise to an electric double layer. The inner layer comprises the preferentially-adsorbed ions whereas the diffuse outer layer consists of counter ions, which are prevented from neutralising the droplet by random thermal motion. The double layer is characterised by the Debye parameter K and defined below (see Chapter 4).

$$K = \left[\frac{2ne^2\nu^2}{\epsilon kT}\right]^{\frac{1}{2}} \qquad (3.9)$$

n = number density of counter ions in bulk solution
e = electronic charge level
ν = valency of counter ions
ϵ = permittivity of solution
k = Boltzmann's constant
T = absolute temperature

The inverse K^{-1} of the parameter K is called the double layer "thickness" and is inversely proportional to the square root of the number density of counter ions in bulk solution. In water-continuous emulsions, where n is large, the double layer thickness is small, typically 10^{-3} - $10^{-2}\mu$m (Becher, 1977). Consequently, a flocculating water droplet has to overcome substantially the entire potential barrier in order to coalesce. Therefore, preferentially adsorbed charge, on dispersed phase droplets, provides a strong stabilising influence in O/W emulsions. In oil-continuous emulsions, however, n is relatively small and so the double layer thickness is significantly larger, being several microns typically (Becher, 1977).

This is equivalent to the droplet separation in a moderately concentrated emulsion. In consequence, the potential barrier is much reduced and the stabilising influence of the adsorbed charge is much less in W/O emulsions.

3.5 Emulsion Rheology

In a Newtonian liquid the shearing stress is proportional to the rate of shear and so its viscosity is constant. For most emulsions, however, viscosity is dependent on the rate of shear. Emulsions exhibit four basic types of flow behaviour: Newtonian, plastic, pseudoplastic and dilatant, as shown in Figure 3.3 (Sherman 1968, Becher, 1977).

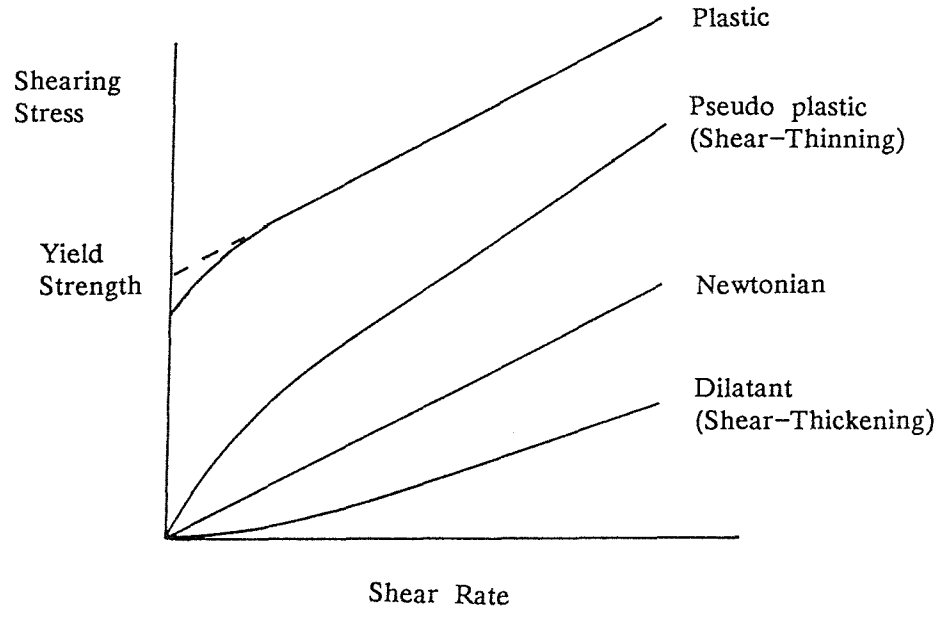

FIGURE 3.3 **Shearing stress as a function of shear rate for various types of flow in emulsions.**

Plastic emulsions have an inherent structure which resists shearing forces completely until the yield strength has been reached. Subsequently, the structure breaks down, giving rise to a linear relationship between shearing stress and rate of shear. Pseudoplastic emulsions behave in a similar way except that they flow as soon as stress is applied and require no initial yield strength to be reached. Dilatant flow is the converse of pseudoplastic flow and is rarely seen in emulsions (Becher, 1977).

In some cases, the flow of an emulsion is dependent on the time of application of the shearing forces as well as the rate of shear. Emulsions exhibiting this type of behaviour are called thixotropic or rheopectic depending, respectively, on whether the viscosity decreases or increases with time. Rheopectic flow is rarely exhibited by emulsions (Becher, 1977).

Sherman (1955) listed the factors which affect emulsion rheology and these are as follows:

(i) Viscosity of the continuous phase (η_c)
(ii) Volume fraction of the dispersed phase (φ)
(iii) Viscosity of the dispersed phase (η_d)
(iv) Type of emulsifying agent and presence of interfacial film
(v) Dispersed phase size distribution
(vi) Electroviscosity.

The viscosity of an emulsion can be seen to be a complicated notion though, in the case of dilute emulsions, Newtonian flow is exhibited (Sherman, 1968). Primarily, however, emulsion viscosity is related to the continuous phase viscosity. If emulsifying agent is dissolved in the continuous phase, it is the viscosity of the solution which is important rather than that of the pure solvent (colloidal agents can have a marked effect on solution viscosity) (Becher, 1977).

The presence of dispersed phase droplets is also of great importance and is usually gauged in terms of the volume fraction φ of the dispersed phase. Einstein's classical expression relating viscosity η to volume fraction φ is (Einstein, 1906):

$$\eta = \eta_c (1 + 2.5\varphi) \qquad (3.10)$$

This equation was derived on hydrodynamic grounds and applies to dilute emulsions ($\varphi < 0.02$) containing non-deformable droplets, between which there are no interactions, and separated by distances greatly in excess of droplet size. Further, it assumes a non-slip condition at the boundary of each dispersed phase droplet.

Various workers have extended eqn. (3.10), using power series in φ, to allow droplet interaction to be accounted for, which arises at higher values of volume fraction φ.

Oliver and Ward (1953) developed the following expression for the viscosity of model emulsions, containing polydisperse rigid spheres, which is valid for values of φ up to about 0.2.

$$\eta = \eta_c/(1 - k\varphi) = \eta_c(1 + k\varphi + k^2\varphi^2 + \ldots) \qquad (3.11)$$

The values of the constant k in eqn. (3.11), calculated from the data of Oliver and Ward, and other workers, are scattered around Einstein's value of 2.5.

Emulsions of volume fraction φ greater than 0.5 generally exhibit non-Newtonian flow behaviour. Hatschek (1911) derived the following expression for such emulsions, which is valid for the linear portion of the shearing stress versus rate of shear curve.

$$\eta = \eta_c/(1 - \varphi^{1/3}) \qquad (3.12)$$

Taylor modified Einstein's relation (3.10) to account for the viscosity of the dispersed phase. The interfacial film is assumed to transmit tangential stress from one phase to the other, leading to circulation of the dispersed phase liquid. Taylor's expression may be written as follows (Taylor, 1932):

$$\eta = \eta_c\left\{1 + 2.5\varphi\left[\frac{\eta_d + 0.4\eta_c}{\eta_d + \eta_c}\right]\right\} \qquad (3.13)$$

Nawab and Mason (1958b) showed that Taylor's expression applied exactly in certain emulsions where circulation of the dispersed phase liquid existed. However, in other emulsions, the presence of emulsifying agent rendered the interfacial film more-or-less rigid. In this case there was no circulation of the dispersed phase liquid and eqn. (3.13) degenerated to eqn. (3.10). Taylor's expression is valid for low values of volume fraction and requires that the dispersed phase droplets remain spherical under shear.

Eqns. (3.10) to (3.13) relate emulsion viscosity η to the volume fraction of the dispersed phase φ but no mention is made of the state of dispersion. However, it is known that homogenization of a coarse emulsion leads to an increase in its viscosity. Sherman (1955) attributes this to an increased interaction between the dispersed phase droplets due to their increase in number and reduction in size. Few expressions for emulsion viscosity incorporate a term for droplet size,

however, the one shown below (due to Raja Gopal, 1960) contains r_m the mean droplet radius (as well as S_c the coefficient of slippage between the droplets and the continuous phase).

$$\eta = \eta_c \left\{ 1 + \frac{2.5\varphi}{(\eta_d+\eta_c)} \left[\eta_d + \frac{2}{5}\eta_c + \frac{2\eta_c\eta_d}{S_c} \left[\frac{1}{r_m}\right] \right] \right\} \qquad (3.14)$$

When dilute emulsions containing charged droplets are sheared, additional energy is dissipated in overcoming the interaction between adsorbed charge on each droplet's surface and ions in its distorted double layer (Conway and Dobry-Duclaux, 1960). Einstein's eqn. (3.10) was modified by von Smoluchowski (1916) to account for this first electroviscous effect to give the following expression (which is presented in SI units).

$$\eta = \eta_c \left\{ 1 + 2.5\varphi \left[1 + \frac{1}{\eta_c\sigma} \left[\frac{2\epsilon_c\zeta}{r} \right]^2 \right] \right\} \qquad (3.15)$$

σ = electrical conductivity of emulsion

ϵ_c = permittivity of continuous phase (= $\epsilon_o K_c$)

ζ = electrokinetic (or zeta) potential of dispersed droplets

Many expressions have been proposed for the viscosity of an emulsion of which eqns. (3.10) to (3.15) are but a sample. Before leaving the topic, it is of interest to consider the effect of inversion on emulsion viscosity. As the volume fraction of dispersed phase increases so does the viscosity of the emulsion (see Figure 3.4). Eventually the emulsion inverts, and when this happens there is generally a sharp drop in viscosity. According to Ostwald's phase-volume theory (Ostwald, 1910), this should occur when the dispersed phase volume fraction reaches about 0.74. However, factors such as the presence of emulsifying agent can change the value drastically, as mentioned previously. The reduction in viscosity is due mainly to the lowering of the dispersed phase volume fraction. There is also an effect due to the change in viscosity of the continuous phase. The section of the curve to the right of the inversion position is merely a reflection of the low-concentration portion of the inverted emulsion.

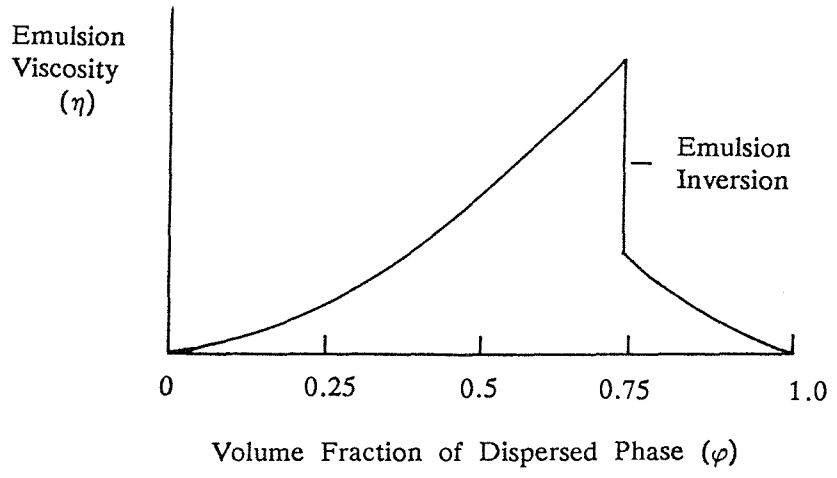

FIGURE 3.4 Emulsion viscosity as a function of volume fraction, showing the effect of inversion.

3.6 Electrical Properties of Dispersions

The early electrical theories of heterogeneous mixtures were based on the assumption that the effective dielectric constant (or conductivity) is a linear function of the dielectric constant (or conductivity) of the bulk phases and their volume fractions (see eqn. (3.16)). Fricke and Curtis (1937) indicated that this was an over-simplification; they argued that some part of the current passes through the interfaces which accumulate charge due to the different electrical properties of the two phases. This phenomenon is called interfacial (Maxwell-Wagner) polarization (see Section 3.6.4) and relies on the two phases having different relaxation times (i.e. $\epsilon_0 K_1/\sigma_1 \neq \epsilon_0 K_2/\sigma_2$). For this reason, the early semi-empirical formulae did not always adequately represent the dielectric contstant or conductivity of the mixture.

A related phenomenon, termed dielectric dispersion, arises when a sinusoidal excitation is used and this is caused by interfacial polarization. Thus, the dielectric constant and conductivity, determined at low frequency, differ from the high frequency limits. [This should not be confused with orientational or dipolar polarization in which, for example, water at 20°C has a dielectric constant of about 80 at frequencies below about 19GHz, which reduces to 1.8 at optical frequencies (Pohl, 1978).]

The state of agglomeration, orientation and deformation (in the case of emulsions) of the suspended phase can be of importance and these matters are discussed more fully below.

3.6.1 Dielectric Constant of a Dispersion of Spherical Particles

Various expressions have been proposed for the dielectric constant in terms of the linear functional relationship, mentioned above, and shown in eqn. (3.16).

$$f(K) = (1 - \varphi)f(K_c) + \varphi f(K_d) \qquad (3.16)$$

K = effective dielectric constant of dispersion
K_c = dielectric constant of suspending medium
K_d = dielectric constant of particulate material
φ = volume fraction of particulate component

Some of the functional forms are:

$$f(K) = K \text{ Wiener (1912) parallel limit} \qquad (3.17)$$
$$= K^{-1} \text{ Wiener (1912) series limit} \qquad (3.18)$$
$$= \log K \text{ Lichtenecker (1926)} \qquad (3.19)$$
$$= K^{\frac{1}{2}} \text{ Beer (Lichtenecker, 1926)} \qquad (3.20)$$
$$= K^{1/3} \text{ Landau and Lifshitz (1960)} \qquad (3.21)$$

Wiener's parallel and series expressions represent the upper and lower limits respectively of K.

It is also possible to develop expressions for the effective dielectric constant of a dispersion by considering a mathematical analysis of the electric fields involved. One of the earliest attempts to do this was made by Rayleigh (1892) who considered a monodisperse, rectangular array of spherical particles; field interactions between a particle and its 128–nearest neighbours were accounted for. Rayleigh's expression was corrected by Runge (1925) and now has the following form (Jones, 1979):

$$K = K_c\left[1 + \frac{3\varphi}{\left[K_d+2K_c\right]/\left[K_d-K_c\right] - \varphi - (\pi/6)\left[K_d-K_c\right]/\left[K_d+4K_c/3\right]\varphi^{10/3}}\right] \qquad (3.22)$$

This expression is intended to be valid for values of the volume fraction φ up to $\pi/6$, the rectangular packed bed limit.

Wiener (1912), assuming dilute dispersions, ignored the $\varphi^{10/3}$ term in eqn. (3.22) to obtain:

$$\left[\frac{K - K_c}{K + 2K_c}\right] = \left[\frac{K_d - K_c}{K_d + 2K_c}\right] \varphi \qquad (3.23)$$

Wagner (1914), derived the same expression for a dilute dispersion containing spherical particles of random distribution.

Considering a process, based on continually increasing the concentration of the dispersed phase by an infinitesimal amount, Bruggeman (1935) was able to modify eqn. (3.23), enabling concentrated dispersions to be considered. The limiting conditions assumed are: $K_c \rightarrow K$, $K \rightarrow K + dK$ and $\varphi \rightarrow (1 - \varphi)^{-1}d\varphi$ which lead to the following differential equation:

$$\frac{\left[2K + K_d\right]}{3K\left[K - K_d\right]}\, dK = \frac{-dK}{3K} + \frac{dK}{K-K_d} = \frac{-d\varphi}{1-\varphi}$$

This equation can be integrated for K in the range K_c to K and φ in the range 0 to φ yielding:

$$\left[\frac{K - K_d}{K_c - K_d}\right]\left[\frac{K_c}{K}\right]^{1/3} = 1 - \varphi \qquad (3.24)$$

Böttcher (1952) modelled the dispersion as a polydisperse random distribution of spheres of both constituents in a ficticious suspending medium of dielectric constant K. The electric field inside an isolated sphere, of dielectric constant K_d, subjected to a uniform background electric field E, is $E_d = 3KE/(2K + K_d)$, and similarly for spheres of the other material. Böttcher substituted the expressions for E_d and E_c into a polarization equation equivalent to eqn. (3.16) with f(K) replaced by $\epsilon_o(K-1)E$:

$$\epsilon_o(K-1)E = (1-\varphi)\epsilon_o(K_c-1)E_c + \varphi\epsilon_o(K_d-1)E_d$$

where $\epsilon_o = 8.854 \times 10^{-12}Fm^{-1}$ (permittivity of free space).

This leads to the following expression for the dielectric constant of the dispersion.

$$\frac{[K - K_c]}{3K} = \left[\frac{K_d - K_c}{K_d + 2K}\right] \varphi \qquad (3.25)$$

Since no distinction is made between which is the dispersed phase and which the continuous phase, Böttcher's eqn. is independent of inversion effects. It is like Wiener's and Wagner's expression [eqn. (3.23)] with K_c replaced by K in the denominator terms.

Kubo and Nakamura (1953) developed a theory based on the increase in polarization of the dispersion brought about by increasing the volume fraction of the dispersed phase. They considered the process of continually adding infinitesimal amounts of the dispersed phase used by Bruggeman in developing eqn. (3.24). Kubo and Nakamura's equation, shown below, is rather complicated and involves the constant $c = 1 - 4\pi/9\sqrt{3} = 0.19387$.

$$\frac{3K_d}{(2+c)K_d+(1-c)} \log\left[\frac{K_d-K}{K_d-K_c}\right] - \frac{[(2+c)K_d-2(1-c)]}{(2+c)[(2+c)K_d+(1-c)]}$$

$$\log\left[\frac{(2+c)K+(1-c)}{(2+c)K_c+(1-c)}\right] = \log(1-\varphi) \qquad (3.26)$$

If c is taken as 1 rather than its proper value of 0.19387, eqn. (3.26) degenerates to Bruggenman's eqn. (3.24).

Frenkel (1948) suggested that the dielectric constant of a dispersion should be dependent on electric double layer effects. Based on this assumption, Fradkina (1950) advanced the following expression for the dielectric constant:

$$K = K_c[1 + 3\varphi(1 - \alpha)/(1 + 2\alpha)] \qquad (3.27)$$

The function α, in eqn. (3.27), depends on the electric double layer surrounding the droplets. For a not-too-dilute aqueous solution of electrolytes dispersed in petroleum, Fradkina has demonstrated that $\alpha \simeq 0$. If the dispersed phase droplets have a dielectric constant K_d, Fradkina has advanced the following expression (Fradkina, 1950):

$$K = K_c[1 + 3\varphi(K_d - K_c)/(K_d + 2K_c)] \qquad (3.28)$$

This is similar in form to Wiener's and Wagner's eqn. (3.23) and Böttcher's eqn. (3.25).

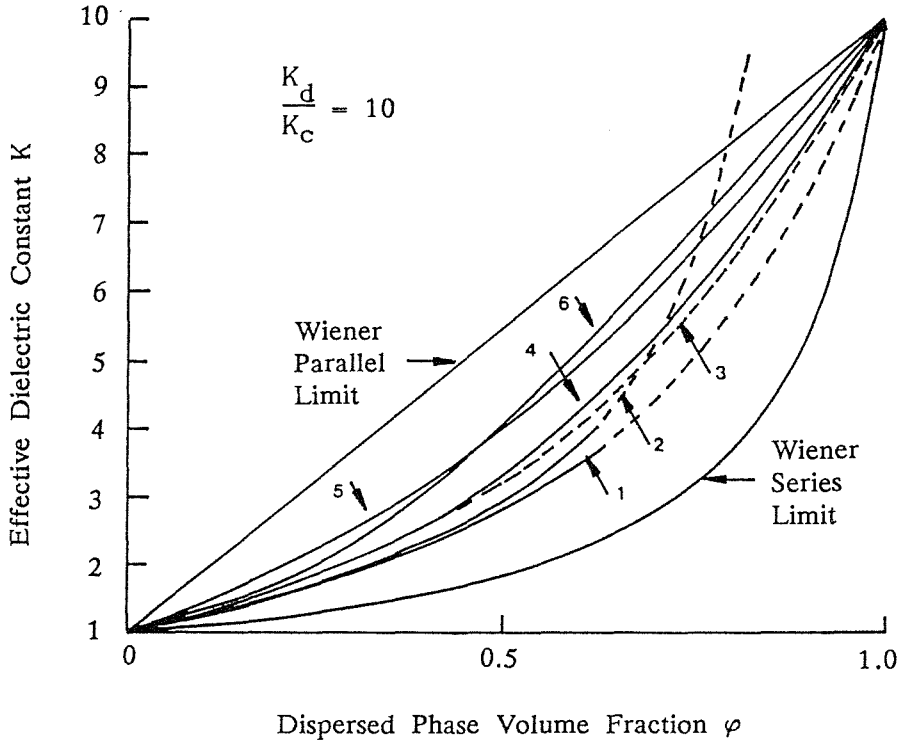

FIGURE 3.5 Comparison of various expressions for the effective dielectric constant K as a function of volume fraction φ: 1 Wiener/Wagner eqn. (3.23); 2 Rayleigh eqn. (3.22); 3 Lichtenecker eqn. (3.16)/(3.19); 4 Bruggeman eqn. (3.24); 5 Landau and Lifshitz eqn. (3.16)/(3.21); 6 Böttcher eqn. (3.25).

3.6.2 Conductivity of a Dispersion of Spherical Particles

The electrical conductivity and dielectric constant play analogous rôles in the theory of electrostatic fields. In consequence, the expressions for conductivity σ are similar, if not identical, to the equivalent expressions for dielectric constant K.

Runge (1925) and Meredith and Tobias (1960a) developed expressions identical to eqn. (3.22) with dielectric constants replaced by conductivities:

$$\sigma = \sigma_c\left[1 + \frac{3\varphi}{(\sigma_d+2\sigma_c)/(\sigma_d-\sigma_c) - \varphi - (\pi/6)(\sigma_d-\sigma_c)(\sigma_d+4\sigma_c/3)\varphi^{10/3}}\right] \qquad (3.29)$$

Similarly, Wagner (1914), Lorentz (1880), Lorenz (1880) and Maxwell (1881) derived expressions equivalent to eqn. (3.23):

$$\left[\frac{\sigma - \sigma_c}{\sigma + 2\sigma_c}\right] = \left[\frac{\sigma_d - \sigma_c}{\sigma_d + 2\sigma_c}\right] \varphi \qquad (3.30)$$

According to de la Rue and Tobias (1959), eqn. (3.24) is also applicable to conductivity:

$$\left[\frac{\sigma - \sigma_d}{\sigma_c - \sigma_d}\right]\left[\frac{\sigma_c}{\sigma}\right]^{1/3} = 1 - \varphi \qquad (3.31)$$

Meredith and Tobias (1960a) found that Rayleigh's eqn. (3.22) was inaccurate near the rectangular packed bed limit ($\varphi = \pi/6$) and attributed this to the omission of higher order terms. When these terms are accounted for, an improved expression is obtained as shown below:

$$\sigma = \sigma_c \left[1 + \frac{3\varphi - 1.227\left[\frac{\sigma_d-\sigma_c}{\sigma_d+4\sigma_c/3}\right]\varphi^{10/3}}{\left[\frac{\sigma_d+2\sigma_c}{\sigma_d-\sigma_c}\right]-\varphi-0.409\left[\frac{\sigma_d+2\sigma_c}{\sigma_d+4\sigma_c/3}\right]\varphi^{7/3} - 0.906\left[\frac{\sigma_d-\sigma_c}{\sigma_d+4\sigma_c/3}\right]\varphi^{10/3}}\right] \qquad (3.32)$$

Meredith and Tobias (1960b) also proposed the following expression for the conductivity of O/W and W/O emulsions of volume fraction $\varphi > 0.2$.

$$\frac{\sigma}{\sigma_c} = \left[\frac{2(1 + Z\varphi)}{2 - Z\varphi}\right]\left[\frac{2 + (2Z - 1)\varphi}{2 - (Z + 1)\varphi}\right] \qquad (3.33)$$

where:

$Z = (\sigma_d - \sigma_c)/(\sigma + 2\sigma_c)$

3.6.3 The Effect of Charged Droplet Migration on Conductivity

It is interesting to note that the expressions for the conductivity of emulsions (in Section 3.6.2) do not account for the effect of free charge carried by dispersed phase droplets migrating in the electric field. This could be an important effect in the case of W/O emulsions, subjected to strong electric fields, since the water droplets can acquire free charge by various means (see Chapter 9, Section 9.8). The effect can be estimated by considering a monodisperse W/O emulsion subjected to a uniform, dc applied electric field. Suppose the emulsion contains n droplets all of which carry the same charge q and travel at the same speed u. The current i flowing between the electrodes of a parallel plate capacitor of cross-sectional area A and plate separation d, containing the emulsion, due to charge transport by droplets is:

$$i = n \times q/(d/u) = nqu/d \qquad (3.34)$$

The charge acquired by a droplet of radius a contacting an electrode, in a uniform electric field E, is (Lebedev and Skal'skaya, 1962 and Cho, 1964):

$$q = \left[\frac{\pi^2}{6}\right] 4\pi a^2 \epsilon_o K_c E \qquad (3.35)$$

where K_c is the dielectric constant of the continuous phase and ϵ_o is the permittivity of free space. The time constant $\tau_c = \epsilon_o K_c/\sigma_c$ is assumed to be large in comparison with droplet transit time between the electrodes so that not much charge leaks away. If the Reynolds number is small Stokes' equation can be used to determine droplet speed by equating the viscous drag and the electrical force as follows, where η_c is the continuous phase viscosity.

$$6\pi\eta_c au = qE \qquad (3.36)$$

Let the conductivity due to the transport of charged particles by σ_t and the current density be J_t, then the following equations hold:

$$J_t = \sigma_t E = i/A \qquad (3.37)$$

By combining eqns. (3.34) to (3.37) the following expression for σ_t can be derived:

$$\sigma_t = \frac{2\pi^5 n a^3 \epsilon_o^2 K_c^2 E^2}{27 A d \eta_c} \qquad (3.38)$$

The volume fraction is given by:

$$\varphi = \frac{(4/3)\pi a^3 n}{Ad}$$

Hence the conductivity due to the migration of charged conducting droplets may be expressed as:

$$\sigma_t = \frac{(\pi^2 \epsilon_o K_c E)^2}{18 \eta_c} \varphi \qquad (3.39)$$

Apparently σ_t is independent of particle size but proportional to the square of the applied electric field. It should therefore be possible to distinguish this kind of conductivity from pure conductivity which is independent of the applied electric field, if Ohm's law holds.

As an example, consider a W/O emulsion of volume fraction $\varphi = 0.5$ where the water has a dielectric constant $K_d = 80$ and the oil has a dielectric constant $K_c = 2.3$, conductivity $\sigma_c = 10^{-11} Sm^{-1} << \sigma_d$ (conductivity of water), and viscosity $\eta_c = 3 \times 10^{-3} Pas$. Suppose also that the applied electric field strength is $E = 10^5 Vm^{-1}$. The expression due to de la Rue and Tobias, eqn. (3.31), gives $\sigma = 8 \times 10^{-11} Sm^{-1}$, whereas eqn. (3.39) gives $\sigma_t = 7.5 \times 10^{-9} Sm^{-1}$ which is two orders of magnitude greater. At low electric field strength, $E = 100 Vm^{-1}$ say, eqn. (3.39) gives $\sigma_t = 7.5 \times 10^{-15} Sm^{-1}$ which is four orders of magnitude smaller than σ. The electric field strength can be seen to be a critical factor therefore.

It should be borne in mind that various assumptions have been made in deriving eqn. (3.39) which must be regarded as an approximation. Eqn. (3.35), for example, assumes that there is only one sphere contacting the electrode and that the other electrode is far away. In fact an emulsion contains many droplets and the actual charge acquired may well be somewhat different.

3.6.4 Interfacial Polarization

The dielectric constants of dispersed systems were considered independently of each other in Sections (3.6.1) and (3.6.2). This approach can be valid if the

measurement frequency is at least an order of magnitude different from the natural frequency ω_o of the dispersion ($\omega_o = 1/\tau = \sigma/(\epsilon_o K)$). More precisely, dielectric constants measured at high frequency ($\omega >> \omega_o$) are independent of conductivity (see eqn. (3.66)) whereas conductivities measured at low frequency ($\omega << \omega_o$) are independent of dielectric constant (see eqn. (3.64)). Similarly, the effects of interfacial polarization are small if the time constants of the two phases are approximately equal ($\epsilon_o K_1/\sigma_1 \simeq \epsilon_o K_2/\sigma_2$). It turns out, also, that dispersion effects, caused by interfacial polarization, are small for O/W emulsions (if the oil phase is non-polar). These results can be obtained by analysing the interfacial polarization phenomenon mathematically.

Interfacial or Maxwell (1892) - Wagner (1914) polarization is characterised by the accumulation of charge at the interface between two dielectric materials having different electrical properties. That is, the time constants of the two materials, which are determined by dielectric constant and conductivity, should not be identical.

The effects of interfacial polarization can be considered, most simply, in terms of two layers of different dielectric materials, situated between parallel plate electrodes (see Figure 3.6).

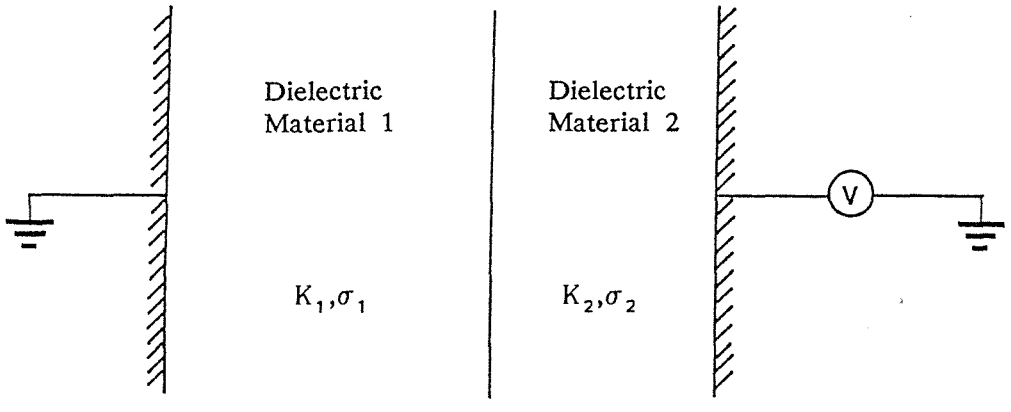

FIGURE 3.6 **Stratified model of binary heterogeneous system.**

This is equivalent to the following electrical circuit containing capacitances and conductances.

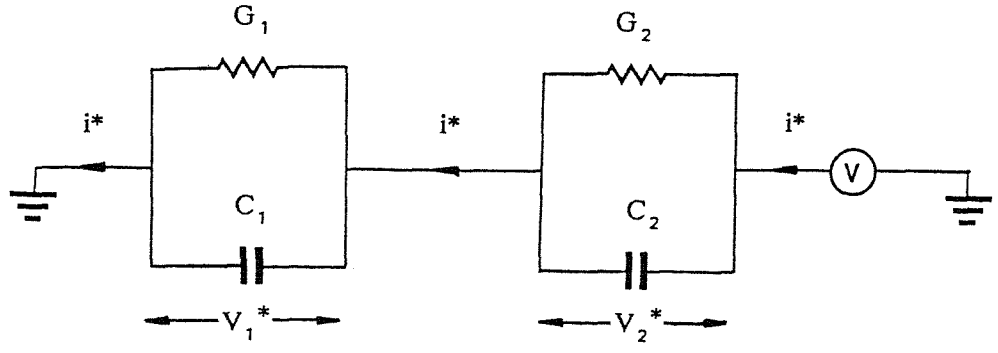

FIGURE 3.7 **Circuit equivalent to system in Figure 3.6.**

In the steady–state (i.e. when transients have decayed), the circuit is most easily analysed in terms of complex quantities (denoted by * superscript). The impedance of the circuits can be determined by considering the complex current i^*.

$$i^* = G_n V_n^* + C_n \frac{dV_n^*}{dt} \quad (n = 1,2) \qquad (3.40)$$

Now $V_n^* = V_n \exp[j(\omega t + \chi_n)]$ where V_n and χ_n are respectively the amplitude and phase of the complex potential V_n^* (n = 1,2), and ω is the angular frequency. Substituting into eqn. (3.40) then gives:

$$i^* = G_n V_n^* + j\omega C_n V_n^* \quad (n = 1,2) \qquad (3.41)$$

Which may be used to define G_n^*:

$$G_n^* = i^*/V_n^* = G_n + j\omega C_n \quad (n = 1,2) \qquad (3.42)$$

Eqn. (3.42) defines the complex conductance G_n^* from which the complex capacitance C_n^* is obtained by dividing by $j\omega$.

$$C_n^* = C_n - jG_n/\omega \quad (n = 1,2) \qquad (3.43)$$

The overall impedance of the circuit is obtained by combining the conductances or impedances as follows (since $V_1^* + V_2^* = V^* = i^*/G^*$):

$$\frac{1}{G^*} = \frac{1}{G_1^*} + \frac{1}{G_2^*} \;,\; \frac{1}{C^*} = \frac{1}{C_1^*} + \frac{1}{C_2^*} \qquad (3.44)$$

By substituting in eqn. (3.44) using eqn. (3.42) or eqn. (3.43), the following eqns. may be obtained (after considerable algebraic manipulation) (Sherman, 1968):

$$G^* = G_\ell + \frac{j\omega\tau (G_h - G_\ell)}{1 + j\omega\tau} + j\omega C_h \qquad (3.45)$$

$$C^* = C_h + \frac{C_\ell - C_h}{1 + j\omega\tau} + \frac{G_\ell}{j\omega} \qquad (3.46)$$

where

$$\lim_{\omega\to o} \mathrm{Re}(G^*) = G_\ell = \frac{G_1 G_2}{G_1 + G_2} \qquad (3.47)$$

$$\lim_{\omega\to \infty} \mathrm{Re}(G^*) = G_h = \frac{G_1 C_2^2 + G_2 C_1^2}{(C_1 + C_2)^2} \qquad (3.48)$$

$$\lim_{\omega\to o} \mathrm{Re}(C^*) = C_\ell = \frac{C_1 G_2^2 + C_2 G_1^2}{(G_1 + G_2)^2} \qquad (3.49)$$

$$\lim_{\omega\to \infty} \mathrm{Re}(C^*) = C_h = \frac{C_1 C_2}{C_1 + C_2} \qquad (3.50)$$

$$\tau = \frac{1}{\omega_o} = \frac{C_1 + C_2}{G_1 + G_2} = \frac{C_\ell - C_h}{G_h - G_\ell} \qquad (3.51)$$

$$G_h - G_\ell = \frac{(C_1 G_2 - C_2 G_1)^2}{(G_1 + G_2)(C_1 + C_2)^2} \qquad (3.52)$$

$$C_\ell - C_h = \frac{(C_1 G_2 - C_2 G_1)^2}{(C_1 + C_2)(G_1 + G_2)^2} \qquad (3.53)$$

The changes in effective conductance, $Re(G^*)$, and effective capacitance, $Re(C^*)$, are shown in Figure 3.8 which does not include the effect of electrode polarization (see Section 3.6.5).

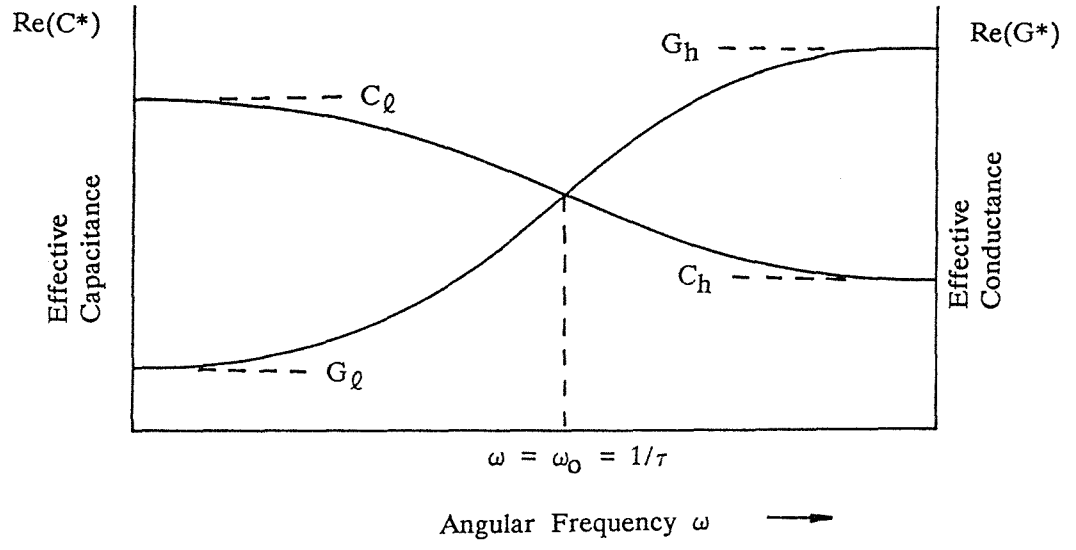

FIGURE 3.8 The effective conductance and capacitance of a dispersion as a function of angular frequency.

It can be seen that the effective capacitance and conductance of a dispersion, comprising two dielectric media, is characterised by a single time constant $\tau = 1/\omega_o$. Dielectric dispersion, as specified by $G_h - G_\ell$ and $C_\ell - C_h$, arises when the time constants of the two media are different (i.e. $C_1/G_1 \neq C_2/G_2$ or $\epsilon_o K_1/\sigma_1 \neq \epsilon_o K_2/\sigma_2$).

The complex plane plot of the dispersion system is shown in Figure 3.9.

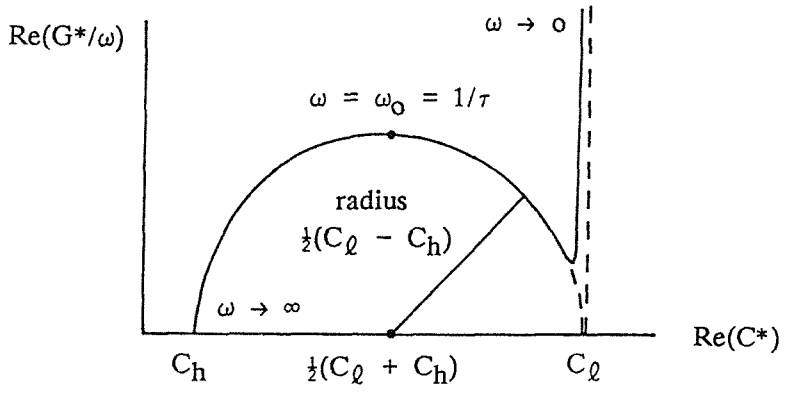

FIGURE 3.9 Complex plane plot showing semicircular-like behaviour of dielectric dispersion.

By specifying the volume fraction φ of the suspended phase, eqns. (3.47) to (3.53) can be re-written in terms of dielectric constant and conductivity using the transformations $G^* \rightarrow \sigma^*$, $C^* \rightarrow \epsilon_o K^*$, $G_1 \rightarrow \sigma_1/(1-\varphi)$, $G_2 \rightarrow \sigma_2/\varphi$, $C_1 \rightarrow \epsilon_o K_1/(1-\varphi)$ and $C_2 \rightarrow \epsilon_o K_2/\varphi$, as first performed by Maxwell (1892). This is not a particularly fruitful exercise, when considering emulsions, since they are not well represented by the binary stratified structure.

In order to represent emulsions in a better way, Wagner (1914) and Hanai (1960) extended eqns. (3.23) and (3.24) respectively to the complex plane by letting $K \rightarrow K^* = K - j\sigma/(\epsilon_o\omega)$ (Sherman, 1968). Hanai's theory is basically an extension of Wagner's theory which allows non-dilute emulsions to be considered (i.e. the volume fraction φ is not limited to being small). Consequently, Wagner's theory should be recoverable from Hanai's theory, by making approximations associated with φ being small. Hence it is only really necessary to consider Hanai's theory. Unfortunately, the frequency dependence in Hanai's theory is difficult to elucidate (as opposed to Wagner's theory which is relatively straightforward). However, the limiting conditions as $\omega \rightarrow 0$ and $\omega \rightarrow \infty$ are quite accessible.

Hanai's results can be obtained by letting $K \rightarrow K^*$, $K_c \rightarrow K_c^*$ and $K_d \rightarrow K_d^*$ in Bruggeman's eqn. (3.24), where the subscripts c and d refer to the continuous medium and dispersed medium respectively. It is convenient to represent $\sigma/(\epsilon_o\omega)$ in the equations by α so that $K^* = K - j\alpha$, etc. Eqn. (3.24) therefore becomes:

$$\frac{K^* - K_d^*}{K_c^* - K_d^*}\left[\frac{K_c^*}{K^*}\right]^{1/3} = 1 - \varphi \qquad (3.54)$$

Now:

$$K^*-K_d^* = [(K-K_d)^2 + (\alpha-\alpha_d)^2]^{\frac{1}{2}}\exp\left[-j\arctan\left[\frac{\alpha-\alpha_d}{K-K_d}\right]\right] \qquad (3.55)$$

$$K_c^*-K_d^* = [(K_c-K_d)^2 + (\alpha_c-\alpha_d)^2]^{\frac{1}{2}}\exp\left[-j\arctan\left[\frac{\alpha_c-\alpha_d}{K_c-K_d}\right]\right] \qquad (3.56)$$

$$K_c^* = (K_c^2+\alpha_c^2)^{\frac{1}{2}}\exp\left[-j\arctan\left[\alpha_c/K_c\right]\right] \qquad (3.57)$$

$$K^* = (K^2+\alpha^2)^{\frac{1}{2}}\exp\left[-j\arctan\left[\alpha/K\right]\right] \qquad (3.58)$$

By substituting eqns. (3.55) to (3.58) into eqn. (3.54), and considering the real and imaginary parts indpendently, it is possible to obtain the following expressions (Sherman, 1968):

$$\frac{\left[\left[K-K_d\right]^2+\left[\alpha-\alpha_d\right]^2\right]\left[K_c^2+\alpha_c^2\right]^{1/3}}{\left[\left[K_c-K_d\right]^2+\left[\alpha_c-\alpha_d\right]^2\right]\left[K^2+\alpha^2\right]^{1/3}} = (1-\varphi)^2 \qquad (3.59)$$

$$\arctan\left[\frac{K\alpha_c-K_c\alpha}{KK_c+\alpha\alpha_c}\right] = 3\arctan\left[\frac{\left[K-K_d\right]\left[\alpha_c-\alpha_d\right]-\left[K_c-K_d\right]\left[\alpha-\alpha_d\right]}{\left[K-K_d\right]\left[K_c-K_d\right]+\left[\alpha-\alpha_d\right]\left[\alpha_c-\alpha_d\right]}\right] \qquad (3.60)$$

Eqn. (3.60) can be simplified by letting:

$$Y = \frac{\left[K-K_d\right]\left[\alpha_c-\alpha_d\right]-\left[K_c-K_d\right]\left[\alpha-\alpha_d\right]}{\left[K-K_d\right]\left[K_c-K_d\right]+\left[\alpha-\alpha_d\right]\left[\alpha_c-\alpha_d\right]} \qquad (3.61)$$

and using the identity:

$$\tan(3\chi) = \tan\chi(3-\tan^2\chi)/(1-3\tan^2\chi)$$

where $\chi = \arctan Y$, the result being:

$$\frac{K\alpha_c - K_c\alpha}{KK_c + \alpha\alpha_c} = \frac{Y(3-Y^2)}{1-3Y^2} \qquad (3.62)$$

The limiting conditions, as $\omega \to 0$ and $\omega \to \infty$, can be found using eqns. (3.59), (3.61) and (3.62). Now $Y \to 0$ as $\omega \to 0$ and as $\omega \to \infty$ (since $\alpha = \sigma/(\epsilon_o\omega)$) and so, near these limits, eqns. (3.61) and (3.62) can be combined to give:

$$\frac{K\alpha_c - K_c\alpha}{KK_c + \alpha\alpha_c} \simeq 3Y = \frac{3\left[K-K_d\right]\left[\alpha_c-\alpha_d\right] - 3\left[K_c-K_d\right]\left[\alpha-\alpha_d\right]}{\left[K-K_d\right]\left[K_c-K_d\right] + \left[\alpha-\alpha_d\right]\left[\alpha_c-\alpha_d\right]} \qquad (3.63)$$

The limiting expressions, at low frequency (for which α, α_c and $\alpha_d \to \infty$), of eqns. (3.59) and (3.63), are respectively:

$$\left[\frac{\sigma_\ell - \sigma_d}{\sigma_c - \sigma_d}\right]\left[\frac{\sigma_c}{\sigma_\ell}\right]^{1/3} = 1 - \varphi \qquad (3.64)$$

$$K_\ell\left[\frac{3}{\sigma_\ell - \sigma_d} - \frac{1}{\sigma_\ell}\right] = 3\left[\frac{K_c - K_d}{\sigma_c - \sigma_d} + \frac{K_d}{\sigma_\ell - \sigma_d}\right] - \frac{K_c}{\sigma_c} \qquad (3.65)$$

Similarly, the limiting expressions, for high frequency (for which α, α_c and $\alpha_d \to 0$), of eqns. (3.59) and (3.63), are respectively:

$$\left[\frac{K_h - K_d}{K_c - K_d}\right]\left[\frac{K_c}{K_h}\right]^{1/3} = 1 - \varphi \qquad (3.66)$$

$$\sigma_h\left[\frac{3}{K_h - K_d} - \frac{1}{K_h}\right] = 3\left[\frac{\sigma_c - \sigma_d}{K_c - K_d} + \frac{\sigma_d}{K_h - K_d}\right] - \frac{\sigma_c}{K_c} \qquad (3.67)$$

Eqn. (3.66) is identical to Bruggeman's Equation (3.24) with $K = K_h$ whereas eqn. (3.64) is identical to de la Rue and Tobias' eqn. (3.31) with $\sigma = \sigma_\ell$.

Eqns. (3.64) to (3.67) can now be considered in relation to O/W and W/O emulsions.

For O/W emulsions (where $\sigma_c >> \sigma_d$ and $\sigma_\ell >> \sigma_d$) eqns. (3.64) to (3.67) reduce to:

$$\frac{\sigma_\ell}{\sigma_c} = (1 - \varphi)^{3/2} \tag{3.68}$$

$$\frac{\sigma_\ell}{\sigma_c} = \left[\frac{2K_\ell - 3K_d}{2K_c - 3K_d}\right] = (1 - \varphi)^{3/2} \tag{3.69}$$

$$\left[\frac{K_h - K_d}{K_c - K_d}\right]\left[\frac{K_c}{K_h}\right]^{1/3} = 1 - \varphi \tag{3.70}$$

$$\frac{\sigma_h}{\sigma_c} = \frac{K_h(K_h - K_d)(2K_c + K_d)}{K_c(K_c - K_d)(2K_h + K_d)} \tag{3.71}$$

For non-polar oils it can be assumed that $K_c >> K_d$, $K_h >> K_d$ and $K_\ell >> K_d$, if the emulsion is not too concentrated. Eqns. (3.69) and (3.70) then imply:

$$K_\ell = K_c(1 - \varphi)^{3/2} = K_h \tag{3.72}$$

Hence, for not too concentrated non-polar O/W emulsions eqn. (3.72) indicates that dielectric dispersion is negligible.

For W/O emulsions (where $\sigma_d >> \sigma_c$ and $\sigma_d >> \sigma_\ell$), eqns. (3.64) to (3.67) reduce to:

$$\frac{\sigma_\ell}{\sigma_c} = \frac{1}{(1 - \varphi)^3} \tag{3.73}$$

$$\frac{K_\ell}{K_c} = \frac{\sigma_\ell}{\sigma_c} = \frac{1}{(1 - \varphi)^3} \tag{3.74}$$

$$\left[\frac{K_h - K_d}{K_c - K_d}\right]\left[\frac{K_c}{K_h}\right]^{1/3} = 1 - \varphi \tag{3.75}$$

$$\frac{\sigma_h}{\sigma_d} = \frac{3K_h(K_c - K_h)}{(K_c - K_d)(K_d + 2K_h)} \qquad (3.76)$$

In contrast to the findings for O/W emulsions, the dielectric dispersion in W/O emulsions is significant (Sherman, 1968).

Hanai's theory of interfacial polarization has been found to be quantitatively correct in the case of O/W emulsions where dielectric dispersion is generally insignificant (Becher, 1977, Sherman, 1968). However, polar oils, such as nitrobenzene, do give rise to dielectric dispersion in O/W emulsions (Hanai et al., 1962) but this is predicted by the theory. Eqn. (3.68) gives the conductivity at the low-frequency limit and eqn. (3.70) gives the dielectric constant at the high-frequency limit.

For W/O emulsions the situation is not so clear cut. Dielectric dispersion arises as predicted by Hanai's theory which means that there are differences between the low and high-frequency limits for both conductivity and dielectric constant. Hanai's experiments on W/O emulsions have validated his theoretical expression for the high-frequency limit of the dielectric constant, given by eqn. (3.75) (Hanai, 1961). Hanai's theoretical expression for the low-frequency dielectric constant, given by eqn. (3.74), is supported by the experimental results of Guilljen (1941) (working with emulsions of mercury in lubricating oil or castor oil) and Pearce (1955) (who worked with emulsions of sea water in fuel oil). Experimental confirmation of Hanai's expression for the low-frequency limit of conductivity, given by eqn. (3.73), has been made by some workers (Sherman, 1968). As regards Hanai's high-frequency limit for conductivity, given by eqn. (3.76), there is little evidence in the literature to validate it. Hanai's own experimental results, for W/O emulsions, depended on the degree of agitation (see Section 3.6.6) applied to the emulsion (Hanai, 1961). As the agitation increased, the experimental results tended towards the theoretical values.

3.6.5 Electrode Polarization

Electrode polarization is a phenomenon associated with low-frequency excitation, although its effects can be apparent up to frequencies as high as 1MHz (Hanai et al., 1960). It is caused by ionic species collecting at the electrodes by electrophoresis, and therefore increases as the conductivity of the dielectric increases, as well as increasing as the applied electric field strength is raised. Electrode polarization is less for O/W emulsions than it is for W/O emulsions, due to the nature of the continuous phase. It is noticeable during the measurement of

dielectric constant at low frequency, its effect increasing as frequency is decreased. When measuring the low-frequency dielectric constant, it is therefore necessary to continue increasing the frequency until the values level off. Clearly, it becomes more difficult for charge to accumulate at the electrodes as frequency increases.

3.6.6 The Effect of Particle Agglomeration on Dielectric Properties

The dielectric properties of disperse systems have been found, experimentally, to depend on the state of agglomeration of the dispersed phase. Parts (1945) was the first to observe this phenomenon and he suggested a correlation between the dielectric and rheological properties of dispersed systems. He experimented with suspensions of carbon black in varnish. A suspension containing 14.2% carbon black had a dielectric constant significantly higher than one containing 12.4% carbon black but, in both cases, the dielectric constant increased in time. The suspension containing the larger proportion of carbon black was found to be much more thixotropic than the other, this property being related to the extent of aggregation; hence the suggested correlation between dielectric and rheological properties.

This effect was investigated extensively by Voet (1947) using various suspensions which were subjected to rotational shear flow by the action of a coaxial viscometer. He measured the dielectric constant of suspensions of carbon black in castor oil, mineral oil and linseed oil, as a function of volume fraction. Simultaneous measurement of the rheological properties was possible. At low values of volume fraction, no change in dielectric constant was found under shearing action. However, as a threshold value was reached (0% for castor oil, 5% for mineral oil and 9% for linseed oil) the effect of shearing became apparent, the dielectric constant decreasing significantly below the rest values. Voet attributed this behaviour to the breaking up of agglomerates under the action of shear forces, since Newtonian flow (particle agglomeration absent) was encountered below threshold concentrations whereas the suspensions exhibited plastic flow (particle agglomeration present) above threshold concentrations.

Similar results were found by Voet for emulsions of 0.5N aqueous sodium hydroxide in mineral oil.

Voet based his analysis on Bruggeman's eqn. (3.24) which, assuming $K_d >> K$, gives:

$$K = K_c/(1 - \varphi)^3 \simeq K_c\ (1 + 3\varphi) \qquad (3.77)$$

Two constants α and δ were incorportated into this equation to account for particle shape and state of agglomeration respectively.

$$K = K_c(1 + 3\alpha\delta\varphi) \qquad (3.78)$$

For spherical particles α assumed the value unity whereas it was greater for non-spherical particles in general, and less for plate-like and thread-like particles. For non-agglomerated suspensions (i.e. those under conditions of high shear), δ was considered to be unity. The value of δ was found to increase with the state of agglomeration and depended on the materials used and the volume fraction.

Hanai (1961) also investigated the dielectric properties of W/O emulsions, subjected to rotational shear forces. He measured the frequency dependence of the dielectric constant and conductivity of W/O emulsions as functions of volume fraction and rotational speed. At high frequencies (> 1MHz) the dielectric constant of the emulsions were found to be independent of rotational speed and to be well represented by Hanai's eqn. (3.75). However, at low frequencies (where the dielectric constant of the dispersed system is dependent on the conductivities of the dispersed and continuous phases) the dielectric constant was found to be dependent on rotational speed (i.e. the state of aggregation of the dispersed phase). The measured values decreased towards the theoretical predictions as the rotational speed was increased and the dispersed phase agglomerates were broken up. Hanai's eqn. (3.74) was used to obtain the theoretical values.

With regard to conductivity, no definite correlation between rotational speed and conductivity, measured at low-frequencies, was obtained. However, the minimum frequency used was 100Hz. All the measured values were less than the values obtained using Hanai's eqn. (3.73).

Limiting values for conductivity at high frequency were not obtained since the maximum frequency used was only 3MHz. The experimental values, measured at this frequency, all lie above the values obtained using Hanai's eqn. (3.71). However, the values decrease towards the predicted values with increasing rotational speed.

3.6.7 Other Factors Affecting the Dielectric Properties of Dispersed Systems

Besides the factors already discussed, others, including the effect of non–spherical particles, orientation and the size distribution of the dispersed phase particles, may be of relevance. Droplet deformation, should the dispersed phase be liquid as in an emulsion, would come under the heading of non–spherical particles. Droplet deformation and orientation can both be initiated by electric fields and mechanical shear forces. These effects will not be discussed further in this thesis.

4. THE ELECTRIC DOUBLE LAYER

Most substances acquire surface charge when brought into contact with a polar medium such as water (Shaw, 1980). The charge may arise from chemical ionisation, preferential ion adsorption and ion dissolution. The surface charge affects the distribution of nearby ions in the continuous phase. Ions of opposite polarity (counter-ions) to the surface charge are attracted to the surface whereas those of like charge (co-ions) are repelled. These attractive and repulsive forces, together with the mixing tendency of thermal motion, lead to the formation of an electric double layer. This can be regarded as comprising an inner region of adsorbed ions and a diffuse region in which the distribution of ions is controlled by electrical forces and random thermal motion (see Figure 4.1).

The simplest quantitative treatment of the double layer is that due to Gouy (1910) and Chapman (1913), which assumes that:

i. The surface is flat, of infinite extent and is uniformly charged.

ii. The ions in the diffuse part of the double layer are point charges distributed spatially in accord with the Boltzmann distribution.

iii. The continuous phase influences the double layer only by virtue of its permittivity which takes the same value everywhere.

iv. Ions in the diffuse part of the double layer are of the same valency.

Suppose that the number density of both counter-ions and co-ions, far from the interface, is n_o. The number density n_i near to the interface can be determined using the Boltzmann distribution:

$$n_i = n_o \exp\left[\frac{-i\nu e\psi}{kT}\right] \qquad (4.1)$$

i = +1 for co-ions and −1 for counter-ions
ν = number of electronic units per ion (valency)
e = electronic unit of charge (1.602×10^{-19}C)
ψ = electrical potential at a distance x from interface
k = Boltzmann's constant (1.381×10^{-23}JK^{-1})
T = absolute temperature

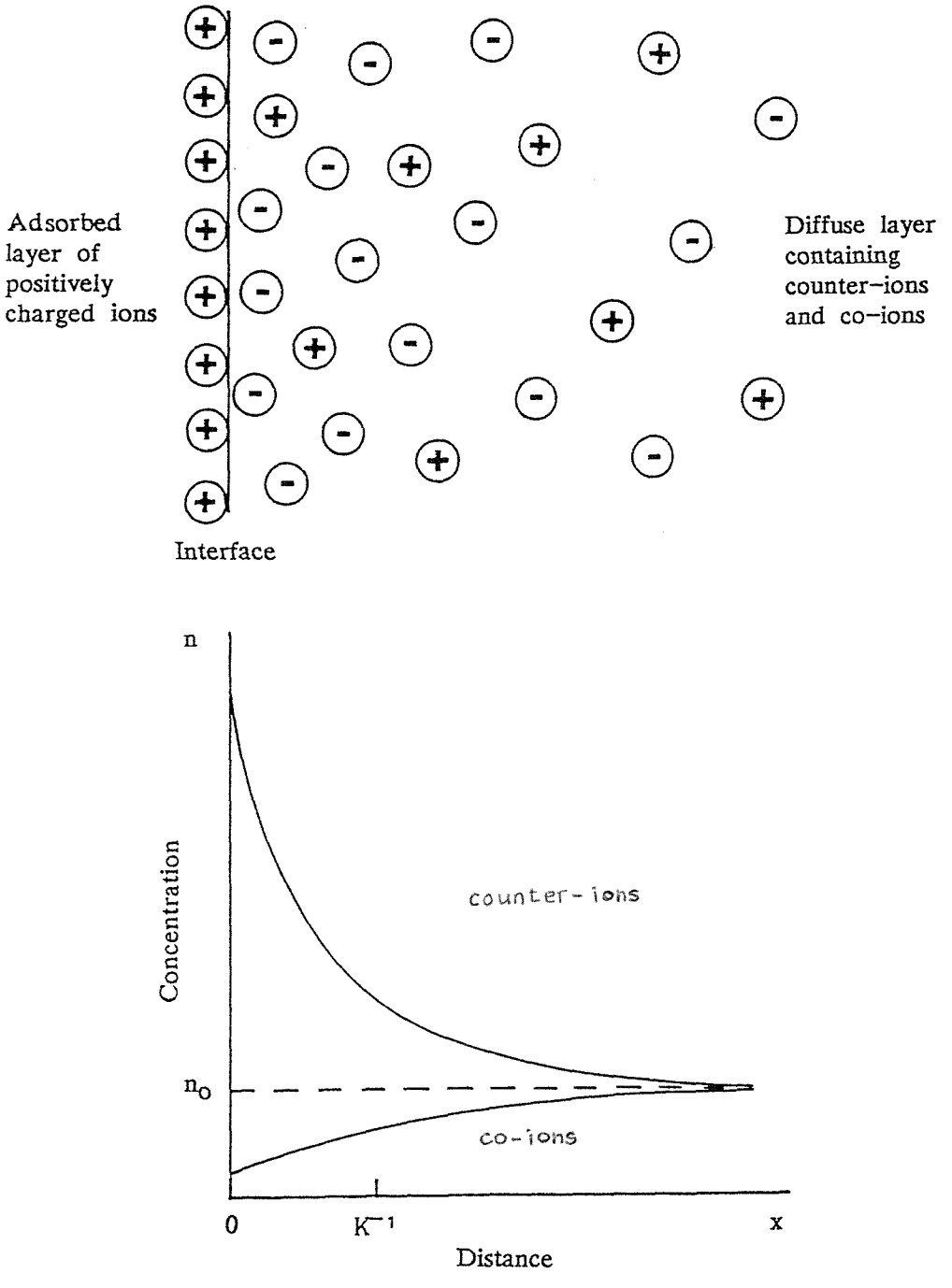

FIGURE 4.1 **Distribution of ions in the electric double layer.**

The net charge density, at points where the electrical potential is ψ, may be obtained using eqn. (4.1):

$$\rho = \nu e(n_{+1}-n_{-1}) = \nu e n_o\left[\exp\left[\frac{-\nu e\psi}{kT}\right] - \exp\left[\frac{\nu e\psi}{kT}\right]\right]$$

$$\rho = -2\nu e n_o \sinh\left[\frac{\nu e\psi}{kT}\right] \qquad (4.2)$$

The electrical potential ψ is related to the charge density ρ by Poisson's equation which in 1-dimension has the form:

$$\frac{d^2\psi}{dx^2} = -\frac{\rho}{\epsilon} \qquad (4.3)$$

where ϵ is the permittivity of the continuous phase.

The 1-dimensional Poisson-Boltzmann equation may be obtained by combining eqns. (4.2) and (4.3):

$$\frac{d^2\psi}{dx^2} = \frac{2\nu e n_o}{\epsilon} \sinh\left[\frac{\nu e\psi}{kT}\right] \qquad (4.4)$$

The boundary conditions to be satisfied are $d\psi/dx = 0$ when $\psi = 0$ (i.e. when $x \to \infty$) and $\psi = \psi_o$ when $x = 0$. Eqn. (4.4) may be integrated as follows:

$$\frac{d}{d\psi}\left[\frac{1}{2}\left[\frac{d\psi}{dx}\right]^2\right] = \frac{d^2\psi}{dx^2} = \frac{2\nu e n_o}{\epsilon} \sinh\left[\frac{\nu e\psi}{kT}\right]$$

Integration gives:

$$\frac{1}{2}\left[\frac{d\psi}{dx}\right]^2 = \frac{2n_o kT}{\epsilon}\left[\cosh\left[\frac{\nu e\psi}{kT}\right] + A\right] \qquad (4.5)$$

Now $d\psi/dx = 0$ when $\psi = 0$ thus $A = -1$ and so eqn. (4.5) becomes:

$$\frac{d\psi}{dx} = \pm 2\left[\frac{2n_o kT}{\epsilon}\right]^{\frac{1}{2}} \sinh\left[\frac{\nu e\psi}{2kT}\right] \qquad (4.6)$$

The negative root must be taken since ψ is assumed to decrease as x increases. Make the following substitutions:

$$B = \left[\frac{2n_o kT}{\epsilon}\right]^{\frac{1}{2}} \qquad (4.7)$$

$$c = \frac{\nu e}{2kT} \tag{4.8}$$

Then eqn. (4.6) may be written:

$$x = -\frac{1}{2B} \int \frac{d\psi}{\sinh(c\psi)} \tag{4.9}$$

Let $y = \cosh(c\psi)$ then eqn. (4.9) becomes:

$$x = -\frac{1}{2Bc} \int \frac{dy}{y^2-1} = \frac{-1}{4Bc} \int \left[\frac{1}{y-1} - \frac{1}{y+1}\right] dy$$

Integration gives:

$$x = \frac{-1}{4Bc} \ell n\left[\frac{y-1}{y+1}\right] + E = \frac{-1}{4Bc} \ell n\left[\frac{\cosh(c\psi)-1}{\cosh(c\psi)+1}\right] + E$$

$$x = \frac{-1}{2Bc} \ell n\left[\tanh\left[\frac{c\psi}{2}\right]\right] + E \tag{4.10}$$

Where E is the constant of integration. Now $\psi = \psi_o$ when $x = 0$ thus:

$$E = \frac{1}{2Bc} \ell n\left[\tanh\left[\frac{c\psi_o}{2}\right]\right] \tag{4.11}$$

Combining eqns. (4.10) and (4.11) gives:

$$2Bcx = \ell n \left[\frac{\tanh(c\psi_o/2)}{\tanh(c\psi/2)}\right] \tag{4.12}$$

Define the Debye parameter K:

$$K = 2Bc = \left[\frac{2n_o \nu^2 e^2}{\epsilon kT}\right]^{\frac{1}{2}} \tag{4.13}$$

Combining eqns. (4.12) and (4.13) and re-arranging gives:

$$\tanh(c\psi/2) = e^{-Kx} \tanh(c\psi_o/2) \tag{4.14}$$

Let $$\beta = \tanh(c\psi_o/2) = (e^{c\psi_o}-1)/(e^{c\psi_o}+1) \qquad (4.15)$$

Combining eqns. (4.14) and (4.15) and re-arranging:

$$\frac{e^{c\psi}-1}{e^{c\psi}+1} = \beta e^{-Kx}$$

$$e^{c\psi}\left[1-\beta e^{-Kx}\right] = 1 + \beta e^{-Kx}$$

$$e^{c\psi} = \left[1+\beta e^{-Kx}\right]/\left[1-\beta e^{-Kx}\right]$$

$$\psi = \frac{1}{c}\,\ell n\left[\frac{1+\beta e^{-Kx}}{1-\beta e^{-Kx}}\right]$$

Using eqn. (4.8) this becomes:

$$\psi = \frac{2kT}{\nu e}\,\ell n\left[\frac{1+\beta e^{-Kx}}{1-\beta e^{-Kx}}\right] \qquad (4.16)$$

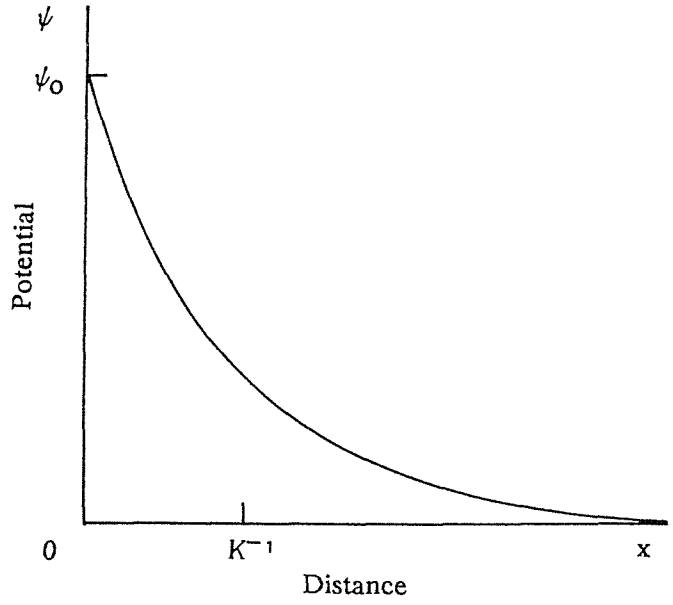

FIGURE 4.2 Potential function of electric double layer.

This equation shows how the potential varies as a function of distance from the plane interface; it decreases from $\psi = \psi_o$, at x = 0, to $\psi = 0$, as $x \to \infty$, as shown in Figure 4.2. If $\nu e\psi_o << 2kT$ (kT/e = 25.6mV at 25°C) then $c\psi_o$ and $c\psi$, in eqn. (4.14), are small (since c is small) and so:

$$\psi = \psi_o e^{-Kx} \qquad (4.17)$$

This is the Debye–Hückel approximation, which shows that the potential decreases exponentially, with distance from the charged interface, at low potentials. When the approximation is not applicable, the potential, given by eqn. (4.16), decreases at a faster than exponential rate near to the charged interface.

The charge density σ_o, of adsorbed charge at the interface, may be determined as follows (since the total charge is zero):

$$\sigma_o = -\int_o^\infty \rho dx$$

Using eqn. (4.2) this becomes:

$$\sigma_o = 2\nu e n_o \int_o^\infty \sinh\left[\frac{\nu e\psi}{kT}\right] dx$$

This may be integrated using eqn. (4.6):

$$\sigma_o = 2\nu e n_o \left[\frac{\epsilon}{2n_o kT}\right]^{\frac{1}{2}} \int_o^{\psi_o} \cosh\left[\frac{\nu e\psi}{2kT}\right] d\psi$$

Integration gives:

$$\sigma_o = (8n_o \epsilon kT)^{\frac{1}{2}} \sinh\left[\frac{\nu e\psi_o}{2kT}\right] \qquad (4.18)$$

For low values of potential, eqn. (4.18) reduces to (using eqn. (4.13)):

$$\sigma_o = \epsilon K \psi_o \qquad (4.19)$$

Eqn. (4.19) shows that $K\psi_o$ is the electric field in the double layer (since $E = \sigma_o/\epsilon$). If the electric double layer is likened to a parallel-plate electrode system, the interface is represented by one plate, whereas the diffuse double layer is represented by a plate separated from the interface by a distance K^{-1}. This shows why K^{-1} is called the double layer thickness. The interface potential ψ_o is related to both the surface charge density σ_o and the ionic composition of the continuous phase (which specifies K, the Debye parameter).

The double layer thickness K^{-1}, given by eqn. (4.13), can also be expressed in terms of concentration of electrolyte c (mol dm^{-3}) since $n_o = N_A c$ where N_A is Avogadro's number (6.023×10^{23} mol^{-1}):

$$K = \left[\frac{2n_o \nu^2 e^2}{\epsilon kT}\right]^{\frac{1}{2}} = \left[\frac{2N_A c \nu^2 e^2}{\epsilon kT}\right]^{\frac{1}{2}} \qquad (4.20)$$

For water, of permittivity $\epsilon = 80\epsilon_o$, having an electrolyte concentration 10^{-3} mol dm^{-3}, the double layer thickness is about 10nm (assuming ν=1). In an oil, the double layer thickness is much larger since the electrolyte concentration is much less. Albers and Overbeek (1959) have pointed out that ionic concentrations of the order of 10^{-10} mol dm^{-3} are possible in benzene. Assuming the permittivity of benzene to be $\epsilon = 2\epsilon_o$, the double layer thickness is about 5μm (assuming ν=1) which is 5×10^3 times the double layer thickness, mentioned above, for water. Eqn. (4.20) shows that the double layer thickness is inversely proportional to the square root of the ionic concentration.

An improved model of the electric double layer was proposed by Stern (1924), who recognised that the error caused by neglecting the finite ionic size was only important in the vicinity of the interface. He proposed dividing the double layer into two parts separated by a plane (the Stern plane), located at a distance from the interface of about the radius of a hydrated ion (see Figure 4.3). Stern assumed that counter-ions would be specifically adsorbed at the interface (where electrostatic and van der Waals' forces overcome thermal agitation) and proposed a Langmuir-type adsorption equilibrium between the ions in the Stern layer and those in the diffuse part of the double layer. The Gouy-Chapman diffuse double layer was assumed to apply beyond the Stern plane.

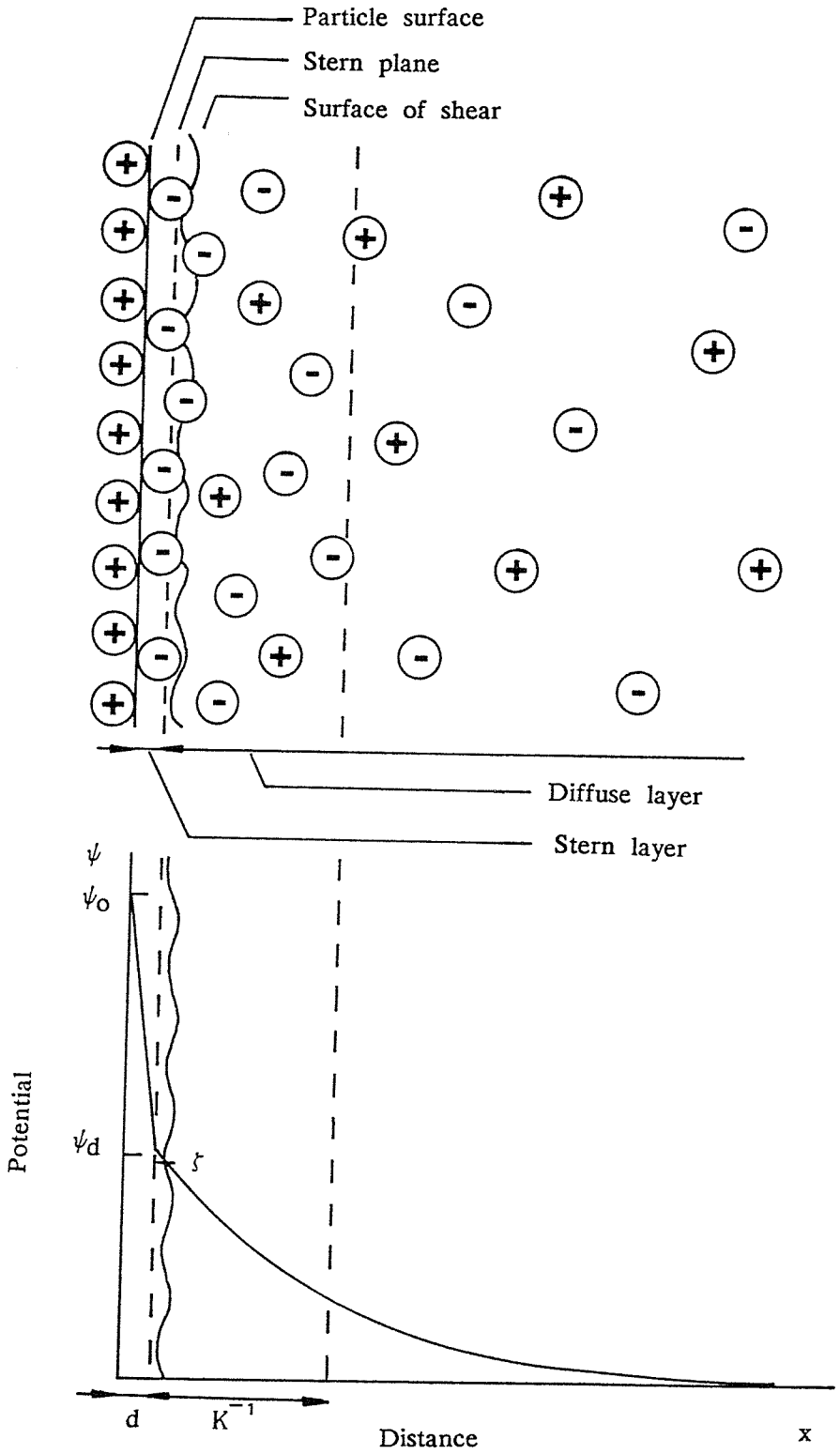

FIGURE 4.3 Potentials in the electric double layer at the interface (ψ_o), the Stern plane (ψ_d) and the shear plane (ζ).

The electrokinetic or ζ-potential, important in electrokinetic measurements, is the electrical potential at the plane of shear (see Figure 4.3), the exact location of which is an uncertain feature of the electric double layer. Usually it is assumed to be located at a small distance further away from the interface than the Stern plane. Though ψ_d is generally slightly larger than ζ, it is customary to assume them to be identical. Typical values of the ζ-potential lie in the range 25–100mV (Sherman, 1968) and values as high as 130mV were obtained by Albers and Overbeek (1959), for water-in-benzene emulsions stabilised by heavy-metal soaps.

In the case of emulsions, an electric double layer will exist on both sides of the interface. The exact form of the potential distribution at the interface will depend on the nature of the ions and surface-active agents present in the system.

The electric double layer, in emulsions, is of interest for two reasons: firstly, a dispersed phase droplet may be acted upon by an electric field, giving rise to an electrophoretic force; secondly, emulsion stability may be conferred, by virtue of a repulsive force between the double layers of two dispersed phase droplets in close proximity. In the case of O/W emulsions, the double-layer potential is small in the outer aqueous phase and so the stability of such emulsions is not great; there is a strong tendency for coalescence to occur in such systems. The double-layer potential can be markedly changed by the presence of surface-active agents at the interface, leading to stable emulsions.

Albers and Overbeek (1959) have studied the stability of W/O emulsions. Although appreciable ζ-potentials were found, they concluded that stability of the emulsion was not conferred by the electric double layer. This was because the double layer thickness was relatively large (several μm), about the distance between droplets in a moderately concentrated emulsion (in which case, the interactions with all neighbouring droplets must be considered).

4.1 Experimental Investigation into the Electric Double Layer of Aqueous Droplets in Oil

In an attempt to measure the electric double layer charge of aqueous droplets in oil, a special cell was constructed. The idea behind the cell was that the terminal speed of descent of a droplet could be modified by the application of an electric field; the field would give rise to an additional force on the droplet, by virtue of its double-layer charge, which could be used to determine the charge.

Cell height was governed by droplet size, in so far as the time of descent should be accurately measurable by stop-watch. A height of about 10cm was found to be appropriate. Optical considerations dictated that the side of the cell should be flat, preferably with a flat face behind for illumination purposes. Consequently, a cell of square cross-section was chosen.

A further requirement was that the electric field should be reasonably uniform between the electrodes, achievable by using a separation small in comparison with electrode size. However, it was also necessary to observe the droplets using a low-power microscope, which limited the object distance. The refractive index n of the oil helped the situation, since the actual observation distance was reduced by the amount $t(1-1/n)$, where t was the light path length in the oil. A satisfactory compromise, between these conflicting interests, was provided by a cell having side length 20cm. Firstly, this gave a minimum ratio of approximately 2:1 for electrode width to electrode separation; such a geometry ensured a reasonably uniform electric field between the electrodes. Secondly, the distance between the objective lens and water droplet assumed a value of 10cm, which reduced to an apparent distance of about 7cm when the refractive index of the oil ($n=1.5$) was accounted for. With this arrangement, a low-power microscope having focal length about 6cm was found to be most appropriate for viewing the water droplets. Such an objective lens, in combination with a low-power eyepiece, gave a reasonable field of view.

The basic cell dimensions were therefore chosen to be 20cm × 20cm × 10cm which gave a volume of approximately four litres. Water droplets were conveniently injected through a small opening in the upper electrode, using a hypodermic needle and syringe or pipette. A means was available for varying the electrode separation. The electrodes were rounded at the corners and edges to minimise non-uniform and intense electric field generation. As a safety measure, the upper electrode was grounded since contact with it was possible when injecting droplets. The lower electrode was supported on perspex legs to keep it away from water which collected at the bottom of the cell.

The electrodes, support rod and collar were made of brass. The cell walls were constructed from glass, though the lid was made from perspex. The main features of the cell are shown in Figure 4.4.

A 16W fluorescent strip lamp, 30cm long, was used to illuminate the droplet trajectory. To reduce convection, a prespex heat shield was introduced between the cell and light source.

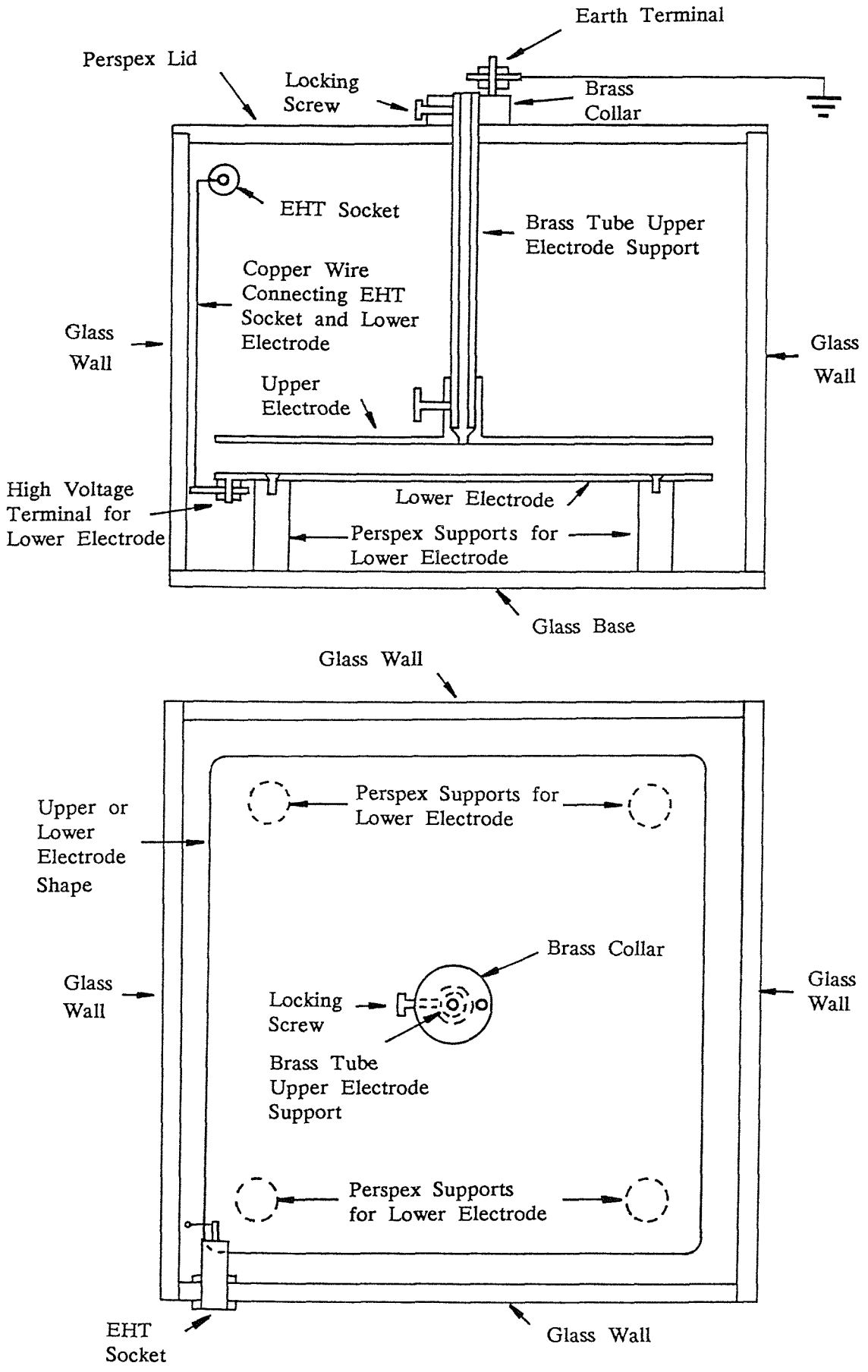

FIGURE 4.4 Cell for investigating electric double layer charge.

In order to facilitate tracking of the water droplets, the low-power microscope was mounted on an x-z co-ordinate slide system.

A supply of water droplets, ranging in diameter from about 25 to 150μm, was obtained by atomizing water into an ancillary beaker, containing the same oil as the cell.

Preliminary tests showed that bulk motions were present in the oil for potential differences greater than about 5kV (perhaps due to electrostriction). If the electric field was kept low, the tendency for water droplets to move out of the microscope field of view was minimised. In certain instances, individual droplets were observed to have their terminal speeds changed and even their direction of travel reversed, by the applied electric field.

Commercial diesel oil (of permittivity $2.3\epsilon_o$, and conductivity $400pSm^{-1}$) was introduced into the cell and ancillary beaker. The sample of water to be used was prepared in the reservoir of an air-blast atomizer. When using deionised water, the reservoir was rinsed several times to remove excess ions from its interior. Saline solution was conveniently produced by adding sodium chloride to the deionised water (it was expedient to perform the experiments using deionised water before those using saline). The atomizer was then used to spray small water droplets into the oil in the ancillary beaker. These were sampled using a pipette which was then introduced into the upper electrode support. Water droplets descended into the inter-electrode space under the influence of gravity. If the flow ceased, it could usually be started again by tapping or slightly squeezing the pipette teat.

The microscope was then focussed onto a falling droplet in the absence of an applied electric field.

The accuracy with which droplet terminal speed could be measured was increased by the number of timings which could be made. With an electrode separation of 5cm, it was usually possible to make at least two measurements with the field on and two with it off, for particles of less than about 110μm diameter. In each case, the time measured was that required for the droplet to traverse half the field of view.

Frequently the droplet moved off course, in which case the microscope had to be re-positioned and re-focussed. Delays were caused by having to reset

the stop-watch, switching the power supply, and noting down times.

The diameter of a droplet was measured, as it traversed the microscope field of view, using a Vernier gauge which positioned cross-wires in the eyepiece. The Vernier gauge was calibrated by focusing the microscope onto a rod of known diameter, situated in the measuring volume.

Measurements made with no applied electric field were used to determine the bulk viscosity of the oil. An auxiliary experiment was performed to determine the density of the diesel oil (which was found to be 830 kg m^{-3}).

4.1.1 Theory

The terminal speed of a charged droplet, situated in a gravitational and electric field, may be found using Stokes' law (see Chapter 3, Section 3.4) as follows:

$$(4/3)\pi a^3 g(\rho_d - \rho_c) + qE = 6\pi\eta_c a u \qquad (4.21)$$

When the electric field is zero eqn. (4.21) gives:

$$u = \frac{2g(\rho_d - \rho_c)a^2}{9\eta_c} \qquad (4.22)$$

The terminal speed u is determined from the time it takes a water droplet to traverse half the microscope field of view. If u is plotted as a function of a^2 then a straight line should result, of gradient m (see Figure 4.5):

$$m = \frac{2g}{9\eta_c}(\rho_d - \rho_c) \qquad (4.23)$$

The coefficient of bulk viscosity η_c, can be determined from eqn. (4.23).

The measurements made, with non-zero electric field, can then be used to determine any charge the droplet may possess. If the terminal speed without the electric field is u_o and with it is u_1, then it is easy to show, using eqn. (4.21), that:

$$q = 6\pi\eta_c a(u_1 - u_o)/E \qquad (4.24)$$

The electric field E here is assumed to be the potential difference between the electrodes divided by electrode separation.

If the charge is assumed to be uniformly distributed over the surface of the droplet, with surface charge density σ, then the charge can be expressed as:

$$q = 4\pi a^2\sigma \qquad (4.25)$$

This can be used in conjunction with the previous eqn. (4.24) to obtain an expression for the surface charge density:

$$\sigma = \frac{3\eta_c}{2Ea}(u_1 - u_o) \qquad (4.26)$$

A droplet of water in oil has a double layer associated with it of a certain thickness K^{-1} and surface charge density σ. Thus, a water droplet in oil is expected to be charged, even if only by the double layer mechanism.

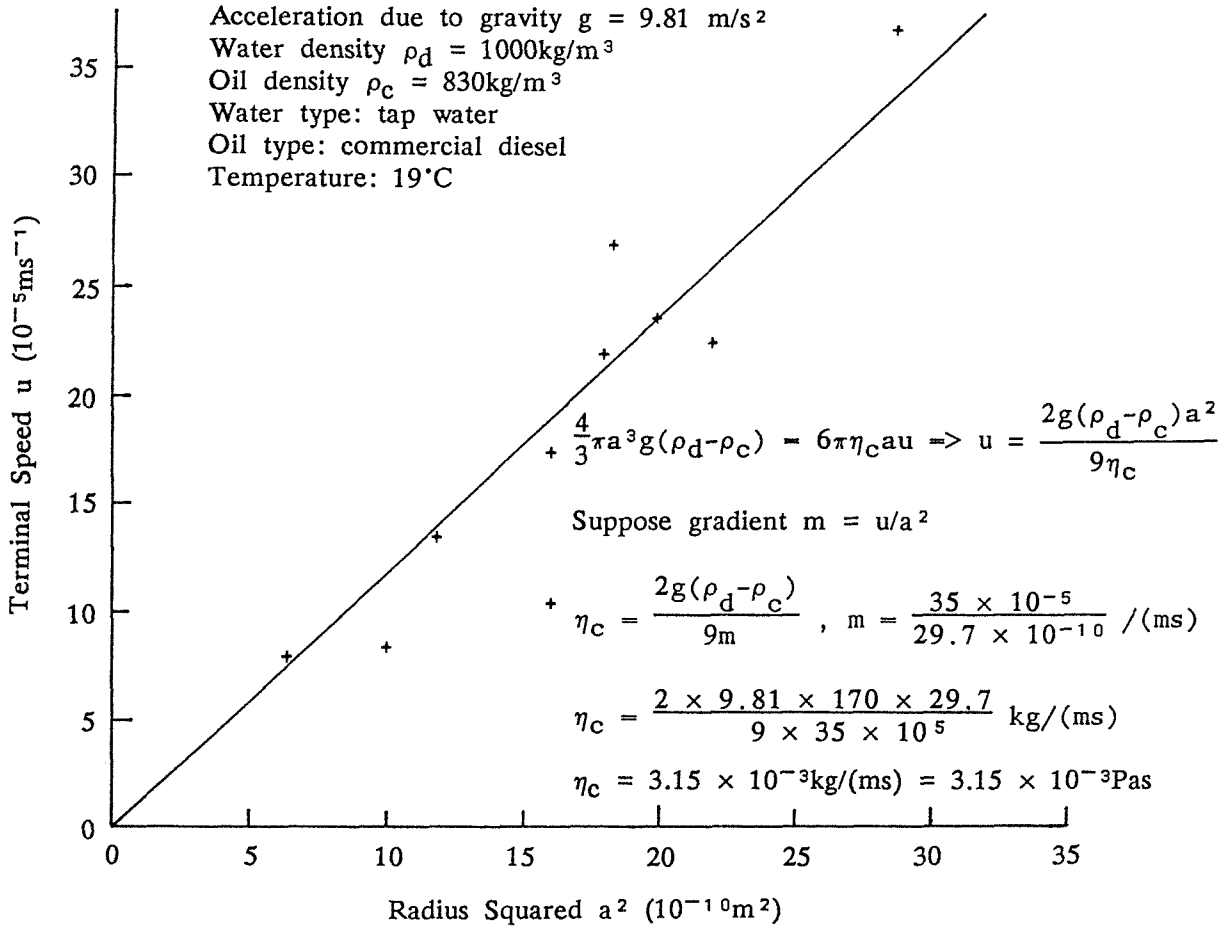

FIGURE 4.5 Graph for determination of oil viscosity.

Electrokinetic measurements can be made to determine ζ the zeta-potential associated with a water droplet in oil. Theoretically, the double layer thickness K^{-1} and surface charge density σ are given by eqns. (4.20) and (4.19) respectively. Following Klinkenberg and van der Minne (1958), the double layer thickness may be expressed in a form different from eqn. (4.20), using the diffusion coefficient Δ_m, and the charge relaxation time τ of the continuous phase.

$$\Delta_m = \frac{kT}{6\pi\eta_c r} \tag{4.27}$$

$$\tau = \frac{\epsilon}{2n_o B\nu e} \tag{4.28}$$

where B is the electrical mobility, of an ion of radius r and valency ν, defined by:

$$B = \frac{\nu e}{6\pi\eta_c r} \tag{4.29}$$

Eqns. (4.27) to (4.29) yield:

$$\Delta_m\tau = \frac{\epsilon kT}{2n_o\nu^2 e^2} \tag{4.30}$$

Combining eqns. (4.20) and (4.30) gives the Debye parameter (inverse of double layer thickness):

$$K = (\Delta_m\tau)^{-\frac{1}{2}} \tag{4.31}$$

The electric double layer potential ψ_o, in eqn. (4.19), is replaced by ζ (the zeta-potential) in the following.

The parameters of interest are listed in Table 1 (tap water), Table 2 (deionised water) and Table 3 (saline). The tabulations give values of: droplet radius measured, droplet radius from graph (calculated from Stokes' law), terminal speed with electric field on, terminal speed with electric field off, charge on droplet (measured), charge density of droplet, and the charge expected from double layer theory. Tables 4.1, 4.2 and 4.3 show that the charge on a water droplet varied; sometimes it was greater than and sometimes less than the expected double layer charge. In some cases the charge was very much greater than would be expected. Both polarities of charge were detected whereas only one polarity would

be expected from double layer theory. The experimental results seem to indicate that there was a charging mechanism in operation, other than the electric double layer. This, quite possibly, was the atomization process in which water droplets were mechanically torn apart. It is reasonable to assume that such a process could produce droplets, with considerable charge, of either polarity, as appears to have been the case.

TABLE 4.1

Water type:	tap water	
Water density:	$1000 kgm^{-3}$	
Oil type:	commercial diesel	
Oil density:	$830 kgm^{-3}$	
Oil conductivity:	$400\ pSm^{-1}$	
Oil dielectric constant:	2.3	
Oil viscosity:	$3.15 \times 10^{-3} Pas$	
Droplet fall distance:	$4.5 \times 10^{-3} m$	
Temperature:	19°C	
Electrode potential:	1kV	
Electrode polarity:	positive	
Electrode separation:	0.05m	
Electric field:	$-20 kVm^{-1}$	
Double layer thickness:	$9.8 \times 10^{-6} m$	
Double layer charge density:	$5.2 \times 10^{-8} Cm^{-2}$	
Diffusion constant:	$1.9 \times 10^{-9} m^2 s^{-1}$	Klinkenberg and van der Minne
Zeta potential:	0.025V	Klinkenberg and van der Minne

Droplet Radius Measured $10^{-5}m$	Droplet Radius From Graph $10^{-5}m$	Terminal Speed Field Off $10^{-3}ms^{-1}$	Terminal Speed Field On $10^{-3}ms^{-1}$	Charge On Droplet $10^{-15}C$	Charge Density On Droplet $10^{-8}Cm^{-2}$	Double Layer Charge $10^{-15}C$
2.53	2.5	0.078	0.079	-0.08	-0.98	0.41
3.16	2.6	0.084	0.102	-1.39	-16.4	0.44
4.16	3.0	0.103	0.143	-3.53	-31.2	0.59
3.43	3.4	0.136	0.137	-0.10	-0.71	0.76
3.16	3.9	0.174	0.141	3.45	20.3	0.99
4.22	4.3	0.218	0.214	0.51	2.20	1.21
4.67	4.4	0.223	0.237	-1.85	-7.60	1.27
4.44	4.5	0.237	0.234	0.40	1.57	1.32
4.28	4.7	0.269	0.254	2.09	7.53	1.44
5.34	5.6	0.369	0.352	2.84	7.21	2.05

TABLE 4.2

Water type:	deionised	
Water density:	$1000 kgm^{-3}$	
Oil type:	commercial diesel	
Oil density:	$830 kgm^{-3}$	
Oil conductivity:	$400 pSm^{-1}$	
Oil dielectric constant:	2.3	
Oil viscosity:	$3.15 \times 10^{-3} Pas$	
Droplet fall distance:	$4.5 \times 10^{-3} m$	
Temperature:	19.6°C	
Electrode potential:	1kV	
Electrode polarity:	positive	
Electrode separation:	0.05m	
Electric field:	$-20 kVm^{-1}$	
Double layer thickness:	$9.8 \times 10^{-6} m$	
Double layer charge density:	$5.2 \times 10^{-8} Cm^{-2}$	
Diffusion constant:	$1.9 \times 10^{-9} m^2 s^{-1}$	Klinkenberg and van der Minne
Zeta potential:	0.025V	Klinkenberg and van der Minne

Droplet Radius Measured $10^{-5}m$	Droplet Radius From Graph $10^{-5}m$	Terminal Speed Field Off $10^{-3}ms^{-1}$	Terminal Speed Field On $10^{-3}ms^{-1}$	Charge On Droplet $10^{-15}C$	Charge Density On Droplet $10^{-8}Cm^{-2}$	Double Layer Charge $10^{-15}C$
1.38	1.87	0.041	0.078	-2.04	-46.4	0.229
1.72	2.45	0.073	0.078	-0.38	-4.97	0.392
2.06	2.87	0.099	0.069	2.53	24.4	0.538
2.06	2.92	0.102	0.103	-0.10	-0.89	0.557
3.09	3.20	0.118	0.172	-5.16	-40.1	0.669
3.09	3.57	0.150	0.154	-0.49	-3.03	0.833
3.78	3.61	0.152	0.196	-4.69	-28.6	0.852
3.78	3.81	0.172	0.129	4.86	26.6	0.949
4.13	4.18	0.205	0.126	9.70	44.2	1.142
7.22	6.56	0.506	0.804	-58.0	-107.3	2.812

TABLE 4.3

Water type:	saline	
Water density:	$1000 kgm^{-3}$	
Oil type:	commercial diesel	
Oil density:	$830 kgm^{-3}$	
Oil conductivity:	$400 pSm^{-1}$	
Oil dielectric constant:	2.3	
Oil viscosity:	$3.6 \times 10^{-3} Pas$	
Droplet fall distance:	$4.5 \times 10^{-3} m$	
Temperature:	22°C	
Electrode potential:	1kV	
Electrode polarity:	positive	
Electrode separation:	0.05m	
Electric field:	$-20 kVm^{-1}$	
Double layer thickness:	$9.8 \times 10^{-6} m$	
Double layer charge density:	$5.2 \times 10^{-8} Cm^{-2}$	
Diffusion constant:	$1.9 \times 10^{-9} m^2 s^{-1}$	Klinkenberg and van der Minne
Zeta potential:	0.025V	Klinkenberg and van der Minne

Droplet Radius Measured $10^{-5}m$	Droplet Radius From Graph $10^{-5}m$	Terminal Speed Field Off $10^{-3}ms^{-1}$	Terminal Speed Field On $10^{-3}ms^{-1}$	Charge On Droplet $10^{-15}C$	Charge Density On Droplet $10^{-8}Cm^{-2}$	Double Layer Charge $10^{-15}C$
1.37	3.1	0.100	0.098	-0.21	-1.76	0.62
2.41	3.2	0.107	0.109	0.22	1.71	0.67
2.41	3.4	0.118	0.097	-2.42	-16.8	0.75
3.09	3.8	0.148	0.152	0.52	2.91	0.93
3.44	3.8	0.149	0.169	2.59	14.2	0.95
4.12	4.1	0.176	0.220	6.15	28.8	1.11
5.15	5.0	0.259	0.264	0.85	2.68	1.65
5.84	5.7	0.338	0.369	6.04	14.6	2.23
6.18	6.2	0.392	0.349	-9.00	-18.9	2.48
6.87	7.0	0.506	0.592	20.4	34.4	3.20

It should be noted that various effects were not accounted for in the foregoing theory, including electrophoretic retardation and the relaxation effect described below.

4.1.2 Electrophoretic Retardation

Under the influence of an electric field, the ions in the mobile part of the double layer, which surrounds the water droplet, show a net movement in a direction opposite to that of the droplet. This creates a local movement of oil which opposes the motion of the droplet and hence slows it down. This phenomenon is known as electrophoretic retardation and is discussed by Shaw (1980).

4.1.3 Relaxation Effect

The movement of a droplet relative to the mobile part of the double layer, results in distortion of the surrounding layer (a spherical double layer surrounds a stationary droplet). This is due to the fact that a finite relaxation time is required for the original symmetry to be restored by diffusion and conduction of the ions. The resulting asymmetric mobile part of the double layer exerts an additional retarding force on the droplet, known as the relaxation effect, as discussed by Shaw (1980). Relaxation can safely be neglected if the droplet radius is less than one tenth the double layer thickness or greater than three hundred times it, as shown in Figure 4.6.

For intermediate values of droplet radius the effect may be significant. Since the double layer thickness, for water droplets in oil, is assumed to be about $10\mu m$, the radii of droplets, for which relaxation effects may be significant, range from $1\mu m$ to 3mm. This includes most water droplets under consideration.

a = droplet radius
B = droplet mobility
K^{-1} = double layer thickness
ζ = zeta potential
ϵ_c = permittivity of continuous phase
η_c = viscosity of continuous phase

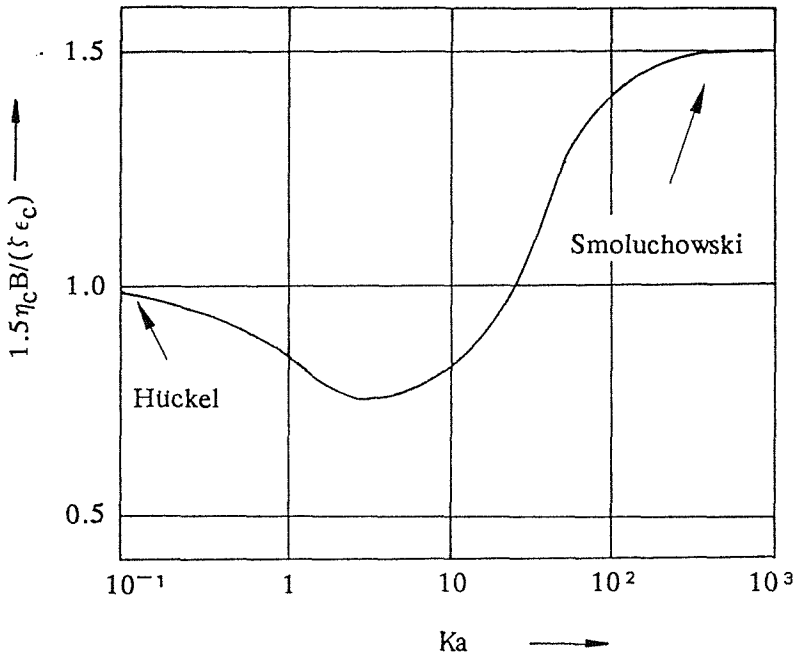

FIGURE 4.6 The relaxation effect (Shaw, 1980).

5. ELECTROSTATIC FORCES ACTING ON WATER DROPLETS IN A W/O EMULSION

The conventional method for calculating the force between two water droplets in a W/O emulsion, the dipole approximation, is only valid if their separation is large in comparison with their sizes. Unfortunately, this does not allow the important situation of droplets in close proximity to be investigated. To overcome this limitation, the Maxwell stress tensor is used to derive the interactive force. The resultant expression is valid for all droplet separations and the dipole approximation can be recovered by considering the limit as the separation becomes large. If the separation is small, a simple force expression can also be deduced. This has only appeared in one publication (Galvin, 1984), as the result of a personal communication to the author of that article from the present author.

Later, the effect of interfacial polarisation on the dipole moment of a droplet is considered, which is usually neglected when calculating the interaction of polarised droplets in an emulsion.

To render the mathematics tractable, droplets are assumed to remain spherical in form, though they are known to deform due to the presence of electrostatic stresses (see Chapter 7).

5.1 The Interactive Force Between Two Conducting Spheres (Bispherical Co-Ordinate Analysis)

Since the water droplets in a W/O emulsion will generally have a large conductivity, with respect to the continuous oil phase, it will presently be assumed that they are perfect conductors.

The most suitable co-ordinate system for the analysis is bispherical co-ordinates (see Appendix A) since these relate directly to the physical system assumed. Laplace's equation in bispherical co-ordinates is as follows (Morse and Feshbach, 1953):

$$\frac{\partial}{\partial\mu}\left[\left[\frac{\sin\eta}{\cosh\mu - \cos\eta}\right]\frac{\partial V}{\partial\mu}\right] + \frac{\partial}{\partial\eta}\left[\left[\frac{\sin\eta}{\cosh\mu - \cos\eta}\right]\frac{\partial V}{\partial\eta}\right]$$

$$+ \frac{\partial}{\partial\lambda}\left[\frac{1}{(\cosh\mu - \cos\eta)\sin\eta}\frac{\partial V}{\partial\lambda}\right] = 0 \qquad (5.1)$$

By letting $V = (2\cosh\mu - 2\cos\eta)^{\frac{1}{2}}v$ eqn. (5.1) can be reduced to (Panchenkov and Tsabek, 1968):

$$\frac{\partial^2 v}{\partial \mu^2} + \frac{\partial^2 v}{\partial \eta^2} + \frac{1}{\sin^2\eta}\frac{\partial^2 v}{\partial \lambda^2} + \cot\eta \frac{\partial v}{\partial \eta} - \frac{v}{4} = 0 \qquad (5.2)$$

If the line of centres of the droplets is aligned with the applied electric field, the solution will be independent of the aziminthal angle λ. The variables μ and η in eqn. (5.2) can be separated by letting $v = A(\mu)B(\eta)$ which yields:

$$\frac{1}{B}\frac{d^2B}{d\eta^2} + \frac{\cot\eta}{B}\frac{dB}{d\eta} = \frac{1}{4} - \frac{1}{A}\frac{d^2A}{d\mu^2} \qquad (5.3)$$

Since the function on the left of eqn. (5.3) is in terms of η only and that on the right only involves μ, it follows that each side of the equation is equal to the same constant $(-n(n+1))$, as μ and η are independent variables. It follows that:

$$\frac{d^2B}{d\eta^2} + \cot\eta \frac{dB}{d\eta} + n(n+1)B = 0 \qquad (5.4)$$

and

$$\frac{d^2A}{d\mu^2} - (n+\tfrac{1}{2})^2 A = 0 \qquad (5.5)$$

Eqn. (5.4) is Legendre's eqn. whose only solutions regular for $\cos\eta = \pm 1$ (corresponding to the z-axis) are the Legendre polynomials $B = P_n(\cos\eta)$ (where $n = 0,1,2,\ldots$). Eqn. (5.5) is easier to deal with and has the following solution:

$$A = M_n\cosh(n + \tfrac{1}{2})\mu + N_n\sinh(n + \tfrac{1}{2})\mu$$

The regular axisymmetric solution of Laplace's equation is therefore a linear combination of the above functions, multiplied by $(2\cosh\mu - 2\cos\eta)^{\frac{1}{2}}$ as follows:

$$V_c = (2\cosh\mu - 2\cos\eta)^{\frac{1}{2}} \sum_{n=0}^{\infty} P_n(\cos\eta)[M_n\cosh(n+\tfrac{1}{2})\mu + N_n\sinh(n+\tfrac{1}{2})\mu] \qquad (5.6)$$

Let E_o be the electric field in the minus z-direction, far from the spheres, where the following is valid:

$$\frac{dV_f}{dz} = E_o \tag{5.7}$$

Eqn. (5.7) is easily solved, its solution being:

$$V_f = V_1 + E_o z = V_1 + \frac{E_o c \sinh\mu}{(\cosh\mu - \cos\eta)} \tag{5.8}$$

The general solution of Laplace's eqn. is therefore the sum of the solutions given by eqns. (5.6) and (5.8):

$$V = V_1 + \frac{E_o c \sinh\mu}{(\cosh\mu - \cos\eta)}$$

$$+ (2\cosh\mu - 2\cos\eta)^{\frac{1}{2}} \sum_{n=0}^{\infty} P_n(\cos\eta)[M_n \cosh(n+\tfrac{1}{2})\mu + N_n \sinh(n+\tfrac{1}{2})\mu] \tag{5.9}$$

Suppose that the two spheres each have radius a and that the separation between their centres is 2b, as shown in Figure 5.1.

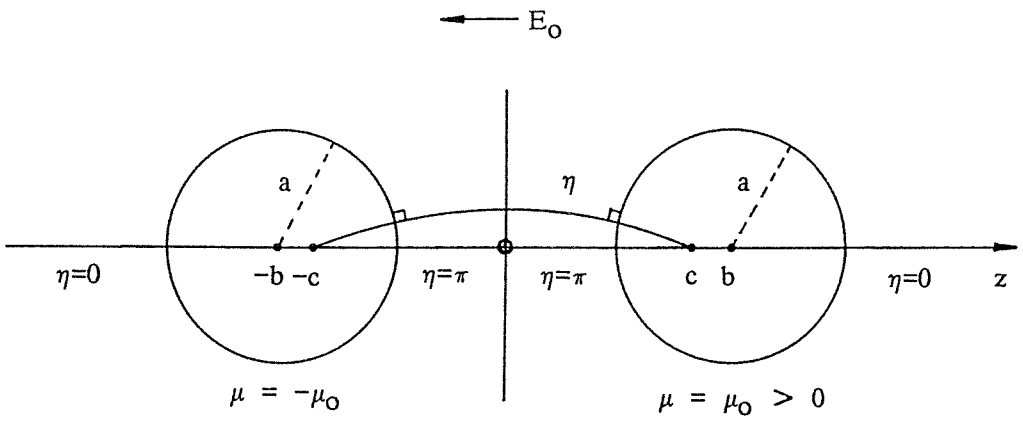

FIGURE 5.1 Representation of two identical spheres in bispherical co-ordinates.

In the bispherical co-ordinate system, $\mu = \mu_o$ defines a spherical surface of radius c $\operatorname{cosech}\mu_o$ whose centre is a distance c $\coth\mu_o$ from the origin (situated half way between the spheres, on the axis of symmetry). Hence a = c $\operatorname{cosech}\mu_o$ and b = c $\coth\mu_o$ in Figure 5.1. The following relations are therefore valid:

$$b = a \cosh\mu_o \tag{5.10}$$

and

$$c = a \sinh\mu_o = b \tanh\mu_o = [b^2 - a^2]^{\frac{1}{2}} \tag{5.11}$$

Suppose that the sphere $\mu = \mu_o$ has potential V_o and that the sphere $\mu = -\mu_o$ has potential $-V_o$. It then follows from eqn. (5.9) that $V_1 = 0$ and $M_n = 0$, for n = 0,1,2,... since only odd functions are valid. Hence the solution of Laplace's equation is:

$$V = \frac{E_o c \sinh\mu}{(\cosh\mu - \cos\eta)} + (2\cosh\mu - 2\cos\eta)^{\frac{1}{2}} \sum_{n=0}^{\infty} P_n(\cos\eta) N_n \sinh(n+\tfrac{1}{2})\mu \tag{5.12}$$

It is now necessary to consider the generating function for Legendre polynomials which may be presented in the form (Panchenkov and Tsabek, 1968):

$$(2\cosh\mu - 2\cos\eta)^{-\frac{1}{2}} = \sum_{n=0}^{\infty} P_n(\cos\eta) e^{-(n+\frac{1}{2})\mu} \tag{5.13}$$

Differentiate eqn. (5.13) partially with respect to μ:

$$\sinh\mu(2\cosh\mu - 2\cos\eta)^{-3/2} = \sum_{n=0}^{\infty} P_n(\cos\eta)(n+\tfrac{1}{2}) e^{-(n+\frac{1}{2})\mu} \tag{5.14}$$

Using eqn. (5.14) it is possible to re-write eqn. (5.12) as follows:

$$V = (2\cosh\mu - 2\cos\eta)^{\frac{1}{2}} \sum_{n=0}^{\infty} P_n(\cos\eta) [E_o c(2n+1) e^{-(n+\frac{1}{2})\mu}$$

$$+ N_n \sinh(n+\tfrac{1}{2})\mu] \tag{5.15}$$

It is now possible to determine the coefficient N_n by letting $V = V_o$ when $\mu = \mu_o$, and using eqns. (5.13) and (5.15):

$$\sum_{n=0}^{\infty} P_n(\cos\eta)\left[-V_o e^{-(n+\frac{1}{2})\mu_o}+E_o c(2n+1)e^{-(n+\frac{1}{2})\mu_o}+N_n \sinh(n+\tfrac{1}{2})\mu_o\right]=0 \qquad (5.16)$$

It follows from eqn. (5.16) that the coefficient of $P_n(\cos\eta)$ must be zero, hence:

$$N_n = [V_o - E_o c(2n+1)]e^{-(n+\frac{1}{2})\mu_o}/\sinh(n+\tfrac{1}{2})\mu_o \qquad (5.17)$$

It will be necessary to determine the electric field in the minus μ-direction (i.e. in the direction of the outward normal from the spherical surface defined by μ) which is given by:

$$E_\mu = -\left[\frac{-1}{h_\mu}\frac{\partial V}{\partial \mu}\right] = \frac{1}{h_\mu}\frac{\partial V}{\partial \mu}$$

Substituting in the Lamé coefficient h_μ from Appendix A:

$$E_\mu = \frac{(\cosh\mu - \cos\eta)}{c}\frac{\partial V}{\partial \mu} \qquad (5.18)$$

In order to determine the value of V_o, it is necessary to invoke the boundary condition that the sphere is uncharged. It is therefore necessary to determine the surface charge density σ, for the sphere $\mu = \mu_o$, which can be expressed as $\sigma = \epsilon E_{\mu_o}$. Before eqn. (5.18) can be used it is necessary to obtain $[\partial V/\partial\mu]\mu = \mu_o$. Thus differentiate eqn. (5.15) partially with respect to μ:

$$\frac{\partial V}{\partial \mu} = \frac{\sinh\mu}{(2\cosh\mu-2\cos\eta)^{\frac{1}{2}}}\sum_{n=0}^{\infty} P_n(\cos\eta)\left[E_o c(2n+1)e^{-(n+\frac{1}{2})\mu}+N_n \sinh(n+\tfrac{1}{2})\mu\right]$$

$$+(2\cosh\mu-2\cos\eta)^{\frac{1}{2}}\sum_{n=0}^{\infty} P_n(\cos\eta)(n+\tfrac{1}{2})\left[-E_o c(2n+1)e^{-(n+\frac{1}{2})\mu}+N_n \cosh(n+\tfrac{1}{2})\mu\right]$$

The first term can be simplified using eqn. (5.15):

$$\frac{\partial V}{\partial \mu} = \frac{V \sinh\mu}{(2\cosh\mu - 2\cos\eta)}$$

$$+(2\cosh\mu-2\cos\eta)^{\frac{1}{2}} \sum_{n=0}^{\infty} P_n(\cos\eta)(n+\tfrac{1}{2}) \left[-E_o c(2n+1) e^{-(n+\frac{1}{2})\mu} + N_n \cosh(n+\tfrac{1}{2})\mu\right]$$

Now use eqn. (5.14) to modify the first term in the above equation:

$$\frac{\partial V}{\partial \mu} = V(2\cosh\mu-2\cos\eta)^{\frac{1}{2}} \sum_{n=0}^{\infty} P_n(\cos\eta)(n+\tfrac{1}{2}) e^{-(n+\frac{1}{2})\mu}$$

$$+(2\cosh\mu-2\cos\eta)^{\frac{1}{2}} \sum_{n=0}^{\infty} P_n(\cos\eta)(n+\tfrac{1}{2}) \left[-E_o c(2n+1) e^{-(n+\frac{1}{2})\mu} + N_n \cosh(n+\tfrac{1}{2})\mu\right]$$

$$\frac{\partial V}{\partial \mu} = (2\cosh\mu-2\cos\eta)^{\frac{1}{2}} \sum_{n=0}^{\infty} P_n(\cos\eta)(n+\tfrac{1}{2}) \left[\left\{V - E_o c(2n+1)\right\} e^{-(n+\frac{1}{2})\mu}\right.$$

$$\left. + N_n \cosh(n+\tfrac{1}{2})\mu\right] \qquad (5.19)$$

Let $\mu = \mu_o$ in the above eqn., in which case $V = V_o$, and use eqn. (5.17) to obtain:

$$\left[\frac{\partial V}{\partial \mu}\right]_{\mu=\mu_o} = (2\cosh\mu_o-2\cos\eta)^{\frac{1}{2}} \sum_{n=0}^{\infty} P_n(\cos\eta)(n+\tfrac{1}{2}) N_n e^{(n+\frac{1}{2})\mu_o} \qquad (5.20)$$

Using eqns. (5.18) and (5.20), the surface charge density σ can now be obtained:

$$\sigma = \epsilon E_{\mu_o} = \frac{\epsilon(\cosh\mu_o - \cos\eta)}{c} \left[\frac{\partial V}{\partial \mu}\right]_{\mu = \mu_o}$$

$$\sigma = \frac{\epsilon}{2c}\,(2\cosh\mu_o - 2\cos\eta)^{3/2} \sum_{n=0}^{\infty} P_n(\cos\eta)(n+\tfrac{1}{2})N_n e^{(n+\frac{1}{2})\mu_o} \qquad (5.21)$$

The charge q carried by the sphere can be found by performing a surface integral of the charge density σ.

$$q = \int_{S_{\mu_o}} \sigma \, dS$$

where

$$dS = \left[\left[h_\eta d\eta\right]\left[h_\lambda d\lambda\right]\right]_{\mu = \mu_o}$$

$$q = \int_o^{2\pi} \int_o^{\pi} \sigma \left[h_\eta h_\lambda\right]_{\mu = \mu_o} \, d\eta d\lambda$$

Substituting in the Lamé coefficients h_η and h_λ from Appendix A:

$$q = c^2 \int_o^{2\pi} \int_o^{\pi} \frac{\sigma \sin\eta \, d\eta d\lambda}{(\cosh\mu_o - \cos\eta)^2}$$

Performing the λ-integration gives:

$$q = 2\pi c^2 \int_o^{\pi} \frac{\sigma \sin\eta \, d\eta}{(\cosh\mu_o - \cos\eta)^2}$$

Substitute in for σ from eqn. (5.21):

$$q = 4\pi\epsilon c \int_o^{\pi} (2\cosh\mu_o - 2\cos\eta)^{-\frac{1}{2}} \sum_{n=0}^{\infty} P_n(\cos\eta)(n+\tfrac{1}{2})N_n e^{(n+\frac{1}{2})\mu_o} \sin\eta d\eta$$

Now use eqn. (5.13) to obtain:

$$q = 4\pi\epsilon c \int_o^{\pi} \sum_{m=0}^{\infty} \sum_{n=0}^{\infty} P_m(\cos\eta) P_n(\cos\eta)(n+\tfrac{1}{2})N_n e^{(n-m)\mu_o} \sin\eta d\eta$$

Using the orthogonality property of Legendre polynomials the above eqn. reduces to:

$$q = 4\pi\epsilon c \sum_{n=0}^{\infty} N_n \qquad (5.22)$$

Now the spheres carry no net charge and so q = 0 in eqn. (5.22) which leads to:

$$\sum_{n=0}^{\infty} N_n = 0 \qquad (5.23)$$

Substituting for N_n using eqn. (5.17) gives:

$$\sum_{n=0}^{\infty} \left[V_o - E_o c(2n+1)\right] e^{-(n+\frac{1}{2})\mu_o} / \sinh(n+\tfrac{1}{2})\mu_o = 0$$

$$\sum_{n=0}^{\infty} 2\left[V_o - E_o c(2n+1)\right]\left[e^{(2n+1)\mu_o} - 1\right]^{-1} = 0$$

$$V_o \sum_{n=0}^{\infty} \left[e^{(2n+1)\mu_o} - 1\right]^{-1} = E_o c \sum_{n=0}^{\infty} (2n+1)\left[e^{(2n+1)\mu_o} - 1\right]^{-1}$$

$$\frac{V_o}{E_o c} = \frac{\sum_{n=0}^{\infty} (2n+1)\left[e^{(2n+1)\mu_o} - 1\right]^{-1}}{\sum_{n=0}^{\infty} \left[e^{(2n+1)\mu_o} - 1\right]^{-1}} \qquad (5.24)$$

This is the required relationship which defines V_o in terms of the other system parameters.

Before going on to derive the interactive force, an example of the use of the analysis so far will be given. If the sphere dimension is made small in comparison with the separation of the spheres (i.e. $\mu_o \to \infty$), the electric field at the surface of the spheres should be identical to that of a single sphere in an

otherwise uniform electric field. The field can be obtained by dividing the surface charge density σ (given by eqn. (5.21)) by ϵ. An approximate form of eqn. (5.21) is used.

$$E_{\mu_o} \simeq \frac{1}{2c} \sum_{n=0}^{\infty} P_n(\cos\eta)(n+\tfrac{1}{2})N_n e^{(n+2)\mu_o}$$

Now N_n, given by eqn. (5.17), can be approximated which leads to:

$$E_{\mu_o} \simeq \frac{1}{c} \sum_{n=0}^{\infty} P_n(\cos\eta)(n+\tfrac{1}{2})\left[V_o - E_o c(2n+1)\right] e^{-(n-1)\mu_o}$$

The limiting behaviour of eqn. (5.24) gives:

$$\frac{V_o}{E_o c} \simeq \frac{\sum_{n=0}^{\infty} (2n+1)e^{-(2n+1)\mu_o}}{\sum_{n=0}^{\infty} e^{-(2n+1)\mu_o}} = \frac{\sum_{n=0}^{\infty} (2n+1)e^{-2n\mu_o}}{\sum_{n=0}^{\infty} e^{-2n\mu_o}} = 1$$

since only the first term in each series contributes as $\mu_o \to \infty$. Thus $V_o = E_o c$ in the limit as $\mu_o \to \infty$ and this may be used to find E_{μ_o} from above:

$$E_{\mu_o} \simeq \sum_{n=0}^{\infty} P_n(\cos\eta)(n+\tfrac{1}{2})[-2E_o n]e^{-(n-1)\mu_o}$$

The only term which contributes in this series, in the limit as $\mu_o \to \infty$, is n = 1 which gives:

$$E_{\mu_o} = -3E_o P_1(\cos\eta) = -3E_o \cos\eta$$

which is the required expression.

The interactive force between the two spheres can be obtained using the Maxwell stress tensor (Panofsky and Phillips, 1978). It is necessary to perform a surface integral of the stress over the surface of one of the spheres ($\mu = \mu_o$) or, alternatively, over the median plane ($\mu = 0$). Both of these surfaces are equipotentials and so the stress tensor considered only has one term. Integration

over the median plane results in a simpler formulation, however, an infinite term is introduced which is cancelled by an identical term corresponding to the bounding surface at infinity (the sphere $\mu = \mu_o$ is effectively enclosed by an infinite box, one side of which is the median plane, the opposite side of which is at infinity). The stress on the median plane, in the minus z-direction is given by:

$$F_m = \frac{\epsilon}{2} \int_{S_o} \left[E_\mu\right]^2_{\mu=0} \, dS$$

In the median plane the elemental area is given by:

$$dS = \frac{c^2 \sin\eta \, d\eta \, d\lambda}{(1 - \cos\eta)^2}$$

since $\mu = 0$. Hence:

$$F_m = \frac{\epsilon c^2}{2} \int_0^{2\pi} \int_0^{\pi} \left[E_\mu\right]^2_{\mu=0} \frac{\sin\eta \, d\eta \, d\lambda}{(1 - \cos\eta)^2}$$

The λ-integration may be performed since the integrand is independent of λ:

$$F_m = \pi\epsilon c^2 \int_0^{\pi} \left[E_\mu\right]^2_{\mu=0} \frac{\sin\eta \, d\eta}{(1 - \cos\eta)^2} \qquad (5.25)$$

The electric field at the median plane can be found, in a convenient form, using eqns. (5.12) and (5.18):

$$\frac{\partial V}{\partial \mu} = E_o c \frac{(1-\cosh\mu\cos\eta)}{(\cosh\mu-\cos\eta)^2} + \frac{\sinh\mu}{(2\cosh\mu-2\cos\eta)^{\frac{1}{2}}} \sum_{n=0}^{\infty} P_n(\cos\eta) N_n \sinh(n+\tfrac{1}{2})\mu$$

$$+ (2\cosh\mu-2\cos\eta)^{\frac{1}{2}} \sum_{n=0}^{\infty} P_n(\cos\eta)(n+\tfrac{1}{2}) N_n \cosh(n+\tfrac{1}{2})\mu$$

Thus from eqn. (5.18)

$$E_\mu = E_o\left[\frac{1-\cosh\mu\cos\eta}{\cosh\mu-\cos\eta}\right] + \frac{\sinh\mu}{2c}\left[2\cosh\mu-2\cos\eta\right]^{\frac{1}{2}}\sum_{n=0}^{\infty} P_n(\cos\eta)N_n\sinh(n+\tfrac{1}{2})\mu$$

$$+\frac{(2\cosh\mu-2\cos\eta)^{3/2}}{2c}\sum_{n=0}^{\infty} P_n(\cos\eta)(n+\tfrac{1}{2})N_n\cosh(n+\tfrac{1}{2})\mu$$

Now at the median plane $\mu=0$ and so:

$$\left[E_\mu\right]_{\mu=0} = E_o + \frac{2^{\frac{1}{2}}}{c}(1-\cos\eta)^{3/2}\sum_{n=0}^{\infty} P_n(\cos\eta)(n+\tfrac{1}{2})N_n \qquad (5.26)$$

Combining eqns. (5.25) and (5.26) gives:

$$F_m = \pi\epsilon c^2E_o^2\int_o^\pi \frac{\sin\eta\, d\eta}{(1-\cos\eta)^2}$$

$$+ 2^{3/2}\pi\epsilon cE_o\int_o^\pi (1-\cos\eta)^{-\frac{1}{2}}\sum_{n=0}^{\infty} P_n(\cos\eta)(n+\tfrac{1}{2})N_n\sin\eta\, d\eta$$

$$+ 2\pi\epsilon\int_o^\pi (1-\cos\eta)\sum_{m=0}^{\infty}\sum_{n=0}^{\infty} P_n(\cos\eta)P_m(\cos\eta)(m+\tfrac{1}{2})(n+\tfrac{1}{2})N_mN_n\sin\eta d\eta$$

The first integral is the infinite one which is cancelled by an identical force on the surface at infinity. By omitting it the interactive force F_i is obtained:

$$F_i = 2^{3/2}\pi\epsilon cE_o\int_o^\pi (1-\cos\eta)^{-\frac{1}{2}}\sum_{n=0}^{\infty} P_n(\cos\eta)(n+\tfrac{1}{2})N_n\sin\eta\, d\eta$$

$$+2\pi\epsilon\int_o^\pi (1-\cos\eta)\sum_{m=0}^{\infty}\sum_{n=0}^{\infty} P_n(\cos\eta)P_m(\cos\eta)(m+\tfrac{1}{2})(n+\tfrac{1}{2})N_nN_m\sin\eta d\eta$$

Use eqn. (5.13) in the first integral and expand the second:

$$F_i = 4\pi\epsilon c E_o \int_o^{\pi} \sum_{m=0}^{\infty}\sum_{n=0}^{\infty} P_m(\cos\eta)P_n(\cos\eta)(n+\tfrac{1}{2})N_n \sin\eta \, d\eta$$

$$+2\pi\epsilon \int_o^{\pi} \sum_{m=0}^{\infty}\sum_{n=0}^{\infty} P_n(\cos\eta)P_m(\cos\eta)(m+\tfrac{1}{2})(n+\tfrac{1}{2})N_nN_m\sin\eta \, d\eta$$

$$-2\pi\epsilon \int_o^{\pi} \sum_{m=0}^{\infty}\sum_{n=0}^{\infty} P_n(\cos\eta)P_m(\cos\eta)(m+\tfrac{1}{2})(n+\tfrac{1}{2})N_nN_m\cos\eta\sin\eta d\eta$$

Use the orthogonality condition for Legendre polynomials in the first two integrals:

$$F_i = 4\pi\epsilon c E_o \sum_{n=0}^{\infty} N_n + 2\pi\epsilon \sum_{n=0}^{\infty} (n+\tfrac{1}{2})N_n^2$$

$$-2\pi\epsilon \int_o^{\pi} \sum_{m=0}^{\infty}\sum_{n=0}^{\infty} P_n(\cos\eta)P_m(\cos\eta)(m+\tfrac{1}{2})(n+\tfrac{1}{2})N_nN_m\cos\eta \, \sin\eta \, d\eta$$

In view of eqn. (5.23) the first summation is zero. The integral above can be performed after using the following recursive identity for Legendre polynomials.

$$(2m+1)\cos\eta \; P_m(\cos\eta) = (m+1)P_{m+1}(\cos\eta) + mP_{m-1}(\cos\eta)$$

Thus:

$$F_i = 2\pi\epsilon \sum_{n=0}^{\infty} (n+\tfrac{1}{2})N_n^2$$

$$-\pi\epsilon\int_o^{\pi} \sum_{m=0}^{\infty}\sum_{n=0}^{\infty} P_n(\cos\eta)\Big[(m+1)P_{m+1}(\cos\eta)+mP_{m-1}(\cos\eta)\Big](n+\tfrac{1}{2})N_nN_m\sin\eta d\eta$$

Using the orthogonality condition for Legendre polynomials in the integral gives:

$$F_i = 2\pi\epsilon \sum_{n=0}^{\infty} (n+\tfrac{1}{2})N_n^2 - \pi\epsilon \sum_{n=0}^{\infty} \left[n\, N_n N_{n-1} + (n+1)N_n N_{n+1} \right]$$

$$F_i = \pi\epsilon \sum_{n=0}^{\infty} N_n \left[(2n+1)N_n - nN_{n-1} - (n+1)N_{n+1} \right] \qquad (5.27)$$

The last two terms in eqn. (5.27) can be combined to give:

$$F_i = \pi\epsilon \sum_{n=0}^{\infty} N_n \left[(2n+1)N_n - 2(n+1)N_{n+1} \right] \qquad (5.28)$$

Having found the general expression for the force of interaction between two conducting spheres, two limits will be considered. The first case corresponds to the separation being large in relation to the dimensions of the spheres ($\mu_o \to \infty$), whereas the second case corresponds to the converse situation ($\mu_o \to 0$).

When considering the force limit, as $\mu_o \to \infty$, it is necessary to use a more precise expression for the term $V_o/(E_o c)$ than was used in the electric field calculation (for which $V_o \simeq E_o c$ was taken). To this end consider the following re-arrangement of eqn. (5.24):

$$\frac{V_o}{E_o c} = 1 + \left\{ \sum_{n=1}^{\infty} 2n \left[e^{(2n+1)\mu_o} - 1 \right]^{-1} \right\} \Big/ \left\{ \sum_{n=0}^{\infty} \left[e^{(2n+1)\mu_o} - 1 \right]^{-1} \right\}$$

For large μ_o this can be approximated by:

$$\frac{V_o}{E_o c} \simeq 1 + \sum_{n=1}^{\infty} 2n e^{-2n\mu_o} \Big/ \sum_{n=0}^{\infty} e^{-2n\mu_o}$$

Approximate the summations by integrals using $\nu = n$:

$$\frac{V_o}{E_o c} \simeq 1 + \int_1^\infty 2\nu e^{-2\mu_o \nu} d\nu \Big/ \int_0^\infty e^{-2\mu_o \nu} d\nu$$

Integration leads to:

$$\frac{V_o}{E_o c} \simeq 1 + \left[\left[\frac{1+2\mu_o}{2\mu_o^2}\right] e^{-2\mu_o}\right] \Big/ \left[\frac{1}{2\mu_o}\right]$$

$$\frac{V_o}{E_o c} \simeq 1 + \left[2 + \frac{1}{\mu_o}\right] e^{-2\mu_o} \simeq 1 + 2e^{-2\mu_o}$$

This expression can now be substituted into eqn. (5.17) to obtain an approximate value of N_n for large μ_o.

$$N_n \simeq 4E_o c\left[e^{-2\mu_o - n}\right] e^{-(2n+1)\mu_o} \qquad (5.29)$$

The first two terms of the force expression, eqn. (5.28), are considered since the rest are of lower order.

$$F_i \simeq \pi\epsilon(N_o^2 - 2N_oN_1 + 3N_1^2 - 4N_1N_2)$$

Now from eqn. (5.29) it follows that:

$$N_o \simeq 4E_o c e^{-3\mu_o},\ N_1 \simeq -4E_o c e^{-3\mu_o} \text{ and } N_2 \simeq -8E_o c e^{-5\mu_o}$$

hence:

$$F_i \simeq \pi\epsilon E_o^2 c^2\left[16e^{-6\mu_o} + 32e^{-6\mu_o} + 48e^{-6\mu_o} - 128e^{-8\mu_o}\right]$$

Neglecting the last term gives:

$$F_i \simeq 96\pi\epsilon E_o^2 c^2 e^{-6\mu_o}$$

Eqn. (5.11), which defines c, is now used:

$$c = a \sinh\mu_o \simeq \frac{a}{2} e^{\mu_o} \text{ for large } \mu_o \text{ thus:}$$

$$F_i \simeq 24\pi\epsilon E_o^2 a^2 e^{-4\mu_o}$$

Eqn. (5.10) is now used which relates b to μ_o:

$$b = a\cosh\mu_o \simeq \frac{a}{2} e^{\mu_o} \quad \text{(for large } \mu_o\text{)}$$

If the separation of the sphere centres is $\Lambda = 2b$ then:

$$e^{-\mu_o} \simeq \frac{a}{2b} = \frac{a}{\Lambda} \quad \text{hence:}$$

$$F_i \simeq 24\pi\epsilon E_o^2 a^2 (a/\Lambda)^4 \qquad (5.30)$$

This equation is just the interactive force between two dipoles that is usually obtained from the dipole approximation (see eqn. (5.53)).

A similar procedure will now be followed to obtain the interactive force for the situation where the separation of the spheres is small in comparison with their dimensions ($\mu_o \to 0$). As before, it is necessary to start off by considering eqn. (5.24), but this time for small μ_o (<0.01). It is possible to approximate the numerator and denominator summations by integrals, however, this is unnecessary since asymptotic representations are given by Buchholz (1957):

$$\sum_{n=0}^{\infty} (2n+1)\left[e^{(2n+1)\mu_o} - 1\right]^{-1} \simeq \frac{\zeta(2)}{2\mu_o^2} + \frac{1}{24} \qquad (5.31)$$

$$\sum_{n=0}^{\infty} \left[e^{(2n+1)\mu_o} - 1\right]^{-1} \simeq \frac{1}{2\mu_o}\left[C + \ell n\left[\frac{2}{\mu_o}\right]\right]$$

$$+ \sum_{m=0}^{N} \frac{B_{2m+2}^2}{(2m+2)!(2m+2)}\left[2^{2m+1} - 1\right]\mu_o^{2m+1} \qquad (5.32)$$

In eqns. (5.31) and (5.32), ζ is the Riemann zeta function ($\zeta(2) = \pi^2/6$), $C \simeq 0.57722$ is Euler's constant, and B_n is a Bernoulli number ($B_0 = 1$, $B_1 = -1/2$, $B_2 = 1/6$, ...). Eqn. (5.24) may therefore be approximated by:

$$\frac{V_o}{E_o c} \simeq \left\{\frac{\pi^2}{12\mu_o^2} + \frac{1}{24}\right\} \Big/ \left\{\frac{1}{2\mu_o}\left[C + \ell n2 + \ell n\left[\frac{1}{\mu_o}\right]\right]\right\} \quad (5.33)$$

Since $\mu_o \to 0$ it can be approximated further:

$$\frac{V_o}{E_o c} \simeq \frac{\pi^2}{6} \frac{(1/\mu_o)}{\ell n(1/\mu_o)} \quad (5.34)$$

In calculating the interactive force, in the limit as $\mu_o \to 0$, it is convenient to use the 3–term force expression given in eqn. (5.27). The coefficients in it, for small μ_o, may be obtained from eqn. (5.17):

$$N_n \simeq \frac{2[V_o - E_o c(2n+1)]}{(2n+1)\mu_o} \quad (5.35)$$

Combining eqns. (5.27) and (5.35) gives:

$$F_i \simeq \frac{4\pi\epsilon}{\mu_o^2} \sum_{n=0}^{\infty} \frac{[V_o - E_o c(2n+1)]}{2(n+1)}$$

$$\times \left\{\left[V_o - E_o c(2n+1)\right] - \frac{n[V_o - E_o c(2n-1)]}{(2n-1)} - \frac{(n+1)[V_o - E_o c(2n+3)]}{(2n+3)}\right\}$$

Grouping terms gives:

$$F_i \simeq \frac{4\pi\epsilon}{\mu_o^2} \sum_{n=0}^{\infty} \frac{V_o[V_o - E_o c(2n+1)]}{(2n+1)} \left[1 - \left[\frac{n}{2n-1}\right] - \left[\frac{n+1}{2n+3}\right]\right]$$

$$F_i \simeq \frac{-8\pi\epsilon}{\mu_o^2} \sum_{n=0}^{\infty} \frac{V_o[V_o - E_o c(2n+1)]}{(2n-1)(2n+1)(2n+3)}$$

$$F_i \simeq \frac{-8\pi\epsilon E_o^2 c^2}{\mu_o^2} \sum_{n=0}^{\infty} \frac{\left[\frac{V_o}{E_o c}\right]\left[\left[\frac{V_o}{E_o c}\right] - (2n+1)\right]}{(2n-1)(2n+1)(2n+3)}$$

Now $c = a \sinh\mu_o \simeq a\mu_o$ for small μ_o hence:

$$F_i \simeq -8\pi\epsilon E_o^2 a^2 \sum_{n=0}^{\infty} \left[\left[\frac{V_o}{E_o c}\right]^2 \frac{1}{(2n-1)(2n+1)(2n+3)} - \left[\frac{V_o}{E_o c}\right] \frac{1}{(2n-1)(2n+3)} \right]$$

The summations may be evaluated as follows:

$$\sum_{n=0}^{N} \frac{1}{(2n-1)(2n+1)(2n+3)} = \frac{-(N+1)^2}{(2N+1)(2N+3)} \rightarrow \frac{-1}{4} \text{ as } N \rightarrow \infty$$

and

$$\sum_{n=0}^{N} \frac{1}{(2n-1)(2n+3)} = \frac{-(N+1)}{(2N+1)(2N+3)} \rightarrow 0 \text{ as } N \rightarrow \infty$$

Hence, for small μ_o, it follows that:

$$F_i \simeq 2\pi\epsilon E_o^2 a^2 \left[\frac{V_o}{E_o c}\right]^2 \qquad (5.36)$$

The previously-derived expression for $V_o/(E_o c)$ (given by eqn. (5.34)), can now be substituted into eqn. (5.36).

$$F_i \simeq \frac{\pi^5}{18} \epsilon E_o^2 a^2 \left[\frac{(1/\mu_o)}{\ell n(1/\mu_o)}\right]^2 \qquad (5.37)$$

When the spheres are very close together ($\mu_o < 0.01$) it is often convenient to relate μ_o to the separation h between the nearest points on the two spheres. Since the spheres each have radius a, and their centres are a distance 2b apart, it follows that:

$$h = 2(b - a)$$

Now eqn. (5.10) gives:

$$b = a \cosh \mu_o = a(1 + 2\sinh^2[\mu_o/2]) \simeq a(1 + \mu_o^2/2)$$

The above two equations give:

$$h \simeq a\mu_o^2 \tag{5.38}$$

Substituting this relation into eqn. (5.37) gives:

$$F_i \simeq \frac{2}{9} \pi^5 \epsilon E_o^2 a^2 \frac{(a/h)}{\ell n^2(a/h)} \tag{5.39}$$

The interactive force between two very close spheres, given by eqn. (5.39), is used later in an analysis of film thinning, applicable to pearl chain formation (see Chapter 6).

Before finishing this bispherical analysis, it is of interest to know the electric field strength between two droplets, almost in contact. This is because electrical breakdown of the intervening film may initiate film rupture and droplet coalescence. The analysis shows that the electric field, in the median plane, on the axis of symmetry, for small μ_o, is:

$$\left[E_\mu\right]_{\substack{\mu=0 \\ \eta=\pi}} = E_o + \frac{2}{c} \sum_{n=0}^{\infty} (-1)^n (2n+1) N_n \tag{5.40}$$

where N_n is approximated by eqn. (5.35) and $V_o/(E_o c)$ is approximated by eqn. (5.34). Similarly, the electric field at the surface of the sphere $\mu = \mu_o$, in the direction of the other sphere is:

$$\left[E_{\mu_o}\right]_{\eta=\pi} \simeq \frac{2}{c} \sum_{n=0}^{\infty} (-1)^n (2n+1) N_n e^{(n+\frac{1}{2})\mu_o} \tag{5.41}$$

Eqns. (5.40) and (5.41) are awkward to deal with since they involve summations, however, the average electric field on the axis of symmetry ($\bar{E}$), has an easier formulation, as shown below (for small μ_o):

$$\bar{E} = \frac{2V_o}{h} = \frac{V_o}{2a\ \sinh^2(\mu_o/2)} \simeq \frac{2V_o}{a\mu_o^2} \qquad (5.42)$$

If eqns. (5.34) and (5.38) are used, eqn. (5.42) becomes:

$$\bar{E} \simeq \frac{2}{3}\pi^2 \frac{(1/\mu_o^2)}{\ell n(1/\mu_o^2)} E_o = \frac{2}{3}\pi^2 \frac{(a/h)}{\ell n(a/h)} E_o \qquad (5.43)$$

It can be appreciated, from the foregoing analysis, that the electric field and the interactive force, between the two spheres, increase without limit as their separation is reduced.

5.2 The Dipole Interaction of Two Uncharged Spheres

The conventional method of calculating the interaction of two uncharged spheres, situated in a uniform applied electric field, will now be investigated. It is considered since the mathematics involved are not too difficult for the case of spheres of differing dipole moment to be analysed, whose line of centres makes an angle θ with respect to the applied field direction. This is important when considering the forces which lead to pearl chain formation (see Chapter 10).

It is a standard result in electrostatics that the dipole moment $\underline{\mu}_i$ of a sphere, of permittivity ϵ_d, situated in a dielectric medium, of permittivity ϵ_c, in the presence of an applied electric field E_o, is as follows (see eqn. (5.126)):

$$\underline{\mu}_i = 4\pi a_i^3 \epsilon_c \left[\frac{\epsilon_d - \epsilon_c}{\epsilon_d + 2\epsilon_c}\right] \underline{E}_o = \frac{4}{3}\pi a_i^3 \alpha_i \underline{E}_o \qquad (5.44)$$

The subscript i in eqn. (5.44) may take the value 1 or 2 depending on which sphere is being considered, the radius of the sphere being a_i.

Another standard result in electrostatics is the interaction energy between two dipoles, of separation Λ, which may be expressed as (Panofsky and Phillips, 1978):

$$U = \frac{1}{4\pi\epsilon_c}\left[\left[\frac{1}{\Lambda^3}\right] \underline{\mu}_1 . \underline{\mu}_2 - \left[\frac{3}{\Lambda^5}\right](\underline{\mu}_1 . \underline{\Lambda})(\underline{\mu}_2 . \underline{\Lambda})\right] \qquad (5.45)$$

Substituting in for the dipole moments, from eqn. (5.44) gives:

$$U = \frac{4\pi\alpha_1\alpha_2 a_1^{\,3} a_2^{\,3} E_o^{\,2}}{9\epsilon_c \Lambda^3}\left[1-3\cos^2\theta\right] = -\frac{2\pi\alpha_1\alpha_2 a_1^{\,3} a_2^{\,3} E_o^{\,2}}{9\epsilon_c \Lambda^3}\left[1+3\cos(2\theta)\right] \quad (5.46)$$

The force in the radial and transverse directions may be established by differentiation of eqn. (5.46) as follows:

$$F_\Lambda = \frac{-\partial U}{\partial \Lambda} = -\frac{2\pi\alpha_1\alpha_2 a_1^{\,3} a_2^{\,3} E_o^{\,2}}{3\epsilon_c \Lambda^4}\left[1+3\cos(2\theta)\right] \quad (5.47)$$

$$F_\theta = \frac{-1}{\Lambda}\frac{\partial U}{\partial \theta} = \frac{-4\pi\alpha_1\alpha_2 a_1^{\,3} a_2^{\,3} E_o^{\,2}}{3\epsilon_c \Lambda^4}\sin(2\theta) \quad (5.48)$$

If $\epsilon_d >> \epsilon_c$ (as in the case of water and oil for which $\epsilon_d = 80\epsilon_o$ and $\epsilon_c \simeq 2.3\epsilon_o$) it follows from eqn. (5.44) that:

$$\alpha_i \simeq 3\epsilon_c \quad (5.49)$$

Eqns. (5.47) and (5.48) may therefore be written as:

$$F_\Lambda = \frac{-6\pi\epsilon_c a_1^{\,3} a_2^{\,3} E_o^{\,2}}{\Lambda^4}\left[1 + 3\cos(2\theta)\right] \quad (5.50)$$

$$F_\theta = \frac{-12\pi\epsilon_c a_1^{\,3} a_2^{\,3} E_o^{\,2}}{\Lambda^4}\sin(2\theta) \quad (5.51)$$

If the line of centres of the droplets is aligned with the applied electric field then $\theta = 0$ and eqn. (5.50) gives:

$$F_\Lambda = -24\pi\epsilon_c a_1^{\,3} a_2^{\,3} E_o^{\,2}/\Lambda^4 \quad (5.52)$$

Suppose the droplets have the same radius $a_1 = a_2 = a$ then:

$$F_\Lambda = -24\pi\epsilon_c E_o^{\,2} a^2 (a/\Lambda)^4 \quad (5.53)$$

This is, of course, the same result as was obtained using bispherical co-ordinates (for large separation of the spheres). The sign change is due to the

fact that, in eqn. (5.53), the force is in the radial direction, the minus sign indicating a force of attraction. Waterman (1965b) has pointed out that, before phase separation takes place, the term $(a/\Lambda)^4$ is constant (since the volume fraction $\varphi = (4\pi/3)(a/\Lambda)^3$), and therefore that the force, on average, is proportional to a^2.

The force of interaction between the spheres, given by eqn. (5.50), is attractive provided $1 + 3\cos(2\theta) \geq 0$, otherwise it is repulsive. The limiting angle θ_o is found from $\cos(2\theta_o) = -1/3$ (see eqn. (5.50)) in which case $\theta_o = 54.7^\circ$ or 125.3°. The force is repulsive for $54.7^\circ \leq \theta \leq 125.3^\circ$ and attractive otherwise, as shown in Figure 5.2.

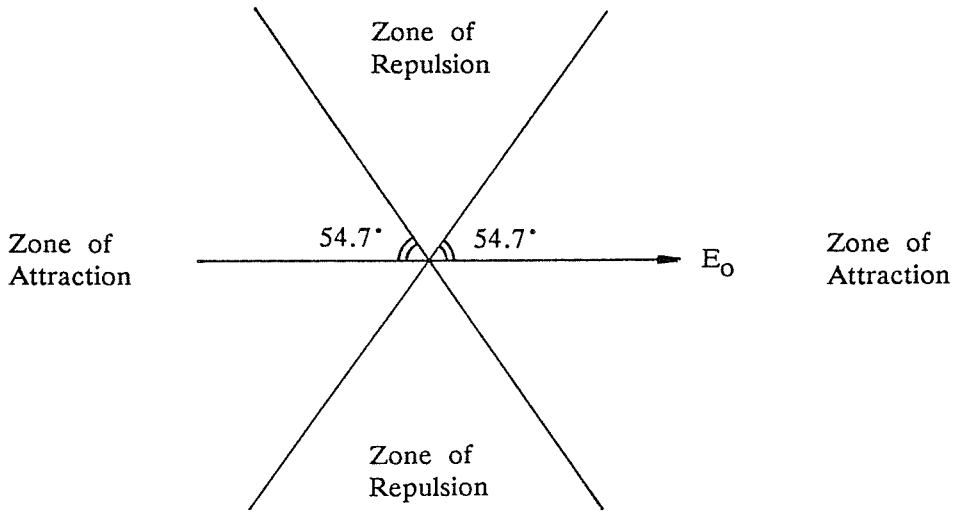

FIGURE 5.2 **Zones of attraction and repulsion associated with two polarized droplets of large separation.**

The force of attraction can be seen to be maximum when $\theta = 0$ and the droplets are aligned with the applied electric field.

The transverse force, given by eqn. (5.51), is of interest since it tends to rotate droplets so that the pair becomes aligned with the applied electric field (which corresponds to the interaction energy, given by eqn. (5.46), being minimum).

The torque, resulting from the transverse force, is maximum when the angle $\theta = 45^\circ$ or 135° and reduces to zero when $\theta = 0^\circ$ or 90°.

Krasny-Ergen (1936) investigated the interaction energy of two identical polarized conducting spheres, situated in a uniform applied electric field. He

compared the interaction energy to the energy associated with Brownian motion kT ($\simeq 4 \times 10^{-21}$J at a temperature of 300K, Boltzmann's constant k being 1.381×10^{-23}JK^{-1}). For droplets of radius 1μm, in contact, the interaction energy is much greater than kT, being $\sim 3 \times 10^{-19}$J for $E = 3 \times 10^{4}$Vm^{-1} and $\epsilon_c = 2.3\epsilon_o$. The two energies only become comparable when the droplet size reduces to about 0.2μm. For droplets larger than this, pearl chain formation should not be hindered by Brownian motion.

Krasny-Ergen's analysis involves the method of images and his expression for interaction energy contains infinite summations. At large separations between the spheres, his expression degenerates to that of eqn. (5.46). For equally-sized spheres in contact, however, the limiting value of his expression is:

$$U = -4\pi\epsilon_c E_o^2 a^3 (f \cos^2\theta + g \sin^2\theta) \qquad (5.54)$$

where:

$$f = 2\left[\sum_{n=1}^{\infty} n^{-3}\right] - 1 = 2\zeta(3) - 1 = 1.404 \text{ and } g = -\sum_{n=2}^{\infty} (-1)^n n^{-3} = -0.099.$$

For comparison purposes, eqn. (5.46) with $\Lambda = 2a$ (which is outside the scope of the equation) may be expressed as:

$$U = -4\pi\epsilon_c E_o^2 a^3 (0.25 \cos^2\theta - 0.125 \sin^2\theta) \qquad (5.55)$$

The coefficients of $\cos^2\theta$ and $\sin^2\theta$ therefore have very different values in the case of spheres in contact. As before, the limiting angle θ_o may be calculated, which defines the zones of attraction and repulsion. Thus, eqn. (5.54) may be solved for U = 0.

$$\tan^2\theta_o = \frac{f}{-g} = \frac{1.404}{0.099}$$

$$\tan\theta_o = 3.766 \text{ which gives } \theta_o = 75.1^\circ \text{ or } 104.9^\circ$$

[N.B. The energy, rather than the force expression, may be used to calculate θ_o here since the radial force is obtained by differentiating the energy partially with respect to Λ (before taking the limit $\Lambda \rightarrow 2a$), which does not affect the angular terms.]

For zero separation, the force of interaction is repulsive when $75.1^\circ < \theta < 104.9^\circ$ and attractive otherwise, as shown in Figure 5.3 (c.f. Figure 5.2 for large separations).

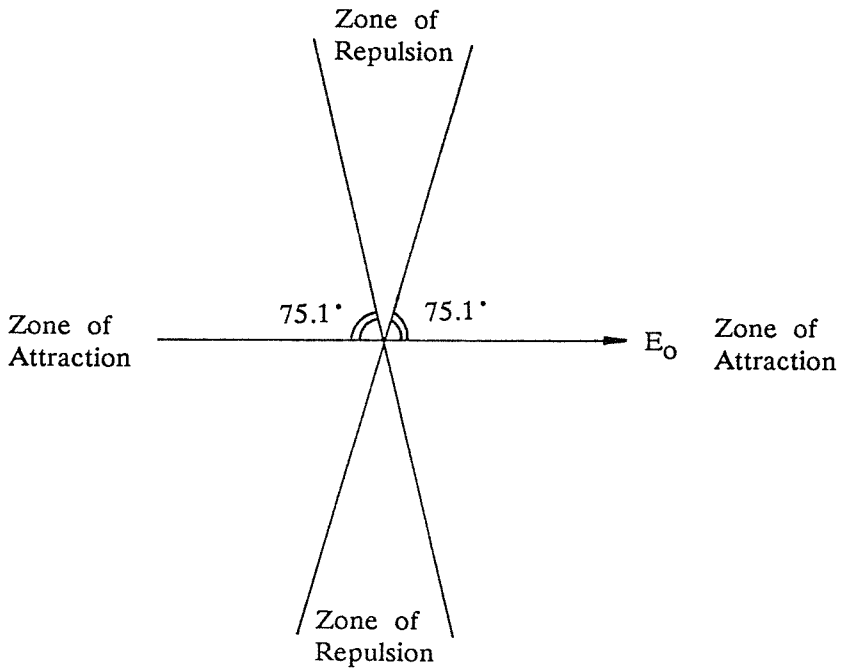

FIGURE 5.3 **Zones of attraction and repulsion associated with two polarised droplets in contact (according to Krasny-Ergen, 1936).**

Davis (1961) has shown, from electrostatic theory, that the force of attraction, directed along the line joining the centres of two identical polarised spheres, is:

$$F_\Lambda = \epsilon_c E_o^2 a^2 [F_1(h/a)\cos^2\theta - F_2(h/a)\sin^2\theta] \qquad (5.56)$$

where h is the minimum separation of the surfaces of the two spheres, and F_1 and F_2 are functions which have been evaluated numerically for various values of h/a.

5.3 Electrophoretic and Dielectrophoretic Forces

Electrophoresis is the translational motion of a charged body in an electric field which may be spatially uniform or non-uniform. The electrophoretic force acting on a charged particle is simply the product of the charge and the local electric field strength:

$$\underline{F} = q\underline{E}$$

If the body is more complicated than a particle, the electrophoretic force may be written in terms of a volume, surface or line integral as follows:

$$\underline{F} = \int \rho \underline{E} d\Omega, \quad \underline{F} = \int \sigma \underline{E} dS \text{ or } \underline{F} = \int p \, \underline{E} d\ell$$

where ρ is the charge per unit volume, σ is the surface charge density and p is the charge per unit length. The direction of the force will depend on the polarity of the electric field.

The total electrostatic force acting on a charged body may not be just the electrophoretic force, since other forces can arise in spatially non-uniform electric fields (i.e. dielectrophoretic forces).

Dielectrophoresis is the translational motion of a neutral body due to the effects of polarization in a non-uniform electric field. The force of interaction between dipoles (eqn. (5.50)) although not normally thought of as being dielectrophoretic must, in fact, be encompassed by that definition since no net charge is carried by either droplet.

The dielectrophoretic force can be derived by considering a simple dipole $\underline{\mu} = q\underline{\ell}$ in a non-uniform electric field $\underline{E}$. The force on the dipole is:

$$\underline{F} = (+q)\underline{E}(\underline{r}+\underline{\ell})+(-q)\underline{E}(\underline{r}) = q[\underline{E}(\underline{r}+\underline{\ell})-\underline{E}(\underline{r})] \qquad (5.57)$$

If $|\underline{\ell}|$ is small, the electric field at the point $\underline{r} + \underline{\ell}$ may be obtained from Taylor's theorem:

$$\underline{E}(\underline{r}+\underline{\ell}) \simeq \underline{E}(\underline{r}) + \ell_1 \frac{\partial \underline{E}(\underline{r})}{\partial x_1} + \ell_2 \frac{\partial \underline{E}(\underline{r})}{\partial x_2} + \ell_3 \frac{\partial \underline{E}(\underline{r})}{\partial x_3}$$

$$\underline{E}(\underline{r}+\underline{\ell}) \simeq \underline{E}(\underline{r}) + \underline{\ell} . \nabla \underline{E} \qquad (5.58)$$

Combining (5.57) and (5.58) gives:

$$\underline{F} = q\underline{\ell} \, . \, \nabla \underline{E} = \underline{\mu} \, . \, \nabla \underline{E} \qquad (5.59)$$

For isotropic dielectrics, where $\underline{E}$ does not vary significantly within the dielectric

volume, the dipole moment is:

$$\underline{\mu} = \alpha\Omega\underline{E} \tag{5.60}$$

where α is the polarisation per unit volume (a constant for the dielectric), Ω is the volume of dielectric considered, and $\underline{E}$ is the electric field within the dielectric.

Consider the following vector identity:

$$\underline{\nabla}(\underline{\mu}.\underline{E}) = \underline{\mu}.\underline{\nabla}\ \underline{E} + \underline{E}.\underline{\nabla}\ \underline{\mu} + \underline{\mu} \times (\underline{\nabla}\times\underline{E}) + \underline{E} \times (\underline{\nabla}\times\underline{\mu})$$

Since the electrostatic field is conservative $\underline{\nabla} \times \underline{E} = 0$ and, by virtue of eqn. (5.60), it follows that $\underline{\nabla} \times \underline{\mu} = 0$, hence:

$$\underline{\nabla}(\underline{\mu}.\underline{E}) = \underline{\mu}.\underline{\nabla}\ \underline{E} + \underline{E}.\underline{\nabla}\ \underline{\mu} = 2\underline{\mu}.\underline{\nabla}\ \underline{E} \tag{5.61}$$

Eqns. (5.59) to (5.61) then give:

$$\underline{F} = \tfrac{1}{2}\ \underline{\nabla}(\underline{\mu}.\underline{E}) = \tfrac{1}{2}\alpha\Omega\underline{\nabla}E^2 \tag{5.62}$$

Thus the dielectrophoretic force is proportional to the volume and polarisability of the dielectric and the gradient of the electric field squared. It follows that the dielectrophoretic force is independent of the electric field polarity, which is not true of the electrophoretic force.

The dielectrophoretic force acting on a spherical particle may be determined once its polarisability has been established. If the particle is small, in relation to the geometry of the electric field, the polarisability may be approximated by assuming that the electric field is locally uniform (apart from the perturbation due to the particle itself). It is a standard result of electrostatics' theory that the dipole moment of a dielectric sphere, placed in a uniform electric field, is (see eqn. (5.126)):

$$\underline{\mu} = 4\pi\epsilon_c \left[\frac{\epsilon_d - \epsilon_c}{\epsilon_d + 2\epsilon_c}\right] a^3\underline{E} \tag{5.63}$$

ϵ_c = permittivity of suspending medium
ϵ_d = permittivity of sphere material
a = radius of sphere
$\underline{E}$ = applied electric field

By comparing eqns. (5.60) and (5.63), and noting that the volume of the sphere is $\Omega = (4/3)\pi a^3$, it is easy to show that the polarisability is:

$$\alpha = 3\epsilon_c(\epsilon_d - \epsilon_c)/(\epsilon_d + 2\epsilon_c) \qquad (5.64)$$

It follows from eqns. (5.62) and (5.63) that the dielectrophoretic force acting on a dielectric sphere is:

$$\underline{F} = 2\pi a^3 \epsilon_d \left[\frac{\epsilon_d - \epsilon_c}{\epsilon_d + 2\epsilon_c}\right] \underline{\nabla} E^2 \qquad (5.65)$$

It can be seen from eqn. (5.65) that the dielectrophoretic force is proportional to the difference in permittivities of the sphere and suspending material. If $\epsilon_d > \epsilon_c$ the particle will move towards the region where the electric field is most divergent; the converse is true if $\epsilon_d < \epsilon_c$. For example, a droplet of water ($\epsilon_d \simeq 80\epsilon_o$), suspended in oil ($\epsilon_c \simeq 2.3\epsilon_o$), will be moved, by dielectrophoresis, to a position where the electric field is stronger and more non-uniform. Since the electric field strength in such regions is invariably high, it follows that the probability of droplet disruption is increased (see Chapter 7).

The dielectrophoretic force, given by eqn. (5.65), is dependent on the term $\underline{\nabla} E^2$ which will be specified by the electrode geometry. For cylindrical geometry, where the inner and outer electrodes have radii r_1 and r_2 respectively, and potential difference V_o, the electric field is:

$$E = \frac{V_o}{r \ell n(r_2/r_1)}$$

from which it follows that:

$$\underline{\nabla} E^2 = \frac{-2}{r^3}\left[\frac{V_o}{\ell n(r_2/r_1)}\right]^2 \hat{\underline{r}} \propto r^{-3}$$

where $\hat{\underline{r}}$ is the unit vector in the radial direction.
For spherical geometry, the radial electric field is:

$$E = \frac{r_1 r_2 V_o}{(r_2 - r_1) r^2}$$

from which it follows that:

$$\underline{\nabla}E^2 = \frac{-1}{r^5}\left[\frac{2r_1r_2V_o}{(r_2 - r_1)}\right]^2 \hat{\underline{r}} \propto r^{-5}$$

In cylindrical and spherical goemetries, therefore, the dielectrophoretic force is critically dependent on the radius concerned. For separation purposes, it is usually preferable to have a more uniform separation force as a function of position. The so-called isomotive geometry, described by Pohl (1978), provides such a force. In isomotive geometry, the potential is described by the following function:

$$V = Ar^{3/2} \sin\left[\frac{3\theta}{2}\right], \quad A \text{ is a constant}$$

The associated electric field is:

$$\underline{E} = \frac{-\partial V}{\partial r}\hat{\underline{r}} - \frac{1}{r}\frac{\partial V}{\partial \theta}\hat{\underline{\theta}} = -\frac{3A}{2} r^{\frac{1}{2}} \sin\left[\frac{3\theta}{2}\right]\hat{\underline{r}} - \frac{3A}{2} r^{\frac{1}{2}} \cos\left[\frac{3\theta}{2}\right]\hat{\underline{\theta}}$$

where $\hat{\underline{\theta}}$ is the unit vector in the transverse direction.
Thus:

$$E^2 = \frac{9A^2}{4} r$$

which leads to:

$$\underline{\nabla}E^2 = \frac{9A^2}{4}\hat{\underline{r}}$$

The dielectrophoretic force, associated with isomotive geometry, is therefore constant and directed radially. A practical electrode arrangement for isomotive geometry is shown in Figure 5.4.

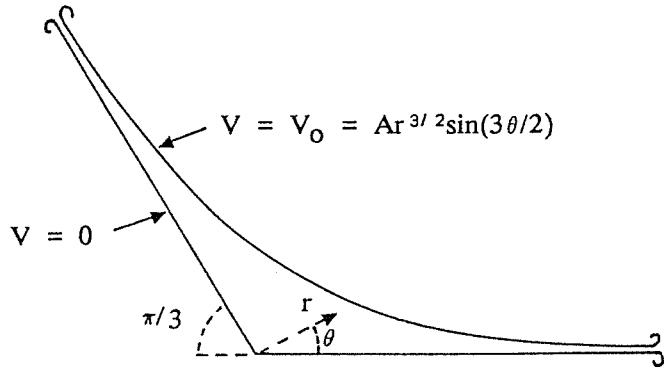

FIGURE 5.4 **Practical electrode arrangement for isomotive geometry.**

5.4 Comparison of Electrophoretic and Dielectrophoretic Forces

Dielectrophoretic forces are usually regarded as being weaker than electrophoretic ones, except in the vicinity of an electrode of high curvature, where the electric field gradients can be very large. A method of comparing the forces, which is relevant to phase separation in emulsions, will now be described. In migratory coalescence (see Chapter 9), the force acting on a charged droplet, in a uniform applied electric field, is electrophoretic and equal to the product of charge and electric field (dielectrophoretic forces are also likely to act on the charged droplet but these are ignored for comparison purposes). The charge assumed to be held by the particle is the maximum charge it can acquire on contacting an energised electrode (Lebedev and Skal'skaya, 1962). Thus the electrophoretic force may be expressed as:

$$F_e = qE = \left[\frac{\pi^2}{6}\right] 4\pi\epsilon_c a^2 E^2 \qquad (5.66)$$

Even though the applied electric field is assumed to be uniform, it is possible for dielectrophoretic forces to arise. This is because the dispersed phase droplets distort the field. When the separation between droplets is small, the electric field gradients can become large, in the neighbourhood of the droplets, causing them to be attracted to one another. The dielectrophoretic force, to be compared with eqn. (5.66), is that associated with two droplets both of which have radius a. The force expression, based on the dipole approximation, has already been established as (see eqn. (5.30)):

$$F_d = 24\pi\epsilon_c E^2 a^2 (a/\Lambda)^4 \qquad (5.67)$$

This assumes that the line of centres, joining the droplets, is aligned with the applied electric field, and that the separation of the droplet centres Λ is not too small (otherwise the dipole approximation becomes invalid).

The electrophoretic and dielectrophoretic forces may be compared by considering their ratio as follows:

$$\frac{F_d}{F_e} = \frac{36}{\pi^2}\left[\frac{a}{\Lambda}\right]^4 \qquad (5.68)$$

Eqn. (5.68) shows that F_d and F_e are comparable at small separations of the droplets (i.e. when $\Lambda \simeq 2a$, the minimum separation).

For small separations, eqn. (5.67) is invalid and it is necessary to represent the dielectrophoretic force using eqn. (5.39), where h is the shortest distance between points on the surfaces of the two droplets.

$$F_d = \frac{2}{9}\pi^5\epsilon_c E^2 a^2 \frac{(a/h)}{\ell n^2 (a/h)} \qquad (5.69)$$

The ratio of F_d and F_e in this case is:

$$\frac{F_d}{F_e} = \frac{\pi^2}{3}\frac{(a/h)}{\ell n^2 (a/h)} \qquad (5.70)$$

Eqn. (5.70) shows that the dielectrophoretic force can far outweigh the electrophoretic force at small separations (i.e. when $h << a$); in fact, the ratio $F_d/F_e \rightarrow \infty$ as $h \rightarrow 0$. At larger separations, however, the electrophoretic force dominates, for example, $F_d/F_e \simeq 3.6 \times 10^{-4}$ when $\Lambda = 10a$.

5.5 The Effect of Interfacial Polarisation on Dipole Moment

If the dispersed phase material cannot be regarded as a perfect conductor (for example distilled water in the context of W/O emulsions), interfacial polarisation (see Chapter 3, Section 3.6.4) will arise, which can affect the dipole moment of a dispersed phase droplet. Forces which depend on the dipole moment such as the interaction force between polarised droplets, will therefore be affected. Since interfacial polarisation is a time-dependent phenomenon, this means that the expression for the dipole moment will be a function of time (and frequency in the case of ac excitation).

The problem can be analysed by considering the section of interface, between the droplet and the suspending medium, shown in Figure 5.5.

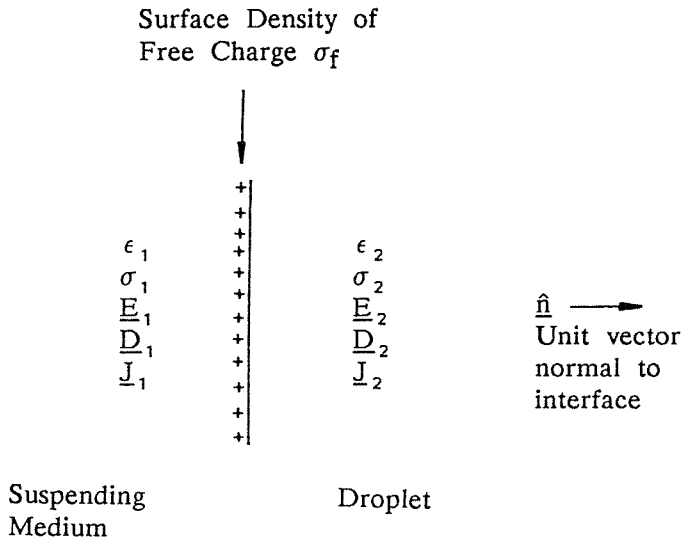

FIGURE 5.5 Incremental interface between droplet and suspending medium showing accumulation of interfacial charge.

The relevant boundary conditions are:

$$\hat{n} \cdot (\underline{D}_1 - \underline{D}_2) = -\sigma_f \tag{5.71}$$

$$\hat{n} \cdot (\underline{J}_1 - \underline{J}_2) = \frac{d\sigma_f}{dt} \tag{5.72}$$

The following constitutive equations also apply which relate the electric displacement $\underline{D}_m$ and the current density $\underline{J}_m$ to the electric field $\underline{E}_m$, as follows:

$$\underline{D}_m = \epsilon_m \underline{E}_m \tag{5.73}$$

$$\underline{J}_m = \sigma_m \underline{E}_m \tag{5.74}$$

where m = 1 or 2, and ϵ_m and σ_m are respectively the permittivity and conductivity of phase m. If the electric field is sinusoidal, of frequency ω, it may be expressed in terms of complex numbers as follows (where $j = \sqrt{-1}$ and $\underline{E}_m$, $\underline{D}_m$, $\underline{J}_m$ and ρ_f are replaced by $\underline{E}_m^*$, $\underline{D}_m^*$, $\underline{J}_m^*$ and ρ_f^* respectively):

$$\underline{E}_m^* = \underline{E}_{om} e^{j\omega t} \qquad (5.75)$$

By eliminating σ_f from eqn. (5.71) and (5.72) then using eqns. (5.73) to (5.75) it follows that:

$$\hat{\underline{n}}.[\epsilon_1^* \underline{E}_1^* - \epsilon_2^* \underline{E}_2^*] = 0 \qquad (5.76)$$

where

$$\epsilon_m^* = \frac{\sigma_m^*}{j\omega} = \epsilon_m - \frac{j\sigma_m}{\omega} \qquad (5.77)$$

The quantities ϵ_m^* and σ_m^* are the complex permittivity and conductivity of phase m (where m = 1 or 2). Poisson's equation and the equation of continuity are also applicable, thus:

$$\underline{\nabla} \cdot \underline{D}_m^* = \rho_f^* \qquad (5.78)$$

and

$$\underline{\nabla} \cdot \underline{J}_m^* + \frac{\partial \rho_f^*}{\partial t} = 0 \qquad (5.79)$$

Eliminating the free charge density ρ_f^* from eqns. (5.78) and (5.79) and using eqns. (5.73) to (5.75) gives:

$$\underline{\nabla} \cdot (\epsilon_m^* \underline{E}_m^*) = 0 \qquad (5.80)$$

Eqn. (5.76) is the boundary condition for no free charge at the interface and eqn. (5.80) is Laplace's equation. Thus, by solving Laplace's equation for the system, using the boundary condition that there is no free charge at the interface, and substituting the complex permittivity ϵ_m^* for ϵ_m, it is possible to account for the effects of interfacial polarisation. For a spherical droplet, the potential outside its surface is conventionally given by (Panofsky and Phillips, 1978):

$$V_1 = \left[\frac{\epsilon_2 - \epsilon_1}{\epsilon_2 + 2\epsilon_1}\right] \frac{a^3}{r^2} E_1 \cos\theta \qquad (5.81)$$

It is therefore necessary to consider the real (or imaginary) part of eqn. (5.82) (depending on whether the applied field corresponds to cos(ωt) or sin(ωt)),

after substitution using eqn. (5.77):

$$V_1^* = \left[\frac{\epsilon_2^* - \epsilon_1^*}{\epsilon_2^* + 2\epsilon_1^*}\right] \frac{a^3}{r^2} E_{01} e^{j\omega t} \cos\theta \qquad (5.82)$$

The dipole moment can then be recovered from the following equation, for the potential of a dipole by letting $V_1 = \mathrm{Re}(V_1^*)$ (applied field related to cos(ωt)):

$$V_1 = \frac{|\underline{\mu}| \cos\theta}{4\pi\epsilon_1 r^2} \qquad (5.83)$$

Hence:

$$|\underline{\mu}| = \frac{4\pi\epsilon_1 r^2}{\cos\theta} \mathrm{Re}\left\{\left[\frac{\epsilon_2^* - \epsilon_1^*}{\epsilon_2^* + 2\epsilon_1^*}\right] \frac{a^3}{r^2} E_{01} e^{j\omega t} \cos\theta\right\}$$

and since $\underline{\mu} \times \underline{E} = 0$ it follows that:

$$\underline{\mu} = 4\pi a^3 \epsilon_1 \mathrm{Re}\left\{\left[\frac{\epsilon_2^* - \epsilon_1^*}{\epsilon_2^* + 2\epsilon_1^*}\right] \underline{E}_1^*\right\} \qquad (5.84)$$

where $\epsilon_m^* = \epsilon_m - j\sigma_m/\omega$ for m = 1 and 2, and $\underline{E}_1^* = \underline{E}_{01} e^{j\omega t}$.

In Pohl's dielectrophoretic force formulation (Pohl, 1978), the multiplicative term ϵ_1 was always replaced by $\bar{\epsilon}_m^*$ (the complex conjugate of ϵ_m^*). Jones and Kallio (1979) preferred to use the formulation of eqn. (5.84). Benguigui and Lin (1981) observed that the expected limits (as $\omega \to 0$ and $\omega \to \infty$) were only obtained using the approach of Jones and Kallio. It is therefore reasonable to assume that Pohl's approach was wrong. In any case, the present derivation shows why the multiplicative term should be ϵ_1 (rather than $\bar{\epsilon}_1^*$) in eqn. (5.84); complex quantities (ϵ_m^*) are only involved in determining the real potential in the suspending medium, after which the dipole moment is related to it using ϵ_1.

This approach will not be followed through, here, since it gives the same result obtained using the analysis which follows; the new approach has the advantage of providing the transient solution as well.

The potentials V_1 outside the droplet and V_2 inside it, and σ_f, the surface density of free charge at the interface, may be expressed in terms of Legendre polynomials as follows (see Figure 5.6 for the geometry).

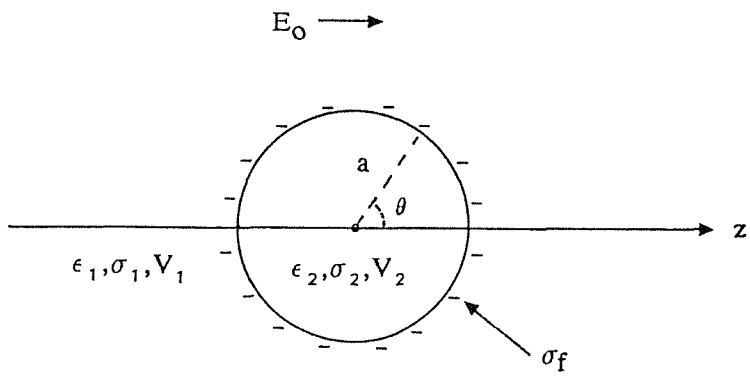

FIGURE 5.6 **Dielectric sphere in uniform electric field.**

$$V_1 = \sum_{n=0}^{\infty} \left[A_n r^n + B_n r^{-(n+1)}\right] P_n(\cos\theta) \qquad (5.85)$$

$$V_2 = \sum_{n=0}^{\infty} \left[C_n r^n + D_n r^{-(n+1)}\right] P_n(\cos\theta) \qquad (5.86)$$

$$\sigma_f = \sum_{n=0}^{\infty} L_n P_n(\cos\theta) \qquad (5.87)$$

To solve the problem, it is necessary to determine the coefficients A_n, B_n, C_n, D_n and L_n. Since V_2 must remain finite as $r \to 0$ it follows that $D_n = 0$ for all n. The potential far from the droplet must be that corresponding to the applied field, that is:

$$V_1 = -Ez = -Er\cos\theta = -ErP_1(\cos\theta) \quad \text{as } r \to \infty$$

Hence $A_n = 0$ for $n \neq 1$ and $A_1 = -E$.

In order to find B_n, C_n and L_n it is necessary to establish three independent relationships between them. The boundary conditions, expressed by

eqns. (5.71) and (5.72) provide two of them, and the third may be found from the further condition that $V_1 = V_2$ when $r = a$. To proceed, the unit vector $\hat{\underline{n}}$, in eqns. (5.71) and (5.72), must be replaced by $-\hat{\underline{r}}$ where $\hat{\underline{r}}$ is the radial unit vector. Similarly, the radial electric field may be expressed as $\hat{\underline{r}} \cdot \underline{E}_m = -\partial V_m/\partial r$ for $m = 1$ and 2. Hence, the required boundary conditions may be expressed as (where ϵ_m and σ_m are respectively the permittivity and conductivity of phase m and m = 1 or 2):

$$\left[\epsilon_1 \frac{\partial V_1}{\partial r} - \epsilon_2 \frac{\partial V_2}{\partial r}\right]_{r=a} = -\sigma_f \qquad (5.88)$$

$$\left[\sigma_1 \frac{\partial V_1}{\partial r} - \sigma_2 \frac{\partial V_2}{\partial r}\right]_{r=a} = \frac{d\sigma_f}{dt} \qquad (5.89)$$

$$\left[V_1 - V_2\right]_{r=a} = 0 \qquad (5.90)$$

Substituting in for V_1, V_2 and σ_f in eqns. (5.88) to (5.90), using eqns. (5.85) to (5.87) gives:

$$\epsilon_1 E P_1(\cos\theta) + \epsilon_1 \sum_{n=0}^{\infty} (n+1) B_n a^{-(n+2)} P_n(\cos\theta) + \epsilon_2 \sum_{n=0}^{\infty} C_n a^{n-1} P_n(\cos\theta)$$

$$= \sum_{n=0}^{\infty} L_n P_n(\cos\theta) \qquad (5.91)$$

$$\sigma_1 E P_1(\cos\theta) + \sigma_1 \sum_{n=0}^{\infty} (n+1) B_n a^{-(n+2)} P_n(\cos\theta) + \sigma_2 \sum_{n=0}^{\infty} C_n a^{n-1} P_n(\cos\theta)$$

$$= -\sum_{n=0}^{\infty} \frac{dL_n}{dt} P_n(\cos\theta) \qquad (5.92)$$

$$EaP_1(\cos\theta) - \sum_{n=0}^{\infty} B_n a^{-(n+1)} P_n(\cos\theta) + \sum_{n=0}^{\infty} C_n a^n P_n(\cos\theta) = 0 \qquad (5.93)$$

By equating coefficients of the Legendre polynomials in eqn. (5.91) to (5.93) the following relations may be obtained (where δ_{1n} is the Kronecker delta):

$$\delta_{1n}\epsilon_1 E + \epsilon_1(n+1)B_n a^{-(n+2)} + \epsilon_2 C_n a^{n-1} = L_n \qquad (5.94)$$

$$\delta_{1n}\sigma_1 E + \sigma_1(n+1)B_n a^{-(n+2)} + \sigma_2 C_n a^{n-1} = -\frac{dL_n}{dt} \qquad (5.95)$$

$$\delta_{1n} aE - B_n a^{-(n+1)} + C_n a^n = 0 \qquad (5.96)$$

Eliminating B_n in eqns. (5.94) and (5.95) using eqn. (5.96) gives:

$$\delta_{1n}(n+2)\epsilon_1 E + [\epsilon_1(n+1)+\epsilon_2]C_n a^{n-1} = L_n \qquad (5.97)$$

and

$$\delta_{1n}(n+2)\sigma_1 E + [\sigma_1(n+1)+\sigma_2]C_n a^{n-1} = -\frac{dL_n}{dt} \qquad (5.98)$$

Eliminating C_n from eqns. (5.97) and (5.98) gives the following differential eqnation:

$$\frac{dL_n}{dt} + \left[\frac{\sigma_1(n+1)+\sigma_2}{\epsilon_1(n+1)+\epsilon_2}\right]L_n = \delta_{1n}(n+2)E\left\{\left[\frac{\sigma_1(n+1)+\sigma_2}{\epsilon_1(n+1)+\epsilon_2}\right]\epsilon_1 - \sigma_1\right\} \qquad (5.99)$$

Now make the following substitution:

$$\tau_n = \frac{\epsilon_1(n+1)+\epsilon_2}{\sigma_1(n+1)+\sigma_2} \qquad (5.100)$$

Hence eqn. (5.99) becomes:

$$\frac{dL_n}{dt} + \frac{L_n}{\tau_n} = \delta_{1n}(n+2)(\epsilon_1/\tau_n - \sigma_1)E \qquad (5.101)$$

Now suppose that the applied electric field is $E = E_o\cos(\omega t)$, then eqn. (5.101) becomes:

$$\frac{dL_n}{dt} + \frac{L_n}{\tau_n} = \delta_{1n}(n+2)(\epsilon_1/\tau_n - \sigma_1)E_o\cos(\omega t) \qquad (5.102)$$

To solve this differential equation make the following substitution:

$$H_n = \delta_{1n}(n+2)(\epsilon_1 - \sigma_1\tau_n)E_o \qquad (5.103)$$

and consider the real part of the following differential equation:

$$\frac{dL_n^*}{dt} + \frac{L_n^*}{\tau_n} = \frac{H_n}{\tau_n} e^{j\omega t} \qquad (5.104)$$

The complementary function of eqn. (5.104) is:

$$L_{nc}^* = M_n^* e^{-t/\tau_n} \qquad (5.105)$$

For the particular integral try:

$$L_{np}^* = Y_n e^{j(\omega t - \chi_n)} \qquad (5.106)$$

Substituting L_{np}^* from eqn. (5.106) into eqn. (5.104) gives:

$$j\omega Y_n e^{j(\omega t - \chi_n)} + \frac{Y_n}{\tau_n} e^{j(\omega t - \chi_n)} = \frac{H_n}{\tau_n} e^{j\omega t}$$

which leads to:

$$Y_n(1 + j\omega\tau_n) = H_n e^{j\chi_n} = H_n(\cos\chi_n + j\sin\chi_n)$$

Thus, equating real and imaginary parts gives:

$$Y_n = H_n\cos\chi_n \qquad (5.107)$$

$$\omega Y_n\tau_n = H_n\sin\chi_n \qquad (5.108)$$

The amplitude Y_n and phase angle χ_n may be found from eqns. (5.107) and

(5.108):

$$Y_n = H_n(1 + \omega^2\tau_n^2)^{-\frac{1}{2}} \tag{5.109}$$

$$\chi_n = \arctan(\omega\tau_n) \tag{5.110}$$

The general solution of eqn. (5.104) is therefore $L_n^* = L_{nc}^* + L_{np}^*$, that is:

$$L_n^* = M_n^* e^{-t/\tau_n} + Y_n e^{j(\omega t - \chi_n)} \tag{5.111}$$

Initially there is no free charge at the interface and so $L_n^* = 0$ when $t = 0$, hence:

$$M_n^* = -Y_n e^{-j\chi_n}$$

This may be substituted back into eqn. (5.111) to give:

$$L_n^* = Y_n\left[e^{j(\omega t - \chi_n)} - e^{-(j\chi_n + t/\tau_n)}\right] \tag{5.112}$$

Now the real part of eqn. (5.112) is the solution of eqn. (5.102) hence:

$$L_n = Y_n\left[\cos(\omega t - \chi_n) - e^{-t/\tau_n}\cos\chi_n\right] \tag{5.113}$$

Substituting in for Y_n is eqn. (5.113) using eqns. (5.109) and (5.103) gives:

$$L_n = \delta_{1n}(n+2)(\epsilon_1 - \sigma_1\tau_n)E_o(1+\omega^2\tau_n^2)^{-\frac{1}{2}}\left[\cos(\omega t - \chi_n) - e^{-t/\tau_n}\cos\chi_n\right] \tag{5.114}$$

Now $\sigma_{1n} = 0$ when $n \neq 1$ and $\delta_{11} = 1$ (properties of Kronecker delta) hence:

$$L_n = 0 \quad \text{for } n \neq 1 \tag{5.115}$$

and

$$L_1 = 3(\epsilon_1 - \sigma_1\tau_1)E_o(1+\omega^2\tau_1^2)^{-\frac{1}{2}}\left[\cos(\omega t - \chi_1) - e^{-t/\tau_1}\cos\chi_1\right] \tag{5.116}$$

A consideration of eqns. (5.115), (5.97) and (5.94) shows that $B_n = C_n = 0$ when $n \neq 1$ and that:

$$3\epsilon_1 E + (\epsilon_2 + 2\epsilon_1)C_1 = L_1 \tag{5.117}$$

and

$$\epsilon_1 E + 2\epsilon_1 B_1 a^{-3} + \epsilon_2 C_1 = L_1 \tag{5.118}$$

Eqns. (5.117) and (5.118) can be used to find B_1 by eliminating C_1, thus:

$$B_1 = a^3\left[\frac{(\epsilon_2-\epsilon_1)E+L_1}{(\epsilon_2+2\epsilon_1)}\right] \tag{5.119}$$

Having determined the coefficients, the potential V_1 outside the droplet, given by Eqn. (5.85), becomes:

$$V_1 = -Er\cos\theta + \frac{B_1}{r^2}\cos\theta \tag{5.120}$$

The second term can be identified as the potential due to a dipole $\underline{\mu}$ where:

$$|\underline{\mu}| = 4\pi\epsilon_1 B_1 \tag{5.121}$$

Thus from eqns. (5.119) and (5.121):

$$|\underline{\mu}| = 4\pi a^3\epsilon_1\left[\frac{(\epsilon_2-\epsilon_1)E + L_1}{(\epsilon_2 + 2\epsilon_1)}\right] \tag{5.122}$$

The dipole moment may therefore be expressed as follows, using eqns. (5.122) and (5.116), bearing in mind that $E = E_o\cos(\omega t)$ and $\underline{\mu} \,//\, \underline{E}_o$:

$$\underline{\mu} = 4\pi a^3\left[\frac{\epsilon_1}{\epsilon_2+2\epsilon_1}\right]\left\{(\epsilon_2-\epsilon_1)\cos(\omega t)\right.$$

$$\left.+3(\epsilon_1-\sigma_1\tau_1)(1+\omega^2\tau_1^2)^{-\frac{1}{2}}\left[\cos(\omega t-\chi_1)-e^{-t/\tau_1}\cos\chi_1\right]\right\}\underline{E}_o \tag{5.123}$$

where the phase angle is defined by eqn. (5.110) with n=1:

$$\chi_1 = \arctan(\omega\tau_1) \tag{5.124}$$

and the time constant is defined by eqn. (5.100) with n=1:

$$\tau_1 = (\epsilon_2+2\epsilon_1)/(\sigma_2+2\sigma_1) \tag{5.125}$$

Eqn. (5.123) defines the dipole moment of the droplet, including transient effects, which results from the application of an electric field $E_o\cos(\omega t)$ at time t=0. Various limits of eqn. (5.123) may be considered as follows. Firstly consider the time limits as $t \to 0$ and $t \to \infty$.

$$\lim_{t\to 0} \underline{\mu} = 4\pi a^3 \epsilon_1 \left[\frac{\epsilon_2 - \epsilon_1}{\epsilon_2 + 2\epsilon_1}\right] \underline{E}_o \tag{5.126}$$

This is the conventional dipole moment as used in eqn. (5.44), with $\epsilon_1 = \epsilon_c$ and $\epsilon_2 = \epsilon_d$.

$$\lim_{t\to\infty} \underline{\mu} = 4\pi a^3 \left[\frac{\epsilon_1}{\epsilon_2+2\epsilon_1}\right] \left\{(\epsilon_2-\epsilon_1)\cos(\omega t) + \frac{3(\epsilon_1-\tau_1\sigma_1)}{(1+\omega^2\tau_1^2)^{\frac{1}{2}}} \cos(\omega t-\chi_1)\right\} \underline{E}_o \tag{5.127}$$

This is the steady-state dipole moment corresponding to an applied electric field of $\underline{E}_o\cos(\omega t)$.

Now consider the frequency limits as $\omega \to 0$ and $\omega \to \infty$.

$$\lim_{\omega\to 0} \underline{\mu} = 4\pi a^3 \left[\frac{\epsilon_1}{\epsilon_2+2\epsilon_1}\right] \left[(\epsilon_2-\epsilon_1) + 3(\epsilon_1-\tau_1\sigma_1)(1-e^{-t/\tau_1})\right] \underline{E}_o \tag{5.128}$$

$$= 4\pi a^3 \epsilon_1 \left[\left[\frac{\epsilon_2-\epsilon_1}{\epsilon_2+2\epsilon_1}\right] + 3\frac{\left[\epsilon_1\sigma_2-\epsilon_2\sigma_1\right]\left[1-e^{-t/\tau_1}\right]}{(\epsilon_2+2\epsilon_1)(\sigma_2+2\sigma_1)}\right] \underline{E}_o \tag{5.129}$$

This is the dipole moment, including transients, for a dc electric field $\underline{E}_o$ applied at time t = 0.

$$\lim_{\omega\to\infty} \underline{\mu} = 4\pi a^3 \epsilon_1 \left[\frac{\epsilon_2-\epsilon_1}{\epsilon_2+2\epsilon_1}\right] \underline{E}_o\cos(\omega t) \tag{5.130}$$

This is the expected dipole moment for high frequencies. Also of interest is the limit as $t \to \infty$ and $\omega \to 0$, which can be obtained from eqns. (5.127), (5.128) or (5.129).

$$\lim_{\substack{\omega\to 0 \\ t\to\infty}} \underline{\mu} = 4\pi a^3 \left[\frac{\epsilon_1}{\epsilon_2+2\epsilon_1}\right]\left[(\epsilon_2-\epsilon_1) + 3(\epsilon_1-\tau_1\sigma_1)\right]\underline{E}_o \qquad (5.131)$$

$$= 4\pi a^3 \epsilon_1 \left[\left[\frac{\epsilon_2-\epsilon_1}{\epsilon_2+2\epsilon_1}\right] + 3\,\frac{\left[\epsilon_1\sigma_2-\epsilon_2\sigma_1\right]}{(\epsilon_2+2\epsilon_1)(\sigma_2+2\sigma_1)}\right]\underline{E}_o$$

$$= 4\pi a^3 \epsilon_1 \left[\frac{\sigma_2 - \sigma_1}{\sigma_2 + 2\sigma_1}\right]\underline{E}_o \qquad (5.132)$$

This is the steady-state dipole moment for a dc electric field. Now the initial dipole moment for a dc electric field can be found by letting $t = 0$ in eqn. (5.129), which happens to give eqn. (5.126). It can be seen that, for a dc applied electric field, the dipole moment varies from:

$$4\pi a^3 \epsilon_1 \left[\frac{\epsilon_2 - \epsilon_1}{\epsilon_2 + 2\epsilon_1}\right]\underline{E}_o \qquad \text{at } t = 0$$

to:

$$4\pi a^3 \epsilon_1 \left[\frac{\sigma_2 - \sigma_1}{\sigma_2 + 2\sigma_1}\right]\underline{E}_o \quad \text{as } t \to \infty.$$

Thus, the force of interaction between two dipoles, which depends on the product of their dipole moments, will vary as a function of time, due to the effects of interfacial polarisation. However, for W/O emulsions the effect is usually small since the dispersed phase permittivity is much greater than that of the continuous phase (i.e. $\epsilon_2 = \epsilon_d >> \epsilon_1 = \epsilon_c$), and the dispersed phase conductivity is much greater than that of the continuous phase (i.e. $\sigma_2 = \sigma_d >> \sigma_1 = \sigma_c$). Thus $(\epsilon_2 - \epsilon_1)/(\epsilon_2 + 2\epsilon_1) \simeq 1$ and $(\sigma_2 - \sigma_1)/(\sigma_2+2\sigma_1) \simeq 1$, with the result that $\underline{\mu} \simeq 4\pi a^3 \epsilon_1 \underline{E}_o$, which is the dipole moment of a perfectly conducting sphere. In W/O emulsions, where the water-like phase cannot be considered to be a perfect conductor, it is necessary to consider the effects of interfacial polarisation as described in the above analysis.

It should be noted that the results of this analysis are reminiscent of the dielectrophoretic force expressions described by Benguigui and Lin (1981), Molinari and Viviani (1978), and Denegri et al. (1977).

6. FILM THINNING THEORY

When a droplet of one liquid settles in a less dense, immiscible liquid onto a flat interface, separating the bulk liquid phases, it rests at the interface for some time before coalescing with the underlying liquid. The rest-time, according to Charles and Mason (1960a), has a roughly Gaussian distribution. In water/oil systems, the mean rest-time generally increases with increasing droplet size, addition of surfactants, and decrease in temperature; it decreases when electrolytes are added to the water phase (Charles and Mason, 1960a).

The temporary stability of the droplet at the interface can be explained in terms of a residual film which drains until the moment of coalescence.

Coalescence of a droplet at a plane interface has been considered by various other workers, such as Brown and Hanson (1965), and Allan and Mason (1961). They investigated the effect of electrostatic forces on coalescence and found that rest-times were reduced. This was because the electrostatic forces enhanced the gravitational force, leading to faster drainage of the intervening film.

Film drainage may also be considered when investigating the coalescence of a pair of droplets. Allan and Mason (1962) used this approach in their studies of droplet coalescence in electric and shear fields.

The geometry of the liquid surfaces, where they face one another, is of importance since this will control film drainage. Deformable droplets are likely to flatten off where one opposes the other at close proximity (see Figure 6.1a). The formation of a dimple (see Figure 6.1b,c) has been observed for gas bubbles approaching a solid interface (Derjaguin and Kussakov, 1939) and the phenomenon has also been seen with liquid droplets and deformable surfaces (Becher, 1977).

Film drainage equations have been considered by many workers, including: Charles and Mason (1960a), Chappelear (1961), Cockbain and McRoberts (1953), Gillespie and Rideal (1956), Elton and Picknett (1957) and Princen (1963). Frankel and Mysels (1962) have calculated the rate of film drainage through the dimple.

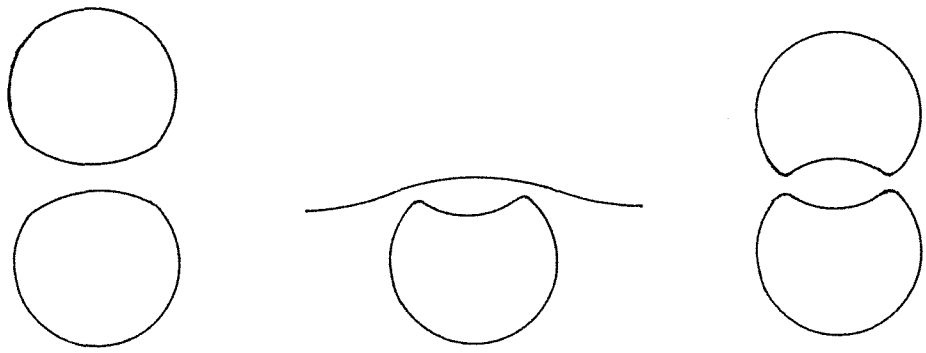

FIGURE 6.1 **(a) Flattening of opposed surfaces of deformable droplets as they approach one another. (b) Dimple formation as a droplet approaches a deformable boundary. (c) Dimple formation in the case of deformable droplets approaching one another.**

The film thinning theory which follows is based on that of Charles and Mason (1960a). They considered a rotationally symmetric rigid surface approaching a stationary rigid plane, as shown in Figure 6.2. The minimum separation of the surfaces at any time was defined as h. The liquid of the intervening film was assumed to be incompressible and to be expelled radially. Inertial effects were ignored and the flow was assumed to be laminar. By equating the mechanical work done by the force F, to the energy dissipated, the following expression was derived.

$$\frac{dh}{dt} = -F\left[6\pi\eta_c \int_0^R (r/\xi)^3 dr\right]^{-1} \qquad (6.1)$$

The upper integration limit R depends on the form of the droplet surface, specified by $z = \xi(r,t)$, as detailed subsequently.

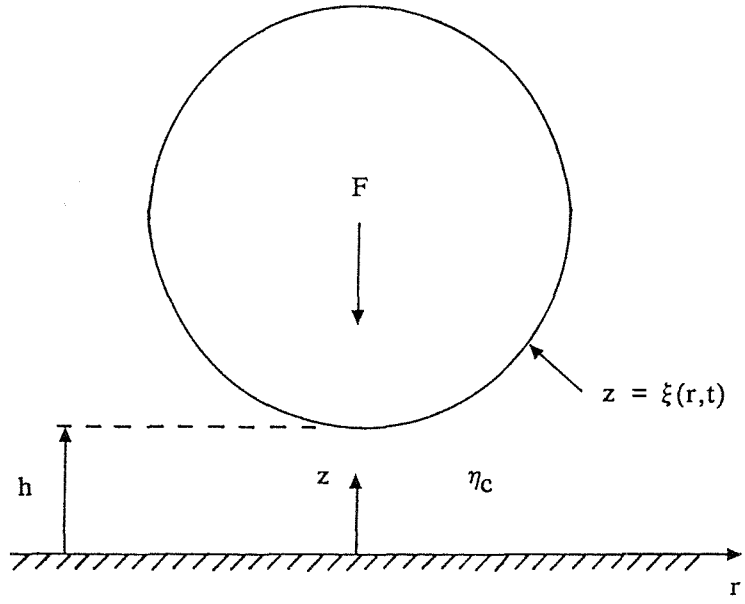

FIGURE 6.2 Sphere approaching a plane boundary under a force of interaction F.

If the lower surface of the droplet assumes a perfectly flat shape, it follows that $\xi(r,t) = h(t)$. For small droplet deformations, the upper limit of integration is:

$$R = \left[\frac{Fa}{2\pi\gamma}\right]^{\frac{1}{2}}$$

where F is the applied force, a is the undeformed droplet radius, and γ is the interfacial tension. Under these circumstances, eqn. (6.1) assumes the form:

$$\frac{dh}{dt} = \frac{-8\pi\gamma^2 h^3}{3\eta_c a^2 F} \qquad (6.2)$$

This equation can be integrated if the force F is known as a function of h, as will be discussed later.

If the lower surface of the droplet is spherical, however, a different approach is necessary. In this case, the upper integration limit is taken as a, the droplet radius, and the surface of the droplet is represented by a parabola (having

radius of curvature a at r = 0) as follows (see Figure 6.3):

$$\xi(r,t) = h(t) + \frac{r^2}{2a}$$

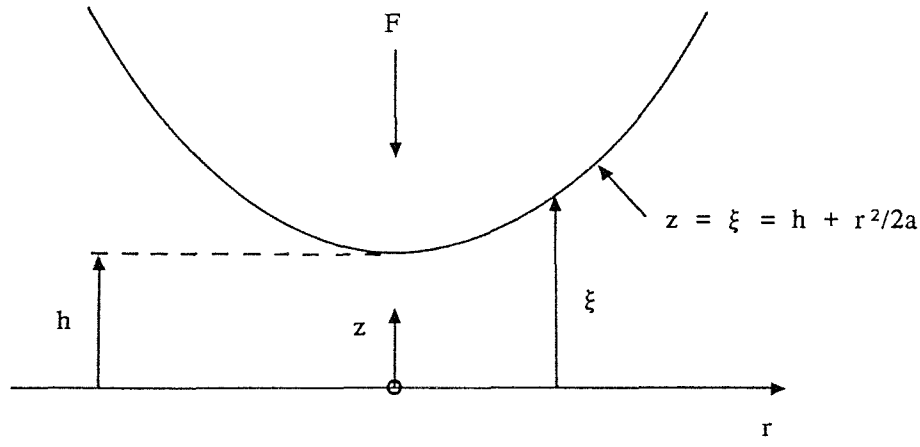

FIGURE 6.3 **Parabolic representation of sphere approaching plane.**

Under these circumstances, eqn. (6.1) has the following form (where it has been assumed that h << a):

$$\frac{dh}{dt} = \frac{-Fh}{6\pi\eta_c a^2} \qquad (6.3)$$

In the case of two droplets approaching one another, one of radius a and the other of radius b, the second droplet must also be represented by a parabola (see Figure 6.4).

The parabolic representations of droplets of radii a and b are:

$$\xi_a(r,t) = h(t) + \frac{r^2}{2a}, \quad \xi_b(r,t) = \frac{-r^2}{2b}$$

and so:

$$\xi(r,t) = \xi_a(r,t) - \xi_b(r,t) = h(t) + \frac{r^2}{2}\left[\frac{1}{a} + \frac{1}{b}\right]$$

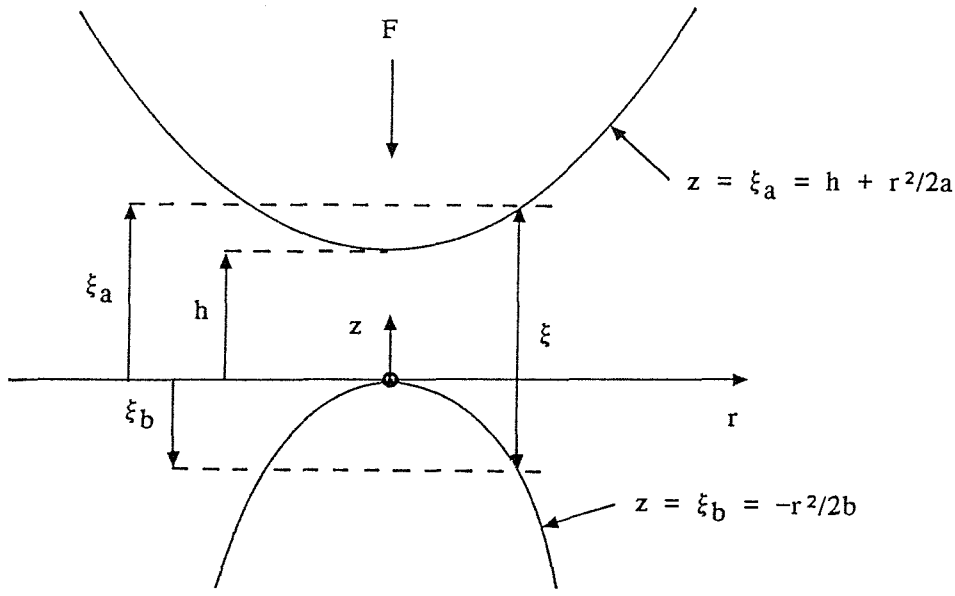

FIGURE 6.4 **Parabolic representation of two spheres approaching one another.**

Under these circumstances, eqn. (6.3) may be modified by letting $1/a \rightarrow 1/a + 1/b$:

$$\frac{dh}{dt} = \frac{-Fh}{6\pi\eta_c}\left[\frac{1}{a} + \frac{1}{b}\right]^2 \qquad (6.4)$$

which is also given by Batchelor (1970). If the droplets are the same size then b = a and eqn. (6.4) becomes:

$$\frac{dh}{dt} = \frac{-2Fh}{3\pi\eta_c a^2} \qquad (6.5)$$

In the subsequent analysis, drainage of the film between two droplets of equal size will be considered. In view of Laplace's law (i.e. $\Delta P = \gamma[1/r_1 + 1/r_2]$ where ΔP is the pressure difference across a surface having principle radii of curvature r_1 and r_2) small droplets are assumed to be undeformable (since ΔP outweighs the effects of externally applied stresses). Large droplets, however, are assumed to be deformable and to flatten off as they approach one another. Thus two regimes are defined: the deformable regime to which eqn. (6.2) applies, and the undeformable regime to which eqn. (6.5) applies. Quite different types of behaviour are expected in these regimes, since eqn. (6.2) involves the interfacial tension γ and the force F appears in the denominator, whereas eqn. (6.5) is independent of γ and F appears in the numerator.

The interactive force between two spheres, polarised in an external electric field, is specified by eqn. (5.39) for droplets in close proximity, that is h < a/100 (the electrostatic force assumes the droplets to be spherical and is therefore an approximation in the case of deformable spheres):

$$F = \frac{2}{9}\pi^5 \epsilon_c E_o^2 a^2 \frac{(a/h)}{\ell n^2(a/h)} \qquad (6.6)$$

Thus, eqn. (6.2) for deformable droplets becomes:

$$\frac{dh}{dt} = \frac{-12\gamma^2 h^4 \ell n^2(a/h)}{\pi^4 \eta_c \epsilon_c a^5 E_o^2} \qquad (6.7)$$

and eqn. (6.5) for undeformable droplets becomes:

$$\frac{dh}{dt} = \frac{-4\pi^4 \epsilon_c a E_o^2}{27\eta_c \ell n^2(a/h)} \qquad (6.8)$$

Eqns. (6.7) and (6.8) can be integrated, to determine h as a function of time, by letting x = a/h.

For deformable droplets, eqn. (6.7) may be integrated to give the time t_d taken by the droplets in moving from an initial separation h_1, to a final separation h_2:

$$t_d = \frac{\pi^4 \eta_c \epsilon_c E_o^2 a^2}{12\gamma^2} \int_{a/h_1}^{a/h_2} \left[\frac{x}{\ell nx}\right]^2 dx \qquad (6.9)$$

The expression above may be integrated by parts then expressed in terms of the logarithmic integral, which is defined as:

$$\ell i(x) = \int_o^x \frac{dy}{\ell ny}$$

Thus eqn. (6.9) becomes:

$$t_d = \frac{\pi^4 \eta_c \epsilon_c E_o^2 a^2}{4\gamma^2} \left[\frac{-x^3}{\ell n(x^3)} + \ell i(x^3)\right]_{a/h_1}^{a/h_2} \qquad (6.10)$$

Similarly, for undeformable droplets, eqn. (6.8) may be integrated to obtain the equivalent time t_u.

$$t_u = \frac{27\eta_c}{4\pi^4\epsilon_c E_o^2}\left[-\frac{1}{x}\left\{1 + (1 + \ell nx)^2\right\}\right]_{a/h_1}^{a/h_2} \qquad (6.11)$$

The times t_d and t_u, plotted as functions of droplet radius a, turn out to be increasing and decreasing respectively, as shown in Figure 6.5.

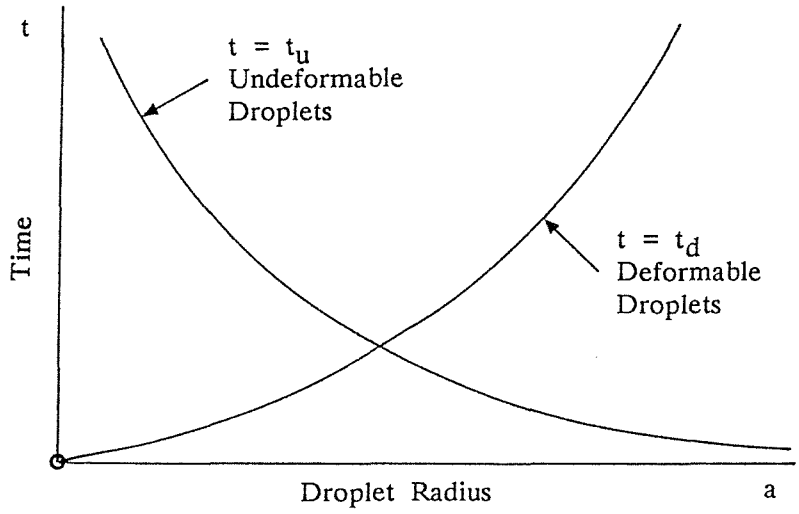

FIGURE 6.5 **The times t_d and t_u plotted as functions of droplet radius a.**

The undeformable and deformable curves, shown in Figure 6.5, suggest that small droplets coalesce readily (being undeformable), and that once they have reached a critical size, a longer time elapses before coalescence can take place (since the droplets flatten off and their relative speed reduces). This is in agreement with the experimental findings that larger droplets are more stable than smaller ones.

It may be possible to increase the maximum separation h, for which these equations are applicable, by improving the definition of F given by eqn. (6.6). This can be accomplished by using the expression given by eqn. (5.33) for $V_o/(E_o c)$, rather than that given by eqn. (5.34), which is used in the short-range force calculation. This would make the final integrations, leading to t_u and t_d, much more difficult though.

The foregoing analysis should be useful for finding the speeds and times involved in the final stages of the approach of two droplets, towards one another, under the influence of electrostatic forces arising from polarisation.

7. DROPLET DISPERSION AND COALESCENCE INHIBITING MECHANISMS WITHIN AN ELECTRO-COALESCER

The phase-separation efficiency of an electro-coalescer is known to increase as the applied electric field strength is increased; this has been established theoretically and experimentally by many workers. However, there is an upper limit beyond which the separation efficiency will reduce, due to droplet dispersion processes (as stated by Waterman (1965b), and Zeef and Visser (1987)) which amounts to re-emulsification. [Some desalter patents, in fact, describe an electrostatic mixing process in which water is added to a W/O emulsion to reduce its salt concentration; the salt water is subsequently removed in an electro-coalescer (Shvetsov et al. (1984), Schmidt (1976), Warren and Prestridge (1980)).] Nevertheless, it is still possible for the maximum phase-separation efficiency to occur, under moderate dispersion conditions, as droplet coalescence is also enhanced; the equilibrium condition is, after all, a balance between dispersive and coalescent processes.

Droplet dispersion can arise in an emulsion as a result of both electrostatic and hydrodynamic stresses. It is likely that both effects will be present simultaneously, though one or other of them may be dominant, depending on the circumstances. To consider the effects independently would therefore be simplistic. However, to do otherwise, apart from qualitatively, would be complicated. Both electrostatic and hydrodynamic stresses manifest themselves in a number of ways which will be dealt with separately.

7.1 Electrostatic Dispersion Mechanisms

An expression for droplet disruption can be obtained from a simple consideration of the forces acting on a sphere (neglecting droplet distortion). By equating the disruptive electrostatic stress to the cohesive surface (or interfacial) tension stress it is possible to obtain:

$$\tfrac{1}{2}\epsilon_o E^2 = \frac{2\gamma}{a} \qquad (7.1)$$

Now, the electric field at the surface of a conducting sphere, in a uniform electric field of strength E_o, is:

$$E = 3E_o \cos\theta$$

where θ is the angle measured from the direction of the applied field. The

electric field strength is maximum at the poles of the sphere ($\theta = 0$ and π) where $|E| = 3E_o$. If this value is used in eqn. (7.1) the following expression is obtained:

$$\frac{a\epsilon_c E_o^2}{\gamma} = \frac{4}{9} = 0.444 \qquad (7.2)$$

The constant on the right-hand side of eqn. (7.2) is likely to be in error due to the fact that droplet distortion has not been accounted for.

The subject has been considered experimentally and theoretically by Taylor (1964). He found that a droplet would elongate, in spheroidal form, to a limited extent (until the ratio of the lengths of the major and minor axes took the value 1.898), before quickly developing an apparently conical end, which would generally oscillate and eject a narrow jet of liquid from its apex (see Section 7.1.1). The critical electric field strength, measured immediately before the onset of the instability (using data from Wilson and Taylor, 1925) was found to agree with the theoretical value (Taylor, 1964) to within 1%.

The deformation and disruption of water droplets, in an electric field, has been investigated by various researchers, often in connection with the distribution of charge in thunderclouds and the mechanisms underlying it (Zeleny (1917), Nolan (1926), Wilson and Taylor (1925), Macky (1931), Rosenkilde (1969), Panchenkov and Tsabek (1968b)).

Zeleny, working with glycerine and water, suspended a droplet from a capillary tube in air and measured the potential required to expel a liquid jet from its surface. He demonstrated that disruption was due to droplet instability rather than ionic current. His experimental data satisfied the following relationship, which he derived using dimensional arguments.

$$\frac{V^2}{a\gamma} = \text{constant} \qquad (7.3)$$

V = potential difference of droplet
a = radius of droplet
γ = surface (or interfacial) tension

Wilson and Taylor (1925) investigated the instability of a soap bubble in an electric field E_o and found that their experimental data were consistent with

eqn. (7.4) (which is presented here in S.I. units and includes the permittivity ϵ_c of the surrounding medium).

$$\frac{a\epsilon_c E_o^2}{\gamma} = 0.205 \qquad (7.4)$$

Macky (1931), working with droplets (of radius 0.85 to 2.6mm) falling in air, and with a vertical or horizontal applied electric field, found that his data satisfied eqn. (7.5) (which is presented here in S.I. units and includes the permittivity ϵ_c of the surrounding medium).

$$\frac{a\epsilon_c E_o^2}{\gamma} = 0.177 \qquad (7.5)$$

The difference between Wilson and Taylor's, and Macky's results may be due to the fact that the droplets in Macky's experiments were falling. They would, therefore, have been subjected suddenly to the electric field and would also have been affected by aerodynamic forces.

Panchenkov and Tsabek (1968b), also developed an expression for the critical electric field strength for disruption of an emulsion droplet. It accounts for the effective dielectric constant of an emulsion due to the presence of dispersed phase droplets (using an expression similar to those shown in Section 3.6.1). The theory is based on an energy approach, U being the sum of the potential energies of the electrostatic and surface tension effects. The balance of forces associated with the two effects is specified by $dU/de = 0$ where e is the droplet eccentricity. The instability condition is specified by $d^2U/de^2 < 0$. By considering these two expressions it is possible to derive the critical electric field strength and the associated droplet eccentricity. The expression for the critical field strength may be written as follows in S.I. units:

$$\frac{a\epsilon_c E_o^2}{\gamma} = \text{constant} \qquad (7.6)$$

This is similar to eqns. (7.2), (7.4) and (7.5). The constant in eqn. (7.6) was specified for an isolated water droplet, and for W/O emulsions of concentration 5%, 10% and 20%; the value of the constant was found to increase with increasing water concentration.

According to Rosenkilde (1969), an uncharged droplet in an applied electric field assumes an approximately prolate ellipsoidal shape. At the point of instability a_1/a_2, the ratio of the lengths of the semi-major and semi-minor axes has a value of 1.838 (c.f. Taylor, 1964) and the following relation holds:

$$\frac{a\epsilon_c E_o^2}{\gamma} = 0.2045 \qquad (7.7)$$

The dimensionless term appearing in eqn. (7.2), (7.4), (7.5), (7.6) and (7.7) is related to the electrostatic Weber number defined below:

$$W_e = 2a\epsilon_c E_o^2/\gamma \qquad (7.8)$$

As the applied electric field strength E_o is increased from zero value, towards the limit, the ratio a_1/a_2 increases as shown in Figure 7.1.

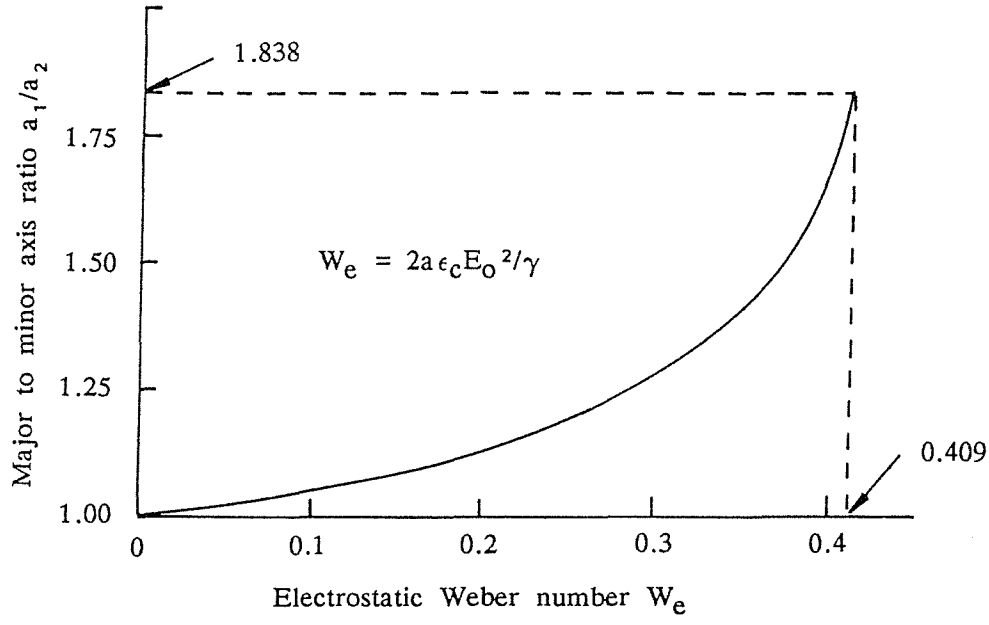

FIGURE 7.1 **Major to minor axis ratio versus electrostatic Weber number (Rosenkilde, 1969).**

The critical electrostatic Weber numbers for Macky (1931), Wilson and Taylor (1925) and Rosenkilde (1969) are 0.354, 0.41 and 0.405 respectively. These are in reasonable agreement with one another. Rosenkilde's value $W_e = 0.405$ is assumed to hold here. Eqn. (7.8), with this value of electrostatic Weber number, has been used to plot the critical electric field as a function of droplet radius (see Figure 7.5 (iv)).

7.1.1 Taylor Cones

Taylor (1964) also analysed the situation where a conducting droplet is deformed, by the applied electric field, to such an extent that it develops a conical protrusion (see Figure 7.2).

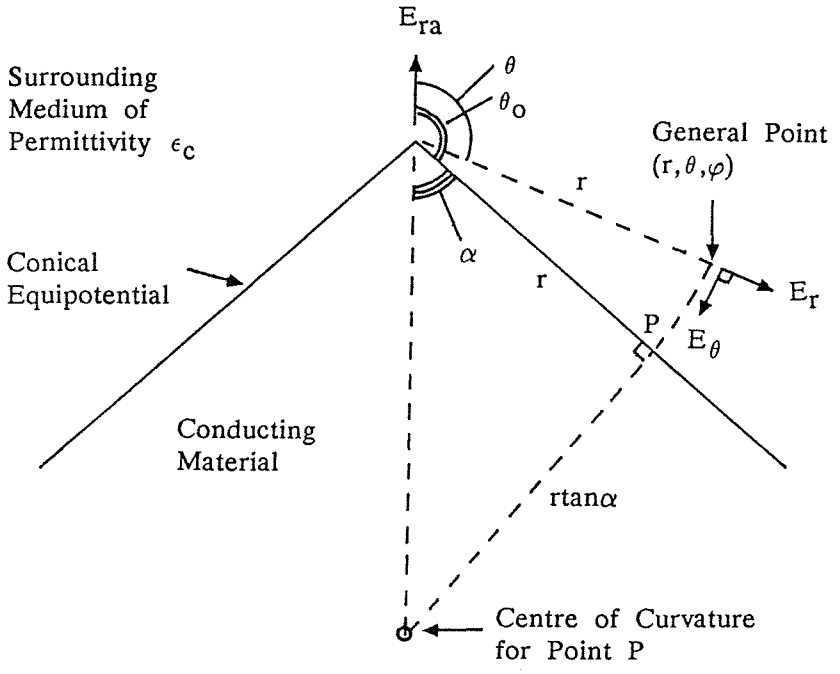

FIGURE 7.2 Taylor cone of semi-vertical angle 49.3°.

The stress at a point on the surface of a cone, due to surface or interfacial tension, is inversely proportional to its distance r from the vertex. If this is to be balanced by electrostatic stress, the electric field normal to the cone must therefore be inversely proportional to the square root of this distance. Such a field is possible if the potential is specified in terms of the conical function $P_{\frac{1}{2}}(\cos\theta)$ (which is a special case of an associated Legendre function) as follows:

$$V = V_o + Ar^{\frac{1}{2}}P_{\frac{1}{2}}(\cos\theta) \qquad (7.9)$$

The conical surface of potential V_o corresponds to $P_{\frac{1}{2}}(\cos\theta) = 0$. Now $P_{\frac{1}{2}}(\cos\theta)$ is finite in the range $0 \leq \theta < \pi$ and has only one zero at $\theta = \theta_o = 130.7099°$ (Taylor (1964)). This fixes the semi-vertical angle of the cone at $\alpha = 49.3°$. The transverse electric field is established from eqn. (7.9) as follows:

$$E_\theta = \frac{-1}{r}\frac{\partial V}{\partial \theta} = \frac{-A}{r^{\frac{1}{2}}}\frac{d}{d\theta} P_{\frac{1}{2}}(\cos\theta) \qquad (7.10)$$

According to Taylor (1964), $dP_{\frac{1}{2}}(\cos\theta)/d\theta = -0.974$ when $\theta = \theta_o$ and so eqn. (7.10) implies:

$$E_{\theta_o} = \frac{-0.974A}{r^{\frac{1}{2}}} \qquad (7.11)$$

The equation governing the balance of interfacial tension and electrostatic stresses is:

$$\frac{\gamma}{r\ \tan\alpha} = \tfrac{1}{2}\epsilon_c E_{\theta_o}^2 \qquad (7.12)$$

Combining eqns. (7.11) and (7.12) gives:

$$\frac{\gamma}{\tan\alpha} = \tfrac{1}{2}\epsilon_c [0.974A]^2 \qquad (7.13)$$

Substituting in $\alpha = 49.3^\circ$ and re-arranging eqn. (7.13) gives:

$$A = 1.347(\gamma/\epsilon_c)^{\frac{1}{2}} \qquad (7.14)$$

The potential at a general point in the surrounding medium is specified by eqns. (7.9) and (7.14):

$$V = V_o + 1.347\left[\frac{\gamma r}{\epsilon_c}\right]^{\frac{1}{2}} P_{\frac{1}{2}}(\cos\theta) \qquad (7.15)$$

The radial electric field may be found from eqn. (7.9) as follows:

$$E_r = -\frac{\partial V}{\partial r} = \frac{-A}{2r^{\frac{1}{2}}} P_{\frac{1}{2}}(\cos\theta) \qquad (7.16)$$

Substituting for A in eqn. (7.16) using eqn. (7.14) gives:

$$E_r = -0.6734\left[\frac{\gamma}{\epsilon_c r}\right]^{\frac{1}{2}} P_{\frac{1}{2}}(\cos\theta) \qquad (7.17)$$

Now $P_{\frac{1}{2}}(\cos\theta) = 1$ when $\theta = 0$ and so the electric field E_{ra} along the axis is given by:

$$E_{ra} = -0.6734 \left[\frac{\gamma}{\epsilon_c r}\right]^{\frac{1}{2}} \qquad (7.18)$$

The axial electric field has an infinite value at the vertex (r=0) where the liquid jet issues from.

Interestingly, eqn. (7.18) may be expressed in a similar way to eqns. (7.2), (7.4), (7.5), (7.6) and (7.7), as follows:

$$\frac{r\epsilon_c E_{ra}^2}{\gamma} = 0.453 \qquad (7.19)$$

however, r is not the droplet radius and E_{ra} is not the field far from the particle, as in the other equations.

Taylor's measurements, with regard to conical interfaces, were made using a special electrode assembly; the lower electrode was basically a frustum of semi-vertical angle 49.3°, whereas the upper one had a profile specified by the relation $r = r_o[P_{\frac{1}{2}}(\cos\theta)]^{-2}$. Experiments were performed on both soap films, and water droplets in transformer oil. Photographic techniques confirmed that the semi-vertical angle of the interface, at the peak of its oscillation, was very close to the predicted value of 49.3°. However, the measured potentials required to produce conical interfaces, were found to be slightly larger than the calculated values (perhaps due to imperfect insulation).

When excess water was present at the apex of the cone, the interface became ogival and the semi-vertical angle was less than 49.3°. However, when there was insufficient water at the apex, the interface tended to be asymmetric and the semi-vertical angle was greater than 49.3°. This goes to show that, even if the electric field is not of the specified form to produce cones, cone-like shapes can be formed on droplets. Waterman's (1965b) paper shows a photograph of two water droplets, in close proximity, one being much larger than the other. The large one, where it faces the small one, has developed a cone-like tip and is dispersing tiny water droplets (towards the smaller droplet). This action relieves the attraction of the spheres for one another and produces charged droplets. Waterman also cites an instability criterion of the kind given by eqns. (7.2), (7.4), (7.5), (7.6) and (7.7), though the numerical value of the constant is not specified.

7.1.2 Inhibition of Coalescence by Contact-Separation Charging

Rather than being a droplet dispersion mechanism, this effect relates to the inhibition of droplet coalescence (both processes are antagonistic to coalescence). It is included here since the expression for the critical field may be expressed in a similar way to the foregoing equations (eqns. (7.2), (7.4), (7.5), (7.6) and (7.7)).

The phenomenon has been described by various researchers such as Sartor (1954), Allan and Mason (1962), and Anisimov and Emel'yanchenko (1976). Two droplets of conducting liquid, suspended in a low-conductivity dielectric material, are attracted to one another (as in dipole coalescence) when an electric field is applied. If the field strength is too great, it is possible for the droplets to come into close proximity and then to be repelled from one another. Apparently, this can even occur when the droplets are in contact and on the point of coalescing (as demonstrated by Anisimov and Emel'yanchenko's photograph). The mechanism responsible for this, suggested by various authors, is an electrostatic discharge. Sartor (1954), who observed water droplets in air, was able to see a fine luminous arc connecting the near surface of the drops, at large field strengths (several kV/cm). Allan and Mason (1962), investigated the coalescence of water droplets in oil. After the initial attraction and repulsion process, in the applied electric field, they found that the droplets could be made to attract one another and coalesce, by removing the field. This confirmed that charge exchange had occurred and that the droplets had become charged. Anisimov and Emel'yanchenko (1976) also investigated the coalescence process of water droplets in oil. They too observed the aforementioned droplet attraction and repulsion behaviour which has been termed contact-separation charging (Zeef and Visser, 1987). A theory was developed by Anisimov and Emel'yanchenko (1976) in which the electrical effects were described using degenerate bipolar co-ordinates. However, the droplets were considered to be spheroids in the calculation of surface tension effects. The expression they derived for the critical electric field strength may be written as:

$$E_o = 0.24 \left[\frac{\gamma}{\epsilon_c a}\right]^{\frac{1}{2}} \qquad (7.20)$$

which can also be presented in the form:

$$\frac{a \epsilon_c E_o^{\,2}}{\gamma} = 0.0576 \qquad (7.21)$$

This expression is shown in Figure 7.5(ii).

7.1.3 Droplet Disruption due to Possession of Charge (Rayleigh Limit)

No analysis has been found in the literature which relates to the disruption of charged droplets in an applied electric field. However, in the absence of an applied field, the Rayleigh limit is valid (Rayleigh, 1882). This may easily be found by equating the disruptive electrostatic stress to the cohesive stress of interfacial tension; internal droplet pressure need not be considered since it becomes zero at the moment of disruption:

$$\tfrac{1}{2}\epsilon_c\left[\frac{q}{4\pi\epsilon_c a^2}\right]^2 = \frac{2\gamma}{a}$$

This leads to the Rayleigh charge limit:

$$q_R = 8\pi(\epsilon_c\gamma a^3)^{\frac{1}{2}} \qquad (7.22)$$

An emulsion droplet, subject also to electrostatic stresses resulting from an applied electric field, will not be able to attain the Rayleigh limit; it will disrupt before the limit is reached.

If droplet charging mechanisms are considered, it is possible to present the Rayleigh limit eqn. (7.22) in the form of the previous equations. The maximum charge a conducting droplet can normally acquire, in an emulsion, is obtained when it contacts a charged electrode. The level of charge is given by the following expression (Lebedev and Skal'skaya (1962), Cho (1964)):

$$q = \left[\frac{\pi^2}{6}\right]4\pi a^2\epsilon_o E_o \qquad (7.23)$$

By substituting this charge into the Rayleigh limit equation (eqn. (7.22)), the desired expresion may be obtained:

$$\frac{a\epsilon_c E_o^2}{\gamma} = \frac{144}{\pi^4} = 1.478 \qquad (7.24)$$

This equation is shown graphically in Figure 7.5(v).

7.2 Hydrodynamic Dispersion Mechanisms

Hydrodynamic dispersion is usually considered in the context of emulsion preparation, within high-shear mixers, where it is desirable. In electro-coalescers, however, which are not usually designed to incorporate mechanical mixing devices (such as paddles, stirrers or turbines), droplet dispersion should be avoided. Even so, it is possible for hydrodynamic dispersion to occur in them.

Hydrodynamic stresses within a W/O emulsion, being processed in a electro-coalescer, may arise directly due to the action of various mechanisms such as: electrostriction (in which pressure gradients are established by non-uniform electric fields), convection, bulk emulsion flow, sedimentation, and electro-osmosis. Such stresses can also be caused, indirectly, by the motion of droplets of the dispersed phase, under the action of the electric field (electrophoresis and dielectrophoresis); electrophoretic effects usually dominate except at short range where dielectrophoretic forces can become large. It should be borne in mind that electrophoretic droplet motion relies mainly on the ability of the droplets to retain their charge (acquired by contacting an electrode for example) since the level of any double-layer charge is likely to be small. This requires that the relaxation time constant (or effectively the conductivity) of the continuous phase should be small. In consequence, electrophoretic droplet motion is likely to be the dominant mechanism in the hydrodynamic dispersion of water droplets in a low-conductivity, continuous oil phase. If the continuous phase conductivity is too large, hydrodynamic droplet dispersion (due to electrostatic effects) may not be possible.

The flow patterns within an electro-coalescer are likely to be highly complex and inhomogeneous; turbulent flow (see Figure 7.3f) may even be possible if the electric field strength is sufficiently large. However, it is conceivable, at least locally, that flow patterns will be similar to certain well-defined flow regimes (see Figure 7.3a-e) such as those investigated by Hinze (1955) and Taylor (1934). Hinze considered deformations caused by viscous stresses and dynamic pressures associated with the following flow regimes:

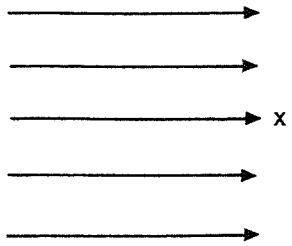

(a) Parallel Flow

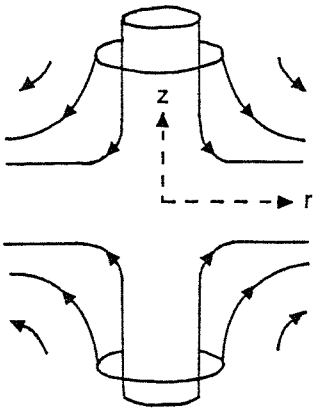

(b) Axisymmetric Hyperbolic Flow

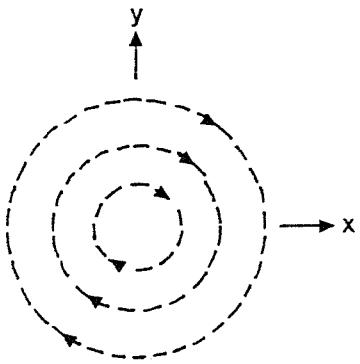

(c) Rotating Flow

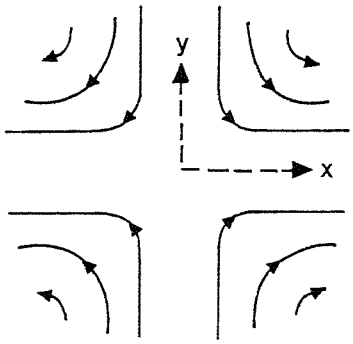

(d) Plane Hyperbolic Flow

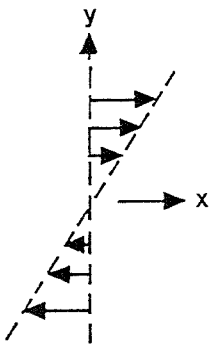

(e) Couette Flow

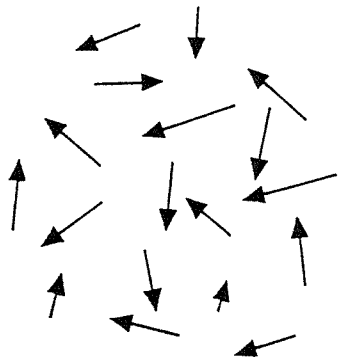

(f) Turbulent Flow

FIGURE 7.3 **Flow patterns which may lead to hydrodynamic droplet disruption.**

Hinze believed that: flow patterns (a), (b) and (c) led to "lenticular" deformation (oblate ellipsoid), flow patterns (d) and (e) led to "cigar-shaped" deformation (prolate ellipsoid), and that droplet breakup was possible for all of these regimes. With regard to emulsification, flow patterns (d) and (e) were thought to be most reasonable (regime (e) being favoured), under conditions of viscous stress (rather than dynamic pressure). Hinze's analysis therefore considered droplet breakup associated with flow patterns (d) and (e). Unfortunately he did not present any analysis for parallel flow, under conditions of viscous stress, which would seem best to match electrophoretic droplet motion.

Hinze also considered turbulent flow (see Figure 7.3f) in which "bulgy" (irregular) deformation of droplets occurred. In turbulent flow, the viscous dissipation of energy occurs in small eddies the length scale δ (typically 25μm, Sherman, 1968) of which was determined by Kolmogoroff (1949) to be:

$$\delta = \left[\frac{\eta_c^{\,3}}{Q\rho_c^{\,3}}\right]^{1/4} \qquad (7.25)$$

where:

Q = rate of energy dissipation per unit mass
η_c = bulk viscosity of continuous phase
ρ_c = density of continuous phase

Hinze considered dispersed phase droplets of diameter $d_m \geq \delta$ for which it was necessary, therefore, to consider dynamic pressure; for small droplets, of diameter $d_m < \delta$, it is appropriate to use the viscous stress formulation. Hinze's analysis considered the force per unit area Ψ to be responsible for deformation and that this was counteracted by the stress γ/d due to interfacial tension γ (d being the diameter of the droplet). The stress Ψ induced (within the droplet) internal flow of speed typically $(\Psi/\rho_d)^{\frac{1}{2}}$, where ρ_d is the density of the dispersed phase. This was associated with viscous stresses of the order of magnitude $\eta_d(\Psi/\rho_d)^{\frac{1}{2}}/d$, where η_d is the bulk viscosity of the dispersed phase. Thus, droplet deformation was assumed to be controlled by the following stresses:

(i) Ψ deforming stress exerted by continuous phase
(ii) γ/d cohesive stress due to interfacial tension
(iii) $\eta_d(\Psi/\rho_d)^{\frac{1}{2}}/d$ viscous stress within droplet.

These can be used to define three dimensionless groups, two of which are

independent. The independent dimensionless groups used are shown below.
Generalised Weber group (i)/(ii):

$$W = \Psi d/\gamma \tag{7.26}$$

Viscosity group (iii)/[(i)(ii)]$^{\frac{1}{2}}$:

$$\sum = \eta_d/(\rho_d \gamma d)^{\frac{1}{2}} \tag{7.27}$$

which is independent of Ψ.

The critical value of the Weber group W_c, at droplet breakup, can be related to the viscosity group $\sum$ as follows:

$$W_c = C[1 + I(\sum)] \tag{7.28}$$

where C is a constant and I is a function (such that $I(\sum) \rightarrow 0$ as $\sum \rightarrow 0$) both of which depend on the flow conditions external to the droplet.

The generalised Weber group admits of two definitions depending on whether Ψ is a stress due to viscous forces (in which case $\Psi = \eta_c S$ where S is the maximum velocity gradient in the external flow field) or, as in the conventional definition, a stress due to dynamic pressure (in which case $\Psi = \rho_c u^2$ where u is the flow speed of the continuous phase in relation to the droplet).

Taylor (1934), in his investigations into droplet deformation and breakup under plane hyperbolic flow and Couette flow, initiated the use of the unconventional form of the Weber group. Hinze interpreted Taylor's results by plotting the critical Weber group W_c as a function of viscosity ratio (η_d/η_c). For plane hyperbolic flow, W_c has a minimum value of roughly 0.2, which corresponds to $\eta_d/\eta_c \simeq 5$, whereas for Couette flow, W_c has a minimum value of roughly 0.7, corresponding to $\eta_d/\eta_c \simeq 2$. Little accuracy is possible in view of the scant data. For low values of η_d/η_c (= 0.0003) there is no droplet breakup for either flow type. Similarly, there is no breakup under Couette flow, for large values of η_d/η_c (= 20). For these types of flow (in which droplet deformation is controlled by viscous forces), it can be concluded that the critical Weber number W_c is a function of viscosity ratio η_d/η_c, and that W_c has a minimum value in the region of 0.2 to 0.7, for η_d/η_c in the region of 2 to 10.

Hinze's investigation into turbulent flow, under conditions of non-coalescence (as for low concentration emulsions), led him to consider $\overline{u^2(d_m)}$, the mean square value of the turbulent velocity fluctuations, over a distance d_m corresponding to the maximum droplet diameter, averaged over the whole flow field. Kolmogoroff (1949) deduced the following expression which relates the average kinetic energy to this distance (in the case of isotropic homogeneous turbulence):

$$\overline{u^2(d_m)} = C_1(Qd_m)^{2/3} \qquad (7.29)$$

where, according to Batchelor (1951), $C_1 \simeq 2$.

Under these conditions, the value of the function I in eqn. (7.28) turns out to be small and so it follows that the critical Weber group is given by:

$$W_c = \rho_c \overline{u^2(d_m)} d_m/\gamma = C$$

Using eqn. (7.29) and re-arranging gives:

$$d_m(\rho_c/\gamma)^{3/5} Q^{2/5} = (C/C_1)^{3/5} \qquad (7.30)$$

Hinze fitted eqn. (7.30) to Clay's experimental data (obtained using two coaxial cylinders, the inner one of which rotated) and found that the constant $(C/C_1)^{3/5}$ took the value 0.725 with a standard deviation of 0.315 (Clay, 1940). From this it follows that the critical Weber group $W_c = 2(0.725)^{5/3} \simeq 1.2$. The value of the numerical constant C is likely to vary from one apparatus to another as is W_c. However, the value found above, for the critical Weber number ($W_c \simeq 1.2$), is not much in excess of the values found previously, for droplet breakup in plane hyperbolic flow ($W_c \simeq 0.2$) and Couette flow ($W_c \simeq 0.7$).

For turbulent flow, in which $d_m \lesssim \delta$, viscous effects are dominant and Kolmogoroff (1949) suggested the use of the following expression for the mean square velocity difference over the distance d_m:

$$\overline{u^2(d_m)} = C_2\rho_c Q d_m^2/\eta_c \qquad (7.31)$$

Shinnar (1961) used this expression, in conjunction with Taylor's unconventional definition of the Weber group, in a manner similar to the following:

$$W = \frac{\eta_c}{d_m} \left[\overline{u^2(d_m)}\right]^{\frac{1}{2}} \times d_m/\gamma$$

Using eqn. (7.31) this becomes:

$$W = C_2{}^{\frac{1}{2}}(\rho_c \eta_c Q)^{\frac{1}{2}} d_m/\gamma \qquad (7.32)$$

Shinnar expressed this as (Sherman, 1968):

$$d_m \left[\frac{\rho_c \eta_c Q}{\gamma^2}\right]^{\frac{1}{2}} = \text{constant} \qquad (7.33)$$

The empirical approach, which leads to the value $W_c \simeq 1.2$ for the case when dynamic pressures dominate viscous stresses, is not available in this case and so no value for the critical Weber group W_c is given. However, from the previously-established values of W_c (0.2, 0.7 and 1.2) it does not seem too unreasonable to consider W_c to be in the range 0.2 to 1.

7.2.1 Presentation of Hydrodynamic Dispersion in Terms of The Expression: $a\epsilon_c E_o{}^2/\gamma$ = constant

It is possible to discuss hydrodynamic dispersion processes, in relation to the applied electric field, by considering the maximum charge a droplet can acquire in an emulsion. This charge is that obtained by the droplet on contacting a charged electrode and is given by eqn. (7.23). The electrical force (electrophoretic) driving the droplet may then be expressed as:

$$F = qE_o = \frac{2}{3} \pi^3 \epsilon_c a^2 E_o{}^2 \qquad (7.34)$$

The terminal droplet speed u may be obtained by equating the driving force F to the drag force F_d. This, however, is governed by Stokes' law if the Reynolds number $R = 2a\rho_c u/\eta_c \leq 1$ otherwise the drag coefficient formulation must be used.

$$F_d = 6\pi\eta_c au \qquad \text{for } R \leq 1 \qquad (7.35)$$

or generally:

$$F_d = \tfrac{1}{2}\rho_c u^2(\pi a^2)C_d \qquad (7.36)$$

where C_d is the drag coefficient of a sphere.

In general, or for Reynolds number R>1, the terminal speed is (from eqns. (7.34) and (7.36)):

$$u = 2\pi E_o \left[\frac{\epsilon_c}{3\rho_c C_d}\right]^{\frac{1}{2}} \qquad (7.37)$$

However, the critical Weber group W_c may be expressed as (assuming the conventional definition):

$$W_c = 2a\rho_c u^2/\gamma = \frac{8\pi^2 a \epsilon_c E_o^{\,2}}{3\gamma C_d} \qquad (7.38)$$

which can be re-arranged to give:

$$\frac{a\epsilon_c E_o^{\,2}}{\gamma} = \frac{3W_c C_d}{8\pi^2} \qquad (7.39)$$

A numerical value may be assigned to the right-hand side of eqn. (7.39) by considering the drag coefficient (see Figure 7.4) which is a function of the Reynolds number:

$$R = 2a\rho_c u/\eta_c = (2a\gamma\rho_c W_c)^{\frac{1}{2}}/\eta_c$$

The value of the critical Weber group W_c is assumed to be in the range 0.2 - 1; the end points of this range are used for specifying the hydrodynamic droplet breakup curves, shown in Figures 7.5(i) and (iii), which are based on eqn. (7.39). The curves are plotted from the data in Tables 7.1 and 7.2 which correspond to the critical Weber numbers 0.2 and 1 respectively. The parameters used are: ϵ_c = $2.3 \times 8.854 \times 10^{-12}Fm^{-1}$, $\gamma = 37 \times 10^{-3}Nm^{-1}$, $\eta_c = 3 \times 10^{-3}Pas$ and ρ_c = $830kgm^{-3}$.

The drag coefficients are determined from the functions specified by eqns. (7.40) to (7.42) (Clift et al., 1978) where w = logR.

For $0.01 < R \leq 20$:

$$\log(C_d R/24-1) = -0.881 + 0.82w - 0.05w^2 \qquad (7.40)$$

For $20 \leq R \leq 260$:

$$\log(C_d R/24-1) = -0.7133 + 0.6305w \qquad (7.41)$$

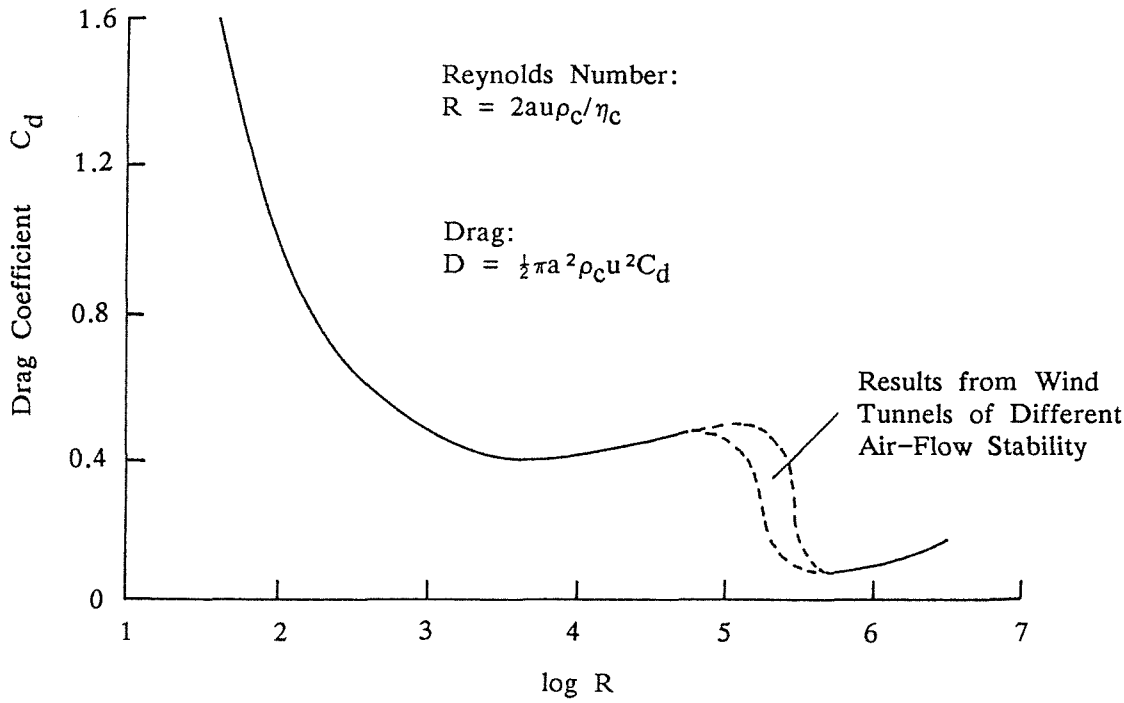

FIGURE 7.4 Drag coefficient for a solid sphere as a function of Reynolds number.

For $260 \leq R \leq 1500$:

$$\log C_d = 1.6435 - 1.1242w + 0.1558w^2 \qquad (7.42)$$

For the droplet size range of interest (1 μm – 1mm), the Reynolds number is greater than unity (see Tables 7.1 and 7.2) which means the hydrodynamic dispersion does not normally occur in the Stokes' law regime.

a(m)	R	$C_d(R)$	$E_o(Vm^{-1})$
10^{-7}	0.3694	68.66	9.736×10^{7}
10^{-6}	1.168	23.62	1.806×10^{7}
10^{-5}	3.694	8.901	3.506×10^{6}
10^{-4}	11.68	3.694	7.142×10^{5}
10^{-3}	36.94	1.874	1.609×10^{5}
10^{-2}	116.8	0.6084	3.725×10^{4}

TABLE 7.1 Hydrodynamic disruption $W_c = 0.2$

a(m)	R	$C_d(R)$	$E_o(Vm^{-1})$
10^{-7}	0.8261	32.32	1.494×10^{8}
10^{-6}	2.612	11.79	2.853×10^{7}
10^{-5}	8.261	4.865	5.795×10^{6}
10^{-4}	26.12	2.310	1.263×10^{6}
10^{-3}	82.61	1.200	2.878×10^{5}
10^{-2}	261.2	0.6863	6.883×10^{4}

TABLE 7.2 Hydrodynamic disruption $W_c = 1$

Figure 7.5 shows the critical electric field as a function of droplet radius for the various droplet dispersion and coalescence inhibiting mechanisms considered. The most critical mechanism appears to be hydrodynamic dispersion ((i) and (iii)) which, for the droplet radius range of interest (1μm to 1mm), corresponds to Reynolds number R>1. The critical electric field of interest ranges from 1 to 20kVcm^{-1}. At the top end of this range, hydrodynamic dispersion can occur for droplets of radius greater than about 22μm. Curve (ii), for contact–separation charging, shows that it is possible for initially–uncharged drops to be prevented from coalescing, if the droplet radius is greater than about 26μm. Curve (iv) shows that a strong electric field can disrupt uncharged drops of radius greater than about 93μm; if the droplet is charged, the likelihood of dispersion is increased. The effect of Taylor–cone dispersion is not included in Figure 7.5, however, it seems reasonable to assume that it may occur when droplets come into close proximity since the electric field can then become very large.

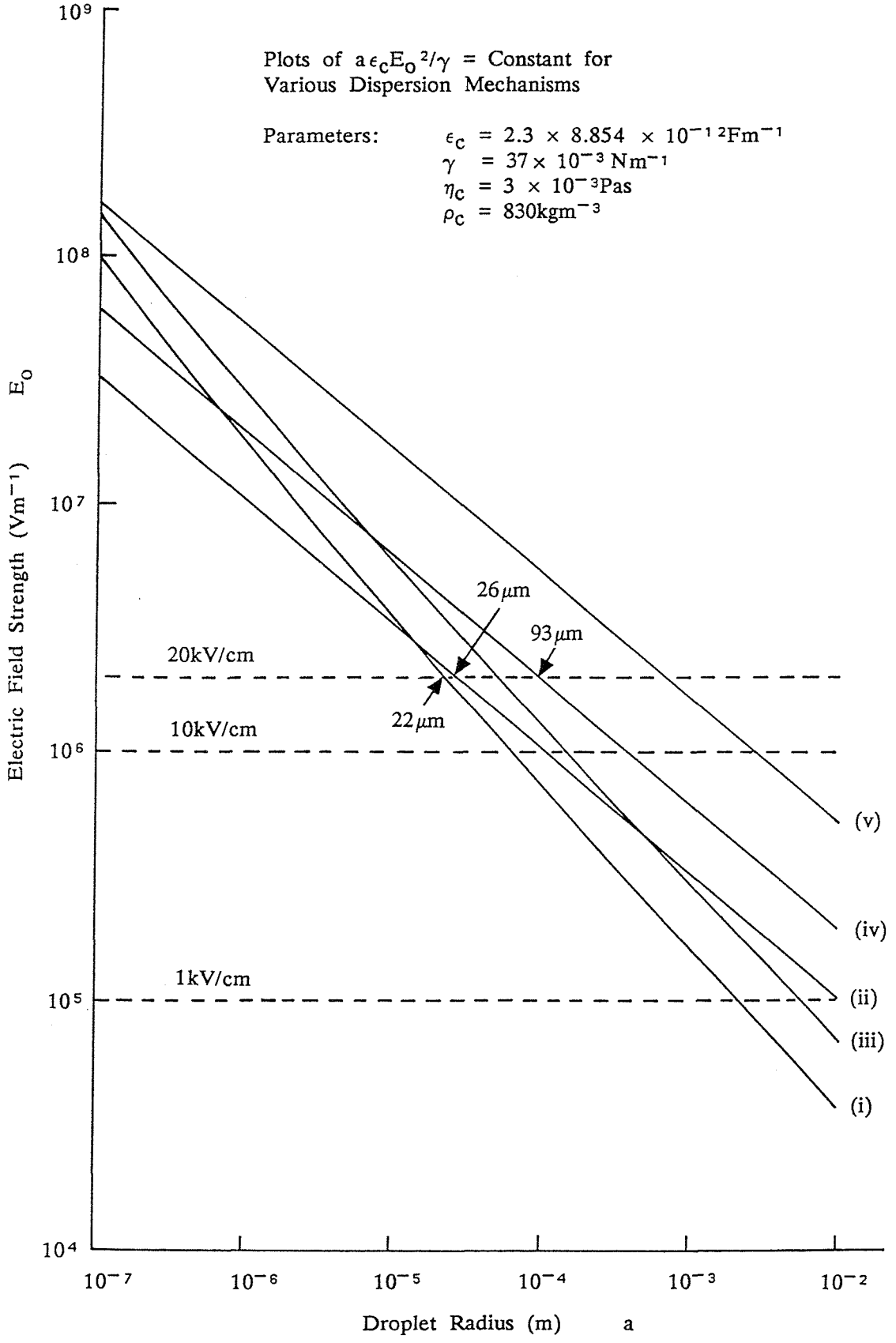

FIGURE 7.5 Critical electric field strength as a function of droplet radius for various dispersion mechanisms: (i) hydrodynamic – W_c = 0.2 (eqn. 7.39), (ii) contact–separation charging (eqn. 7.21), (iii) hydrodynamic – W_c = 1 (eqn. 7.39), (iv) strong electric field (eqn. 7.7), (v) modified Rayleigh limit (eqn. 7.24).

8. EMULSION FORMATION

Emulsions may be formed inadvertently, as is the case when water, as well as oil, are drawn from an oil well; emulsification results from the agitation induced by pumping. The purposeful formation of emulsions, however, is of great importance in the paint, food and pharmaceutical industries. Indeed, W/O emulsions are formed purposefully, at oil refineries, during the desalting process. The preparation of emulsions, hopefully reproducible ones, is also of importance in their scientific study (in order to investigate coagulation kinetics for example).

In some systems, minimal effort of emulsification is involved, such as in spontaneous emulsification or the Briggs intermittent shaking technique (Briggs, 1920). In most practical cases, however, emulsions are prepared using brute force. The presence of emulsifying agent reduces the time required for emulsification, and the emulsification energy since the interfacial tension is lowered. In the older literature, emulsification energy was calculated in terms of the energy required to create new interface. However, this vastly underestimates the energy requirements, since the work done in setting up the liquid motion is neglected. The viscous energy involved can be calculated using simple models of the emulsification process, such as those proposed by Monk (1952) and Subramanyam and Raja Gopal (1966).

8.1 Industrial Emulsification Techniques

Most practical emulsions are made using mixers, colloid mills or homogenizers. Efficient mixing is obtained using a propeller or turbine stirrer in a cylindrical vessel having baffles attached to the walls. The diameter of emulsion droplets produced by mixers is typically $5\mu m$.

A colloid mill incorporates a fixed stator surface and high-speed rotor, separated by a narrow gap where the liquids to be emulsified flow and are subjected to high shear forces. The diameter of droplets is typically $2\mu m$ in emulsions prepared using a colloid mill.

Emulsification is achieved in a homogenizer by forcing the liquids to be emulsified through a small orifice (of area ~ $10^{-4}cm^2$) under very high pressures (up to 5000psi) (Sherman, 1968). This process results in the formation of a fine emulsion having droplets of diameter less than about $1\mu m$.

8.2 Ultrasonic Emulsification

There are three basic types of ultrasonic generator, namely: the piezoelectric transducer, in which a mechanical deformation is produced by an electric field; the magnetostriction transducer, in which a magnetic field gives rise to a mechanical deformation in a ferromagnet; the Pohlman liquid jet whistle (Janovsky and Pohlman, 1948), in which a blade is caused to vibrate at its resonant frequency by the flow of liquid, and which has the advantage of not requiring complex electronic circuitry (Sherman, 1968).

Two mechanisms are thought to be responsible for ultrasonic emulsification, these being surface wave instability and cavitation. Both mechanisms lead to ligaments of one liquid being formed in the other, which are then subject to classical Rayleigh breakup (Rayleigh, 1879). A Rayleigh–Taylor surface wave instability can arise when an interface, between two liquids is accelerated from the less dense to the denser liquid (Gopal, 1963).

In the case of cavitation, a cavitational nucleus is required to be present, which may be produced by: thermal fluctuations giving rise to a vapour bubble; very tiny specks of foreign matter causing breaks in the liquid structure; gas bubbles prevented from dissolving by surface films; ionisation due to cosmic rays or other radiation (Sirotyuk, 1963). In the dilational phase, a cavitation nucleus grows to large size, subsequently collapsing in the implosion phase. The liquid in the vicinity of the cavity is accelerated towards the cavitational centre and may pull with it a ligament from any nearby interface (Sherman, 1968).

A threshold intensity, below which cavitation does not arise, exists and is frequency dependent (Neduzhii, 1965); it increases from about $0.1 Wcm^{-2}$ at 1kHz to $10 Wcm^{-2}$ at 10MHz, showing that cavitation is more easily produced at lower frequencies (Sherman, 1968).

The surface wave instability is understood to be responsible for emulsification in systems where the density difference between the phases is large, such as mercury/water emulsions (Sherman, 1968). Cavitation, however, is thought to be the mechanism responsible for emulsification in the case of water/oil systems.

The temperature dependence of ultrasonic emulsification by cavitation is complex; as temperature increases, the interfacial tension and continuous phase viscosity decrease, which help the emulsification process. However, cavitation reduces as temperature is increased, and this is thought to be the dominant effect (Clayton, 1943).

8.3 Condensation Method of Emulsification

Emulsions can be prepared by injecting the vapour of one liquid below the surface of the other liquid which forms the continuous phase of the emulsion (Sumner, 1933). The vapour condenses on to nuclei within the continuous phase, as its temperature is lowered, thus forming dispersed phase droplets. Condensation nuclei can be natural specks of dust, ions or artificially introduced seeds. Nuclei, in the form of tiny droplets of diameter about $10^{-2}\mu m$, can be produced spontaneously under conditions of relatively high supersaturation; such nuclei are formed by the aggregation of vapour molecules, which is probabilistic in nature (Clayton, 1943). Excess material in the supersaturated vapour deposits on the nuclei which then grow in size. Though the concentrations of such emulsions is low, droplets of diameter $20\mu m$ can readily be produced (Sherman, 1968).

8.4 Emulsification by Aerosol Dispersal

An emulsion can be formed by introducing aerosol droplets to the continuous phase liquid. Aerosols can be prepared by various methods but the following two techniques lead to virtually monodisperse emulsions.

The first technique utilises electrostatic dispersal (Nawab and Mason, 1958a). It may be achieved by passing the liquid to be dispersed through a narrow metal capillary which is held at high electrical potential with respect to a counter electrode submerged in the continuous phase liquid. Charged droplets are caused to issue from the tip of the capillary by the strong electric field there. These then pass into the other liquid so forming an emulsion, a process which may be assisted by stirring. Emulsions with concentrations as high as 30% may be prepared, having droplets of diameter ranging from 1 to $10\mu m$ (Sherman, 1968).

The second technique relies on the preparation of an aerosol by the evaporation–condensation method. Such an aerosol is charged electrically, using a corona discharge, and then bubbled through the continuous phase to form the emulsion. Emulsions having diameters in the range 0.5 to $2\mu m$ can be prepared using this method (Wachtel and La Mer, 1962).

8.5 Orifice Mixing

An emulsion can be produced by injecting one liquid phase into another, as by Richardson (1950). Disintegration of the liquid jet is governed by viscous

and inertial forces, flow velocity being a critical parameter. Only very coarse emulsions can be obtained unless a critical flow velocity u_o is attained. This can be found from Ohnesorge's equation as follows (Ohnesorge, 1936):

$$\frac{\eta_d}{(\rho_d \gamma d_o)^{\frac{1}{2}}} = 2000 \left[\frac{\eta_d}{u_o \rho_d d_o}\right]^{4/3}$$

η_d = dispersed phase viscosity
ρ_d = dispersed phase density
d_o = diameter of orifice
γ = interfacial tension
u_o = critical flow velocity

8.6 Electrostatic Emulsification

This technique is sometimes used in the desalting process, in oil refineries, to mix water with oil containing salty water droplets prior to phase separation (Schmidt (1976), Shvetsov et al. (1984), Warren and Prestridge (1980)). A prerequisite of this method is that the water must aready be dispersed in the oil, to a reasonable extent. Very strong electric fields can be generated in the mixture by applying EHT voltage to one or more electrodes situated in the oil. These fields polarise and elongate the water droplets to such an extent that they are disrupted into smaller droplets. The process is described more fully in Chapter 7.

8.7 Time Required for Emulsification

When an emulsion is being created two opposing effects arise, namely disruption and coalescence of the dispersed phase. Initially, relatively few droplets are present and disruption is the dominant process. However, with the passage of time, the droplets become smaller and hence less susceptible to breakup, subject to the same disruptive forces. The fact that there are more droplets present leads to a higher probability of collision and coalescence. Thus, an equilibrium state must be arrived at, in some time, for which the two opposing effects of disruption and recombination balance (Roth, 1956). This time, as well as the limiting values of concentration, droplet size, and other properties are governed by the precise conditions pertaining; that is, the types of liquid and emulsifier involved, temperature, and the method of emulsification.

Several workers, notably Raja Gopal (1959), have investigated the influence of time on emulsification, and the consensus of opinion is that agitation beyond the

optimum time is of little value. Mean droplet size reduces rapidly at first, gradually attaining a limiting value in 1–5min. Emulsion viscosity, stability and concentration vary in a similar fashion with agitation time.

Generally, it is difficult to quantify the change in emulsion concentration with time. However, under the idealised conditions pertaining during ultrasonic emulsification, the rate of dispersion is found to be approximately proportional to the interfacial area A between the bulk liquids, and the rate of recombination is found to be approximately proportional to Ωc^2 (coalescence by binary collision process), where Ω is the emulsion volume and c its concentration. This leads to the following differential equation governing the change in emulsion concentration with time, where α and β are constants of proportionality (Krishnan et al. 1959):

$$\frac{d}{dt}(\Omega c) = \alpha A - \beta \Omega c^2$$

This is easily solved, its solution being shown below:

$$c = \left[\frac{\alpha A}{\beta \Omega}\right]^{\frac{1}{2}} \tanh\left\{\left[\frac{\alpha \beta A}{\Omega}\right]^{\frac{1}{2}} t\right\}$$

Under typical conditions of emulsification, c increases rapidly initially and effectively reaches a steady-state in a matter of minutes.

8.8 Effect of Agitation Intensity on Emulsification

Many investigators have considered emulsification in simple mixers. Attempts have been made to correlate experimental parameters with specific area S (Sherman, 1968) which is the interfacial area per unit volume of emulsion. The specific area is found to increase as density difference $|\rho_c - \rho_d|$ increases and interfacial tension γ reduces. It is also found to increase as the speed of rotation n and stirrer diameter d_s increase, and as the containing tank diameter d_t decreases. The viscosities of the two phases have an effect but they only play minor rôles. The expression given by Rodger et al. (1956), for propeller mixers in tanks, is shown below with the viscosity factor omitted.

$$S \propto \frac{1}{d_t}\left[\frac{\rho_c n^2 d_s^3}{\gamma}\right]^{1/3} \exp\left[\frac{3.6}{\rho_c}|\rho_c - \rho_d|\right]$$

The term $\rho_c n^2 d_s^3/\gamma$ is the Weber number which gives a measure of the disruptive interfacial shear forces in relation to the cohesive forces arising due to interfacial tension. The expression allows experimental factors to be scaled and reasonably describes emulsification in simple mixers having tanks with baffles.

Though the above expression is applicable to simple mixers, it is not unreasonable to assume that the degree of emulsification correlates with shear stress, interfacial tension and density difference, in a similar way, for other emulsification techniques.

8.9 The Influence of Temperature on Emulsification

In many respects, an increase in temperature is advantageous to emulsification, mainly because viscosity and interfacial tension are lowered (Sutheim, 1946). (A possible exception to this is ultrasonic emulsification since a rise in temperature militates against cavitation.) This is particularly true in the case of oil phases which can be highly viscous or even solid at normal temperatures. Experience has shown that 160°F (71°C) is a good temperature for emulsification (Clayton, 1943); especially in some instances, as this is the temperature of sterilization. However, it is not advisable to increase the temperature too much since troublesome steam bubbles may form, and volatile or essential constituents evaporate.

Another point to consider is that the speed of most chemical reactions increases with rising temperature, approximately doubling with every 10°C rise. Thus emulsifying agents are likely to be decomposed more quickly by reactions such as hydrolysis and ion exchange at elevated temperatures. This is particularly critical in the case of emulsions, in view of the enormous interfacial area involved.

As mentioned earlier, steady-state emulsification involves a balance between the disruption and agglomeration of droplets. This balance is bound to be affected by changes in temperature, and so emulsion concentration, droplet size distribution and other properties can be expected to change accordingly.

8.10 Emulsification Methods Considered During Experimentation

The aim here was to develop an emulsification technique which was convenient to use and which would give reasonably reproducible results. Four techniques were tried, namely: centrifugal mixing, condensation, and two ultrasonic methods, all of which are described below.

8.10.1 Centrifugal Mixing

This system comprised, basically, a 3ℓ reservoir and centrifugal pump, in a closed loop (as in Section 9.12). After passing through the centrifugal pump, the emulsion was returned to the reservoir. Initially, the reservoir was filled with known quantities of water and oil. High shear forces, generated at the tips of the impeller blades, emulsified the water and oil mixture. After being recycled for a few minutes, the emulsion assumed a uniform consistency. Generally, more oil than water was used, leading to the production of W/O emulsions. The pump speed could be varied between 280 and 2789 rpm (determined by stroboscope) by controlling its input voltage. At maximum speed, the flow rate was 40ℓ/min. The coarseness of the emulsions reduced as pump speed increased, as would be expected. In general, much coarser emulsions were generated by this method than by ultrasonic emulsification. Such emulsions were observed, using a nephelometer (see Section 9.11), to have a lower initial turbidity and higher settling rate than ultrasonically prepared emulsions.

8.10.2 Condensation Method

The method described here is a variation of the condensation technique, described earlier (Section 8.3), where a vapour (dispersed phase) is injected into the continuous liquid phase.

Approximately equal quantities of water and oil were placed in a glass jar which was then sealed. The mixture was shaken and when the air bubbles had cleared the oil phase, above the water/oil interface, was observed to be turbid, indicating that a W/O emulsion had been formed. The jar and contents were then placed in a thermostatically–controlled water bath, which had been preheated to 60°C, and left for one hour at this temperature. During this period, the oil phase cleared as the water droplets either settled out, at the interface, or were dissolved in the oil. A pipette was then used to transfer some of the warm oil into a preheated cuvette, in order to perform turbidity measurements (see Section 9.11), using the nephelometer. A thermocouple was immersed in the oil so that a cooling curve could be obtained simultaneously. The results are shows in Figure 8.1. As cooling proceeded, from the initial temperature of 45°C, the turbidity of the oil increased due to the precipitation of small water droplets. After about 30 minutes, when the temperature had dropped to 32°C, the turbidity peaked at 8NTU, after which sedimentation caused the turbidity to decrease.

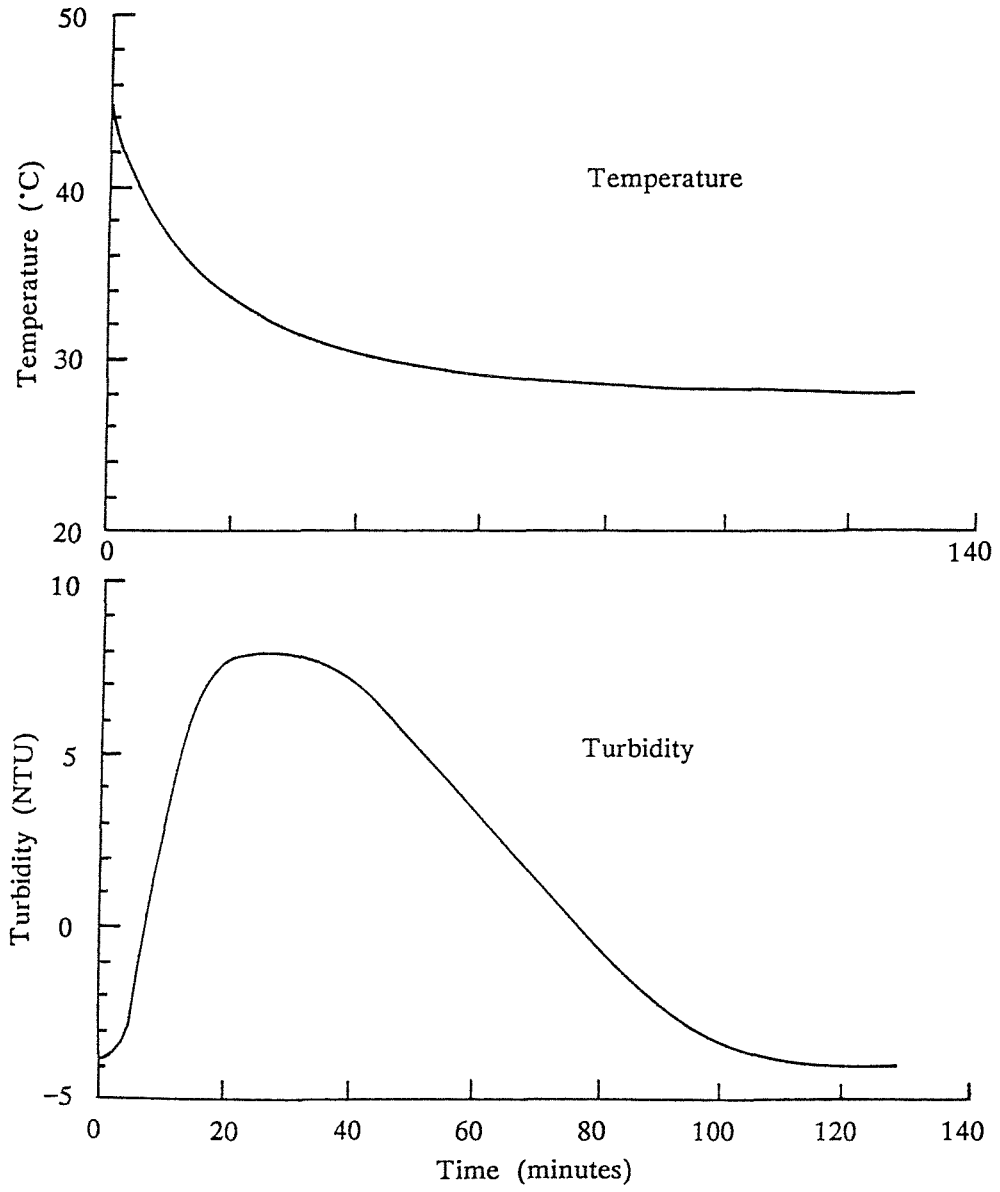

FIGURE 8.1 **Cooling and turbidity curves for a W/O emulsion in a cuvette (no electric field applied).**

After about 110 minutes, the emulsion had resolved leaving a pure oil phase. This was apparent, as the turbidity had reduced to that of pure oil (−4NTU). The concentration in this instance must have been very low since, in the case of ultrasonically prepared emulsions, the turbidity value was typically 700NTU for a water concentration of about 750ppm.

In another condensation experiment, the procedure described above was adopted, except that the oil was transferred into a cold cuvette. Water droplets precipitated out immediately, as can be seen from Figure 8.2. The turbidity value

peaked at 120NTU (much higher than in the previous example) after about 5 minutes (shorter than the time obtained previously). The corresponding cooling curve was not obtained. A higher rate of cooling, therefore, produced a more concentrated emulsion which resolved, by sedimentation, in about 3 hours.

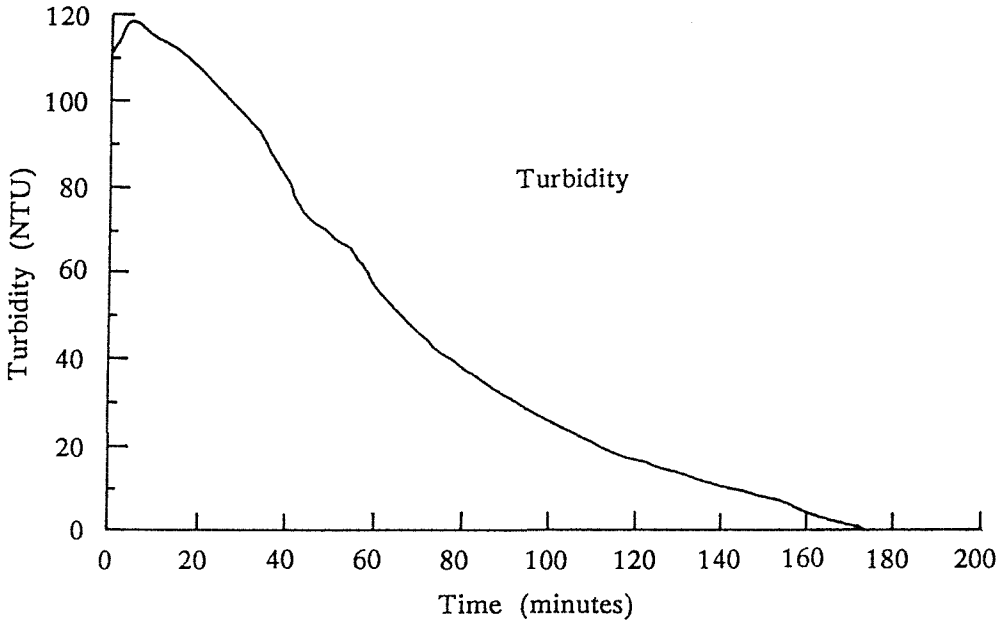

FIGURE 8.2 **Turbidity of a W/O emulsion prepared by precipitation (no electric field applied).**

It was decided not to adopt this method for general experimentation since: it was inconvenient and took a long time to produce an emulsion; the concentrations of the emulsions produced were low and not easily determined; the emulsions were much coarser than those prepared ultrasonically.

8.10.3 Ultrasonic Preparation of Emulsions Using a Piezoelectric Transducer

This technique is said to have advantages over other methods, so far as laboratory studies are concerned, because accurate control of the sound energy is possible and emulsification can be performed under well-defined conditions (Sherman, 1968). The apparatus used for this purpose is shown in Figure 8.3. The emulsifier unit itself consists of a perspex cylinder with a 10cm focal length parabolic, piezoelectric transducer, mounted by its rim, at the bottom. The large mismatch of acoustic impedance, at the solid/gas interface, ensured that most of the sound energy was reflected, so augmenting the forward beam (Sherman, 1968).

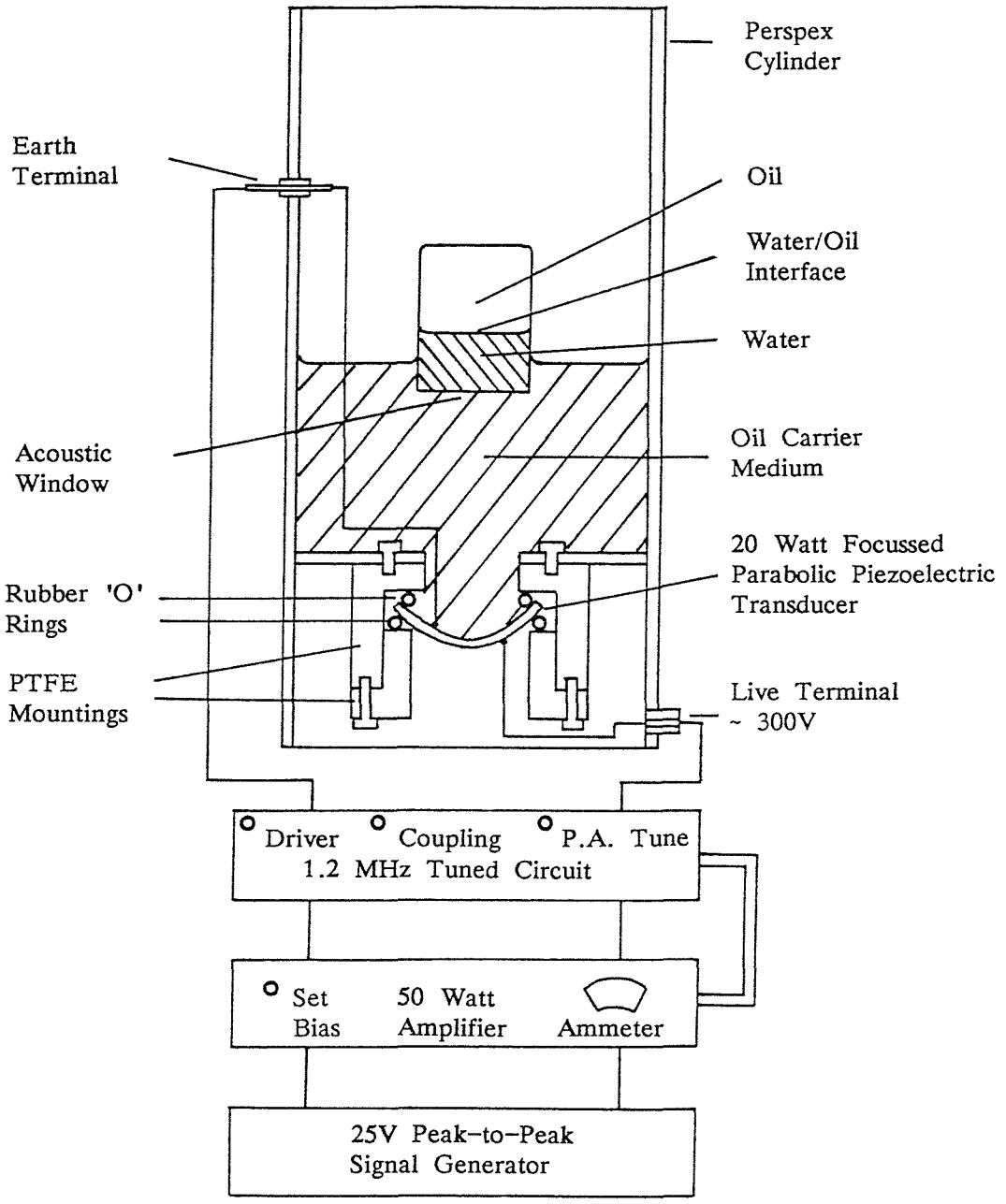

FIGURE 8.3 **Piezoelectric ultrasonic emulsifier unit.**

The emulsifier unit was driven by a radio frequency source comprising signal generator, tuned circuit and amplifier. A large fraction of the electrical energy supplied was converted into sound energy when the piezoelectric transducer was driven at its resonant frequency of 1.2MHz.

The cylinder was filled with oil which acted as a carrier medium for the sound waves. An emulsion was prepared by introducing a vessel, containing the water and oil to be emulsified, into the carrier medium such that the sound energy focussed at the water/oil interface within it. The sound energy passed through an acoustic window, at the bottom of the vessel, and after many minutes' agitation, the mixture became emulsified. The lower portion comprised a low–turbidity (see Section 9.11) O/W emulsion whereas the upper portion was a turbid (850NTU) W/O emulsion.

The disadvantage of this method was that the concentration of water could not readily be obtained. In an attempt to overcome this problem, the procedure was modified so that the vessel contained only the required amounts of water and oil. The water phase consisted, initially, of a small droplet, situated at the bottom of the oil, onto which the sound energy was focussed. After many minutes' agitation, the droplet became white in appearance, showing that it had taken in many tiny oil droplets to form an O/W emulsion. Not much water, however, was caused to disintegrate and form a W/O emulsion.

8.10.4 Ultrasonic Emulsification Using Magnetostriction

The most convenient way of preparing emulsions was to use an ultrasonic bath, with water as the carrier medium for the sound. Sound waves were induced in the water using the principle of magnetostriction (in which a change in magnetic field causes the dimensions of a ferromagnetic material to alter).

An emulsion was prepared by adding a measured volume of water, using a micro–syringe, to a known volume of oil, contained in a stainless steel cup. The cup (with a lid on to prevent water droplets from the carrier medium entering inadvertently) was then placed in a supporting frame, so that it contacted the carrier medium. An emulsion could be formed, in a matter of minutes, by subjecting the mixture in the cup to ultrasonic irradiation. In some instances the water droplet, residing at the bottom of the cup, took in tiny oil droplets so forming globules of O/W emulsion. This tended to happen when larger amounts of water were added. In the majority of cases, however, a W/O emulsion was formed. These emulsions were found to be relatively stable, typically taking a day to resolve by sedimentation. This showed that the average drop size in the emulsion was quite small. Very turbid emulsions could usually be produced, showing that the water concentration was high (all the water having been emulsified).

The advantages of this technique are that it is convenient, the water concentration is known, and relatively stable emulsions can be formed. Unfortunately, the technique did not give very good reproducibility. This may have been due to: inaccuracies in the amount of water dispensed using the micro-syringe, temperature differences, different positions of the stainless steel cup within the body of the ultrasonic bath, and different contact areas between the cup and the carrier medium. However, it was thought to be the best of the available methods, and when it was chosen as the standard emulsification technique, an agitation period of 5-minutes was decided upon.

9. DROPLET COALESCENCE IN W/O EMULSIONS

9.1 Coalescence

Essentially, coalescence is the combination of two dispersed phase droplets into a single, larger droplet. The process can be broken down into the five stages shown below, though some workers (e.g. Becher, 1977) classify stages (i) and (ii) as flocculation, and stages (iii) to (v) as coalescence.

(i) Long-range flocculation: the coming together of two droplets, to close proximity, under the influence of the prevailing forces.

(ii) Short-range flocculation (film thinning): the drainage of the intervening film, once the droplets are in close proximity, under the action of the prevailing forces.

(iii) Collision: the contact of flocculating droplets.

(iv) Film rupture: the rupture of the intervening film.

(v) Unification of droplets: the flowing together of the liquid in the two droplets to form a single larger droplet.

Coalescence is the converse of dispersion (disruption, emulsification or atomisation). All of the forces which produce emulsification (e.g. those resulting from electrostatic, hydrodynamic, mechanical, or acoustic stresses) can also give rise to coalescence, if the intensity of the mechanism is reduced. Often, both processes will occur simultaneously; once the equilibrium state has been achieved, during emulsification, coalescence and dispersion are balanced. Coalescence can also result from sedimentation and Brownian motion.

The five coalescence stages defined above will now be considered in greater detail.

9.1.1 Long-Range Flocculation

There are several mechanisms by which droplets, initially separated by a large distance, can be brought into close proximity. Brownian motion is one such mechanism. This is usually of importance in dipole coalescence, where the droplets are not significantly charged, since the dipole force of interaction is small at long-range. Sedimentation is another such mechanism, in which larger particles

settle at greater speeds than smaller ones, which gives the possibility of large and small droplets coming into close proximity. In migratory coalescence (see Section 9.8) the mechanism is electrophoresis which relies on the droplets being charged. The droplets may possess a double layer charge and, if they have contacted an electrode, a larger level of free charge might have been acquired. The most favourable situation is where droplets of opposite polarity collide head-on, giving the best chance of coalescence. If migratory coalescence is to be effective, the dispersed phase droplets must retain their free charge long enough to traverse the inter-electrode space; this requires that the continuous phase be of low conductivity. The electrophoretic force acting on a charged particle is simply the product of electric field and charge:

$$F = qE \tag{9.1}$$

If the droplet is conducting and has become charged by contacting an electrode then (Lebedev and Skal'skaya, 1962):

$$F = \left[\frac{\pi^2}{6}\right] 4\pi a^2 \epsilon_c E^2 \tag{9.2}$$

Sadek and Hendrick's paper shows how electrophoretic forces can lead to coalescence of droplets and a change in the size distribution of such droplets (Sadek and Hendricks, 1974) (see also Section 9.9.1).

9.1.2 Short-Range Flocculation (Film Thinning)

Electrophoretic forces act in short-range as well as long-range flocculation, however, dielectrophoretic forces can become very large, for small separations between droplets, and may even be the dominant mechanism. The force of interaction between two equally-sized droplets (of radius a), which are polarised in an external electric field E, is as follows, if their separation h << a (see eqn. (5.39)):

$$F = \frac{2}{9} \pi^5 \epsilon_c E^2 a^2 \frac{(a/h)}{\ell n^2 (a/h)} \tag{9.3}$$

This force leads to drainage of the intervening film of liquid between the flocculating droplets. Two expressions apply to the thinning rate (dh/dt) of the film, dependent on whether the droplets are deformable or undeformable. For undeformable droplets of radius a, the rate of film thinning is given by (see eqn. (6.5)):

$$\frac{dh}{dt} = \frac{-2Fh}{3\pi\eta_c a^2} \qquad (9.4)$$

If the droplets deform slightly, so that their opposing faces flatten off, the rate of film thinning is given by (see eqn. (6.2)):

$$\frac{dh}{dt} = \frac{-8\pi\gamma^2 h^2}{3\eta_c a^2 F} \qquad (9.5)$$

These film drainage equations are considered more fully in Chapter 6 which covers film thinning theory.

9.1.3 Droplet Collison

According to Owe Berg et al. (1963), droplets in air can come into contact with one another, as evidenced by their flattened surfaces of contact, before the liquid in the two droplets starts to flow together a short time later. If there is an intervening film of immiscible liquid, however, it would appear that the droplets do not necessarily have to collide before film rupture and coalescence occur. Thus, the work of Charles and Mason, 1960a, (in which the coalescence of a droplet at a plane interface, and with an applied electric field, was considered) the film thickness varied from 6 - 203μm at the moment of film rupture. The film thicknesses were, however, calculated (see eqn. (9.6) below) rather than observed, and the coalescence was not between a pair of droplets.

In Ansimov and Emel'yanchenko's (1976) paper, concerning contact-separation charging (see Chapter 7, Section 7.1.2), there is a photograph of two water droplets, in oil, apparently coalescing. However, charge transfer occurs between the droplets (due to an electrostatic discharge, presumably), which subsequently separate and are repelled from one another. This suggests that droplets can contact one another if there is an intervening film of immiscible liquid.

9.1.4 Film Rupture

As mentioned above, Charles and Mason (1960a) have investigated the ruputre of the intervening film, which is a precursor of coalescence. For droplets coalescing at a bulk interface, due to gravitational settling, they found the distribution of rest-times to be approximately Gaussian. This suggested to them that film rupture and coalescence were governed by random statistics.

Assuming that the surface free energy was converted completely into kinetic energy of the liquids displaced from and entering the hole, Charles and Mason extended Dupré's (1869) analysis for rupture velocity to obtain:

$$u = \left[\frac{4\gamma}{(\rho_1 + \rho_2)h}\right]^{\frac{1}{2}} \qquad (9.6)$$

where:

γ = interfacial tension

ρ_i = density of phase i, for i = 1 and 2

h = film thickness

If the rupture velocity u is known (from high speed photography), eqn. (9.6) can be used to estimate the film thickness at the moment of rupture.

Owe Berg et al. (1963) consider the time of coalescence to be the time from the moment of collision of the droplets, to the moment of rupture of the intervening film. They define coalescence to be the formation of intermolecular bonds between the droplets, and suggest two mechanisms by which bonds can be switched from within the droplets to across their interface. In the first mechanism, bonds are broken and new ones formed. However, in the second mechanism, the bonds are not broken but, rather, are gradually re-arranged. The breaking of bonds is favoured by energy supply in the form of an electrical discharge between the droplets (which are assumed to have a potential difference V). The near surfaces of the droplets can be thought of as having a capacitance C, in which case the energy associated with the electrical discharge may be represented by $CV^2/2$. [That the droplets can be in contact and yet have a potential difference, must relate to the fact that the intermolecular bonds are within the droplets initially, rather than across their interface.] It is then reasoned that the rate of coalescence, in the case of bond breaking, is proportional to $\epsilon_d V^2$ where ϵ_d is the permittivity of the droplet material. In the case of bond re-arrangement, the rate of bond re-orientation (and hence coalescence) is proportional to μE where μ is the dipole moment of the bonds and E is the electric field . Now μ is known to be proportional to $(\epsilon_d - 1)^{\frac{1}{2}}$, and E is proportional to V, hence it follows that the rate of coalescence is proportional to $(\epsilon_d - 1)^{\frac{1}{2}}V$ for the case of bond re-arrangement.

Owe Berg et al. (1963) measured the coalescence times (typically milliseconds) of various liquids (distilled water, hydrochloric acid solutions, and

amyl, butyl, isopropyl, ethyl and methyl alcohols) and found the results consistent with their theory. At potential differences below a threshold level, the rate of coalescence appears to be consistent with the gradual re-arrangement of molecular bonds, and is proportional to $(\epsilon_d - 1)^{\frac{1}{2}}V$. However, at higher values of potential difference, the coalescence rate is consistent with energy supply at the interface, and is proportional to $\epsilon_d V^2$. The threshold value of potential difference depends on the droplet permittivity but is typically 6V. The delay in coalescence is pointed out as being an aspect of surface tension.

9.1.5 Unification of Droplets

This is just the flowing together of liquid from the two droplets to form a single, larger droplet. The process is essentially hydrodynamic in nature and lasts milliseconds typically. This last stage of coalescence does not appear to have been analysed in the literature.

9.2 Coalescence Involving Sedimentation

Coalescence by sedimentation can occur when droplets of differing size, which settle at different rates, collide with one another. The phenomenon is of importance in aerosols, where it has been studied by such workers as Findeisen (1932), Langmuir (1948), Fuchs (1964) and Sartor (1954).

Centrifugation (in a centrifuge or cyclone) can be thought of as an extension of sedimentation, in which the acceleration due to gravity g is replaced by $\omega^2 r$, where ω is the angular velocity and r is the radius concerned. Since the radial acceleration ($\omega^2 r$) can be made much larger than g, it follows that coalescence by sedimentation will be increased accordingly. The use of centrifuges and cyclones is a practised technique in the separation of emulsions.

9.3 Coalescence Involving Brownian Motion

Friedlander and Wang, 1966, investigated the coalescence of dispersions by Brownian motion, and found the droplet size distributions to be self preserving. The shape of the distributions depended on the volume fraction and number density of the dispersed phase droplets. Wang and Friedlander, 1967, also investigated coalescence under conditions of simultaneous Brownian motion and laminar shear flow.

Volkov and Krylov, 1972a, investigated the coalescence of

low-concentration (< 1% by volume) W/O emulsions, to which an ac electric field was applied. Their analysis was based on coagulation kinetics, the coagulation constant of which depended on Brownian motion and electrostatic effects. They suggested a method of determining the integral characteristics of an emulsion (mean size, variance, and symmetry coefficient), as a function of time, without the need to solve the coagulation kinetics of the distribution function itself (see Section 9.10.1).

9.4 Coalescence Involving Shear Forces

The coalescence of dispersed phase droplets, due to laminar shear flow, has been studied by Bartok and Mason, 1959. They described the behaviour of two-body collision doublets of fluid spheres suspended in a liquid undergoing Couette flow. Allan and Mason, 1962, extended this work, with special emphasis on the effect of electric fields and charge on doublet behaviour and coalescence.

9.5 Coalescence Involving Electrostatic Forces

Sadek and Hendricks (1974) and Zeef and Visser (1987) have considered coalescence processes occurring in a W/O emulsion, having low-conductivity oil phase, to which a steady electric field is applied. The dispersed phase water droplets are assumed to be brought into close proximity, one with another, by electrophoretic action. The droplets must therefore be charged (by contacting the electrodes) and must retain their charge long enough to cross the inter-electrode gap (which is why low-conductivity oils are necessary) (see Section 9.8). Sadek and Hendricks (1974) (see Section 9.9.1) considered the effect of migratory coalescence on the size distribution of dispersed phase droplets. They found that the size distribution was of self-preserving type, in that it was of fixed form when plotted as a function of a/a_m (where a_m is the mean droplet radius of the size distribution as a function of time).

Zeef and Visser's (1987) work on coalescence was more mechanistic in nature. They developed an expression for droplet growth, in terms of the time required for flocculation and that required for film rupture and coalescence. This was used to determine the electro-coalescer residence time, that is the time required for the growing droplets to settle out under the influence of gravity (as pioneered by Williams and Bailey, 1983).

Williams and Bailey, 1983, developed a model for droplet growth based on dipole coalescence (see Section 9.10.2). This was used to determine the emulsion

resolution time, of the assumed monodisperse W/O emulsion, under the influence of a steady electric field. Using a laser light scattering technique, Williams and Bailey, 1984, measured the change in size distribution of a W/O emulsion, subjected to a steady electric field, as a function of time (see Section 9.13).

The coalescence of W/O emulsions using insulated electrodes, has been investigated experimentally by Bailes and Larkai (1981, 1982, 1984) and Galvin (1984), and theoretically by Joos and Snaddon (1985). In order to establish a strong electric field within the emulsion, it is necessary to apply a time varying waveform; a low-frequency, unidirectional pulsed excitation was considered in the above cases. Bailes and Larkai (1982, 1984) deduced a relationship between the collision frequency of droplets and the electrical current supplied.

Volkov and Krylov, 1972b, investigated the coalescence of relatively high-concentration ($>$ 1% by volume) W/O emulsions, under the influence of an ac applied electric field. It was necessary for them only to consider dielectrophoretic forces. They were able to determine the integral characteristics of the emulsion without the need to solve the coagulation kinetic of the distribution function itself (see Section 9.10.1). Joos, Snaddon and Johnson, 1984, measured the changes in the size distribution of a neutrally buoyant W/O emulsion, subjected to a 60Hz ac electric field, using a light scattering technique (Malvern Particle and Droplet Size Analyser). They also developed an expression for droplet growth in terms of an average coalescence time, which was determined from the system parameters.

9.6 Partial Coalescence

The simplest way of studying coalescence is to consider a droplet of Phase 1 liquid (e.g. water) settling gently onto a flat interface separating the Phase 1 (e.g. water) and Phase 2 (e.g. oil) liquids in bulk. This technique was used by Charles and Mason, 1960b, for various immiscible systems. They found that the Phase 1 droplet only coalesced with the underlying bulk Phase 1 liquid after resting at the interface for some time. In many of the systems coalescence was incomplete as the primary droplet was succeeded by a smaller secondary droplet. The cycle can also be repeated by the secondary droplet. In water/benzene systems, as many as eight stages of partial coalescence have been observed, and it is probable that additional stages yielded sub-micron droplets. Occasionally, a large primary droplet simultaneously yielded two secondary droplets, of unequal size.

Charles and Mason analysed the behaviour in terms of the disintegration of an unstable jet of liquid according to Rayleigh (1879), Weber (1931) and Tomotika (1935).

The formation of secondary droplets was found to be dependent on the viscosity ratio η_d/η_c of the two phases; when η_d/η_c was less than 0.02 or greater than 11, no secondary droplets were formed.

The application of a vertical dc electric field was found to reduce the number of stages of partial coalescence. If the electric field strength was sufficiently large, coalescence was single staged.

It seems possible that the phenomenon of partial coalescence could occur when a pair of liquid droplets coalesce. However, it would appear from the literature that no such observations have been made.

Since the application of an electric field, of sufficient magnitude, can prevent partial coalescence, it is likely that electrostatically induced droplet coalescence will be single staged.

9.7 Limited Coalescence

Under some circumstances, the coalescence rate of dispersed phase droplets, in an emulsion, proceeds until a limiting size is reached and the size distribution becomes roughly uniform. Wiley, 1954, has termed this behaviour limited coalescence. It is believed to be related to the adsorption of emulsifying agent at the interface. The phenomemon has been discussed in more detail in Chapter 10, with regard to the stability of droplets in pearl-chains.

9.8 Migratory Coalescence

Migratory coalescence is the term given to the coalescence of dispersed phase droplets, in a W/O emulsion, as a result of electrophoretic forces, arising from an applied electric field (see Figure 9.1). The droplets must therefore possess charge which they may acquire in a number of ways:

(i) ionisation (due to chemical reaction) (Alexander and Johnson, 1949).

(ii) preferential adsorption of ions at the interface (electrical double layer) (Alexander and Johnson, 1949).

Droplet size exaggerated in comparison with electrodes

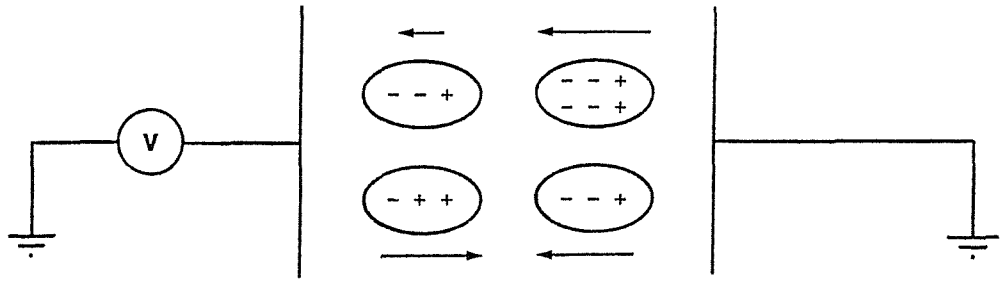

FIGURE 9.1 Migratory coalescence. Electrophoretic forces lead to the collision of droplets; coalescence is assisted by dipole attraction and droplets having charges of opposite polarity.

(iii) frictional charging (Alexander and Johnson, 1949).

(iv) contact-separation charging (Anisimov and Emel'yanchenko, 1976).

(v) droplet disruption (Macky, 1931 and Taylor, 1964).

(vi) contact with charged electrode (Lebedev & Skal'skaya, 1962 and Cho, 1964).

The most important of these mechanisms is probably (vi). A spherical, conducting particle acquires (at most) the charge, specified by eqn. (9.7), on contacting a charged electrode in a parallel plate system.

$$q_o = \left[\frac{\pi^2}{6}\right] 4\pi a^2 \epsilon_c E \qquad (9.7)$$

To account for such effects as non-spherical, or dielectric particles, it is customary to multiply the charge, given by eqn. (9.7), by a constant η_q. This relates to the efficiency of charging and so $0 < \eta_q < 1$.

This charge is not bound to the droplet, by any physical means, and will gradually leak away by conduction through the continuous phase. The process is exponential in form and governed by the permittivity ϵ_c and conductivity σ_c of the continuous phase.

Some of the other charges, such as the double layer charge q_ζ, are physio-chemically bound to the droplet and cannot, therefore, be conducted away by the continuous phase.

The total charge held by a droplet, which has contacted an electrode, may therefore by expressed as (Vygovski et al., 1980):

$$q = \eta_q q_o e^{-\sigma_c t/\epsilon_c} + q_\zeta \qquad (9.8)$$

If inertial effects are neglected and Stokes' law is assumed to hold (as by Vygovski et al., 1980), the following differential equation applies:

$$6\pi\eta_c a \frac{dx}{dt} = qE \qquad (9.9)$$

By combining eqns. (9.7) to (9.9), ignoring q_ζ and integrating (between the limits 0 and X for the x variable, and 0 and ∞ for the t variable), it is possible to obtain:

$$X = \frac{\eta_q a(\pi\epsilon_c E)^2}{9\eta_c\sigma_c} \qquad (9.10)$$

This is the distance travelled by the droplet, under the influence of the applied electric field, before its charge is completely conducted away by the continuous phase (assuming that it does not interact with any other particle meanwhile). If the continuous phase conductivity σ_c is too great, the charge held by the droplet leaks away rapidly, and the distance X, over which the applied field can drive the droplet, is small. Sadek and Hendricks, 1974, suggest that the droplet should be able to traverse the inter-electrode gap, which may therefore be identified with X. Such a definition would ensure that the droplet could be driven into many collisions with other droplets (in reality it would probably not be able to traverse between the electrodes without undergoing coalescence).

Migratory coalescence is applicable in the case of W/O emulsion where the continuous phase is a distillate (of conductivity about $10^{-11} - 10^{-12}Sm^{-1}$). For example, X = 15mm if the parameters in eqn. (9.10) are: $\eta_q = 1$, a = 5μm, $\epsilon_c = 2.3 \times 8.854 \times 10^{-12}Fm^{-1}$, E = $10kVcm^{-1}$, $\eta_c = 3 \times 10^{-3}Pas$, and $\sigma_c = 5 \times 10^{-11}Sm^{-1}$.

Panchenkov et al., 1970, measured the velocity of charged water droplets, in a low–conductivity oil, which was subjected to a uniform electric field. The oil used was a mixture of vaseline oil (ρ_c = 877kgm^{-3}, $\epsilon_c = 2.2\epsilon_o$) and carbon tetrachloride (ρ_c = 1597kgm^{-3}, $\epsilon_c = 2.288\epsilon_o$) in such proportions as to provide a neutrally buoyant system. A photographic technique was used to record the trajectory of a droplet between the vertical, parallel–plate electrodes, which had a 20mm separation. On release from a grounded capillary, the droplet moved at a velocity consistent with it having a double layer charge. The speed of the droplet increased as it approached an electrode. On contacting the electrode, the droplet was repelled back towards the other electrode at a much greater speed, and then continued to oscillate between the electrodes at this speed. This behaviour is consistent with the droplet having acquired a charge, much greater than the double layer charge, on contacting an electrode.

Panchenkov et al., 1970, found that the speed of the droplet increased as its salinity was raised, according to the following expression (which was derived assuming Stokes' law to be applicable):

$$u = (1+0.458c^{0.546})(1-e^2)^{7/6}(\pi^2/9)\epsilon_c E_o^2 a/\eta_c \qquad (9.11)$$

where e is the eccentricity of the droplet as it contacts an electrode, which is given by:

$$e = \frac{3}{2}\left[\frac{\epsilon_c a E_o^2}{\gamma}\right]^{\frac{1}{2}} \qquad (9.12)$$

u = droplet speed
c = sodium chloride concentration (mol dm^{-3})
ϵ_c = permittivity of oil phase
E_o = applied electric field strength
a = droplet radius
γ = interfacial tension between water and oil.

9.9 Coalescence Models

There appear to be two main ways of modelling the coalescence of dispersed phase droplets in an emulsion. The first is statistical in nature and considers the emulsion macroscopically. The emulsion is specified by a droplet size distribution, and equations involving coagulation kinetics are solved, in order to describe how the distribution changes with the passage of time. Sadek and

Hendricks' model (see Section 9.9.1) and Volkov and Krylov's model (see Section 9.10.1) are encompassed by this definition.

The second method is mechanistic in nature and considers the emulsion microscopically (i.e. in terms of the behaviour of a single pair of droplets). Zeef and Visser's (1987) electrophoretic coalescence model is of this kind, as is the author's dielectrophoretic model, to be discussed subsequently (see Section 9.10.2).

9.9.1 Migratory Coalescence Model (The Coagulation Kinetics Approach)

In Sadek and Hendrick's (1974) analysis, of the electrical coalescence of water droplets in low-conductivity oil, eqn. (9.9) is used to specify the terminal speed (dx/dt = u) of a droplet (the double layer charge and exponential decay terms are neglected). This is then used to define the coagulation rate constant between two species of droplets:

$$K_{mn} = \beta(a_m + a_n)^2(u_m + u_n) \qquad (9.13)$$

where u_i is the terminal speed and a_i is the radius of a droplet of species i. In eqn. (9.13), the parameter β is a geometric factor determined by the spatial distribution of droplets and the electrode separation, the second term represents the collision cross-section, and the third term represents the relative velocity between droplets. The coagulation rate constant is then used in a differential equation which specifies the rate of formation of a species of droplets:

$$\frac{dN_M}{dt} = -\sum_{n=0}^{\infty} K_{Mn}N_M N_n + \tfrac{1}{2}\sum_{m=0}^{M} K_{m,M-m}N_m N_{M-m} \qquad (9.14)$$

The first term on the right-hand side of eqn. (9.14) represents the rate of disappearance of species M, whereas the second term represents the formation of species M from droplets of smaller species. Sadek and Hendricks solved eqn. (9.14) numerically and concluded that the size distribution of droplet species was self preserving (i.e. it had a single form in terms of droplet radius normalised according to the mean droplet radius).

9.10 Dipole Coalescence

Dipole coalescence is the name given to the coalescence of dispersed phase droplets, in a W/O emulsion, as a result of the droplets being polarised in an

external applied electric field, resulting in an attractive force of interaction (see Figure 9.2)

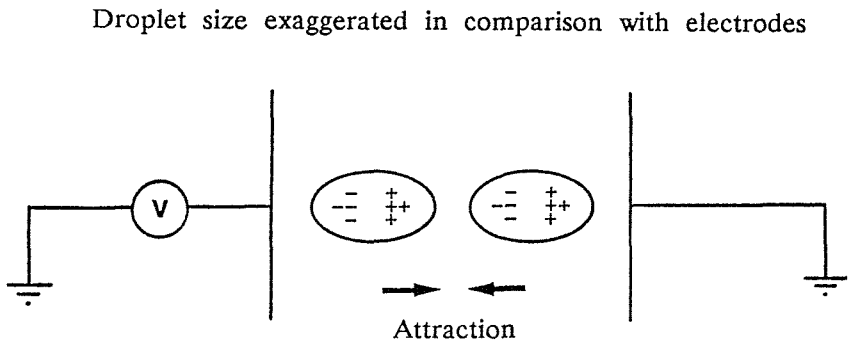

FIGURE 9.2 Dipole coalescence. The applied electric field causes the neutral water droplets to polarise and attract one another by dielectrophoresis.

9.10.1 Dipole coalescence Model (The Coagulation Kinetics Approach)

Volkov and Krylov (1972b) consider the coagulation kinetics of a relatively concentrated (>1% by volume) W/O emulsion as described below.

A spatially uniform ac electric field is applied to the emulsion in order to obviate electrophoretic effects. The interactive force between emulsion droplets is therefore dielectrophoretic in nature.

The analysis utilises the function $n(\Omega,t)$ which is the number density of particles, per unit volume, having volume Ω at time t, from which the total number N of particles per unit volume, at time t, may be obtained:

$$N(t) = \int_0^\infty n(\Omega,t)\,d\Omega \qquad (9.15)$$

The function $n(\Omega,t)$ satisfies the following integro-differential equation (c.f. eqn. (9.14)):

$$\frac{\partial}{\partial t} n(\Omega,t) = \tfrac{1}{2} \int_0^\Omega K(\Omega_1,\Omega-\Omega_1)\,n(\Omega_1,t)\,n(\Omega-\Omega_1,t)\,d\Omega_1$$

$$-n(\Omega,t) \int_0^\infty K(\Omega_1,\Omega)\,n(\Omega_1,t)\,d\Omega_1 \qquad (9.16)$$

where $K(\Omega_1,\Omega)$ is a coagulation rate function which specifies the rate at which particles of volume Ω_1 and Ω coagulate. The first term on the right-hand side of eqn. (9.16) corresponds to the rate of creation of droplets of volume Ω, by coalescence of smaller droplets, whereas the second term corresponds to their destruction, by coalescence with any other size of droplet.

By intergrating eqn. (9.16), with respect to droplet volume Ω, between the limits $\Omega = 0$ and $\Omega = \infty$, it is possible to obtain the following differential equation in N:

$$\frac{dN}{dt} = -\tfrac{1}{2} \langle\langle K \rangle\rangle N^2 \qquad (9.17)$$

where:

$$\langle\langle K \rangle\rangle = \frac{1}{N^2} \int_0^\infty n(\Omega,t) \int_0^\infty K(\Omega_1,\Omega) n(\Omega_1,t)\, d\Omega_1\, d\Omega \qquad (9.18)$$

Similarly, by multiplying eqn. (9.16) by the droplet volume Ω throughout, and then integrating between the limits $\Omega = 0$ and $\Omega = \infty$, it is possible to obtain another differential equation:

$$\frac{d\langle\Omega\rangle}{dt} = \tfrac{1}{2} N \langle\langle K \rangle\rangle \langle\Omega\rangle \qquad (9.19)$$

where:

$$\langle\Omega\rangle = \frac{1}{N} \int_0^\infty \Omega n(\Omega,t)\, d\Omega \qquad (9.20)$$

The term $\langle\Omega\rangle$, in eqn. (9.20), is the average droplet volume for the distribution of droplets.

By combining eqns. (9.17) and (9.19) the following differential equation is obtained:

$$\frac{d\langle\Omega\rangle}{dN} = \frac{-\langle\Omega\rangle}{N} \qquad (9.21)$$

Eqn. (9.21) is easily solved, using the initial conditions that $N = N_o$ and $\langle\Omega\rangle = \langle\Omega_o\rangle$ when $t = 0$:

$$N\langle\Omega\rangle = N_o\langle\Omega_o\rangle \qquad (9.22)$$

This is simply a statement of the conservation of dispersed phase volume (before phase separation).

By considering the coagulation rate function $K(\Omega_1,\Omega)$ dimensionally (i.e. assuming that it can be specified by ϵ_c, E, η_c, Ω_1 and Ω), it can be shown that:

$$K(\Omega_1,\Omega) = \frac{2\epsilon_c E^2}{\eta_c}\,\Omega\,\Phi(\Omega_1/\Omega) \qquad (9.23)$$

where Φ is an unspecified function.

Now $K(\Omega_1,\Omega) = K(\Omega,\Omega_1)$, by symmetry, and so eqn. (9.23) can be expressed as:

$$K(\Omega_1,\Omega) = \frac{\epsilon_c E^2}{\eta_c}\,[\Omega\Phi(\Omega_1/\Omega) + \Omega_1\Phi(\Omega/\Omega_1)] \qquad (9.24)$$

Assuming Φ to be a slowly varying function, (i.e. $\Phi = \alpha$, an experimentally definable constant), eqn. (9.24) becomes:

$$K(\Omega_1,\Omega) = \frac{\alpha\epsilon_c E^2}{\eta_c}\,(\Omega_1 + \Omega) \qquad (9.25)$$

By substituting for $K(\Omega_1,\Omega)$ in eqn. (9.18) using eqn. (9.25), and appealing to eqns. (9.15) and (9.20), the following expression is obtained:

$$\langle\langle K\rangle\rangle = \frac{2\alpha\epsilon_c E^2}{\eta_c}\,\langle\Omega\rangle \qquad (9.26)$$

This may now be used in eqn. (9.17):

$$\frac{dN}{dt} = \frac{-\alpha\epsilon_c E^2}{\eta_c}\,\langle\Omega\rangle N^2 \qquad (9.27)$$

By using eqn. (9.22), eqn. (9.27) becomes:

$$\frac{dN}{dt} = \frac{-\alpha\epsilon_c E^2}{\eta_c} N_o\langle\Omega_o\rangle N \qquad (9.28)$$

Eqn. (9.28) may now be integrated to give:

$$N = N_o \exp\left[-\frac{\alpha\epsilon_c E^2}{\eta_c} N_o\langle\Omega_o\rangle t\right] \qquad (9.29)$$

Volkov and Krylov obtained satisfactory agreement between their theory and measurements (for continuous phase viscosities of 2.2×10^{-2} and 5.4×10^{-2}Pas, and electric field strengths of 2, 3 and 4kVcm^{-1}). For example, for E = 4kVcm^{-1} and $\eta_c = 2.2 \times 10^{-2}$Pas, they obtained $\alpha = 3.1 \times 10^{-3}$ and $\langle\Omega_o\rangle = 1.9 \times 10^{-7}$cm^3 (i.e. initial average droplet radius $\langle a_o\rangle \simeq 36\mu$m).

In eqn. (9.29) the term $N_o\langle\Omega_o\rangle$ can be identified with the volume fraction φ. Eqn. (9.22) shows that $N/N_o = \langle\Omega_o\rangle/\langle\Omega\rangle$ and so eqn. (9.29) may be written:

$$\langle\Omega\rangle = \langle\Omega_o\rangle \exp\left[\frac{\alpha\epsilon_c E^2\varphi}{\eta_c} t\right] \qquad (9.30)$$

This can be expressed in terms of droplet radius as follows:

$$\langle a\rangle = \langle a_o\rangle \exp\left[\frac{\alpha\epsilon_c E^2\varphi}{3\eta_c} t\right] \qquad (9.31)$$

Eqns. (9.30) and (9.31) are expressions of droplet growth, as a function of time, which are exponential in form.

It should be noted that Volkov and Krylov's analysis is strictly applicable to the situation before phase separation gets underway, since the volume fraction $\varphi = N_o\langle\Omega_o\rangle = N\langle\Omega\rangle$ is assumed to be constant.

9.10.2 Dipole Coalescence Model (Mechanistic Approach)

A W/O emulsion comprises a collection of water droplets, the dispersed phase, suspended in a background of oil, the continuous phase. Droplets which are not small enough to be kept in suspension by the effects of Brownian motion attain a terminal speed of descent under the gravitational field of the Earth. These eventually collide and coalesce with the rising free-water interface. Coalescence between droplets settling at different rates, and that due to Brownian motion, can occur but these effects are assumed to be negligible. The terminal speed of a droplet is calculated according to Stokes' law. After a sufficiently long time, all the falling water droplets in the emulsion coalesce with the rising free-water interface. When this occurs the water and oil phases become separate and the emulsion is said to be resolved. The time it takes for this to occur is the emulsion resolution time.

When an external electric field is applied to the W/O emulsion, the water droplets polarise and are attracted to one another by dipole coalescence.

The aim of inducing droplet coalescence is to create larger droplets which have increased rates of descent. The potency of this method is attributable to the fact that droplet terminal speed is proportional to radius squared, according to Stokes' law.

An emulsion is usually characterised by a droplet size distribution which can present difficulties in theoretical treatments. To render the calculations tractable, it is assumed that the emulsion is monodisperse, cubically packed, and characterised by a representative droplet radius. This allows the derivation of an expression for droplet growth rate which can be used for the determination of emulsion resolution time.

When an electric field is applied to a W/O emulsion the suspended water droplets polarise and elongate in the direction of the field. The exact shape of the droplet is governed by the electrostatic stresses generated at its surface which are balanced by the effects of interfacial tension. The shape can usually be approximated by an ellipsoid but here it will be assumed to remain spherical, for mathematical convenience. The expression for the dipole coalescence force between two droplets of equal size, which are aligned with the applied electric field is (see eqns. (5.30) and (5.53)):

$$F = 24\pi\epsilon_c(a/\Lambda)^4 a^2 E^2 \qquad (9.32)$$

This assumes that the continuous phase permittivity ϵ_c is much less than that of the dispersed phase ϵ_d (valid for W/O emulsions). The droplet radius is taken as a, and E is the uniform applied electric field.

Eqn. (9.32) is only a good approximation when the particle separation $\Lambda >> 2a$ but is presently assumed to be valid for $\Lambda \geq 2a$ as by Fuchs (1964). He considers the force of attraction to be balanced by viscous drag, according to Stokes' law, and obtains the following expression (which has been modified to account for the permittivity of the continuous phase):

$$6\pi\eta_c au = 24\pi\epsilon_c a^6 E^2/\Lambda^4 \qquad (9.33)$$

The equation of motion of water droplets, ignoring inertial effects, is therefore as follows, where u is the speed of each droplet relative to the continuous phase:

$$\frac{-d\Lambda}{dt} = 2u = \frac{8\epsilon_c a^5 E^2}{\eta_c \Lambda^4} \qquad (9.34)$$

Now the unit lattice, for the case of a cubically packed emulsion, is a cube with one droplet at each vertex. Consequently, the unit lattice contains the volume of one complete dispersed phase droplet. If the emulsion is monodisperse and contains droplets of radius a, cubically packed with separation Λ, the volume fraction φ of the dispersed phase is therefore:

$$\varphi = \frac{4}{3}\pi\left[\frac{a}{\Lambda}\right]^3 \qquad (9.35)$$

Eqn. (9.34) can be integrated as follows to determine the time it takes for two water droplets to become coincident. Initially the droplets are assumed to be a distance Λ apart whereas the separation becomes zero at time t later.

$$t = \frac{\eta_c}{40\epsilon_c E^2}\left[\frac{\Lambda}{a}\right]^5 = \frac{\eta_c}{40\epsilon_c E^2}\left[\frac{4\pi}{3\varphi}\right]^{5/3} \qquad (9.36)$$

Eqn. (9.36), originally presented by Fuchs (1964), can be used to gain some insight into the time required for the resolution of a W/O emulsion but it should be borne in mind that it is only applicable to the coalescence of a pair of water droplets. In order to obtain a more meaningful expression, the artificial process described below may be considered. As before, the emulsion is assumed to be

monodisperse and cubically packed (at the end of each stage of coalescence). Suppose that the action of the applied electric field causes alternate emulsion droplets to move in the direction of the field and the interspersed ones to move anti-parallel to the field. The approach of each droplet to its nearest neighbour produces a collection of couplets, as shown in Figure 9.3. Each couplet comprises a pair of water droplets which move towards one another.

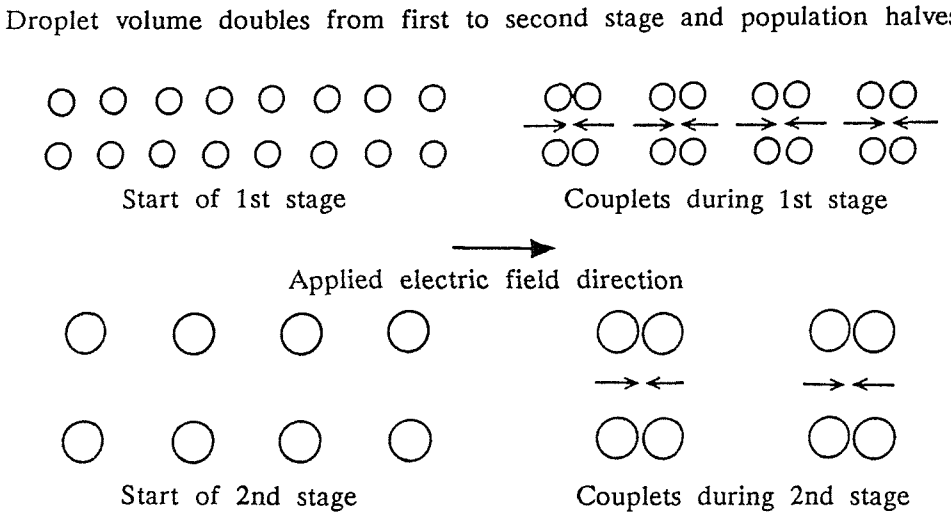

FIGURE 9.3 **Artificial coalescence process. Action of the applied electric field in promoting couplets.**

When the droplets forming each couplet coalesce the first stage of coalescence is completed. The original population of droplets is halved, though each has twice its original volume. The volume fraction of dispersed water remains fixed despite this coalescence process. The newly-formed droplets are then considered to re-arrange themselves into a cubically packed formation, prior to the second stage of coalescence. The second, and subsequent, stages of coalescence follow precisely the first-stage pattern.

The droplets which undergo the aforementioned stage-by-stage coalescence process simultaneously descend under the influence of gravity. Eventually the process ends when the droplets, which were initially in the surface layer of the emulsion, have grown in size, descended to the rising free-water interface and coalesced with it. The resolution time of the emulsion can therefore be determined by considering the descent time of a growing water droplet. Although the artificial coalescence model is discrete in nature, the mathematics used to describe the process are continuous in form. The continuous growth pattern of a droplet can be established by combining eqn. (9.34), with sign reversed, and eqn. (9.35):

$$\frac{1}{\Lambda}\frac{d\Lambda}{dt} = \frac{8\epsilon_c E^2}{\eta_c}\left[\frac{3\varphi}{4\pi}\right]^{5/3} \qquad (9.37)$$

The solution of this differential equation is easily obtained, the initial value of droplet separation Λ being Λ_o:

$$\Lambda = \Lambda_o \exp\left\{\frac{8\epsilon_c E^2}{\eta_c}\left[\frac{3\varphi}{4\pi}\right]^{5/3} t\right\} \qquad (9.38)$$

Eqns. (9.35) and (9.38) can now be used to give the continuous growth pattern of a droplet of initial radius a_o:

$$a = \left[\frac{3\varphi}{4\pi}\right]^{1/3}\Lambda, \qquad a_o = \left[\frac{3\varphi}{4\pi}\right]^{1/3}\Lambda_o$$

$$a = a_o \exp\left\{\frac{8\epsilon_c E^2}{\eta_c}\left[\frac{3\varphi}{4\pi}\right]^{5/3} t\right\} \qquad (9.39)$$

Suppose that the resolution time of the emulsion is τ. This is the time it takes for a droplet with continuously growing radius to fall from the top of the emulsion, at level H, to the final water/oil interface, at level φH. Let h be the height of a water droplet, the descent speed w of which may be calcualted from Stokes' law as follows:

$$6\pi\eta a w = \frac{4}{3}\pi a^3(\rho_d - \rho_c)$$

$$w = \frac{2g}{9\eta_c}(\rho_d - \rho_c)a^2 = \beta a^2 \qquad (9.40)$$

where ρ_d and ρ_c are the densities of the dispersed and continuous phases respectively. The equation of motion of the descending droplet is given by:

$$\frac{dh}{dt} = -w = -\beta a^2 \qquad (9.41)$$

This may be integrated using the previously-mentioned height limits and eqn. (9.39):

$$\int_{H}^{\varphi H} dh = -\beta a_o^2 \int_{o}^{\tau} \exp\left\{\frac{16\epsilon_c E^2}{\eta_c}\left[\frac{3\varphi}{4\pi}\right]^{5/3} t\right\} dt$$

$$H(1-\varphi) = \frac{\beta a_o^2 \eta_c}{16\epsilon_c E^2}\left[\frac{4\pi}{3\varphi}\right]^{5/3}\left\{\exp\left[\frac{16\epsilon_c E^2}{\eta_c}\left[\frac{3\varphi}{4\pi}\right]^{5/3}\tau\right]-1\right\}$$

This can be re-arranged to give an expression for the resolution time of the emulsion:

$$\tau = \frac{\eta_c}{16\epsilon_c E^2}\left[\frac{4\pi}{3\varphi}\right]^{5/3} \ell n\left[1+\frac{16\epsilon_c E^2}{\beta\eta_c a_o^2}\left[\frac{3\varphi}{4\pi}\right]^{5/3} H(1-\varphi)\right] \qquad (9.42)$$

Eqn. (9.42) has the expected limiting value as the electric field strength E becomes vanishingly small:

$$\tau = \frac{H(1-\varphi)}{\beta a_o^2} \qquad (9.43)$$

The maximum droplet radius a_τ can be found by substituting τ for t in eqn. (9.39) and using eqn. (9.42):

$$a_\tau = \left[a_o^2 + \frac{72\epsilon_c E^2}{g(\rho_d-\rho_c)}\left[\frac{3\varphi}{4\pi}\right]^{5/3} H(1-\varphi)\right]^{\frac{1}{2}} \qquad (9.44)$$

Interestingly enough, this expression is independent of the continuous phase viscosity η_c.

Although real emulsions are seldom monodisperse, it is considered reasonable to take, as representative, the droplet radius a_o which corresponds to the peak of the volume fraction distribution.

If the applied electric field strength E is not of steady value, it should be replaced by the root-mean-square value in the equations.

It is interesting to compare the equations of droplet growth given by the coagulation kinetics approach (eqn. (9.31)) and the mechanistic approach (eqn. (9.39)). The expressions are similar, both showing exponential growth of droplet radius with the passage of time.

In order to test the applicability of eqn. (9.42), some experiments were performed to measure the resolution time of W/O emulsions. A turbidimetric technique (see Section 9.11) was used to monitor the water droplet content. Since the nephelometer is very sensitive (1NTU $\simeq$ 1ppm by volume of water) it was necessary to make measurements on low volume fraction emulsions (i.e. $\varphi \leq$ 750ppm).

W/O emulsions were prepared by ultrasonically agitating known amounts of distilled water and diesel oil. Each newly-prepared emulsion was then placed in a cuvette, of square cross-section, immediately prior to testing in the nephelometer.

A pair of vertically-orientated electrodes were quickly lowered into the emulsion, to enable it to be subjected to an electric field. Each electrode measured 60mm high by 19mm wide, the separation between them being 16mm.

The nephelometer sensors were situated half-way up the cuvette which meant that emulsions appeared to be resolved when, in fact, there were still suspended droplets below sensor level. This was accounted for by replacing $H(1-\varphi)$ by $H-S$ in eqns. (9.42) to (9.44), where S is the sensor height (30mm). An emulsion was considered to be resolved when its turbidity became equal to that of the pure oil. It was difficult to assess accurately the end-point of a turbidity decay curve due to noise. To overcome this problem, the end-point was defined as that time when the emulsion turbidity had reduced to within 5NTU (Nephelometric Turbidity Unit) of the oil turbidity. This level was arbitrarily chosen and corresponded to less than 1% of the initial emulsion turbidity. Consequently the measured resolution times of the W/O emulsions were underestimated.

Measurements were made on W/O emulsions, of volume fraction $\varphi = 750 \times 10^{-6}$, with the cuvette electrodes energised at voltages in the range 500V to 8kV dc. The results are shown in Figure 9.4 and are compared with the theoretical curve obtained from eqn. (9.42). It can be seen that the agreement between theory and experiment is reasonable over the range of potentials given. The experimental parameters are: H = 60mm, S = 30mm, $\eta_c = 3 \times 10^{-3}$Pas, $\rho_c = 830\text{kgm}^{-3}$, $\rho_d = 1000\text{kgm}^{-3}$, $\epsilon_c = 2.3 \times 8.854 \times 10^{-12}\text{Fm}^{-1}$, $a_o = 4\mu$m.

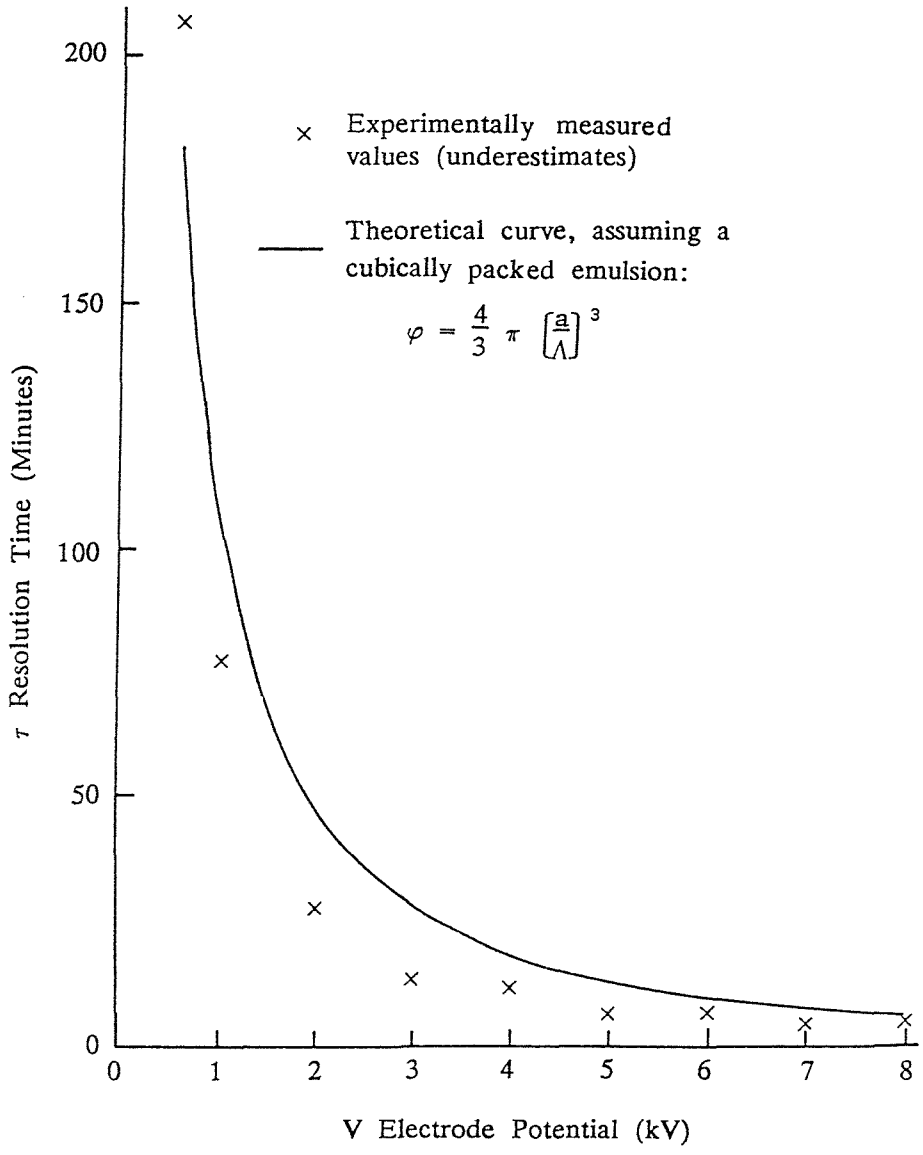

FIGURE 9.4 Comparison of theoretical and measured resolution times for a water-in-oil emulsion ($\varphi = 750 \times 10^{-6}$).

A sedimentation technique was used to determine the water volume fraction distribution of the ultrasonically-prepared W/O emulsions. This was derived from the turbidity decay curve of such an emulsion, settling under gravity, in the absence of an applied electric field, assuming that no coalescence took place (see Section 9.11.1). The volume fraction distribution was also measured using a laser diffraction technique described by Swithenbank et al., 1976 (using the Malvern Particle and Droplet Size Analyser)(see Section 9.13). Both methods showed that the peak of the distribution occurred at a radius of approximately 4μm. This was the value chosen for a_o, the radius representative of water droplets in the emulsion.

Although simplifying assumptions have been made, concerning droplet size distribution and spatial arrangement, the model correctly predicts the manner in which resolution time decreases, with increasing electric field strength, in an experimental system.

The above theoretical derivation is somewhat simplistic since it assumes a perfectly efficient coalescence mechanism. In reality this is not the case since emulsion droplets are not cubically packed and are rarely monodisperse. Even if droplets collide, there is no certainty of them coalescing. These points can be accounted for in the theory by modifying the droplet growth expression (eqn. (9.39)). This is most conveniently achieved by including a multiplicative factor δ in the exponent. The term δ is geometrical in nature and will depend on such factors as volume fraction, droplet size distribution and the spatial distribution of dispersed phase droplets. It is apparent that δ is experimentally derivable and that $0 < \delta \leq 1$. It is likely that δ will vary during the course of an experiment, in view of its geometric character. To include δ in the analysis it is only necessary to replace ϵ_c by $\epsilon_c\delta$ in eqns. (9.38), (9.39), (9.42) and (9.44).

9.10.3 Extension of the Mechanistic Theory to Flowing Emulsions

The above theory can be extended to account for the conditions of steady upward flow, found in most electro-coalescers. Suppose that a droplet, of initial radius a_o, enters the electro-coalescer at the bottom, and is carried upwards into the treating space at a uniform flow speed F (as shown in Figure 9.5). On reaching the lower electrode, the droplets start to grow in size, as a result of coalescence in the electric field E. Consider a droplet to have radius a when it is at height h above the lower electrode. Its speed there is βa^2 (eqn. (9.40)) relative to the upward flowing emulsion. Since the emulsion flow speed is F, it follows that the upward speed of the droplet, relative to the electro-coalescer, is:

$$dh/dt = F - \beta a^2 \qquad (9.45)$$

Suppose that the electro-coalescer is designed so that the speed of the droplet is zero when it reaches the upper electrode. It follows that:

$$F = \beta[a(t_e)]^2 \qquad (9.46)$$

where t_e is the time taken by the droplet in rising between the lower and upper electrodes. Now eqn. (9.39) may be re-written as:

$$a = a_o e^{Lt} \qquad (9.47)$$

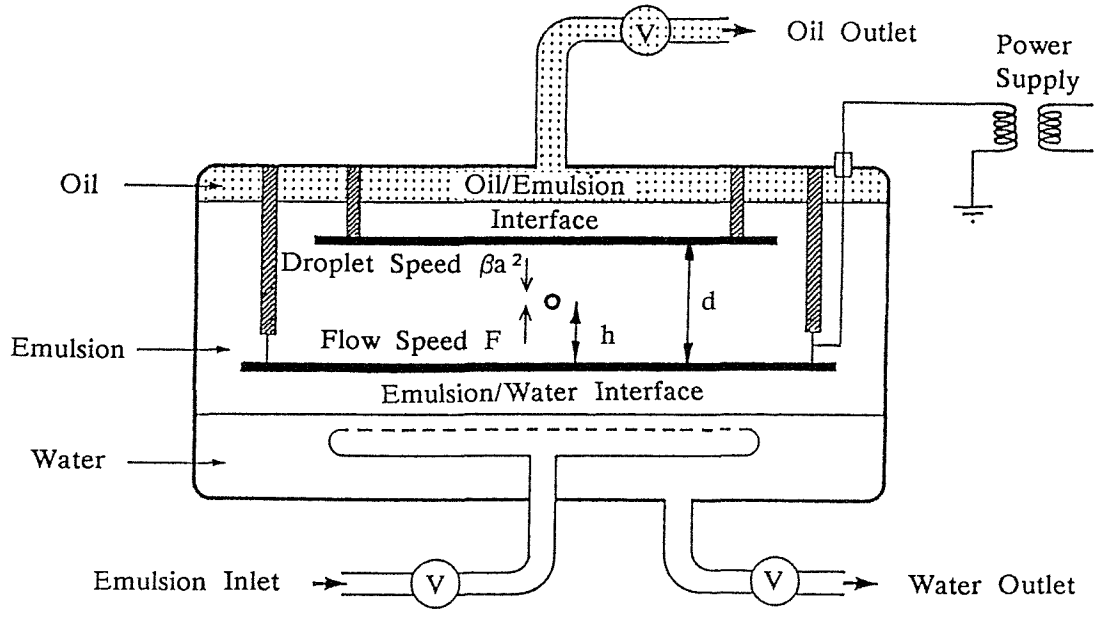

FIGURE 9.5 **Upward flow in practical electro-coalescer.**

where

$$L = \frac{8\epsilon_c E^2}{\eta_c}\left[\frac{3\varphi}{4\pi}\right]^{5/3} \qquad (9.48)$$

The time t_e may be established from a consideration of eqns. (9.46) and (9.47):

$$F = \beta a_o{}^2 e^{2Lt_e}$$

Re-arrangement leads to:

$$t_e = \frac{1}{2L}\,\ell n\left[\frac{F}{\beta a_o{}^2}\right] \qquad (9.49)$$

The required separation (d) of the electrodes may now be established by integrating eqn. (9.45) between the limits 0 and d, for the h variable, and between the limits 0 and t_e, for the t variable:

$$\int_0^d dh = \int_0^{t_e} (F - \beta a_o{}^2 e^{2Lt}) dt$$

$$d = Ft_e - \frac{\beta a_o{}^2}{2L}\left[e^{2Lt_e} - 1\right]$$

Using eqn. (9.49) this becomes:

$$d = \frac{\beta a_o{}^2}{2L}\left\{1 + \left[\frac{F}{\beta a_o{}^2}\right]\left[\ell n\left[\frac{F}{\beta a_o{}^2}\right] - 1\right]\right\} \qquad (9.50)$$

It should be noted that the electric field is specified by E = V/d, for parallel plate electrodes, where V is the potential difference between the electrodes. In consequence, eqn. (9.50) takes on the following form, after using eqn. (9.48).

$$\frac{8\epsilon_c V^2}{d\eta_c}\left[\frac{3\varphi}{4\pi}\right]^{5/3} = \frac{\beta a_o{}^2}{2}\left\{1 + \left[\frac{F}{\beta a_o{}^2}\right]\left[\ell n\left[\frac{F}{\beta a_o{}^2}\right] - 1\right]\right\}$$

Re-arranging gives d explicitly:

$$d = \frac{16\epsilon_c V^2}{\eta_c \beta a_o{}^2}\left[\frac{3\varphi}{4\pi}\right]^{5/3} \Big/ \left\{1 + \left[\frac{F}{\beta a_o{}^2}\right]\left[\ell n\left[\frac{F}{\beta a_o{}^2}\right] - 1\right]\right\} \qquad (9.51)$$

Eqn. (9.51) gives the required electrode separation in terms of the other electro-coalescer parameters. Its applicability can be gauged using the known characteristics of a Howmar electro-coalescer, which are as follows: d = 0.31m, V = 34000V (peak), $\eta_c = 1.76 \times 10^{-3}$Pas, $\rho_c = 880 kgm^{-3}$, $\rho_d = 1000 kgm^{-3}$, $F = 1.97 \times 10^{-3} ms^{-1}$, $a_o = 5\mu m$. Though the oil is treated with 5% wash water, most of it falls out before the treating space and so the volume fraction is taken as $\varphi = 0.01$. It follows from eqn. (9.40) and the above parameters that $\beta = 1.486 \times 10^5 m^{-1}s^{-1}$. Eqn. (9.51) can now be used to show that d = 0.44m (the value of V^2 has been halved to account for the RMS value), which is in fairly good agreement with the actual value of 0.31m for electrode separation (which should be less than d).

If a smaller value of electrode separation were to be used, the electric field would be stronger and the droplets would fall out before reaching the upper

electrode. The electrode separation should not be reduced too much, however, since the increase in electric field strength could lead to re-emulsification (see Chapter 7).

9.11 The Use of Turbidity to Monitor Coalescence in Emulsions

Turbidity is an expression of the optical property of a material which causes light to be scattered and absorbed rather than transmitted directly through it. Devices which measure turbidity are called turbidimeters; those that work by light absorption are called absorptometers whereas those that work by light scattering are termed nephelometers. Absorptometers are not sensitive to small turbidities, maximum signal strength corresponds to minimum turbidity, and negative response is exhibited in that signal strength decreases with increasing turbidity. Nephelometers, on the other hand, can be highly sensitive to small turbidities, minimum signal strength corresponds to minimum turbidity, and a direct response is exhibited in that the signal increases with increasing turbidity. The unit of turbidity is called the NTU which stands for Nephelometric Turbidity Unit.

In order to monitor the turbidity of W/O emulsions, a Drott TRM-LD nephelometer is used, which has a range of 0 - 1000NTU. In this instrument, a photodiode, situated opposite the light source, regulates the current supply to the lamp, in such a way that the output current from the photodiode remains unchanged. This compensates automatically for sample colour, lamp ageing, temperature dependence, and the spectral sensitivity difference between the two photodiodes. The second photodiode is situated at right angles to the first, in the same horizontal plane, in order to measure scattered light. Its output current is proportional to the amount of scattered light, up to 500NTU. Beyond 500NTU the output becomes non-linear and the reading has to be adjusted using a correction curve.

To measure the turbidity of a liquid, a sample of it is poured into a cuvette, which must then be placed in the body of the nephelometer, and covered with a top to prevent the entry of extraneous light. The cuvette is square in cross-section, of dimension 20mm, and 70mm high which gives a maximum sample volume of 25mℓ. The lamp and photodiodes are situated at a level corresponding to approximately half-way up the cuvette.

In order to apply an electric field to an emulsion, while it is in the nephelometer, a pair of vertically-orientated electrodes are used (see Figure 9.6 and Plate 4,a). The cuvette electrodes are each 18mm wide by 68mm high and

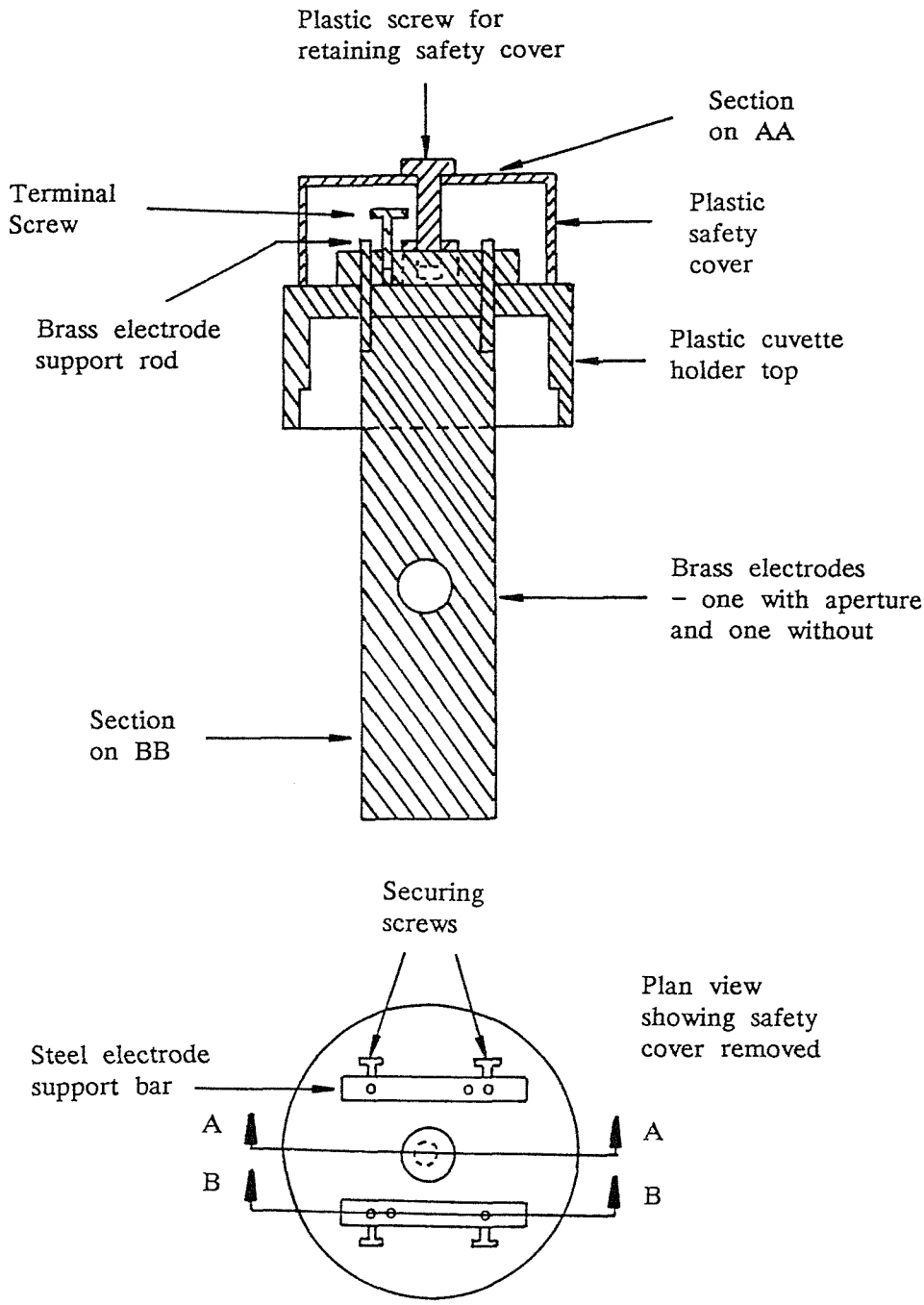

FIGURE 9.6 Schematic diagram of cuvette electrode (approximately full size).

separated from one another by a 16mm gap. One of the electrodes is constrained to have a hole in it, to allow scattered light to reach the measuring photodiode. The presence of the electrodes within the cuvette does affect the output of the nephelometer but this can be accounted for by using a second correction curve (obtained by measuring the turbidity of various emulsions with and without the electrodes present in the cuvette).

The turbidity of an emulsion, as a function of time, is obtained by

recording the nephelometer output using a chart recorder. The turbidity reading must then be modified to account for the previously-mentioned corrections.

When working with clear oils, negative turbidities were encountered; this was because the nephelometer was calibrated for water which has a different refractive index from oil.

Experiment showed that the turdibity of a W/O emulsion, prepared ultrasonically, was approximately proportional to the volume fraction of dispersed water, where 1NTU corresponded to about 1ppm by volume of water.

9.11.1 Determination of the Droplet Size Distribution of a W/O Emulsion Using Turbidity

The turbidity of a W/O emulsion, settling under gravity (with no electric field applied), is expected to decrease rapidly at first, as the larger droplets settle out, and then more slowly as the smaller droplets are left in suspension. At a particular moment in time, and at a particular level in an emulsion (e.g. sensor height), the turbidity is only dependent on those droplets less than a certain size. Droplets larger than this critical size will already have descended to at least the level considered. Thus, if Stokes' law is assumed to apply, the critical size can be determined from the system parameters. It can be appreciated, therefore, that the emulsion turbidity curve, (a function of time) contains information about the droplet size distribution.

It is shown, in Appendix E, how to determine the droplet size distribution (or equivalently the volume fraction distribution) of a W/O emulsion from a turbidity decay curve. Coalescence by Brownian motion and differential sedimentation is, of course, assumed to be negligible; coalescence would change the distribution. In fact, the distribution does change, as a function of time, due to settling which is a truncation effect.

The initial portion of the turbidity decay curve was found to be virtually exponential in nature, and this has been assumed in Appendix E. It is possible that droplet coalescence did occur, and this could explain the observed faster-than-exponential settling, with the passage of time. The volume fraction distribution, derived from the emulsion turbidity decay curve (according to Appendix E), is shown in Figure 9.7. It ranges from about 1 to 20μm in radius with the peak at about 3.5μm. Also shown in Figure 9.7 is the number density distribution, which was obtained from the volume fraction distribution by dividing

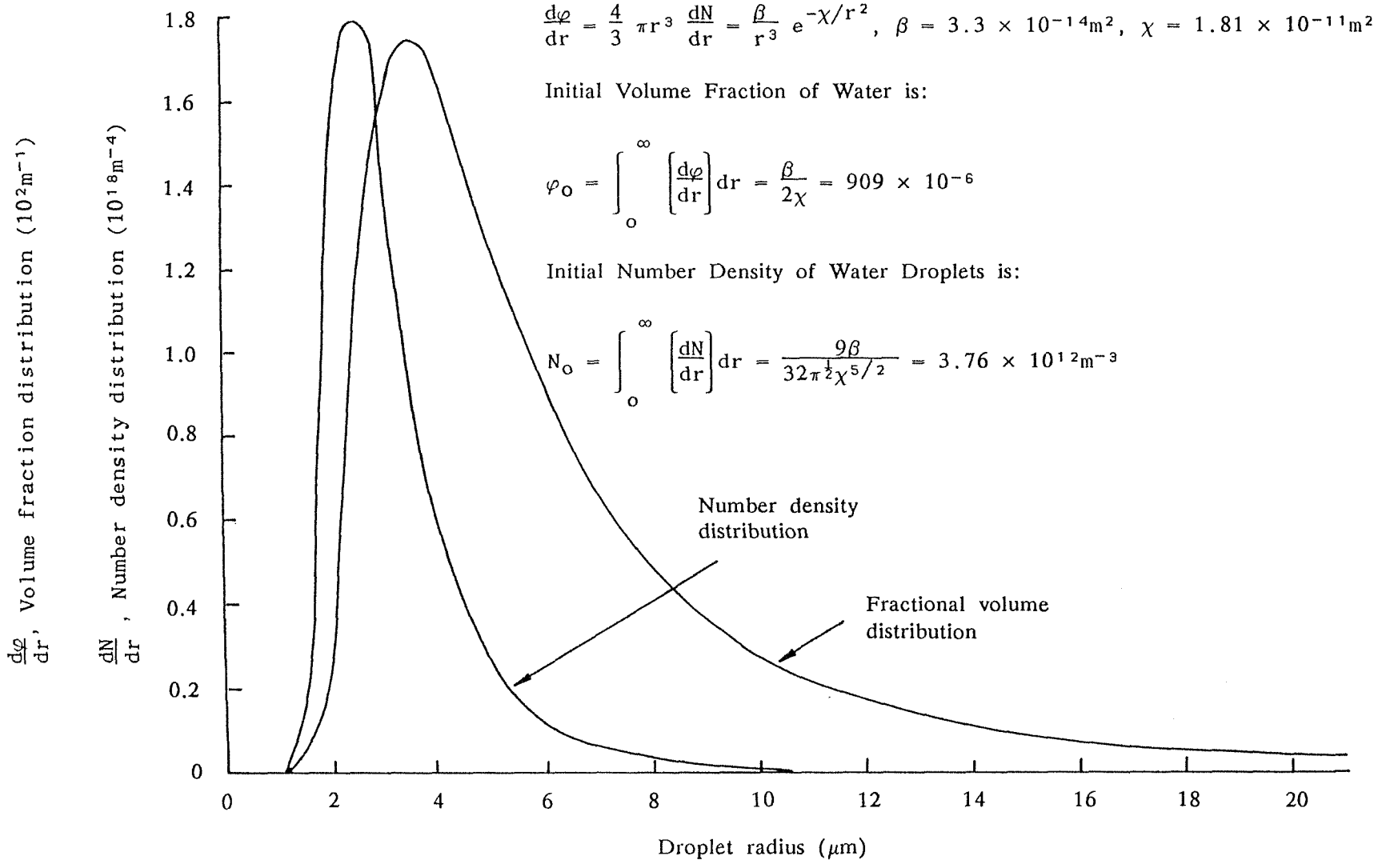

FIGURE 9.7 **Volume fraction and number density distributions of a W/O emulsion ($\varphi \simeq 0.1\%$) as determined by a sedimentation technique.**

by the droplet volume, for the particular size considered. In this case, the peak occurs at the smaller size of 2.5μm radius. By integrating the number density distribution, it can be shown that the emulsion had an initial number density of about $4 \times 10^{12} m^{-3}$ (its initial volume fraction was ~ 0.1%).

In Section 9.13 , the measurement of the volume fraction distribution of an ultrasonically prepared W/O emulsion (and how it changes in time) is discussed. In fact, it turns out to be bimodal rather than unimodal as suggested by the simplistic sedimentation theory.

9.11.2 A Turbidimetric Investigation of Electrical Coalescence in Low-Concentration W/O Emulsions

One of the disadvantages of working with low-concentration (< 0.1% by volume) W/O emulsions is that it is difficult to measure the level of dispersed water. In systems where the concentration of water is greater than about 1%, it is possible to measure the level of free water, which is similar to the approach of Bailes and Larkai (1981) who measured dispersion band depth. The turbidimetric technique, however, offers a number of advantages. Firstly, it is possible to measure dispersed phase water concentrations down to about 1ppm; the turbidity being roughly proportional to the concentration of dispersed water. Secondly, if an electric field is applied to a W/O emulsion within the cuvette, it is possible to monitor the water content, in situ, as a function of time (using a chart recorder to record the nephelometer output). One disadvantage of the technique is that it relies on the medium being transparent, and so is inapplicable to fuel oils and crudes which are black and opaque. It is, however, applicable to diesel oil, gas oil and other distillates. Since the latter are of low and the former of high conductivity, it is apparent that the turbidimetric technique is not suitable for high-conductivity oils. In order to investigate electrical coalescence in high-conductivity oils, the anti-static additive ASA-3 was dissolved in a low-conductivity (~ $10 pSm^{-1}$) transparent diesel oil. Whereas only 0.4ppm of ASA-3 is required to make aviation fuel safe, from the buildup of excess charge during pumping, a seemingly disproportionate amount, 200ppm, was needed to produce a 730-fold increase in conductivity of the diesel oil.

Ultrasonic emulsification, using diesel oil doped with ASA-3, appeared to be different from the case for undoped diesel. This was apparent from the turbidity decay curves (see Figures 9.13 and 9.14) which exhibited a maximum turbidity some time after cessation of agitation; there was no such maximum for undoped diesel (see Figures 9.8 to 9.12). The maximum occurred in the case of electrified emulsions and also when no electric field was applied. This effect may have been due to the ASA-3 behaving as a surface-active agent or to the increased ionic concentration which affects the electric double layer.

During the course of experiments on undoped diesel oil, the conductivity of the diesel was found to increase significantly (by nearly an order of magnitude e.g. from 8 to 59pSm^{-1}). This was believed to have been due to ions leaching out of the brass electrode material; such could have been prevented by the use of gold or platinum coated electrodes.

Emulsion temperature was also observed to increase above ambient during experiments, in the range 6 - 9°C, depending on oil conductivity and potential difference between the electrodes. This increase was due to heating from the nephelometer light source and Joule heating of the emulsion.

Emulsions were prepared by ultrasonically agitating (for 5 minutes) equilibrated diesel oil and water. The diesel oil having been stored in contact with free water, to reduce any tendency for it to absorb dispersed water during experiments. Oil in contact with a source of free water will absorb water until it becomes saturated, at which time the system has reached a state of equilibrium. Similarly, oil in contact with the atmosphere will absorb an amount of water which is approximately proportional to the relative humidity of the surrounding air (Zaky and Hawley, 1973).

The ultrasonic emulsification technique, though convenient to use, did not give very good repeatability. Thus, the initial turbidity of emulsions, produced under identical conditions, tended to vary.

Described below are the results of a number of experiments performed with potential differences ranging from 0 to 500V (dc and RMS).

9.11.3 Electrical Separation of Doped and Undoped W/O Emulsions Using Weak AC and DC Fields

During the experiments described here, potential differences up to 500V dc and 500V RMS ac were applied between the cuvette electrodes. A mains-frequency transformer was used to provide the 50Hz ac excitation whereas a stabilized power supply provided the dc excitation.

The W/O emulsions were prepared ultrasonically using doped (high conductivity) and undoped (low conductivity) diesel oil, as described earlier (see Section 9.11.2).

The results of seven experiments are shown in Figures 9.8 to 9.14. In each case, the W/O emulsion was prepared by ultrasonically agitating 15$\mu\ell$ water in 20 mℓ diesel oil, for five minutes (leading to 750ppm W/O emulsions). Figures 9.8 to 9.12 are for emulsions prepared using diesel oil undoped with ASA-3. Figures 9.13 and 9.14, however, are for emulsions prepared using diesel oil doped with ASA-3 (which increased the continuous phase conductivity by a factor of about 730). When comparing Figures 9.8 to 9.13, the criterion for efficient droplet coalescence and phase separation is rapid reduction of turbidity (since this corresponds to the rapid removal of dispersed phase droplets from the emulsion). It can be seen from Figures 9.8 to 9.12 that phase separation rate improves as the potential difference (and hence electric field strength) increases, for both dc and ac fields. Figures 9.9 to 9.14 show that phase separation is better for dc than ac fields. In fact, 150V dc gives more efficient phase separation than 500V RMS ac (which may be a reflection of how small the dipole coalescence forces are at low concentrations of water). Figures 9.13 and 9.14, in which the diesel oil has been doped with ASA-3 (to increase the continuous phase conductivity), also show that better phase separation results from dc than ac fields. This is somewhat surprising, since it is usually assumed that dc and ac fields are comparable, with regard to separation efficiency, for high-conductivity oils (since the effects of migratory coalescence are small). However, when it is remembered that the water concentration is low, which gives rise to small dipole coalescence forces, and that there is probably migratory coalescence due to double layer charge (which cannot relax away from droplets in the high-conductivity, continuous oil phase), the result does not seem unreasonable. The benefit of using a dc rather than ac electric field is most clearly demonstrated by Figure 9.13 in which the potential difference was switched from 150V RMS ac to 150V dc after 1080 minutes; after switching over, the phase separation rate increased dramatically. By comparing Figure 9.9 with Figure 9.13, and Figure 9.10 with Figure 9.14, it can be seen that phase separation was most efficient in the emulsions having undoped continuous oil phases

(i.e. low conductivity), for both dc and ac electric fields. This may have been due to the emulsions having been stabilized by the addition of ASA-3.

The turbidity decay curves, shown in Figures 9.8 to 9.14, have been processed from the raw chart recorder traces. Such chart recorder traces are frequently noisy and to obtain the general trends from them, such noise has been smoothed out. The noise is possibly due to water droplet floccules passing through the sensing volume in the nephelometer cuvette. As they pass, the turbidity increases for a short time, then decreases when they are no longer in a position to scatter light. When a large dc potential difference is used, the noise amplitude can be very high, sometimes swinging through 100NTU in a few minutes. It is less at the start and towards the end of an experiment. If a smaller dc potential difference is used, the same behaviour occurs but the amplitude of the noise is less. However, when an ac coalescing field is applied, the chart recorder trace is not noisy and consequently does not require smoothing. The same is true for W/O emulsions made with diesel oil doped with ASA-3, no matter what type of coalescing field is applied, whether it be ac or dc. This behaviour may be connected with the conductivity of the oil.

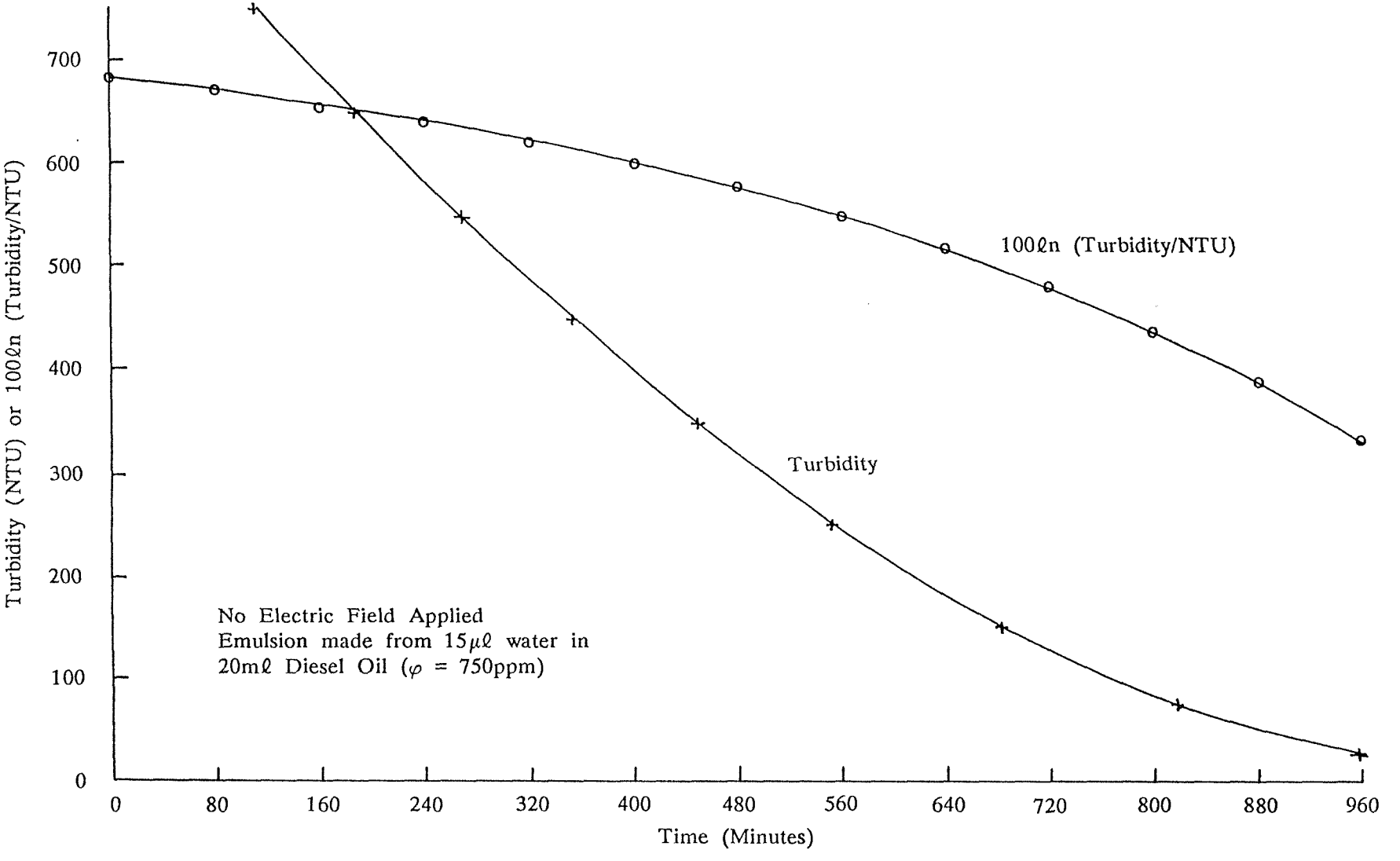

FIGURE 9.8 **Turbidity decay curve for a 750 ppm undoped W/O emulsion with no electric field applied.**

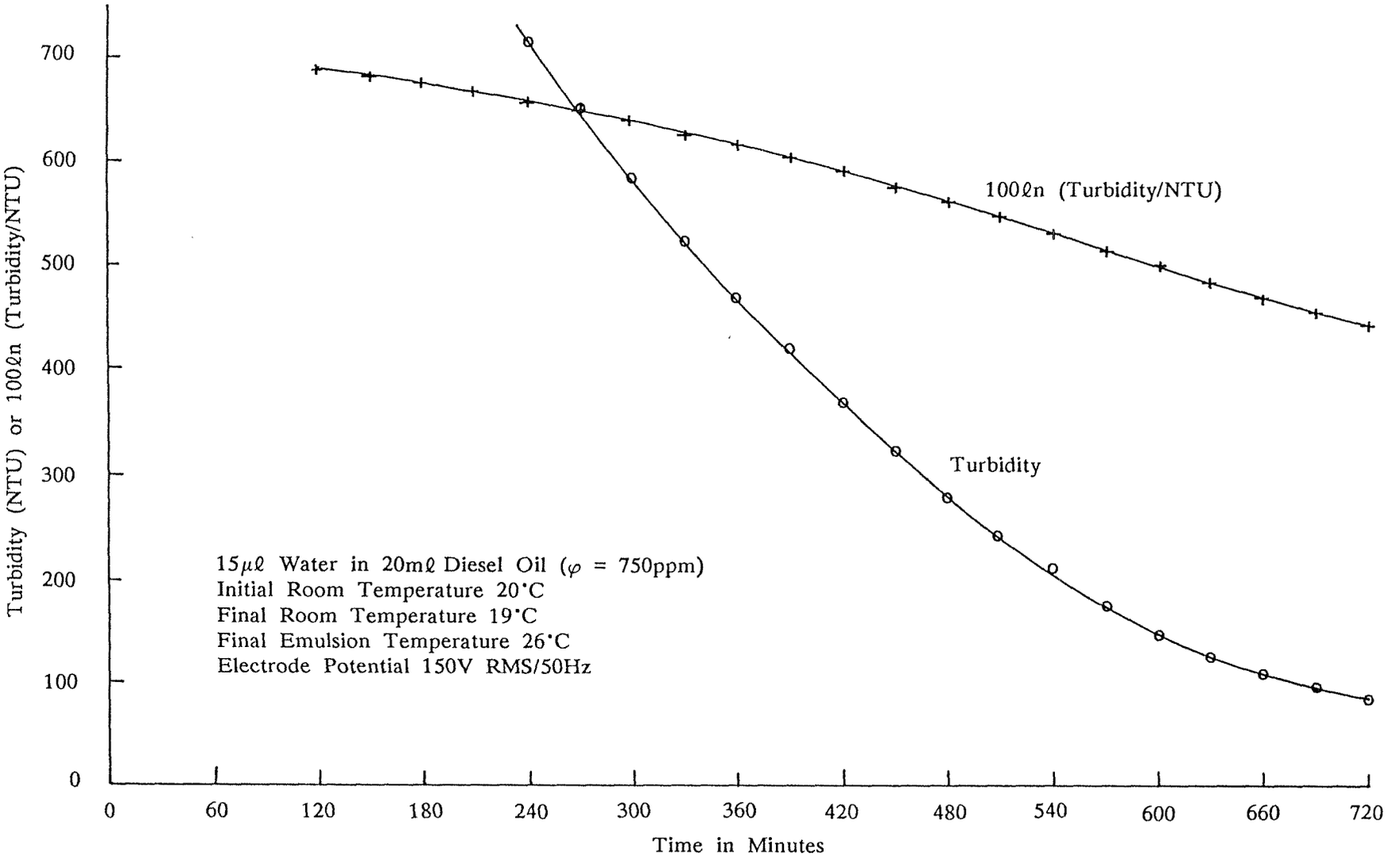

FIGURE 9.9 **Turbidity decay curve for a 750 ppm undoped W/O emulsion with 150V RMS, 50Hz ac excitation applied to test-cell electrodes.**

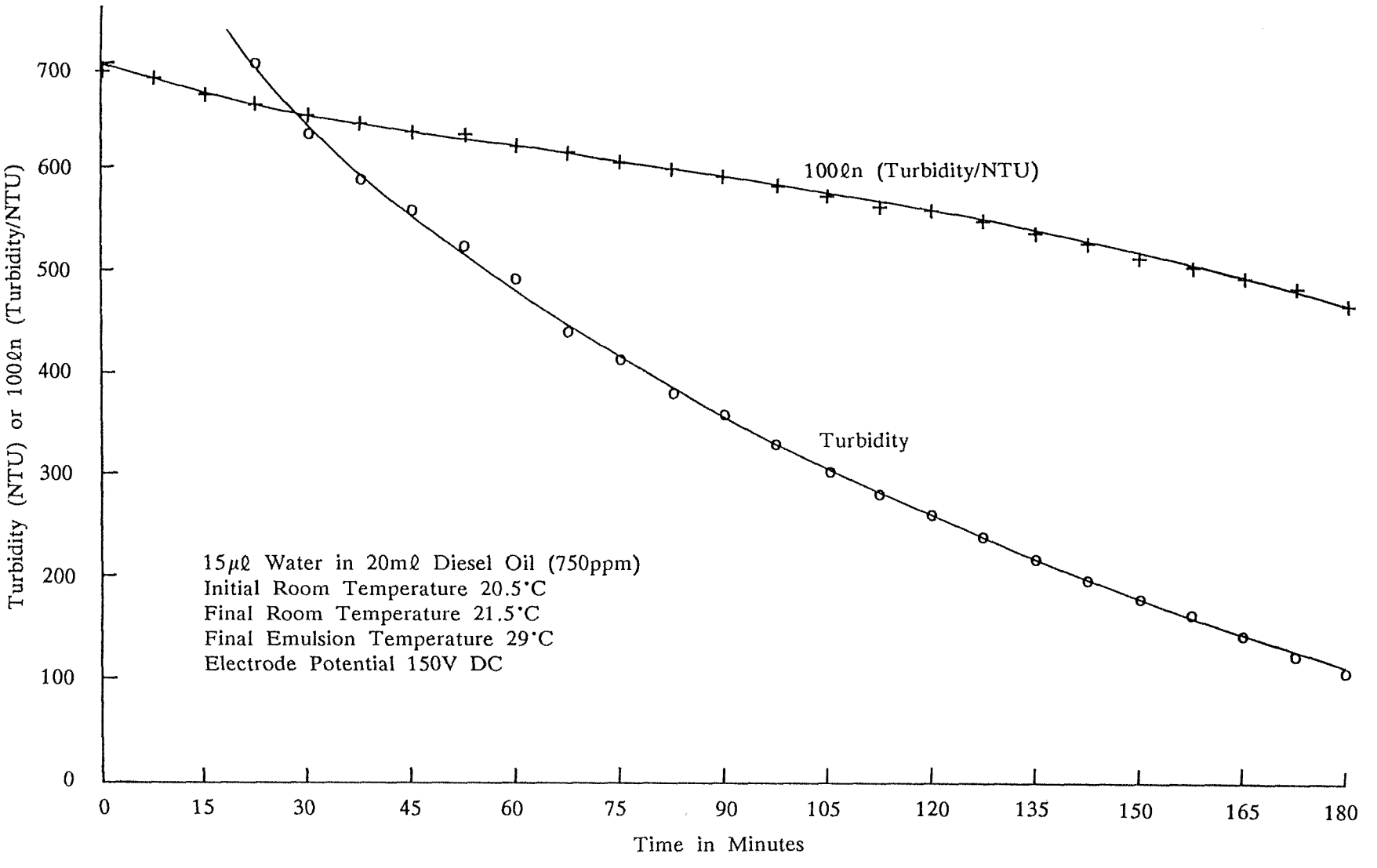

FIGURE 9.10 **Turbidity decay curve for a 750 ppm undoped W/O emulsion with 150V dc applied to test-cell electrodes.**

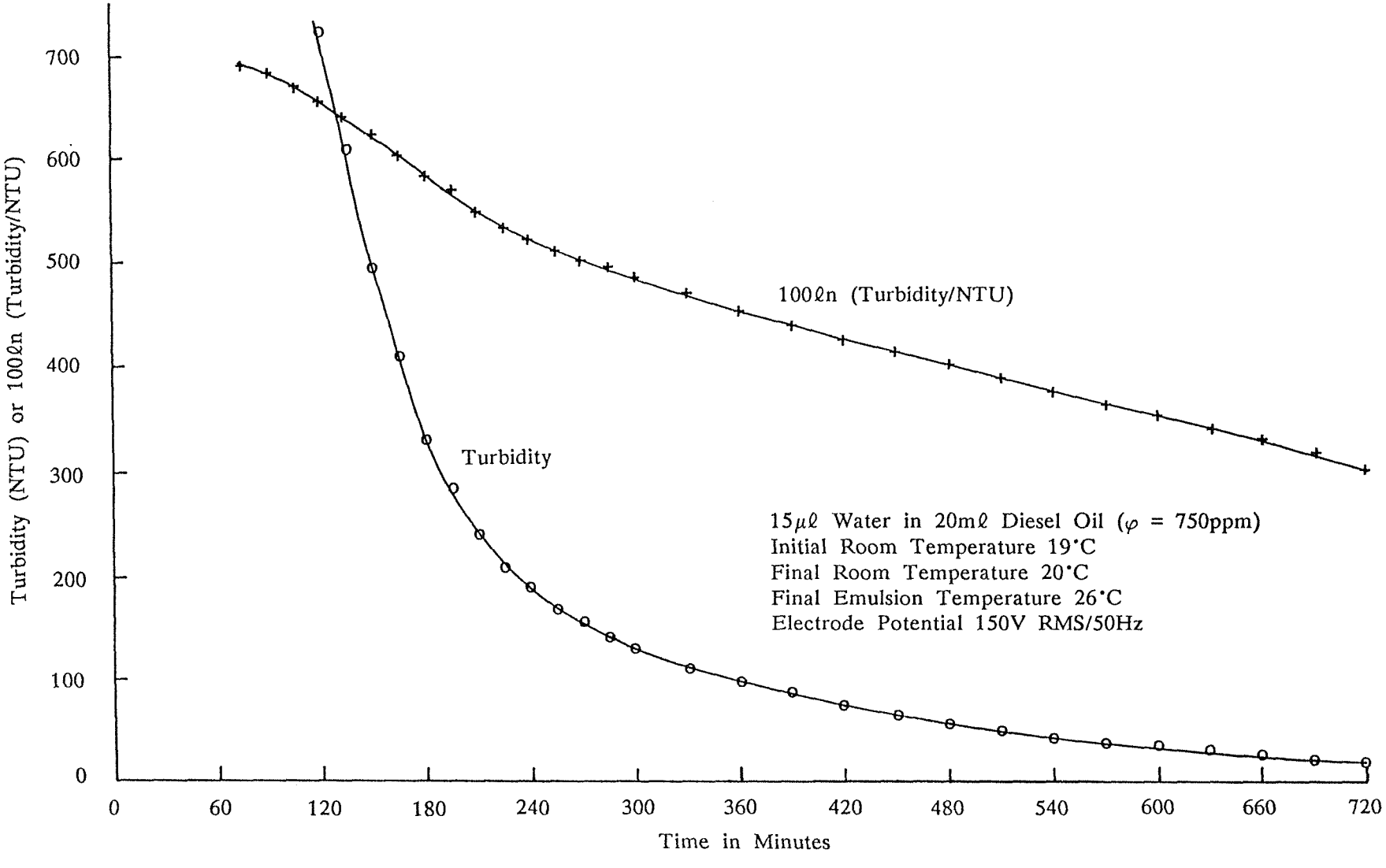

FIGURE 9.11 **Turbidity decay curve for a 750 ppm undoped W/O emulsion with 500V RMS, 50Hz ac excitation applied to test-cell electrodes.**

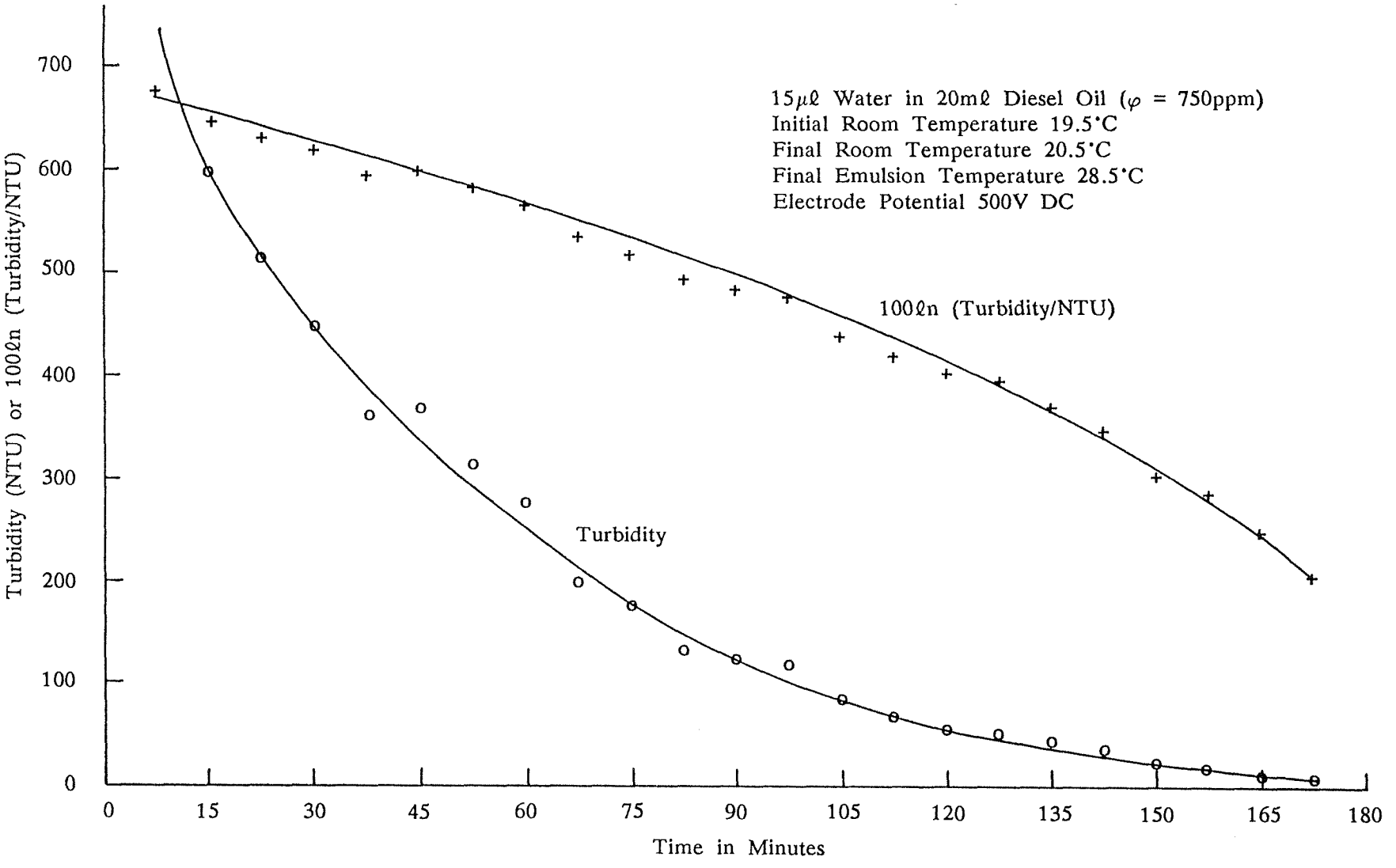

FIGURE 9.12 **Turbidity decay curve for a 750 ppm undoped W/O emulsion with 500V dc applied to test-cell electrodes.**

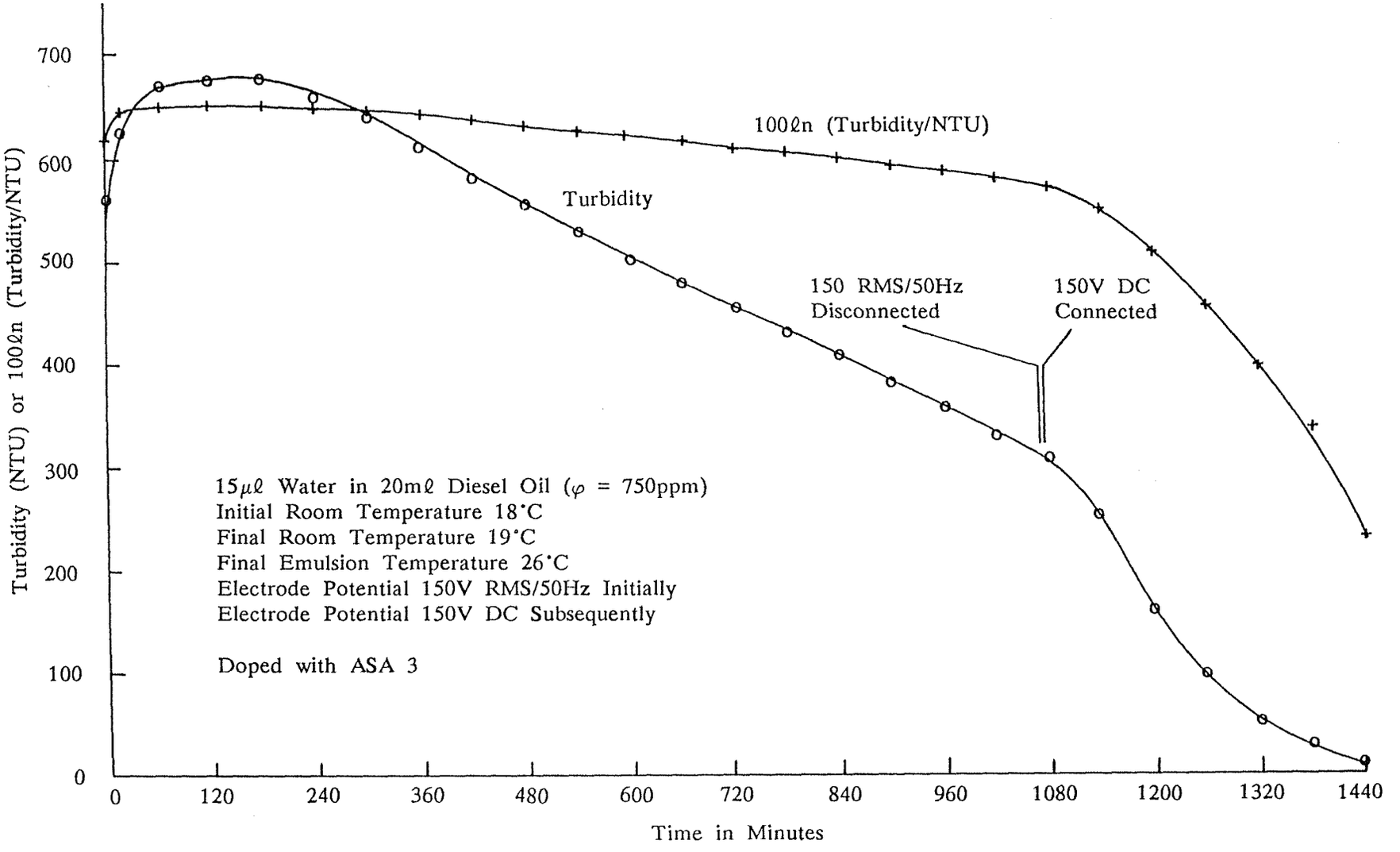

FIGURE 9.13 **Turbidity decay curve for an ASA–3 doped W/O emulsion. A 150V RMS ac excitation was applied for the first 1080 minutes, which subsequently was changed to 150V dc.**

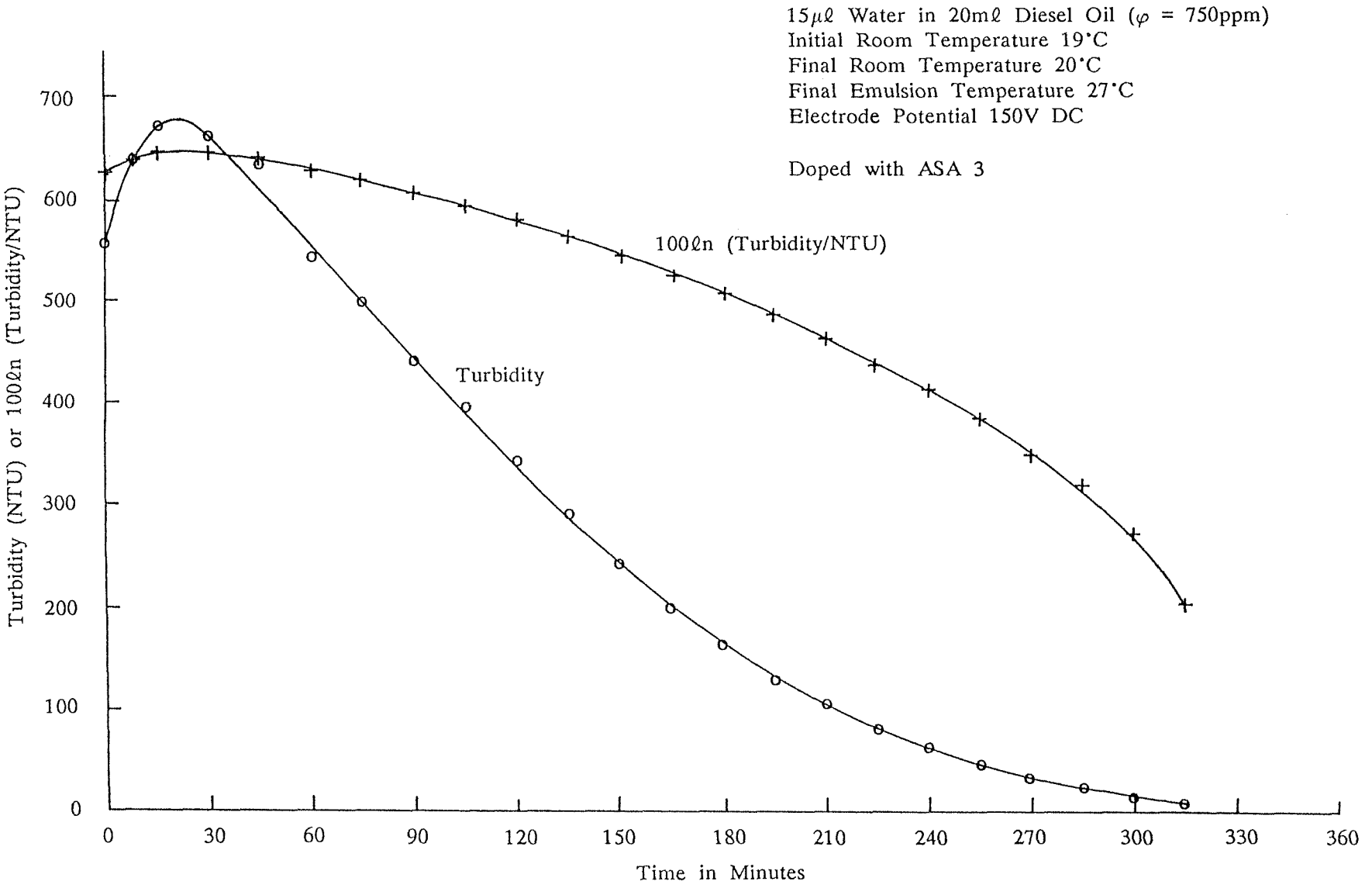

FIGURE 9.14 **Turbidity decay curve for an ASA–3 doped W/O emulsion with 150V dc applied to the test–cell electrodes.**

9.12 Closed-Loop Emulsification and Electro-Coalescer System

The closed-loop emulsification and electro-coalescer system was designed to demonstrate, qualitatively, the principles underlying the electrostatic resolution of W/O emulsions. It comprises a centrifugal pump, flow meter, horizontal electro-coalescer, main reservoir, drain valve, and an injection-inlet/sampling port which can be isolated between two ball valves (see Figure 9.15 and Plate 4,b). The pump can operate at flow rates up to 40 litre/min and is capable of dispersing the water phase, which forms about one third of the system volume (the remainder being diesel oil). Pump speed can be varied between 280 and 2780 RPM by adjusting the pump input voltage. The main reservoir is fitted with an anti-surge pipe and has a sloping bottom to prevent the accumulation of water. The electro-coalescer has a square cross-section, of dimension 2.54cm, and is 30cm long. It is constructed in perspex and has externally-mounted electrodes at its top and bottom surfaces. the lower electrode is grounded and the upper one connected to a power supply. To enable a strong electric field to be applied to the emulsion, within the electro-coalescer, a time-varying potential difference must be applied between the electrodes (see Chapter 11). Two types of power supply can be used; one is a simple transformer, the other is the triode-valve modulator unit (described in Chapter 11) which enables the application of a unidirectional, pulsed electric field.

W/O emulsions are created by the centrifugal pump; high shear forces, at the tips of the impeller blades, disperse the water phase into small droplets. The emulsion then flows upwards, through a flow meter, into the horizontal electro-coalescer, from where it returns to the main resevoir. Experiments can either be performed with the emulsion stationary or flowing.

The interaction of the electric field with the W/O emulsion was observed at high flow rates. When no electric field was applied, the emulsion flowing through the electro-coalescer had a smooth, laminar appearance. However, if an electric field was applied, the appearance of the emulsion became turbulent. When the modulator unit was used, with a low-frequency input, the turbulence in the emulsion was synchronous with the supply frequency.

In some experiments, the flow was allowed to stop (by disconnecting the electrical supply to the pump) after the emulsion had reached an equilibrium state, prior to energizing the electrodes. When an electric field was applied to the emulsion, it became substantially resolved (i.e. two distinct phases were apparent)

in a matter of seconds. When a potential difference of 5kV RMS ac was applied to the electro-coalescer electrodes, using a mains frequency transformer, the separation process lasted about six seconds (see Plate 5, a, b and c).

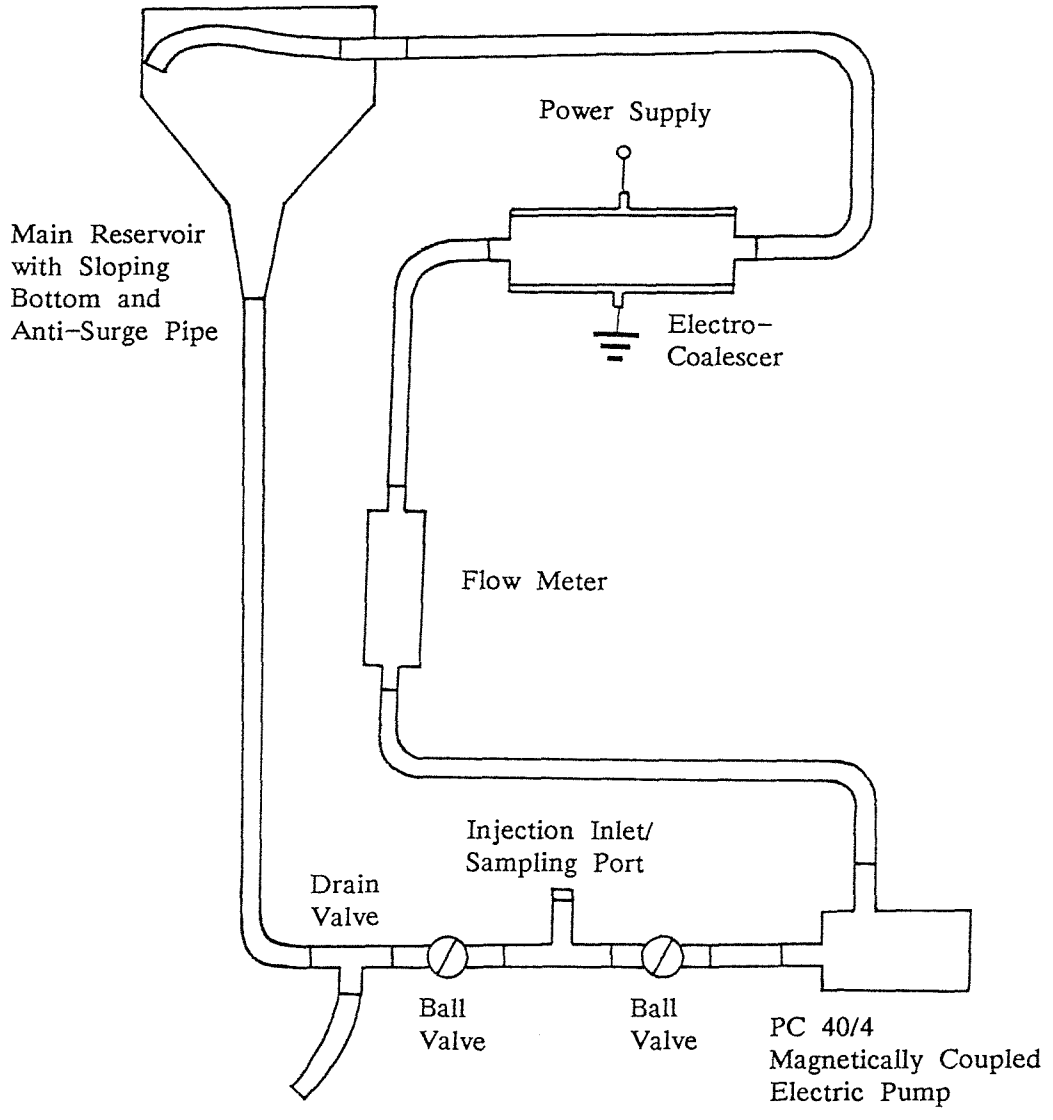

FIGURE 9.15 Closed-loop emulsification and electro-coalescer system.

A different type of experiment was possible with a flowing emulsion. In this case, the emulsion was allowed to attain an equilibrium state with the electric field on. The flow rate was then gradually reduced until the emulsion in the electro-coalescer took on a wedge-shaped appearance (see Figure 9.16). Above the wedge of emulsion, a separated oil phase developed and below it a separated water phase. The separated bulk oil phase had a slightly turbid appearance, indicating that it still contained some dispersed water, though only a minimal amount.

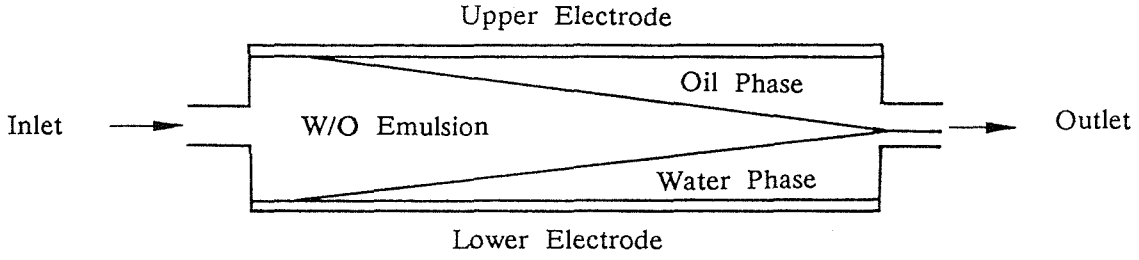

FIGURE 9.16 **Wedge-shaped appearance of W/O emulsion flowing through the electro-coalescer at low flow rates.**

9.13 Changes in the Size Distribution of a W/O Emulsion Due to Electric Field Induced Coalescence

Specially prepared emulsions of distilled water in silicone oil were used in this study, of water content generally less than 0.1% by volume (i.e. volume fraction $\varphi \simeq 10^{-3}$). The silicone oil had a density of $820 kgm^{-3}$, a kinematic viscosity of $10^{-6} m^2 s^{-1}$ and an electrical conductivity of less than $1 pSm^{-1}$.

Emulsion preparation consisted of adding a measured volume of water to the oil, followed by ultrasonic agitation of the mixture for five minutes. Emulsions, prepared in this way, were transferred to a quartz test cell, of square cross-section, to enable droplet size distributions to be measured using an optical technique. Two brass electrodes could be positioned in the cell, in order to subject the test emulsion to an electrostatic field while droplet size distributions were determined simultaneously. The electrodes measured 18mm wide by 68mm high and were separated by a gap of 16mm. One electrode was normally earthed and the other raised in potential to various levels, up to 4kV, by means of a stabilized dc supply.

Droplet size distributions were determined using a Malvern Particle and Droplet Size Analyser (HSD 2600) which utilises a technique based on the Fraunhoffer diffraction of a collimated beam of monochromatic laser light (as discussed by Swithenbank et al., 1976). The optical arrangement used in the measurements is shown in Figure 9.17.

A lower size limit of $1 \mu m$ applied to the experimental technique since a diffraction pattern could only be formed when the droplet diameter was greater than the wavelength ($0.6328 \mu m$) of the helium/neon laser radiation source. A

Fourier transform lens focussed the stationary light pattern on to a multi-ring photodetector and the measured light energy was transformed into a volume size distribution using computer software.

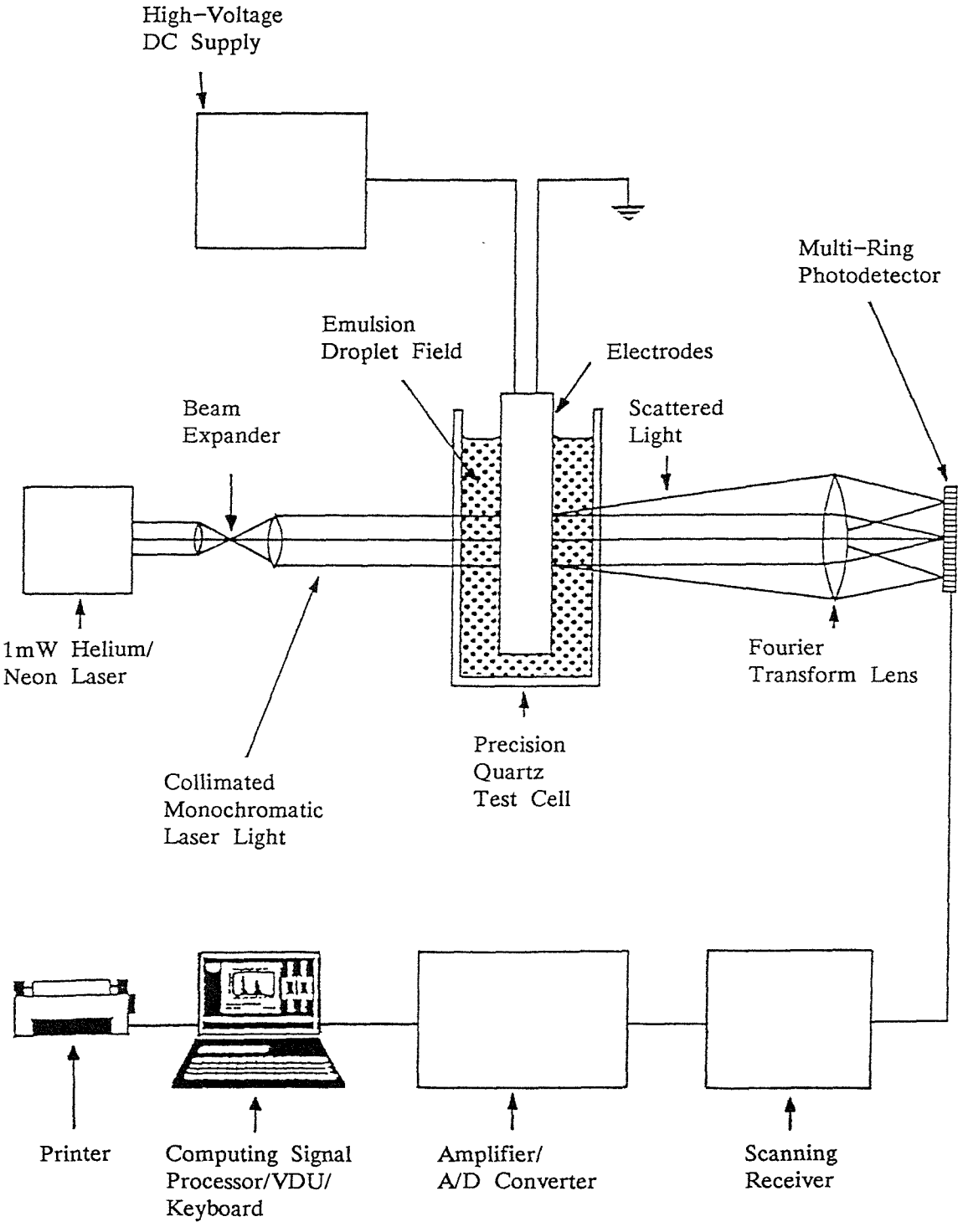

FIGURE 9.17 **Optical arrangement for measuring the droplet size distribution of an emulsion using a laser light scattering technique.**

When an emulsion becomes less turbid, due to natural or electric-field-induced coalescence, a measure of the rate at which the process proceeds is the turbidity of the emulsion itself. Turbidity is related to the attenuation of a light beam passing through an emulsion and may be measured, using the laser sytem, by considering the light energy falling on the central detector (of the multi-ring photodetector). The measurement parameter, in this case, is the fractional obscuration of the laser light.

It was possible to perform, automatically, a sequence of experiments on an emulsion, keeping the time interval constant between one experiment and the next. If the effect of using an electric field was to be considered, such a sequence was initiated immediately the field had been established, having performed an initial experiment with the field off (to determine the background levels). Data from all the experiments in a sequence were stored for subsequent analysis.

The results of sequential experiments performed with dc potential differences of 0, 3 and 4kV maintained between the test cell electrodes are now discussed. In all cases, the time interval between consecutive experiments was 6-seconds (there being a maximum of 24 experiments in each sequence); the time interval used was arbitrarily chosen and could have been much less than or much greater than the 6-seconds used. The sequence of experiments performed with no electric field applied to the emulsion serves as a control for comparison purposes.

Since there is a density difference between the water and oil phases, sedimentation of water droplets occurs. Initially, however, droplets which fall out of the measuring volume (which is several centimetres below the emulsion surface in the test cell) are replaced by similar ones from above. This assumes that the initial emulsion is homogeneous and holds even in the presence of an applied electric field (which causes the droplet size distribution to change by inducing coalescence).

The maximum electric field strength used was $2.5 kVcm^{-1}$ which is unlikely to have caused droplet disruption by any of the droplet breakup mechanisms (discussed in Chapter 7).

Volume size distributions of water droplets are presented in histogram form in Figures 9.18 and 9.19. With no electric field applied to the emulsion, a sequence of size distributions was recorded. The length of this sequence was 138s, during which time there was very little change in the droplet size distribution. The first and last histograms in the sequence are shown in Figures 9.18a and 9.18b

respectively. The absence of significant change in the distribution, over the period of 138s, suggests that the effects of Brownian motion and sedimentation led to negligible droplet coalescence during this period. When an electric field was applied to the emulsion, rapid changes in droplet size distribution were recorded, as illustrated by the histograms in Figure 9.19 (which were obtained for a potential difference of 3kV applied between the test cell electrodes). Changes in the droplet size distribution were due to dipole coalescence and migratory coalescence (the oil phase conductivity was sufficiently low) induced by the applied electric field. It can be seen that the initial bimodal distribution transformed into a unimodal distribution, accompanied by a shift to larger droplet sizes. Coalescence explains the shift to larger sizes and the change in form of the size distribution is not unreasonable. Naively, perhaps, the bimodal distribution may be approximated by two independent, monodisperse aqueous systems, corresponding to the peak values. The electrostatic coalescence of monodisperse aqueous emulsions was considered by Sadek and Hendricks (1974) whose numerically-obtained results were presented in normalised, cumulative form. It can be seen from their results that the size distributions broaden in time and that the peaks shift to larger sizes.

Band Number	Size Band (μm)	
	Lower	Upper
1	1.2	1.5
2	1.5	1.9
3	1.9	2.4
4	2.4	3.0
5	3.0	3.9
6	3.9	5.0
7	5.0	6.4
8	6.4	8.2
9	8.2	10.5
10	10.5	13.6
11	13.6	17.7
12	17.7	23.7
13	23.7	33.7
14	33.7	54.9
15	54.9	118.4

TABLE 9.1 Size bands of the Malvern Size Analyser (63mm focal length Fourier transform lens) corresponding to the fractional volume size distributions shown in Figures 9.18 and 9.19.

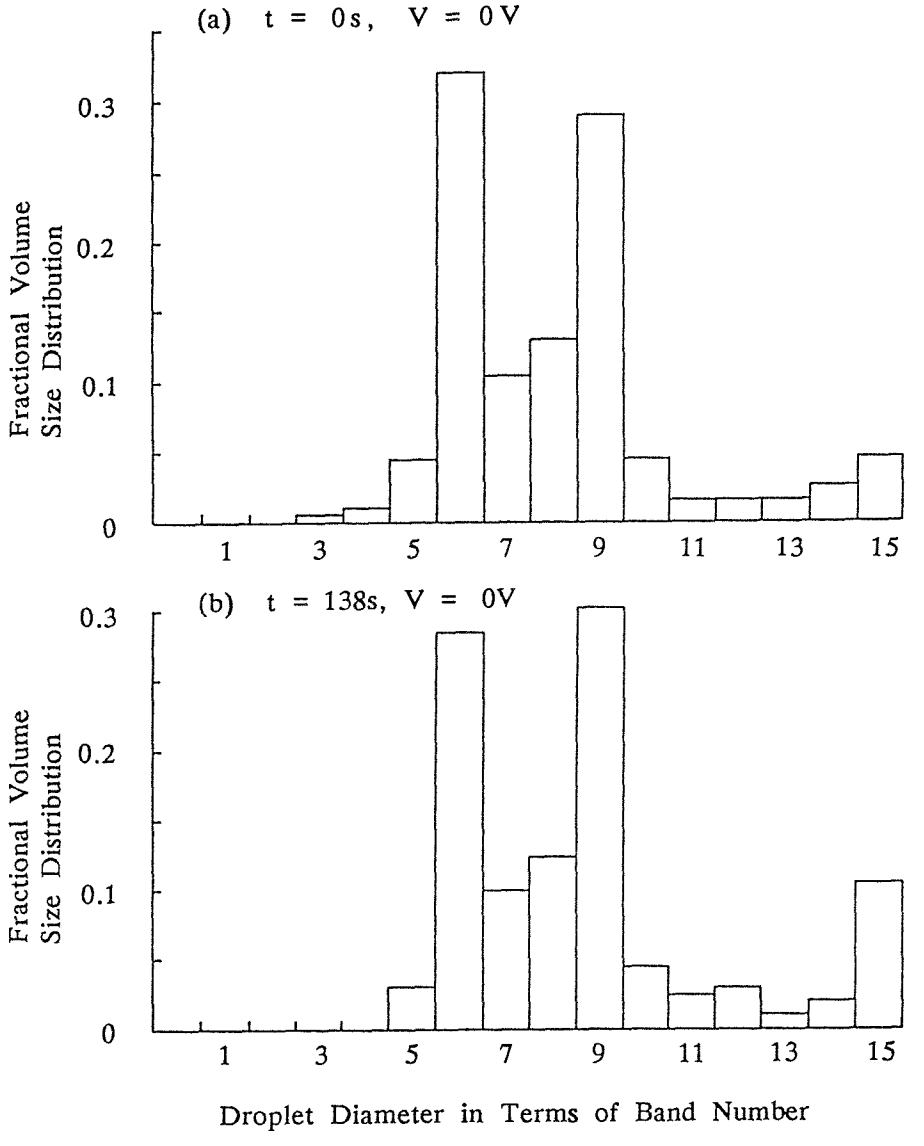

FIGURE 9.18 a and b are the first and last distributions in an experimental sequence performed with no potential difference between the test cell electrodes.

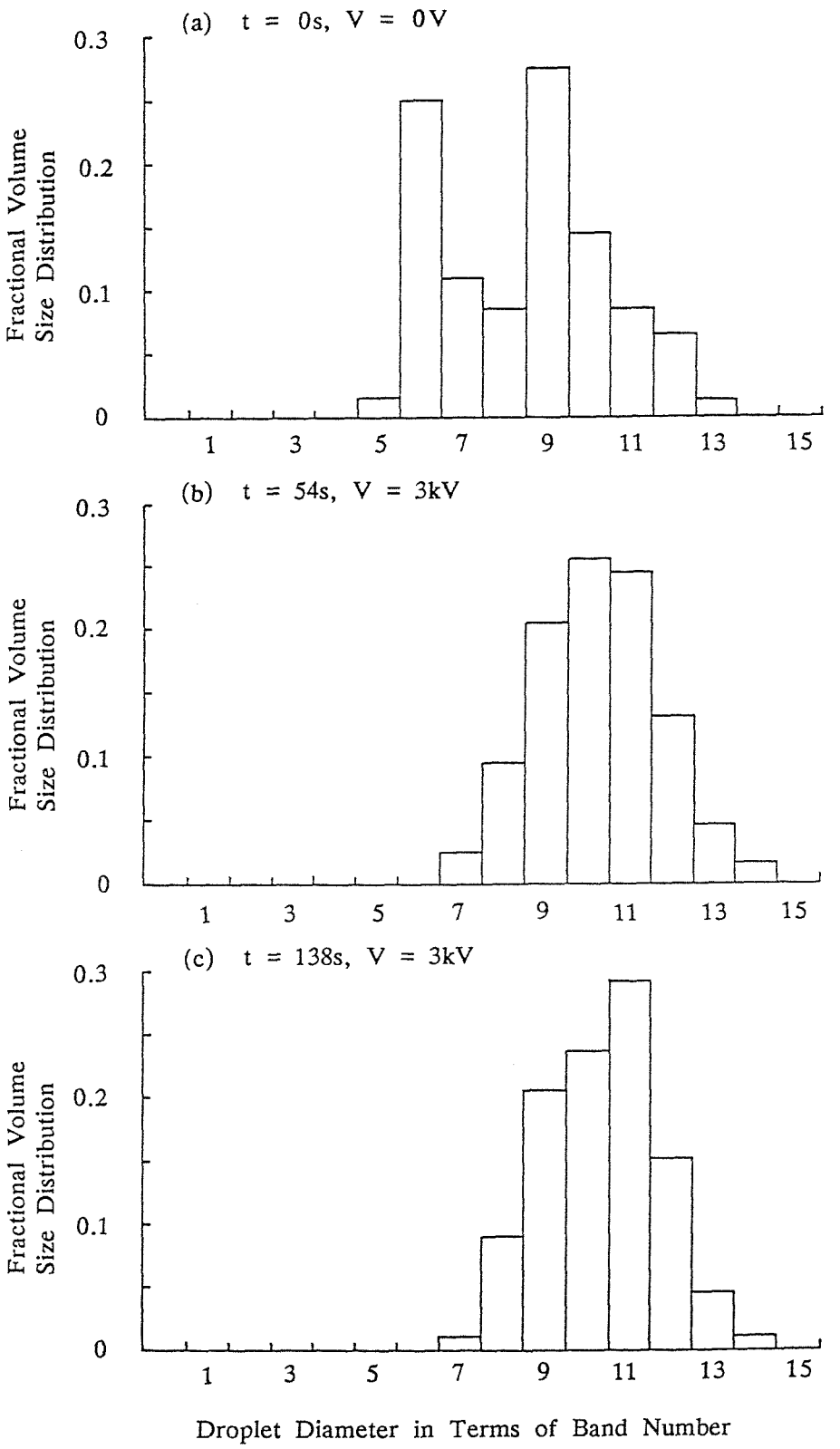

FIGURE 9.19 a to c are a selection of distributions from an experimental sequence performed with a potential difference of 3kV between the test cell electrodes.

By superimposing the size distributions of two initially monodisperse emulsions (assuming them to be mutually independent) the tendency to form a unimodal distribution is apparent. In practice, the cross-coupling effect, due to droplets of one (initially monodisperse) system coalescing with droplets of the other (initially monodisperse) system, increases this tendency, as does the fact that real emulsions cannot be perfectly monodisperse.

The ultrasonic preparation of emulsions appears to have been fairly repeatable, the volume size distributions being typified by Figures 9.18a and 9.19a which correspond to the first experiments in the sequences performed at potential differences of 0 and 3kV respectively. Another point of interest here is that the droplets in the first peak (in Figures 9.18a and 9.19a), of band size 3.9 - 5μm, are about twice the size of those in the second peak, which has band size 8.2 - 10.5μm. This suggests that the sizes of the droplets, corresponding to the two peaks, may possibly be associated with the fundamental and second harmonic frequencies of the ultrasonic vibration.

With the passage of time, the fractional obscuration of an emulsion was found to decrease and this reflects the coalescence processes which occur, causing the emulsion to become clearer (see Figure 9.20). It was found that the fractional obscuration reduced slowly due to the coalescence effects of Brownian motion and sedimentation; however, when a strong electric field was applied to the emulsion, it decreased rapidly at first then approached a limiting value asymptotically, as in Figure 9.20. The stronger the electric field the more rapid was the decrease in fractional obscuration. It should be noted that the graphs shown in Figure 9.20 are normalised, with respect to the initial fractional obscuration, to account for the effects of different water concentrations of the emulsions; the intial values are shown by the graphs. The fractional obscuration is akin to the turbidity of an emulsion, which was used in Section 9.10.2 as a method of monitoring the water content of an emulsion (leading to the emulsion resolution time).

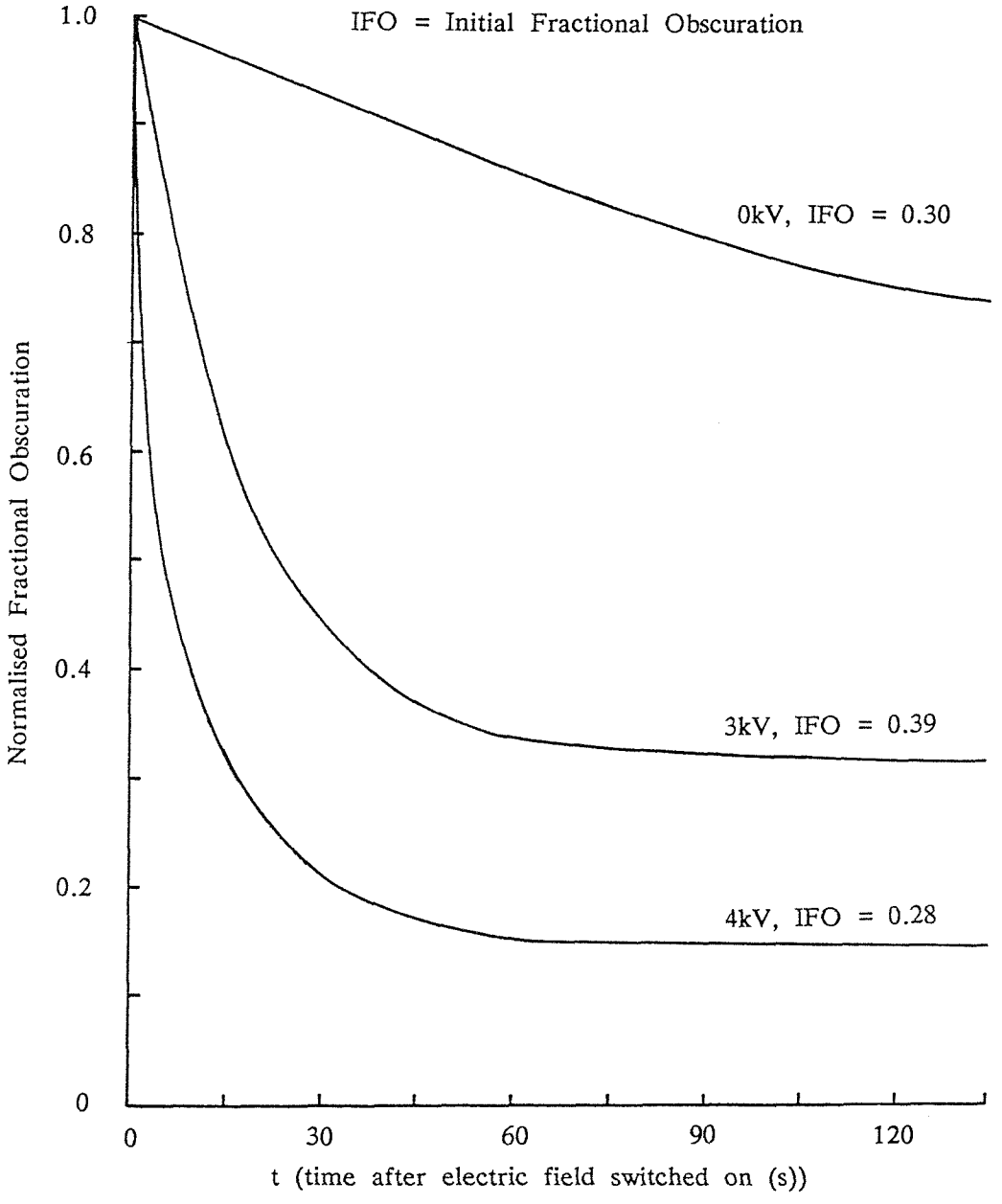

FIGURE 9.20 **Fractional obscuration, normalised to its initial value, plotted as a function of time for potential differences of 0, 3 and 4kV applied between the test cell electrodes.**

By considering the cumulative volume distribution, it is possible to calculate the volume median diameter associated with the 50% level. This was done for each experiment in the sequences corresponding to potential differences of 0, 3 and 4kV between the test cell electrodes. The volume median diameter is observed to increase with time in all cases, as shown in Figure 9.21. Again, this is evidence of the coalescence processes which occur in the emulsion. If no electric field is

applied the volume median diameter increases slowly; however, when a strong electric field is applied to the emulsion, it increases rapidly at first, then more slowly. The graphs shown in Figure 9.21 are normalised, with respect to the initial volume median diameter, to account for the effects of different water concentrations of the emulsions; the initial values are noted by the graphs.

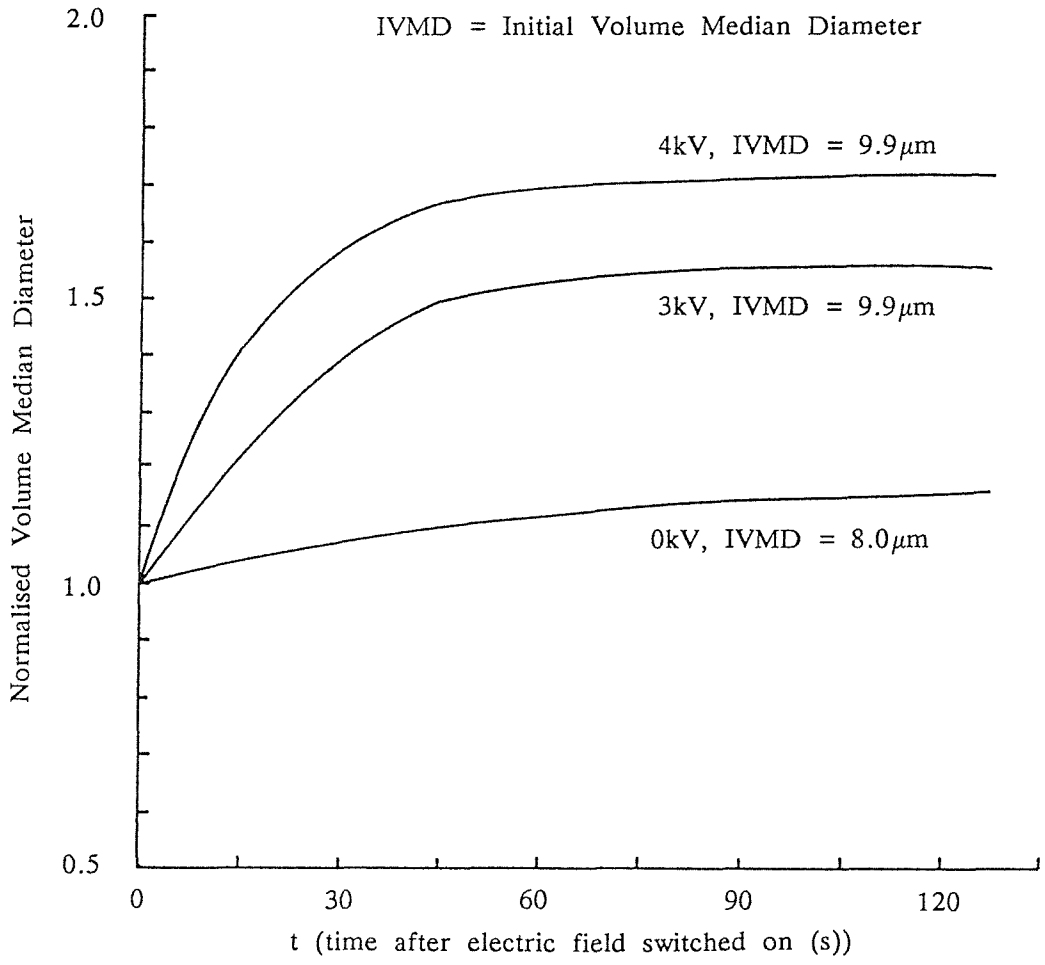

FIGURE 9.21 Volume median diameter, normalised to its initial value, plotted as a function of time for potential differences of 0, 3 and 4kV applied between the test cell electrodes.

It has been established that the size distribution of W/O emulsion droplets, and how it changes in time, can be determined in situ, while the electric field is on, using a light scattering technique. The coalescence effects of Brownian motion and sedimentation have been shown to be small in comparison with dipole and migratory coalescence caused by strong electric fields (for water droplets of mean size less than 10μm diameter suspended in silicone oil). W/O emulsions, initially having bimodal distributions become unimodal following the application of an

electric field. The fractional obscuration of a W/O emulsion decreases and its volume median diameter increases with time, following the application of an electric field (provided droplet dispersion mechanisms do not cause significant re-emulsification).

A knowledge of the size distributions of the water droplets in W/O emulsions, subjected to electric fields, and how they change in time, could be of value in the design of commercial electro-coalescers. Such knowledge should enable the optimization of electrode design and energisation. The criterion normally used would be the maximisation of electrostatic coalescence and concomitant minimisation of re-emulsification processes.

10. THE FORMATION OF PARTICLE CHAINS IN ELECTRIFIED SUSPENSIONS

When an electric field is applied to certain types of suspension, the formation of particle chains can occur which align themselves with the electric lines of force. Winslow (1949) and Hollmann (1950) observed chaining in suspensions of semiconductor particles in paraffin.

Putilova et al. (1950) observed particle chaining in the following systems: carbon black in benzene, aluminium in petrol, zinc and barium stearates in petrol and mineral oil.

Pearce (1954) investigated the chaining of various materials (copper, zinc, aluminium, carbon, carborundum, magnesite, porcelain, perspex, glass and quartz) suspended in oil (insulating oil, commercial paraffin, de-asphalted fuel oil, untreated fuel oil, and white spirit containing 4% calcium naphthenate in solution), and exposed to a dc or 50Hz ac electric field (both of which produced similar effects). He found that the conducting particles formed chains whereas the insulating ones did not, and concluded that it was the conductivity of the particle and not just its permittivity which was of importance (interfacial polarisation cannot reduce the dipole moment in the case of conducting particles, as discussed in Section 5.5).

In the case of emulsions, the chains (known as pearl chains) are formed from dispersed phase droplets. The formation of pearl chains in emulsions has been investigated by Muth (1927) and Kuczynski (1929), using high-frequency ac fields (20kHz - 2MHz in the case of Kuczynski). Kuczynski showed, from energy considerations, that pearl-chain formation was to be expected. Pearce investigated pearl-chain formation in W/O emulsions and presented an analysis of the forces (dielectrophoretic) to explain their formation. He also made the observation that particle chains can result if the electric field is uniform or divergent and if the supply is ac or dc.

The biological aspects of pearl-chain formation were considered analytically by Saito and Schwan (1961), whose analysis was mainly concerned with the time constants involved in chain formation.

Krasny-Ergen (1936) developed an expression for the interaction energy of a pair of polarised conducting spheres (see Section 5.2) which degenerated to

simple forms for large and small separations. For droplets in close proximity to one another (or even in contact), he concluded that Brownian motion could not deflocculate them, if the electric field strength was sufficiently large, and therefore that pearl-chains could develop in an emulsion subjected to an electric field.

Before going on to discuss the forces responsible for the creation of particle chains, it is worth mentioning that they can only be formed in the absence of disruptive effects. For example, if there is hydrodynamic disturbance, due perhaps to excessive speed of flow, then chain formation will be limited. This was demonstrated in Galvin's work, in which a W/O emulsion flowed through a parallel-plate electro-coalescer (Galvin, 1984). The speed of flow was such as to prevent the build-up of pearl chains comprising more than four water droplets. In the case of Bailes and Larkai's almost identical system, in which the flow speed was lower, pearl chains developed readily, and shorted out the electrodes if they were not insulated from one another (Bailes and Larkai, 1981). The situation was recognised long ago in McKibben's 1919 patent which indicates that the emulsion should be moved through the electric field at such a velocity as to break up or prevent the persistence of chains of polarised globules of liquid entrapped between the electrodes.

10.1 Forces Involved in the Formation of Particle Chains

The forces involved in particle chain formation, in electrified suspensions, may be found most conveniently if the particles are assumed to be spherical. In the case of emulsions, where the particles are droplets, this is a very reasonable assumption, apart from the problems of droplet distortion. By considering the interaction between a pair of spherical particles, it can be seen how particle chains evolve.

Pohl (1978) suggested that a threshold electric field strength existed, below which pearl chains would not form due to thermal effects. He developed an expression for the interaction energy of two identical polarised spheres, assuming the dipole approximation (which included the mutual polarisation effect):

$$U_i = \frac{-8\pi a^6 E_o^2}{\Lambda^3} \epsilon_c \left[\frac{\epsilon_d - \epsilon_c}{\epsilon_d + 2\epsilon_c}\right]^2 \left[1 - \frac{1}{4}\left[\frac{\epsilon_d - \epsilon_c}{\epsilon_d + 2\epsilon_c}\right]\right]^{-1} \quad (10.1)$$

Pohl assumed this to be valid at zero separation (i.e. $\Lambda = 2a$), which is not strictly true since the dipole approximation does not then hold, and identified the so-called "critical bunching energy" with the average translational energy kT/2:

$$-U_{crit} = \pi a^3 E_o^2 \epsilon_c \left[\frac{\epsilon_d - \epsilon_c}{\epsilon_d + 2\epsilon_c}\right]^2 \left[1 - \frac{1}{4}\left[\frac{\epsilon_d - \epsilon_c}{\epsilon_d + 2\epsilon_c}\right]\right]^{-1} = \frac{kT}{2}$$

By re-arranging this equation, it is possible to establish the critical field for chain formation:

$$E_{crit} = \left[\frac{kT}{2\pi a^3 \epsilon_c}\right]^{\frac{1}{2}} \left[\frac{\epsilon_d + 2\epsilon_c}{\epsilon_d - \epsilon_c}\right] \left[1 - \frac{1}{4}\left[\frac{\epsilon_d - \epsilon_c}{\epsilon_d + 2\epsilon_c}\right]\right]^{\frac{1}{2}} \qquad (10.2)$$

Saito and Schwan (1961) presented a similar expression in their paper.

In view of the foregoing remarks, eqn. (10.2) is at best an approximation. However, it does give some idea of the threshold electric field strength for particle chaining. It shows that the threshold electric field strength reduces as particle size increases, being proportional to $a^{-3/2}$. Krasny-Ergen's interaction energy for polarised, conducting spheres in contact (see Section 5.2, eqn. (5.54)) similarly leads to (Krasny-Ergen, 1936):

$$E_{crit} = \left[\frac{kT}{8\pi[2\zeta(3)-1]\epsilon_c a^3}\right]^{\frac{1}{2}} \qquad (10.3)$$

where $2\zeta(3)-1 = 1.404$ (and ζ is the Riemann zeta function).

The forces concerned with chain formation have already been discussed in some detail (see Chapter 5). They are dielectrophoretic in nature, and arise since the particles polarise in the applied electric field. For large separations of the particles, the radial and transverse components, of the interactive force, are proportional to the volumes of the particles, the square of the applied electric field strength, and inversely proportional to the fourth power of the separation (see eqns. (5.50) and (5.51)). They also depend on the angle θ which the line of centres of the particles makes with the applied electric field. If $\theta < 54.7^\circ$ or $125.3^\circ < \theta < 180^\circ$, the radial force is attractive, otherwise it is repulsive (see Figure 5.2). The transverse force tends to align the line of centres of the particles with the applied electric field. Thus, even if the particles are oriented such that the radial force is repulsive, the transverse force will eventually alter their orientation until it is attractive. Thus pairs of particles tend to attract one another and align themselves with the electric field. As the separation of the particles reduces, the dipole approximation becomes invalid and other force

expressions apply. Krasny-Ergen (1936) has considered the limit, of the interaction energy, as the droplets come into contact. At such small separations, the angle governing the regions of attraction and repulsion increases. Thus for $\theta < 75.1^{\circ}$ or $104.9^{\circ} < \theta < 180^{\circ}$ the radial force is attractive otherwise it is repulsive (see Figure 5.3).

Having seen how particles flocculate in pairs, it is not difficult to imagine how these pairs attract a third particle or how two pairs come together. If the process is repeated, chains comprising many particles can build up.

10.2 The Stability of Droplets in Pearl Chains

The formation of pearl chains is perhaps more complicated than that of particle chains, since droplet stability must be considered. Thus, droplets coming together as a pair will either coalesce or just flocculate.

The coalescence of emulsion droplets, at a rate which reduces to zero, as the droplets approach a limiting size and approximately uniform size distribution, has been termed "limited coalescence" by Wiley (1954). The phenomenon is frequently observed in emulsions stabilised by finely-divided solids and should also be applicable in the case of emulsions stabilised by surface-active agents (Becher, 1977).

Pearce (1954) was of the opinion that the droplets, comprising the pearl chains in his W/O emulsions, were stabilised by electrical double layer effects. He erroneously (for want of a better value) based his calculations for W/O emulsions, on the double layer thickness (5nm) proposed by Lewis (1934) for an oil-in-aqueous system. However, the concentration of ions in an oil is so low that the double layer thickness for W/O systems may be as large as several microns (Becher, 1977), that is about three orders of magnitude greater than for O/W systems.

Albers and Overbeek (1959) have investigated the relation between flocculation and the electric double layer, in W/O systems, and they concluded that there was no stabilising effect (the reverse being true for O/W systems).

The mechanism which stabilises water droplets in W/O emulsions may not be fully understood, however, such a mechanism must exist otherwise pearl chains would not form (instead droplets would continue coalescing and fall out under gravity).

10.3 Experimentation into the Behaviour of Water Droplets in an Electrified W/O Emulsion

A microscopic electrode cell (see Figure 10.1 and Plate 1,a) was designed and constructed in order to investigate the behaviour of water droplets, in a W/O emulsion, under the influence of an applied electric field. One of the main requirements was that the cell should be easily cleanable. This was achieved by using upper and lower cell plates, machined from perspex, which could be attached to one another using securing screws. A glass plate and rubber 'O' ring, for sealing purposes, could be sandwiched between the cell plates. The upper cell contained two laterally drilled holes to accommodate the 1mm diameter brass rod electrodes. The dimensions of the cell receptacle were approximately 7mm square by 4mm deep (much deeper than that used by Pearce (1954) which was only 0.1mm deep and did not give much scope for sedimenting particles).

A dc potential difference could be applied to the electrodes using a stabilised high-voltage power supply. However, it was unnecessary to work at potential differences greater than 300V, since the electrode separation was small enough (5mm) to allow sufficiently large electric fields to be generated at this level.

W/O emulsions were prepared by agitating 10$\mu\ell$ of distilled water in 25mℓ of diesel oil, for about a minute, using an ultrasonic bath (see Section 8.10.4). This created dilute W/O emulsions of volume fraction ~400ppm. A disposable pipette was used to transfer several droplets of emulsion to the receptacle of the microscopic electrode cell.

The microscope was usually focussed onto the edge of one of the electrodes, during experiments, but could also be adjusted to view the inter-electrode space. Either a ×39 or ×200 microscope magnification was used. The lower magnification gave a good overall view whereas the higher one was better for observing detail. When photographs were to be taken, the eyepiece was removed and replaced with an extension tube and camera. The overall print (see Plates 1-3) magnifications, corresponding to the above microscope magnifications, were calculated to be ×27 and ×130 respectively (taking into account print enlargement from the 35mm negative).

Before the electrodes were energised, it was possible to see circulating motion of the emulsion which was caused, presumably, by thermal convection due to heat transmission from the microscope light source.

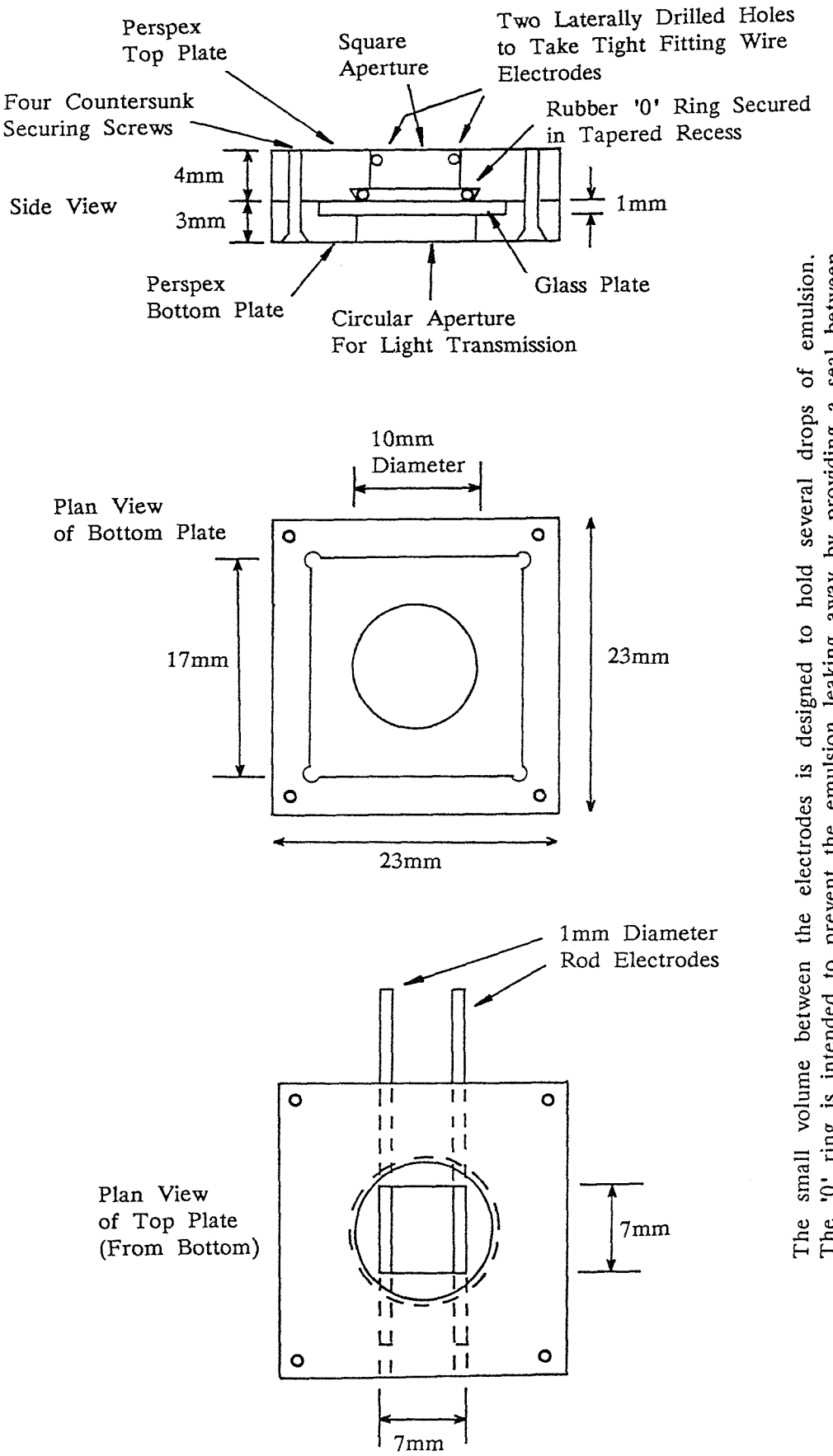

The small volume between the electrodes is designed to hold several drops of emulsion. The '0' ring is intended to prevent the emulsion leaking away by providing a seal between the perspex top and glass slide which is located in a recess in the bottom perspex plate. The complete assembly is held together by four screws.

FIGURE 10.1 Microscopic electrode cell (approximately twice full size).

Potential differences of between about 100 and 300V, applied to the electrodes, were found to be most suitable. For potential differences lower than 100V there was little effect whereas those over 300V caused too much motion of the emulsion. The average electric fields, associated with the above potential differences, were $20kVm^{-1}$ and $60kVm^{-1}$ respectively, assuming the electrode separation to have been 5mm. In fact, the electric field was non-uniform since the electrodes were rods and the cell had perspex boundaries. Dielectrophoretic forces were therefore present, the greatest values being associated with the surfaces of the electrodes.

The effect of applying an electric field, of average strength between 20 and $60kVm^{-1}$, to the W/O emulsion was easily observed by its action on the droplet motion. Soon after its application, it was possible to see the formation of pearl chains which aligned themselves with the applied electric field (see Plate 1,c and Plate 3,l). Interfacial effects, such as double layer repulsion or limited coalescence (see Section 9.7) apparently prevented the droplets from coalescing, even though the electric field tended to induce such an action. It was interesting to observe the formation of pearl chains and trees (a pearl chain with droplet branches) mainly on the negative electrode (see Plate 2,e and g). Many such floccules were also to be seen in the inter-electrode region (see Plate 1,d) as were single droplets. Very few, sometimes none at all, were to be found attached to the positive electrode (see Plate 2,f and h). It would appear, therefore, that the water droplets had an affinity for the negatively-charged electrode. When the polarity of the power supply was reversed, the pearl-chains and trees formed on the other electrode. This suggests that the floccules generally possessed a net positive charge (a particle may possess charge due to having contacted an electrode; by virtue of the electrical double layer, the polarity depending on the type of surface-active agent present; by frictional contact which, by Coehn's (1898) rule, would make water droplets charge positively in oil). It would seem that the pearl chains and trees formed at the negative electrode or in the bulk emulsion. Those found attached to the positive electrode (see Plate 2,f) may well have formed at the negative electrode, become charged negatively, and then travelled across due to the effects of electrophoresis.

Frequently, pearl chains or trees, moving in the bulk emulsion, joined ones attached to the negative electrode, so elongating them. Sometimes a droplet, pearl chain or tree was observed to bounce off an electrode (see Plate 1,b) or off a droplet, pearl chain or tree attached to an electrode. Associated with this behaviour, on occasion, was the oscillation of a droplet or pearl chain between a fixed tree and one drifting in the inter-electrode region. In Plate 1,c the end

pearl chain was observed to oscillate between the second pearl chain and the negative electrode. Such oscillation occasionally resulted in the coalescence of a number of water droplets. This behaviour is compatible with charge transfer. A positively charged or neutral tree in the bulk emulsion would be attracted to another attached to the negative electrode. The free tree would then become negatively charged and be repelled into the bulk emulsion. Sometimes only the end part of the free tree participated in this kind of behaviour, giving rise to an oscillation.

Quite rarely, a continuous droplet bridge formed between the electrodes (see Plate 1,c), and on one occasion, two such bridges existed simulataneously. The droplet bridges were typically stable for several minutes before dispersing. Occasionally, a pearl chain was attracted laterally to the bridge and observed to combine with it. Sometimes the base of the bridge would shift along the electrode to one side or the other of the cell.

As the potential was increased above 300V, the pearl chains and trees were forced off the electrodes into the bulk emulsion. Occasionally, a long pearl chain was observed to bounce along an electrode towards the edge of the cell, to which it adhered subsequently.

Multi-phase droplets could also be observed on occasion. It was sometimes possible to see tiny droplets of oil in motion within the water droplet, in the continuous oil phase (evidence of a dual or multiple emulsion). The motion of the tiny oil droplets inside was observed to change when the potential difference between the electrodes was reduced or increased. Typical water droplet behaviour and configurations are shown schematically in Figure 10.2.

One conclusion that can be drawn from the microscopic observations relates to coalescence of the water droplets. It is clear that the tiny water droplets, initially present in an emulsion, coalesce in the applied electric field to form the water droplets and floccules which subsequently can be observed. However, once the droplets achieve a certain size (about 15-45μm) they do not readily coalesce with one another even though they appear to be in contact. This shows why it may be necessary to use chemical demulsifiers, in electro-coalescers, in order to enhance coalescence by influencing the interfacial properties of the emulsion.

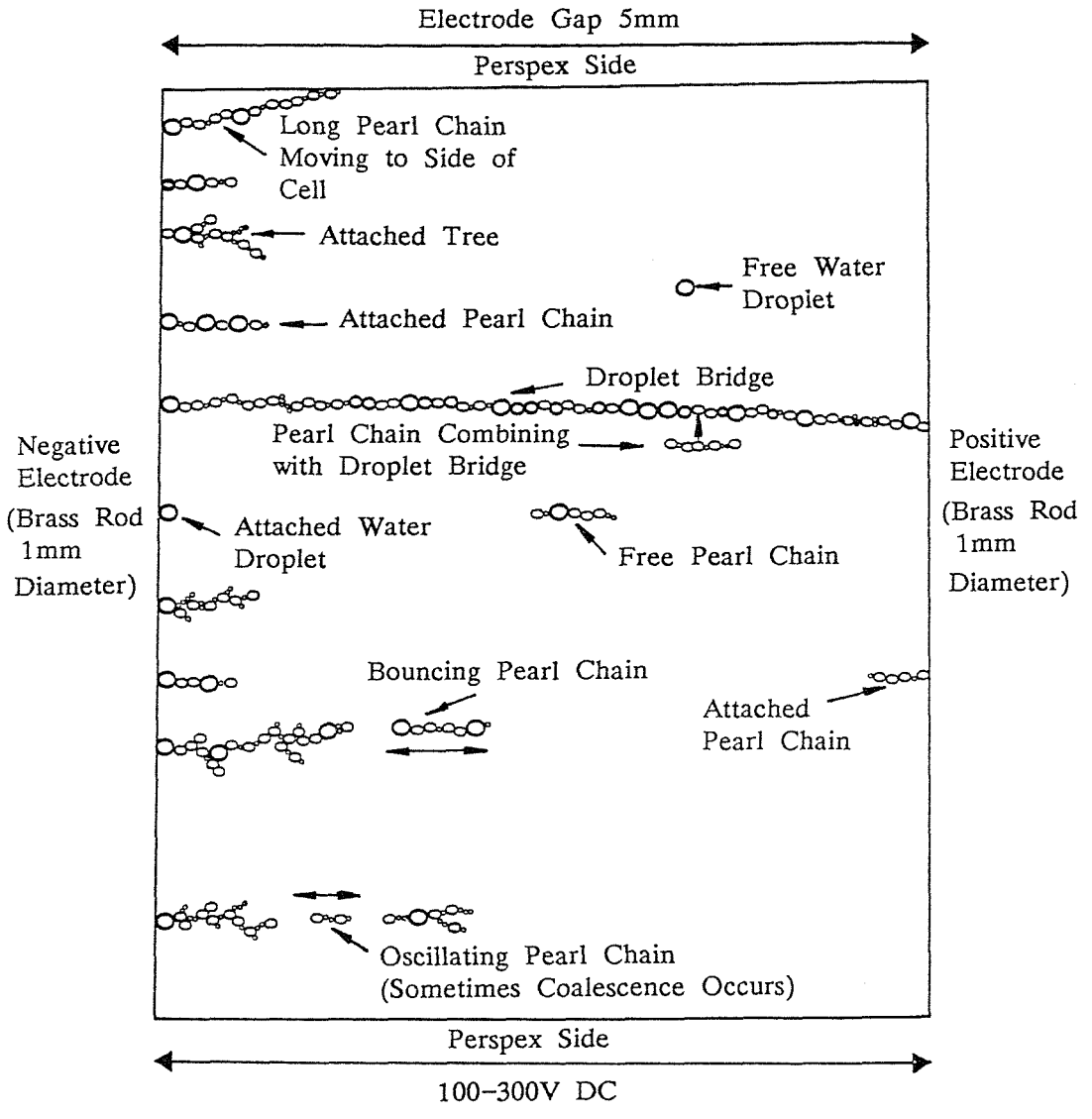

FIGURE 10.2 **The behaviour of water droplets, in a W/O emulsion, to which an electric field has been applied.**

11. THE USE OF INSULATED ELECTRODES

There are advantages to be gained from using insulated electrodes to separate high volume fraction W/O emulsions. If uninsulated electrodes were to be used, to apply an electric field to such an emulsion, pearl chains could soon form a low-resistance bridge between them which would short-circuit the power supply. The probability of this happening increases as electrode separation reduces and emulsion flow speed (in the case of continuous operation) is decreased. Bailes and Larkai (1981) encountered this difficulty during experimentation, in which emulsion flowed through their electro-coalescer at speeds of up to 3.7mm/s. They found that the problem could be overcome by using perspex to insulate the electrodes, and applying a pulsed dc electric field.

Galvin (1984), using an almost-identical experimental set-up (apart from having a smaller electro-coalescer), apparently did not encounter the problem of water droplets bridging the electrodes. In fact, the largest pearl chain he observed, using high-speed photography, comprised four water droplets. This was probably because emulsion flowed through his electro-coalescer at higher speeds, typically 13.3mm/s. One of his conclusions was that insulation served no useful purpose and that current limiters could be used, should short circuiting arise. This might not be a good solution, however, since the electric field strength would be reduced if the current were limited. Similarly, there would be disadvantages in switching off the coalescer until the droplet bridges dispersed.

The use of insulated electrodes has appeared in the patent literature, as has the almost-equivalent procedure of energising the electrodes via a capacitor; evaluations of electro-coalescer performances have not been presented.

11.1 Some Theoretical Aspects of Electrode Insulation

Consider a plane boundary between two dielectric materials having permittivities ϵ_1 and ϵ_2, and conductivities σ_1 and σ_2 respectively. Suppose also that the electric fields within the dielectrics, of strengths E_1 and E_2 respectively, are normal to the interface and in the same direction. When the fields are initiated, there is no free charge at the interface and so the normal component of electric displacement is continuous there:

$$\epsilon_1 E_1 = \epsilon_2 E_2$$

Re-arrangement gives:

$$\frac{E_2}{E_1} = \frac{\epsilon_1}{\epsilon_2} \qquad (11.1)$$

Generally speaking, free charge will subsequently accumulate at the interface until equilibrium is achieved. This is due to interfacial (Maxwell-Wagner) polarisation as described in Section 5.5. Under equilibrium conditions, the normal component of current density is continuous at the interface:

$$\sigma_1 E_1 = \sigma_2 E_2$$

Re-arrangement gives:

$$\frac{E_2}{E_1} = \frac{\sigma_1}{\sigma_2} \qquad (11.2)$$

It can be appreciated from Eqns. (11.1) and (11.2) that the electric field ratio will change unless the time constants of the two dielectric media are identical (i.e. unless $\tau_1 = \tau_2$ where $\tau_i = \epsilon_i/\sigma_i$ for i = 1,2). The electric field strength ratio E_2/E_1 can therefore drop in value from its initial value of ϵ_1/ϵ_2 to σ_1/σ_2 in the steady-state, should $\sigma_1 << \sigma_2$ (since ϵ_1 and ϵ_2 do not usually differ greatly).

Suppose that one of the dielectric materials being considered is a W/O emulsion of effective permittivity ϵ_2 and conductivity σ_2, and that the other is an insulator (e.g. perspex) of permittivity ϵ_1 and conductivity σ_1. The emulsion is complex to model since its dielectric properties are dependent on those of its constituent phases and the volume fraction of the dispersed phase (as described in Sections 3.6.1 and 3.6.2). Similarly, the action of the electric field will result in water droplet coalescence and phase separation. In general, the emulsion will therefore comprise three bands: one of separated oil, one of emulsion and one of separated water. The dielectric properties of the emulsion are therefore also time dependent.

In order to render the analysis tractable, the emulsion will be regarded as a simple dielectric but this simplification must be borne in mind when interpreting the results.

In the analysis, it is only necessary to consider one interface, even if both electrodes are insulated (with the same material). This can be demonstrated as follows:

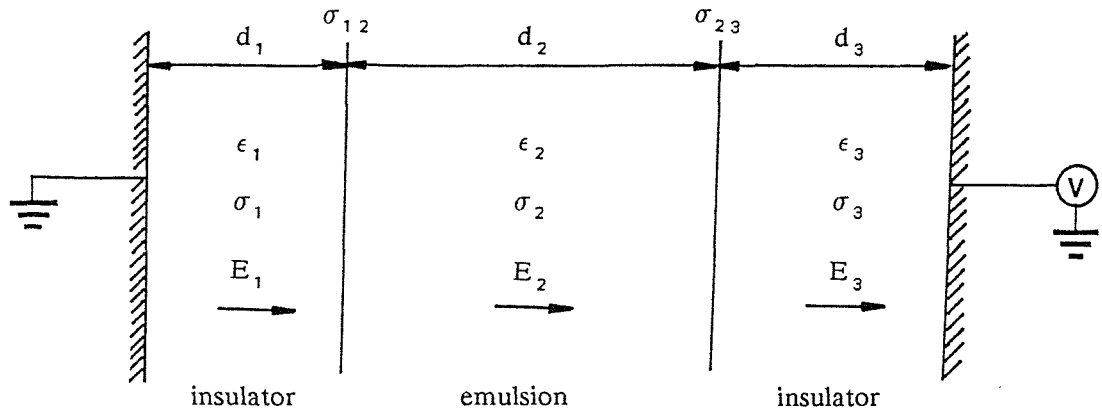

FIGURE 11.1 Capacitor comprising three lossy dielectrics in series.

In Figure 11.1 the terms σ_{12} and σ_{23} represent the surface density of free charge at the interfaces. The following boundary conditions apply:

$$-\epsilon_1 E_1 + \epsilon_2 E_2 = \sigma_{12} \tag{11.3}$$

$$\sigma_1 E_1 - \sigma_2 E_2 = \frac{d\sigma_{12}}{dt} \tag{11.4}$$

$$-\epsilon_2 E_2 + \epsilon_3 E_3 = \sigma_{23} \tag{11.5}$$

$$\sigma_2 E_2 - \sigma_3 E_3 = \frac{d\sigma_{23}}{dt} \tag{11.6}$$

Eqns. (11.3) and (11.5) imply:

$$-\epsilon_1 E_1 + \epsilon_3 E_3 = \sigma_{12} + \sigma_{23} \tag{11.7}$$

Eqns. (11.4) and (11.6) imply:

$$\sigma_1 E_1 - \sigma_3 E_3 = \frac{d}{dt}(\sigma_{12} + \sigma_{23}) \tag{11.8}$$

Now if it is assumed that both electrodes are insulated with the same material, eqns. (11.7) and (11.8) become:

$$-\epsilon_1(E_1 - E_3) = \sigma_{12} + \sigma_{23} \qquad (11.9)$$

$$\sigma_1(E_1 - E_3) = \frac{d}{dt}(\sigma_{12} + \sigma_{23}) \qquad (11.10)$$

Eqns. (11.9) and (11.10) may be combined to give:

$$\frac{d}{dt}(\sigma_{12} + \sigma_{23}) = -\frac{\sigma_1}{\epsilon_1}(\sigma_{12} + \sigma_{23})$$

This differential equation is easily solved:

$$\sigma_{12} + \sigma_{23} = A \exp\left[-\frac{\sigma_1}{\epsilon_1} t\right] \qquad (11.11)$$

The constant A is determined from the sum of the initial interfacial free charges. Since the initial interfacial free charges are assumed to be zero, it follows that A = 0 and so eqn. (11.11) implies that $\sigma_{12} + \sigma_{23}$ is always zero. Eqn. (11.9) then implies that $E_1 = E_3$ for all values of time $t \geq 0$.

The potential difference V of the electrodes can be expressed as follows:

$$V = d_1E_1 + d_2E_2 + d_3E_3$$

Now $E_3 = E_1$ hence:

$$V = (d_1 + d_3)E_1 + d_2E_2$$

Consider the two insulators to be lumped together so that $d_1 + d_3 \rightarrow d_1$ then:

$$V = d_1E_1 + d_2E_2 \qquad (11.12)$$

It is therefore necessary to solve the set of independent eqns. (11.3), (11.4) and (11.12).

Eqns. (11.3) and (11.4) imply:

$$\sigma_1E_1 + \epsilon_1 \frac{dE_1}{dt} = \sigma_2E_2 + \epsilon_2 \frac{dE_2}{dt} \qquad (11.13)$$

This is, effectively, an expression for the conservation of current passing through the dielectric media. Eqns. (11.12) and (11.13) can now be combined to give:

$$\frac{\sigma_1}{d_1}(V-d_2E_2) + \frac{\epsilon_1}{d_1}\frac{d}{dt}(V-d_2E_2) = \sigma_2E_2 + \epsilon_2\frac{dE_2}{dt}$$

$$(\epsilon_1d_2+\epsilon_2d_1)\frac{dE_2}{dt} + (\sigma_1d_2+\sigma_2d_1)E_2 = \sigma_1V + \epsilon_1\frac{dV}{dt} \qquad (11.14)$$

Let:

$$\omega_o = 1/\tau = (\sigma_1d_2+\sigma_2d_1)/(\epsilon_1d_2 + \epsilon_2d_1) \qquad (11.15)$$

$$\alpha = \sigma_1/(\epsilon_1d_2 + \epsilon_2d_1) \qquad (11.16)$$

$$\beta = \epsilon_1/(\epsilon_1d_2 + \epsilon_2d_1) \qquad (11.17)$$

Eqn. (11.14) may therefore be expressed as:

$$\frac{dE_2}{dt} + \omega_oE_2 = \alpha V + \beta\frac{dV}{dt} \qquad (11.18)$$

Suppose that the driving function is $V = V_o\cos(\omega t)$ then eqn. (11.18) becomes:

$$\frac{dE_2}{dt} + \omega_oE_2 = \alpha V_o\cos(\omega t) - \beta\omega V_o\sin(\omega t) \qquad (11.19)$$

This differential equation is easily solved and has the following solution:

$$E_2 = Be^{-\omega_o t} + \left[\frac{\alpha^2 + \omega^2\beta^2}{\omega_o^2 + \omega^2}\right]^{\frac{1}{2}} V_o\cos(\omega t + \chi) \qquad (11.20)$$

The phase angle χ is given by:

$$\tan\chi = \frac{\omega(\beta\omega_o - \alpha)}{\alpha\omega_o + \beta\omega^2} \qquad (11.21)$$

The constant B in eqn. (11.20) is determined by letting $\epsilon_1E_1 = \epsilon_2E_2$ when $t = 0$. Using eqn. (11.12) it can be seen that this is equivalent to letting $E_2 = \beta V_o$ when $t = 0$. Bearing this in mind and considering eqn. (11.20) leads

to:

$$\beta V_o = B + \left[\frac{\alpha^2 + \omega^2\beta^2}{\omega_o^2 + \omega^2}\right]^{\frac{1}{2}} V_o \cos\chi$$

Using eqn. (11.21) this becomes:

$$\beta V_o = B + \left[\frac{\alpha\omega_o + \beta\omega^2}{\omega_o^2 + \omega^2}\right] V_o$$

This may be re-arranged to give:

$$B = \omega_o V_o \left[\frac{\beta\omega_o - \alpha}{\omega_o^2 + \omega^2}\right] \qquad (11.22)$$

The steady-state solution is obtained by ignoring the transient solution in eqn. (11.20) which tends to zero as $t \to \infty$.

$$E_{2,s}(\omega) = \left[\frac{\alpha^2 + \omega^2\beta^2}{\omega_o^2 + \omega^2}\right]^{\frac{1}{2}} V_o \cos(\omega t + \chi) \qquad (11.23)$$

[Eqn. (11.23) could have been derived by applying eqn. (3.42) to obtain $G_1^* V_1^* = G_2^* V_2^*$, then using this in conjunction with $V_1^* + V_2^* = V_o e^{j\omega t}$ to specify V_2^*, the real part of which should be considered. This approach has not been adopted since it does not yield the transient solution.]

Suppose that the applied waveform is constant which can be represented by letting $\omega = 0$. The solution is given by eqns. (11.20), (11.21) and (11.22).

$$E_{2,o}(t) = V_o\left[\beta e^{-\omega_o t} + \frac{\alpha}{\omega_o}\left[1 - e^{-\omega_o t}\right]\right] \qquad (11.24)$$

The electric field changes from $E_{2,o}(0)$, the initial state, to $E_{2,o}(\infty)$, the final state, where:

$$E_{2,o}(0) = \beta V_o = \epsilon_1 V_o/(\epsilon_1 d_2 + \epsilon_2 d_1) \qquad (11.25)$$

$$E_{2,o}(\infty) = \alpha V_o/\omega_o = \sigma_1 V_o/(\sigma_1 d_2 + \sigma_2 d_1) \qquad (11.26)$$

If a very good insulator (such as perspex) is used then $\sigma_1 << \sigma_2$ and eqn. (11.26) implies:

$$E_{2,0}(\infty) \simeq \frac{\sigma_1 V_o}{\sigma_2 d_1} << \frac{\epsilon_1 V_o}{(\epsilon_1 d_2 + \epsilon_2 d_1)} = E_{2,0}(0) \qquad (11.27)$$

This means that, in the case of a constant applied voltage, the electric field is initially high but soon falls to a very low value. The fall time is governed by the relaxation time defined in eqn. (11.15). Since the electric field strength E_2 is required to be high, in order to resolve the emulsion, it is clear that a constant applied voltage is ineffective.

The amplitude of the steady-state solution $E_{2,S}(\omega)$, as given by eqn. (11.23), is frequency dependent. It varies from $\hat{E}_{2,S}(0)$ at zero frequency to $\hat{E}_{2,S}(\infty)$ at very high frequencies, where:

$$\hat{E}_{2,S}(0) = \alpha V_o/\omega_o = E_{2,0}(\infty) \qquad (11.28)$$

$$\hat{E}_{2,S}(\infty) = \beta V_o = E_{2,0}(0) \qquad (11.29)$$

The lower and upper frequency limits, of the steady-state solution, are therefore identical, respectively, to the final and initial values of the transient solution for constant applied voltage. Hence, from eqn. (11.27), it follows that:

$$\hat{E}_{2,S}(0) << \hat{E}_{2,S}(\infty)$$

Consequently, the steady-state electric field amplitude increases as frequency is increased.

Of interest is the electric field amplitude at frequency ω_o, which can be obtained from Eqn. (11.23):

$$\hat{E}_{2,S}(\omega_o) = \frac{V_o}{\sqrt{2}} (\alpha^2/\omega_o^2 + \beta^2)^{\frac{1}{2}}$$

Using eqns. (11.15) to (11.17) this becomes:

$$\hat{E}_{2,S}(\omega_o) = \frac{V_o}{\sqrt{2}} \left[\left[\frac{\sigma_1}{\sigma_1 d_2 + \sigma_2 d_1} \right]^2 + \left[\frac{\epsilon_1}{\epsilon_1 d_2 + \epsilon_2 d_1} \right]^2 \right]^{\frac{1}{2}}$$

If $\sigma_1 << \sigma_2$ then it follows that:

$$\hat{E}_{2,s}(\omega_o) \simeq \frac{V_o\beta}{\sqrt{2}} = \frac{V_o}{\sqrt{2}}\left[\frac{\epsilon_1}{\epsilon_1 d_2+\epsilon_2 d_1}\right] = \frac{1}{\sqrt{2}}\hat{E}_{2,s}(\infty)$$

Thus, the electric field strength in the emulsion, at frequency ω_o (corresponding to the system time constant τ), is 71% of the high-frequency limit. It should therefore be possible to obtain good emulsion resolution by operating at frequency ω_o (where the cyclical frequency $f_o = \omega_o/(2\pi) = 1/(2\pi\tau)$).

It is of interest to examine the current i passing between the electrodes, which for the present considerations, is the product of current density (given by eqn. (11.13)) and electrode area S.

$$i/S = \sigma_2 E_2 + \epsilon_2 \frac{dE_2}{dt} \qquad (11.30)$$

Eqn. (11.20) can be used to substitute in for E_2:

$$i/S = \sigma_2\left[\omega_o V_o\left[\frac{\beta\omega_o-\alpha}{\omega_o^2+\omega^2}\right]e^{-\omega_o t} + \left[\frac{\alpha^2+\omega^2\beta^2}{\omega_o^2+\omega^2}\right]^{\frac{1}{2}} V_o\cos(\omega t+\chi)\right]$$

$$-\epsilon_2\left[\omega_o^2 V_o\left[\frac{\beta\omega_o-\alpha}{\omega_o^2+\omega^2}\right]e^{-\omega_o t} + \left[\frac{\alpha^2+\omega^2\beta^2}{\omega_o^2+\omega^2}\right]^{\frac{1}{2}} \omega V_o\sin(\omega t+\chi)\right] \qquad (11.31)$$

For large values of ω, $\chi \to 0$ (from eqn. (11.21)) and eqn. (11.31) becomes:

$$i/S \simeq \beta V_o[\sigma_2\cos(\omega t)-\omega\epsilon_2\sin(\omega t)] \simeq -\beta V_o\omega\epsilon_2\sin(\omega t)$$

$$i/S \to \infty \text{ as } \omega \to \infty.$$

The current increases without limit as the frequency of operation tends to infinity. In reality, a power supply cannot provide infinite current or a waveform of infinite frequency. The maximum frequency of operation will therefore be determined by the ability of the power supply to provide current.

The maximum steady-state field amplitude, βV_o, obtained by using very high frequencies, can also be achieved by requiring that $\alpha = \omega_o\beta$ (as can be seen from eqn. (11.23)). This is equivalent to the expression $\epsilon_1/\sigma_1 = \epsilon_2/\sigma_2$, as can

be deduced from eqns. (11.15), (11.16) and (11.17). When this condition is valid, the time constants of the two phases are identical and there is no interfacial polarisation. The condition that the time constants should be as close as possible requires that the value of σ_1 be increased towards that of σ_2, and that ϵ_1 be reduced. However, there is not much scope for reducing the permittivity and in any case this would tend to reduce the field amplitude βV_0 (according to eqn. (11.17) which defines β). Eqn. (11.17) can also be used to demonstrate that the field amplitude is increased by reducing the thickness of insulation d_1 (which also makes β less dependent on ϵ_1 since, as $d_1 \rightarrow 0$, $\beta \rightarrow 1/d_2$ (ϵ_1 cancelling)).

Thus there are three ways of increasing the electric field in the emulsion, namely by: increasing the frequency of the applied waveform; increasing the conductivity of the insulating dielectric; reducing the width of the insulating dielectric. All of these measures increase the current drawn by the electro-coalescer and hence increase its power consumption.

It is also apparent that the applied waveform should have zero mean value, otherwise there would be a leakage current and charge accumulation at the interface between the insulator and the emulsion. In practice, the time constants of the two phases cannot be made the same since this would necessitate σ_1 being of similar magnitude to σ_2, contradicting the requirement that the phase 1 dielectric should be an insulator. If the time constants of the two phases were to be made identical, the electric field amplitude would be independent of frequency. Though this has been shown to be impracticable, the requirement to operate at as high a frequency as possible (disregarding power supply current limitations) is relaxed by reducing the difference between the time constants of the two dielectrics.

There are also practical implications with regard to reducing the thickness of insulation, d_1, since this could lead to electrical breakdown problems if taken to extremes.

If it is possible to obtain efficient phase separation by the above means, it must still (usually) be commercially viable. In order to obtain cost-effective operation, the power consumption must be minimised without compromising separation efficiency. Some indication of the economic viability of operating at higher currents can be obtained from the petroleum industry, where it is acceptable to treat crude oil, of conductivity typically $10^{-9}Sm^{-1}$, using electro-coalescers with uninsulated electrodes. This suggests that it would be reasonable to use an insulating dielectric having a similar conductivity.

11.2 The Effect of Insulation on Waveform Shape

Consider a periodic voltage waveform (of period T) applied across insulated electrodes between which there is an emulsion. According to Fourier analysis, this waveform can be expressed as a linear combination of sinusoidal components having frequencies inversely proportional to T. The voltage waveform across the emulsion can then be obtained from a consideration of the steady-state solution given by eqn. (11.23). It can be seen that the amplitudes of the sinusoidal components are frequency dependent and that they tend to increase with frequency. In consequence, the voltage waveform appearing across the emulsion will be different in form from the one applied across the electrodes.

Apart from a sinusoid, one of the simplest periodic waveforms is a square wave. If the period of the square wave T is less than or equal to the system time constant τ ($= 1/\omega_0$, defined by eqn. (11.15)), interfacial polarisation will be small and the voltage across the emulsion will not be significantly attenuated. If $T >> \tau$, however, interfacial polarisation will be important and the voltage appearing across the emulsion will be attentuated, except for small time intervals following a step change in voltage (see eqn. (11.24)).

The application of a square wave to an emulsion, via insulated electrodes, has been considered practically by Bailes and Larkai (1981), and Galvin (1984), and theoretically by Joos and Snaddon (1985). In all of these cases the square wave was unidirectional (the peak amplitudes varying between zero and some positive value), the rise time being relatively large and the fall time small (see Figure 11.2).

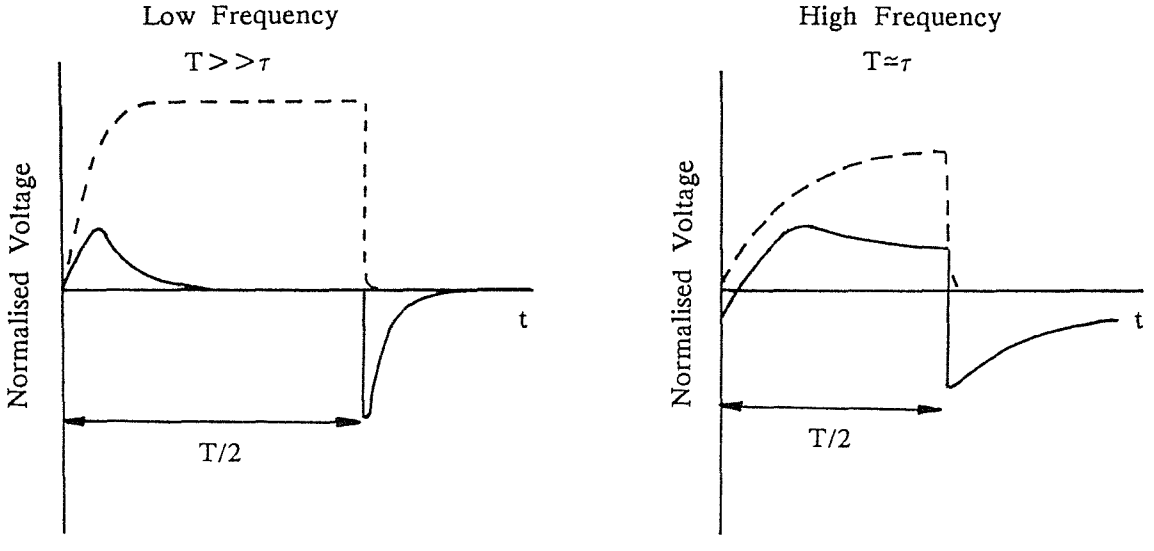

FIGURE 11.2 Normalised voltages across a W/O emulsion (solid line) and across the insulated electrodes (dotted line) for low and high frequencies.

Bailes and Larkai, and Galvin state that the insulation affects the voltage waveform appearing across the emulsion, as predicted earlier. Joos and Snaddon calculate the effect and its frequency dependence, producing waveforms similar to those shown in Figure 11.2. These waveforms are like those measured by Galvin (1984) whose paper shows a photograph of a typical oscilloscope trace. Galvin shows experimentally, and Joos and Snaddon show theoretically, that the RMS voltage drop across the emulsion increases with frequency until limited by the power supply. This limitation corresponds to the inability of the power supply to provide current at high frequencies and is related to the capacitive load of the electro-coalescer system.

11.3 Limitations Imposed by Real Power Supplies

As mentioned earlier, the upper frequency limit, for electro-coalescer operation, is usually determined in part by the power supply used. Practically, it is difficult to obtain high voltages at high frequency since this requires the generation of large currents and hence power. Even the simple transformer, usually regarded as an efficient electrical device, suffers "transformer losses" at high frequency.

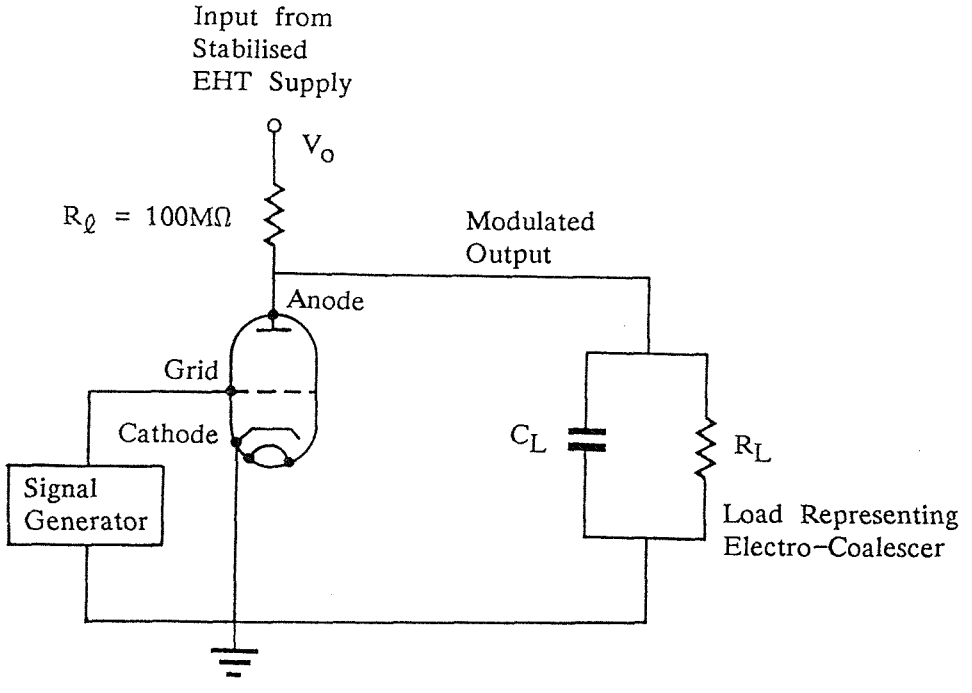

FIGURE 11.3 Modulator unit utilising high-voltage triode (PD 500) for controlling stabilised EHT supply.

The method used by Bailes and Larkai (1981) and Galvin (1984) (and considered theoretically by Joos and Snaddon (1985)) relies on a triode valve which can be operated at anode voltages as high as 25kV. A stabilised power supply is connected to the anode via a current-limiting resistor, as shown in Figure 11.3. The grid voltage is determined by the output of a signal generator. The electro-coalescer load is represented by a parallel RC network. When the grid voltage is negative the valve is a poor conductor, since the electrons in the vicinity of the cathode are prevented from reaching the anode. In this state, the anode voltage soon (governed effectively by the time constant $R_\ell C_L$) reaches the working level of $V_o R_L/(R_L+R_\ell)$. If $R_\ell << R_L$ (as assumed) the anode voltage can almost attain the output voltage V_o of the EHT supply. However, when the grid voltage is positive, the valve becomes a good conductor (of resistance R_v say) since electrons can travel from the cathode to the anode. Under these circumstances, the charge held by the capacitor C_L, and that supplied through the current-limiting resistor R_ℓ, is soon neutralised. The capacitor C_L is discharged according to the time constant $R_v C_L$ which is very much smaller than the charging time constant $R_\ell C_L$ since $R_v << R_\ell$. In this case, the anode voltage assumes the value $V_o R_v/(R_v+R_\ell)$ which is very much less than V_o since $R_v << R_\ell$ (typically $R_v <$ 1MΩ whereas R_ℓ = 100MΩ).

It can be appreciated that the low-voltage signal generator waveform modulates the stabilised EHT voltage. The anode voltage assumes a low level when the grid voltage is positive. However, when the grid voltage is negative the anode voltage will follow the grid voltage, as defined by the signal generator waveform. The anode and grid voltage waveforms may differ in shape due to the different charging and discharging time constants ($R_\ell C_L$ and $R_v C_L$ respectively) of the circuit. The anode voltage, for a square wave grid voltage, for example, will exhibit a slow rise and fast fall (as shown in Figure 11.2).

The shape of the anode voltage will also be determined by the frequency of operation. If the frequency is high, the anode voltage will have insufficient time to rise to a large value before its rapid decay. The maximum frequency of operation can be estimated from the expression $f = 1/(2\pi R_\ell C_L)$. As R_ℓ and C_L increase the maximum frequency of operation reduces. In the absence of the electro-coalescer $C_L = C_v \simeq$ 8pF which is the capacitance of the valve. This defines the absolute maximum operating frequency to be about 200Hz, assuming R_ℓ is not reduced. At frequencies of operation higher than this, the anode voltage reduces in amplitude. When the electro-coalescer is present, the maximum operating frequency is reduced by virtue of the increased capacitive load. It can therefore be appreciated that this represents a constraint on the physical dimensions

of the electro-coalescer since $C_L = A\epsilon/d$ (for a parallel plate system), where A is the plate area and d is a measure of electrode separation. (The proper expression for C_L is more complex than this since an emulsion and insulator are involved). In order to keep C_L low it is necessary to make A small and d large. Unfortunately this means that the size of the electro-coalescer must be kept small. Similarly, increasing d reduces the electric field strength within the emulsion, which results in less efficient phase separation.

As examples, the electro-coalescers of both Bailes and Larkai (1981) and Galvin (1984) will be considered. The first step is to calculate the effective dielectric constant (K_2) and conductivity (σ_2) of the emulsion. In order to do this it is necessary to determine the characteristic frequency f_o of the emulsion. The following expression, due to Wagner, may be used. Though it is strictly valid for dilute emulsions, it should give some idea of the characteristic frequency of a concentrated emulsion (having volume fraction $\varphi = 0.5$ in the examples) (Sherman, 1968):

$$\tau_o = \frac{1}{2\pi f_o} = \left[\frac{2K_c+K_d+\varphi(K_c-K_d)}{2\sigma_c+\sigma_d+\varphi(\sigma_c-\sigma_d)}\right]\epsilon_o \qquad (11.32)$$

Since the emulsion is of W/O type it follows that $\sigma_c << \sigma_d$ and $K_c << K_d$, hence eqn. (11.32) implies:

$$f_o = \frac{\sigma_d}{2\pi K_d \epsilon_o} \qquad (11.33)$$

For the present purpose, σ_d is taken as the conductivity of Bailes and Larkai's (1981) System A aqueous phase ($8 \times 10^{-5} Sm^{-1}$), this being less than that of their System B aqueous phase. The dielectric constant of the aqueous phase K_d is assumed to be 80. Eqn. (11.33) then gives the characteristic frequency of the emulsion as about 19kHz. Since this is much greater than the experimental frequencies used (which were less than 1kHz), this justifies the use of the low-frequency values for the effective dielectric constant and conductivity of the emulsion. Thus the emulsion dielectric constant K_2 is equal to K_ℓ as given by Hanai's eqn. (3.74), and the emulsion conductivity σ_2 is equal to σ_ℓ as given by Hanai's eqn. (3.73). Since $\varphi = 0.5$ this means that $K_2 = K_\ell = 8K_c$ and $\sigma_2 = \sigma_\ell = 8\sigma_c$, where K_c and σ_c are respectively the dielectric constant and conductivity of the continuous phase (i.e. the organic phase). Having determined the effective dielectric constant K_2 and conductivity σ_2 of the emulsion it is now possible to

consider the system comprising the perspex insulator (K_1,σ_1) and the emulsion (K_2,σ_2). The theory of Section (3.6.4) will be used for this purpose and so it is necessary to specify the capacitance C and conductance G of each component rather than their dielectric constant K and conductivity σ. This is achieved using eqns. (11.34) and (11.35) below where A represents cross-sectional area and d_n represents thickness (n = 1 for insulator, n = 2 for emulsion).

$$C_n = A\epsilon_o K_n/d_n \qquad (11.34)$$

$$G_n = A\sigma_n/d_n \qquad (11.35)$$

The values of C_n and G_n can now be used to determine C_ℓ and C_h, the low and high frequency limits of capacitance, and the characteristic time constant τ of the insulator/emulsion system; eqns. (3.49) to (3.51) are used for this purpose. The effective load capacitance C_L can then be found by considering the real part of eqn. (3.46), resulting in:

$$C_L = Re(C^*) = C_h + \frac{(C_\ell - C_h)}{1 + (\omega\tau)^2} \qquad (11.36)$$

Clearly the capacitive load C_L, of the electro-coalescer, is dependent on the frequency ($\omega = 2\pi f$) used. For the present purpose, f will be taken as 8Hz since this is the optimum frequency of operation for Bailes and Larkai's (1981) apparatus.

Firstly, Bailes and Larkai's (1981) System B will be considered, for which the organic phase has dielectric constant K_c = 1.315 and conductivity σ_c = 4.0nSm^{-1}. The effective dielectric constant and conductivity of the emulsion are therefore (from above) $K_2 = 8K_c$ = 10.52 and $\sigma_2 = 8\sigma_c$ = 32.0nSm^{-1} respectively. The perspex insulator has dielectric constant K_1 = 3.5 and conductivity σ_1 = 0.316pSm^{-1}. Bailes and Larkai's (1981) electro-coalescer has cross-sectional area A = 3.17 $\times$ 10^{-2}m^2 (17.8cm $\times$ 17.8cm) and height 2.54cm. Following their suggestion, however, the emulsion band depth is taken as d_2 = 1cm, since a free water phase is present at the bottom of the coalescer. Though various thicknesses of insulator were considered the value d_1 = 6mm is here taken as representative. The capacitances and conductances of the insulator/emulsion system are therefore: C_1 = 164pF, G_1 = 1.67pS, C_2 = 295pF and G_2 = 0.101μS (from eqns. (11.34) and (11.35)). The low and high frequency limits of capacitance and the time constant of the insulator/emulsion system turn out to be C_ℓ = 164pF, C_h = 105pF and τ = 4.53ms, respectively (using eqns. 3.49 - 3.51). At a frequency of 8Hz,

the capacitive load (given by eqn. (11.36)) therefore has the value C_L = 161pF. The triode valve presents a capacitance of 8pF in parallel with this and so the total load capacitance becomes C_L = 169pF. The capacitive load is charged through a current-limiting resistor of value R_ℓ = 100MΩ and so the charging time constant ($\tau_c = R_\ell C_L$) is 16.9ms. This corresponds to a power supply operating frequency ($f_s = 1/(2\pi\tau_c)$) of about 9Hz, above which the voltage amplitude will be attenuated. Since this is less than the characteristic frequency ($f_c = 1/(2\pi\tau)$) 35Hz (see eqn. (3.51)) of the insulator/emulsion system, the voltage drop available across the emulsion will be substantially less than that available between the electrodes. Similarly, the voltage drop across the emulsion will be attenuated as the power supply operating frequency is increased above 9Hz. The situation could be improved by reducing the cross-sectional area A of the coalescer or, preferably, by reducing the value of the current-limiting resistor R_ℓ. By reducing R_ℓ to 10MΩ, it would still be possible to obtain 10kV at the output of the EHT supply since the greatest current drawn would then be 1mA (the maximum output current of the 30kV Brandenburg EHT supply). This would raise the maximum power supply operating frequency to the much healthier value of about 90Hz (twice the system characteristic frequency).

The situation is different in the case of Galvin's (1984) apparatus since his electro-coalescer is much smaller. The dielectric constant and conductivity of Galvin's organic phase are K_c = 2.5 and σ_c = 3.5nSm^{-1}. The effective dielectric constant and conductivity of the emulsion are therefore $K_2 = 8K_c$ = 20 and $\sigma_2 = 8\sigma_c$ = 28.0nSm^{-1} respectively. The perspex insulator is assumed to have a dielectric constant K_1 = 3.5 and conductivity σ_1 = 0.316pSm^{-1}, as before. Galvin's electro-coalescer has cross-sectional area A = 10^{-3}m^2 (1cm × 10cm) and height 5cm. Since the flow speed in Galvin's coalescer is nearly an order of magnitude greater than that in Bailes and Larkai's, the emulsion band depth is taken as the coalescer height d_2 = 5cm (since no free water layer is specified and is therefore assumed not to exist). The thickness of the perspex insulation is 3mm. The capacitances and conductances of the insulator/emulsion system are therefore: C_1 = 10pF, G_1 = 0.105pS, C_2 = 3.5pF and G_2 = 0.64nS (from eqns. (11.34) and (11.35)). From these it follows that the low and high frequency limits of capacitance and the time constant of the insulator/emulsion system are C_ℓ = 10pF, C_h = 2.6pF and τ = 21.1ms respectively (using eqns. 3.49 - 3.51). At a frequency of 8Hz, the capacitive load (given by eqn. (11.36)) has the value C_L = 6.1pF. Since the triode valve presents a capacitance of 8pF in parallel with this, the total load capacitance becomes 14pF. As before, the capacitive load is assumed to be charged through a current-limiting resistor R_ℓ of value 100MΩ and so the charging time constant ($\tau_c = R_\ell C_L$) is 1.41ms. This corresponds to a

power supply operating frequency ($f_s = 1/(2\pi\tau_c)$) of about 113Hz, above which the voltage amplitude will be attenuated. This is much greater than the characteristic frequency ($f_c = 1/(2\pi\tau)$) 7.5Hz of the insulator/emulsion system, and so the voltage drop available across the emulsion will be a large proportion of that available between the electrodes. Galvin's results do, in fact, show that the RMS voltage drop across the emulsion rises as the operating frequency is increased up to, and a little beyond, the 113Hz value calculated; it is subsequently attenuated greatly as the frequency increases to 1kHz.

11.4 Miscellaneous Aspects of Electrode Insulation

Two interesting phenomena are apparent from Galvin's (1984) experiments, in which a W/O emulsion is subjected to an electric field using insulated or uninsulated electrodes. The first relates to the conflict between electrostatic and hydrodynamic effects when low-frequency waveforms are used. For frequencies up to about 10Hz, the coalescence effectiveness is not as high as would be expected for uninsulated electrodes, bearing in mind that the mean field strength is virtually unattenuated. In fact, it is only marginally better than the situation in which insulated electrodes are used, where the field strength is greatly attenuated. Galvin explains this in terms of hydrodynamic mixing during the half-period when the emulsion is not subjected to an electric field. This explanation would appear to be reasonable and has implications with regard to the choice of continuous or batch processing. During batch processing, presumably, hydrodynamic mixing should not arise at low frequencies or, indeed, at any frequency. However, in the case of continuous processing it would have to be contended with.

One way of removing hydrodynamic mixing would be to raise the voltage of the counter electrode, which is usually grounded, to half the maximum voltage of the energised electrode, for example. In this way, the electric field applied to the emulsion would never be zero, except transiently. However, the field strength would be halved and since coalescence forces are dependent, primarily, on the square of the field strength, coalescence effectiveness would be reduced by a factor of about four. Since the electric field would be applied for twice the time, however, the overall coalescence effectiveness would be halved. This disadvantage would have to be weighed in relation to the advantage of not having to suffer low-frequency hydrodynamic mixing.

The second phenomenon, which Galvin did not discuss, is concerned with the use of uninsulated electrodes at frequencies above 10Hz. Apparently, the mean emulsion drop size, for a dc electric field, is less than that for a pulsed field

having an equivalent or even smaller RMS field strength. This may be due to interfacial instabilities (e.g. droplet oscillation, Marangoni effect) or possibly the half-period during which the electric field is off. In fact, de Brey (1926) suggests that it is the peak voltage drop which is of importance in coalescence. There may be something in this, though the modern consensus of opinion (e.g. Galvin (1984), Joos and Snaddon (1985), Williams and Bailey (1983), Volkov and Krylov (1972b)) is that it is the mean square field strength which is of primary importance in determining coalescence effectiveness.

The use of a triode valve modulator and waveform generator, to produce unidirectional pulses, is quite complicated in relation to the use of a simple transformer, and may not be justified. For a given electric field amplitude, the RMS field of the unidirectional pulsed waveform is identical to that of a sinusoid produced using a transformer. Though coalescence effectiveness is believed to be related primarily to the RMS field strength, there may be some differences due to the secondary effects already mentioned (e.g. interfacial instabilities and migratory coalescence).

12. ELECTRO-COALESCER PATENT INFORMATION

Although the Applied Electrostatics Group at the University of Southampton already held many patents relating to the dehydration and cleaning of fuel by electrostatic methods, many more were located by computer searches performed in 1979, 1980, 1985 and 1986. The following table summarises the data bases and search methods used for these searches.

SEARCH DATE	DATA BASE	SEARCH METHOD
16.11.79	INSPEC	KEYWORD
11.12.79	BIOSIS	"
"	CHEM. ABS.	"
28.1.80	WORLD PATENTS INDEX (WPI)	KEYWORD
31.1.80	" " "	"
20.9.85	APIPAT	KEYWORD
"	CHEM. ABS.	"
"	WORLD PATENTS INDEX (WPI)	"
"	WORLD PATENTS INDEX (LATEST) (WPIL)	"
6.3.86	PATSEARCH	CITATION
"	WORLD PATENTS INDEX (WPI)	CLASSIFICATION CODE & KEYWORD
7.3.86	WORLD PATENTS INDEX (LATEST) (WPIL)	"

Searching by classification code and keyword turned out to be the most efficient method producing 61% relevant information. The citation search came next producing 45% relevant information.

Appendix B lists relevant patents held before any computer searches were performed; all are the British equivalents of basic American patents. Appendix C lists the patents located by computer searches in 1979/80 and Appendix D lists those located by computer searches in 1985/86.

It is interesting to note that most of the patents, relating to the separation of water-in-oil emulsions, originate in the Soviet Union and the United States; the remainder originate in such countries as Canada, Japan, Great Britain, Germany and France.

12.1 Overview of Information Contained in Patents

Although the use of an electric field for resolving an emulsion may appear novel, the method was first patented in 1911. F G Cottrell took out the pioneering patents US 987114/5/6/7 in this connection, claiming that the water particles are subject to electrostatic forces dependent upon the relative potentials and dielectric constants of the materials in contact and caused to coalesce into masses easily removed by settling or centrifugation. Since then, many hundreds of patents have been filed on the subject of electrical dehydration and desalting. Electric treater specifications differ appreciably from one patent to another, and design trends have changed over the years. From reading a selection of patents, it would appear that electric treater design has been more of an art than a science in the past. Improvements have apparently been made in a stage-by-stage process. As an example of the different design concepts which appear, consider the following extracts from patents. The patent GB 953841 (1963) extract reads, "The invention also provides apparatus for electrically resolving oil-continuous dispersions including a plurality of cells disposed side by side, central electrodes in said cells insulated therefrom, there being long and narrow inter-electrode treating spaces within the cells between the cell walls and the central electrodes, metering orifices adjacent to the exit ends of the cells, and a high-voltage source of potential connected between the cells and the central electrodes establishing high-voltage electric fields in said treating spaces." Compare and contrast this with patent US 3661746 (1972), an extract of which reads, "A spatial uniform electric field is provided by an electrode means within the treating vessel so that the dispersion flowing along the vertical flow axis passes perpendicularly through planes of constant potential. In the treater, the electric field is established between an energised electrode and an upstream electric ground, such as a grounded electrode, which are spaced vertically from one another. More particularly, the energised electrode is constructed of an electrically conductive metal into a foraminous form and is positioned substantially horizontally in the treating vessel. The energised electrode has a planar surface presented toward the emulsion inlet. Insulators support the energised electrode in electrical isolation from the walls of the treating vessel. The energised electrode extends substantially across the entire cross-section of the treating vessel transverse to the flow of fluid along the vertical flow axis."

For details of a typical modern electric treater design, see Figure 12.1 which shows the main components.

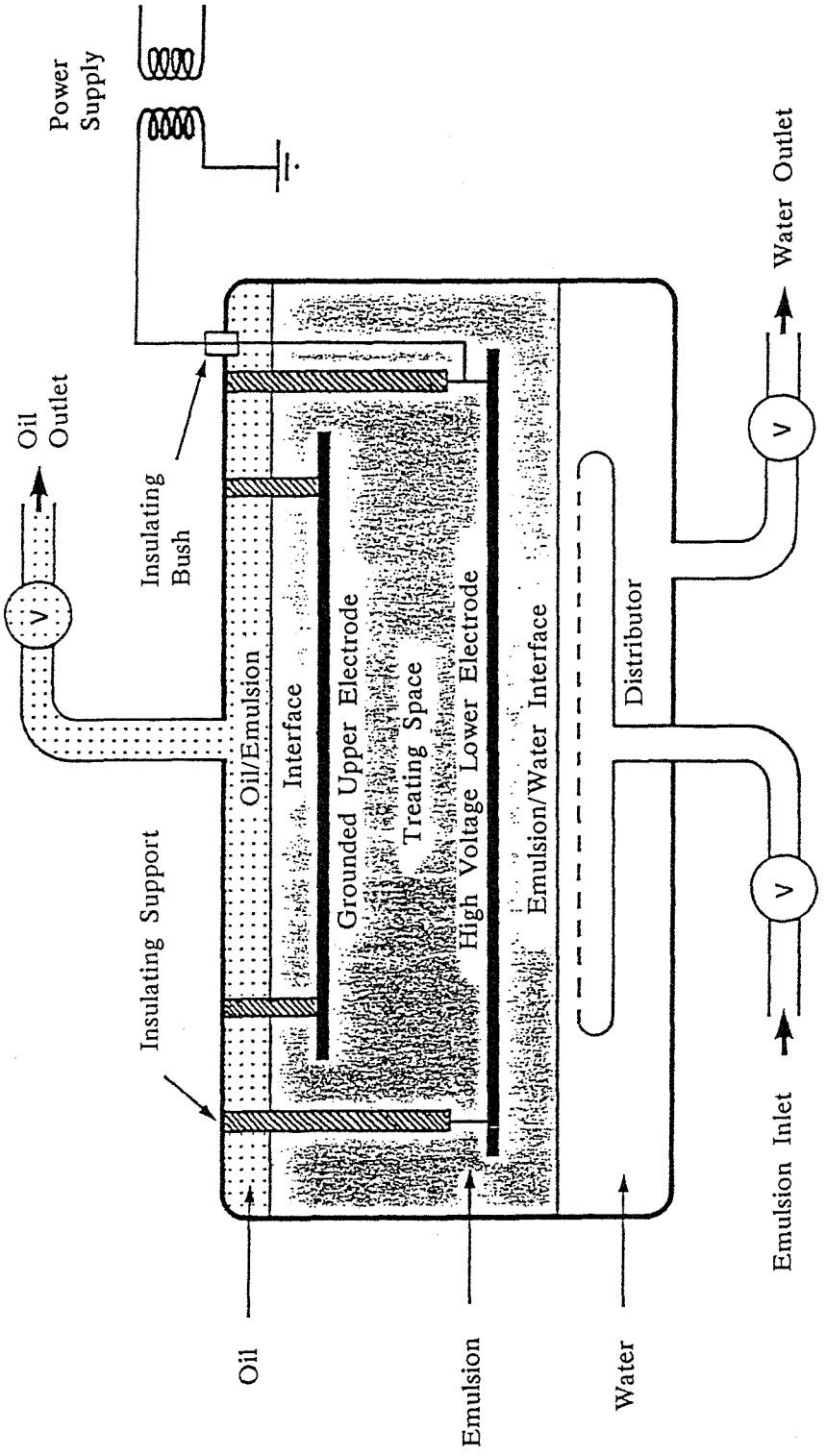

FIGURE 12.1 Typical electric treater design.

It would appear from the patent abstracts that many different techniques and combinations of techniques are used for separating W/O emulsions. These are listed as follows:

(i) Gravitational settling
(ii) Heating
(iii) Chemical demulsification
(iv) Electrostatic field separation
(v) Centrifugation
(vi) Cyclone separation
(vii) Ultrasonic irradiation
(viii) Magnetic separation
(ix) Aeration
(x) Microwave radiation
(xi) Tribocharging
(xii) Charge injection

All these techniques are concerned with causing or assisting the coalescence of water droplets; as the size of a water droplet increases so does the speed with which it can be removed from the continuous oil phase.

The most conventional method of treatment relies on separation in an electrostatic field, after the emulsion has been heated and the appropriate chemical demulsifier added. This treatment process is sometimes combined with centriguation or, more latterly, cyclone separation.

In all cases where an electrostatic field is used, the electrodes are housed in a container into which the emulsion is introduced. The container is usually cylindrical in shape and made from metal. In some cases it may be made from a dielectric material or shaped in the form of a sphere (to increase residence time in the electric field as the flow speed reduces). The container may also house such internal devices as capacitance or conductivity probes, interface level sensors, filters containing fibres or glass beads, baffles, screens and deflecting plates.

The electrodes themselves are multifarious in design. In some cases uniform electric fields are thought desirable whereas in others non-uniform fields are preferred, perhaps to obtain benefit from dielectrophoretic effects. There may be only one recognisable electrode, the other being the metal container itself or the free water at the bottom. Alternatively, many electrodes may be used. If an

electrode is situated normal to the flow direction it must be perforated to allow the emulsion to pass through it, into the treating space where the electric field is intense. Otherwise, it may be of solid construction. In some designs, the electrodes are corrugated or may have projections such as discs or needles which distort the electric field.

In electro-coalescers where a separate tank is used for settling, the droplet size increases in the flow direction; since electrostatic re-emulsification occurs more readily the larger the droplet, the electric field intensity is often decreased in the downstream direction to prevent dispersion of water droplets. The converse is true when droplets coalesce and settle out in the opposite direction to the emulsion flow.

Another important consideration is the way the electrodes are energised. A very convenient method is to use ac excitation, at the frequency of the local supply (50 or 60 Hz), for which transformers only are necessary. This excitation is usually adopted for the treatment of high conductivity oils such as crudes. In the case of gas oil and distillates, separation efficiency is improved by using dc excitation. Unfortunately, this involves the use of rectifying circuitry. In some cases "dual polarity" separation is employed in which both ac and dc excitations are used, in conjuction with independent electrode systems within the electric treater. Also described in the literature is separation using a three-phase supply, which by necessity involves the use of at least three electrodes. Also described in the literature is separation using pulsed excitation (unidirectional or bipolar); the advantage of using a pulse is that, during the fast rise and fall of the electric field intensity, the water droplet surface is destabilized (especially helpful in the case where surfactant is present) enhancing coalescence. It is also worth mentioning here that sometimes, the electrodes in a treater, are resistively or capacitively coupled to their power supply.

The surfaces of the electrodes may be insulated from the emulsion by a dielectric material. This can prevent shorting but there are disadvantages since dc energisation and migratory coalescence are rendered ineffective.

Electrodes are sometimes coated with hydrophilic or hydrophobic layers either to attract water droplets or to prevent their accumulation.

Latterly, in some patents the treating space is filled with fibres or dielectric beads to form an electrofilter.

Some patents are worthy of individual mention because of their novel design features. In SU 432170 the emulsion is made to flow through a polyfluoroethylene resin casing which faces a corona discharge. In US 3799856 a hydrocarbon stream is desalted by establishing a water content of less than 1%, increasing the temperature until all the water is dissolved in the oil, and then passing the stream through an electrofilter which removes the salt crystals. In US 3567619 aqueous and solid contaminants are removed from hydrocarbon fuels by using a charged emitting screen electrode and a conductive fibrous collecting bed downstream. In EP 159909 a charge injection technique is used to separate particulates or water droplets from oil and can also be used for dehazing fuel oil. In SU 1127613 a perforated dielectric diaphragm with inserted dielectric rods, situated in the inter-electrode space, is described . In GB 2136323 use is made of a surfactant-treated permeable membrane, connected to an electric current source, which acts as a percolating electrode through which the emulsion passes. Increased dehydrator efficiency is claimed in SU 1007695 which describes a treater equipped with several pairs of corona discharge and earthed electrodes inclined at angles of 30° - 90° from the treater axis. In GB 2123716 it is claimed that efficiency of water removal can be increased by over 25 times by using electrodes made from directionally solidified eutectic rather than stainless steel. Described in EP 96739 is a pair of electrodes, spaced to form a passageway in which each electrode consists of a material which varies in electrical conductivity, in a predetermined direction, within the passageway. In SU 993976 a treater is described, in which a sphere having metallized surface moves reciprocally between the electrodes transferring charge and collecting water droplets; the separation efficiency is claimed to be increased by a factor of 2 - 2.5. In SU 912204 coaxial mesh electrodes are used in conjunction with an earthed impeller shaft with blades, there being negative partitions at the side. In SU 865325 the outer ring electrode has a dielectric lining whereas the inner electrode is an inverted truncated cone grounded by capacitors. In SU 850122 coaxial electrodes are used, separated by ferromagnetic particles. Described in SU 829130 is a technique whereby positively charged particles are introduced to the peripheral zone, negatively charged particles to the central zone, the two streams being mixed by dielectric swirlers subsequently. In SU 82711 a perforated dielectric screen is situated between the electrodes. In SU 770547 coagulation and precipitation of aviation fuel impurities is achieved by using rotating discs, of different metal surfaces, to generate charge by triboelectrification. In SU 889035 the positive electrode is made from a container holding metal turnings.

To summarise, it is clear that many different separation techniques are applicable but their diversity suggests that an optimum design has not yet been achieved. In fact, there may not be an optimum design since the nature of the emulsion is so variable (oil viscosity, water content, surface–active agent content, etc.).

OVERALL SUMMARY AND CONCLUSIONS

Chapter 2

1. Water is often produced with oil since it generally underlies the oil in the geological formations from which the oil is drawn.

2. As the production life of a well is extended, the proportion of water increases, especially if secondary recovery techniques are used.

3. The high shear forces created by pumping a mixture of water and oil through pipes, valves and other equipment creates an emulsion, usually of the W/O type.

4. The emulsification process may be aided by emulsifying agents, which can occur naturally in an oil, leading to the production of a stable emulsion.

5. The presence of dispersed water in oil is undesirable for a number reasons: (i) it increases pumping costs since the emulsion viscosity is greater than that of the oil; (ii) throughput is reduced since water as well as oil has to be pumped; (iii) the water contains salts which lead to corrosion in pipelines and refineries; (iv) the water contains sediment which causes erosion and can stabilize emulsions by accumulating at the water/oil interface.

6. Pipeline authorities normally accept crude charge from oilfields if the brine content is at most 0.5–2%.

7. Desalting is practised at refineries, prior to distillation, in order to prevent corrosion, erosion, plugging and scaling. The hydrolysis of chlorides, especially at temperatures above 120°C, leads to the evolution of hydrochloric acid. Not only is this extremely corrosive itself, but the experience of refiners indicates that corrosion due to hydrogen sulphide is increased in its presence.

8. The use of caustic materials to neutralize hydrochloric acid, if used to excess, can lead to stress corrosion (caustic embrittlement) in refinery metals.

9. Contamination of refined fuel, by sea water, can occur during shipping. When the fuel is used to power gas turbines, it is good practice to desalt it, on site, prior to combustion. This is because hot corrosion can lead to severe damage to turbine blades and stators, necessitating an expensive overhaul and unscheduled shut–down.

10. In the treatment of distillate fuels, chemical reagents, such as sulphuric acid and caustic, are used to remove contaminants in the "scrubbing" process. Dispersed phase droplets are then removed by electrical treatment, as in the desalting process.

11. In the desalting process, 3 to 5% fresh water is added to the crude oil and thoroughly mixed with it. The dispersed fresh water droplets coalesce with the brine droplets, in the applied electric field, then settle out gravitationally at an increased rate. This reduces the concentration of salt in the oil. Sediments are also removed during the desalting operation.

12. The electrical dehydration of crude, at the oilfield, is practised in order to reduce the brine content to meet the specification of pipeline authorities.

13. The electrical treatment of W/O emulsions was instituted in 1909. It is a simple, efficient and cost effective process which is widely used in the oil field and at refineries.

14. The electrical treatment of W/O emulsions relies on the coalescence of water droplets in the presence of an intense electric field. The water droplets polarise in the electric field and are attracted to one another in a process which is called dipole coalescence. Dipole coalescence is independent of field polarity and arises no matter whether the electric field is stable or oscillatory. However, ac fields are generally used, due to their convenient implementation, especially during the dehydration and desalting of crude. Another form of electrical coalescence, termed migratory coalescence, occurs in low–conductivity oils. It relies on the dispersed aqueous droplets being charged, leading to electrophoretic motion and collision. Migratory coalescence is important in the scrubbing of distillate fuels since dipole coalescence forces become very small as the mean droplet separation increases.

15. The use of heat is beneficial, in the separation of emulsions, since it reduces the viscosity and cohesion of the interfacial film, and the viscosity

of the oil. It also increases the solubility of the oil phase for stablizer and increases the rate of diffusion of stabilizer into the oil.

16. Chemical destabilizers are generally used in the electrical treatment of emulsions to improve the efficiency of the separation process. They displace stabilizing chemicals from the water/oil interface, reduce the thickness of the interfacial film and render it susceptible to rupture. The choice and amount of destabilizer to be used is decided empirically.

17. Modern desalting plants typically reduce the salt content of a crude by 95%. The sodium content is routinely reduced to the 3ppm level in a single stage, and below 1ppm during two stages of electrically-assisted separation. Typically 50 to 75% of sediment is also removed during the desalting process.

18. The costs of desalting are outweighed by the savings that can be made from increased oil throughput, reduced consumption of chemicals, and reductions in corrosion and labour costs.

19. The power consumption, for electrical treatment, varies typically between 0.2kWhr/1000bbl, for distillate fuel treatment, and 36kWhr/1000bbl, for desalting a heavy crude.

20. The cost of installing equipment for the electrical treatment of oil is affected by an economy of scale in that it increases as the cube root of the capacity of the treater. Thus the cost little more than doubles in going from a unit able to treat 20000bdp to one capable of treating 200000bpd.

21. The throughput rate of electric treaters generally ranges from about 20000 to 200000bpd.

22. The amount of water which can be removed from an oil depends on its electrical conductivity. Thus crude oil can be dehydrated down to a level of about 0.1% whereas, for distillates, the limit can be as low as 10ppm. This is because migratory coalescence can be taken advantage of in the case of low-conductivity distillates. In high-conductivity oils, migratory coalescence is ineffective since the required charge on the water droplets soon relaxes away in the continuous oil phase.

23. The electrical treatment of oils is very attractive since it is inexpensive, no moving parts are involved (unlike centrifuges) and operation periods measured in years can be obtained (with the occasional shutdown for removal of sediment and cleaning).

24. As the complexity of refinery operations increases, with the advent of new processes, so has their sensitivity to contaminants in the crude oil charge. When this is considered, in conjunction with the ever-increasing demands of user specifications, it can be appreciated that there is a requirement for increasing the efficiency of electric treaters.

Chapter 3

25. The kind of emulsion that results when water and oil are thoroughly mixed together depends on a number of factors including: the type of emulsifying agent present, the phase-volume ratio, the method of emulsification. The phase of greatest volume usually forms the continuous phase.

26. Emulsions generally have polydisperse size distributions. The diameters of dispersed phase droplets are typically in the range 0.1-10μm, though some droplets outside this range are likely to be present.

27. Interfacial tension is an important property of emulsions since it governs the ease with which new interface can be created.

28. The presence of small amounts of emulsifying agent in an emulsion can confer stability to it by drastically reducing the interfacial tension between the phases. That a small amount of emulsifying agent can have such a profound effect is related to the polar-non-polar architecture of the molecule; the polar end has an affinity for water whereas the non-polar end has an affinity for oil, which explains why it is positively adsorbed at an oil/water interface.

29. The phase in which the emulsifying agent is more soluble will generally be the continuous one; agents which are hydrophobic promote W/O emulsions whereas those which are hydrophilic promote O/W emulsions.

30. The presence of emulsifying agent often immobilizes the surface of a dispersed phase droplet. This means that its sedimentation velocity is

better described by Stokes' theory than that due to Rybczynski and Hadamard (which accounts for circulation of liquid within the droplet).

31. The terminal speed of a sedimenting particle is proportional to its diameter squared, acceleration due to gravity and density difference between the phases, and inversely proportional to the continuous phase viscosity.

32. Emulsions can be stabilized by the repulsion of dispersed phase droplets carrying charges of the same polarity. Such charge may arise due to chemical ionisation, ion adsorption or frictional contact.

33. Surface elasticity (Marangoni and Gibbs effects) causes a thinning liquid lamella (such as that between droplets prior to coalescence) to be approximately uniform in thickness; interfacial tension increases where the lamella thins down thus healing points of potential rupture.

34. The electric double layer can have a stabilizing effect in the case of O/W emulsions but this is not the case for W/O emulsions. This is believed to be related to the electric double layer thickness which is small (10^{-3} - $10^{-2}\mu$m) in the case of O/W emulsions but large (several μm) for W/O emulsions.

35. The dielectric constant and conductivity of an emulsion can depend on the dispered phase volume fraction, state of agglomeration of the dispersed phase droplets, and the frequency of electrical excitation. Many expressions have been proposed to account for these effects.

36. In an emulsion, the conductivity tends to increase and the dielectric constant tends to reduce as the applied frequency increases. This is known as dielectric dispersion which can be significant in O/W emulsions, where the oil phase is non-polar (e.g. nitrobenzene), and in W/O emulsions. Dielectric dispersion is caused by interfacial polarization.

37. The conductivity of a W/O emulsion is increased by charge carried by water droplets migrating between the electrodes, in the case of a dc applied field. The effect becomes important when the electric field strength is large.

38. Electrode polarization can lead to the measurement of high dielectric constant at low frequency (sometimes extending to 1MHz) and is caused by

the accumulation of ionic species near the electrodes. It increases as the continuous phase conductivity and applied electric field strength are increased, and is more noticeable in W/O than O/W emulsions (due to the nature of the continuous phase).

39. The dielectric properties of emulsions are also affected by the non-sphericity, orientation and size distribution of the dispersed phase droplets.

Chapter 4

40. The electric double layer, in emulsions, is of interest for two reasons. Firstly, a dispersed phase droplet may be acted upon by an electric field giving rise to an electrophoretic force (important in migratory coalescence). Secondly, emulsion stability (in the case of O/W emulsions) may be conferred by virtue of a repulsive force between the double layers of neighbouring dispersed phase droplets.

Chapter 5

41. Using the bispherical co-ordinate system, it is possible to solve Laplace's equation for two droplets, situated in a uniform applied electric field (if it is assumed that they do not distort from spherical form). The solution can be used to derive the force of interaction between the droplets. By considering the limit, as the droplets become far apart, it is possible to recover the conventional dipole interaction force. Alternatively, the limit as the droplets become very close may be considered; this yields a simple relationship which may be used in film drainage theory.

42. Before phase separation occurs, in the electrostatic resolution of a W/O emulsion, the dipole coalescence force is proportional to droplet radius squared (i.e. a^2). This is because the multiplier term $(a/\Lambda)^4$, in the force expression (where Λ is droplet separation), is initially constant being related to the volume fraction φ by the expression $\varphi = (4\pi/3)(a/\Lambda)^3$. Subsequently, however, the force falls off rapidly as $\varphi \rightarrow 0$.

43. If the line of centres of two polarised droplets, of large separation, is less than 54.7° from the direction of the applied electric field, the droplets will attract one another. Otherwise, there will be a force of repulsion between them. A torque is also established which tends to align the droplets with

the applied electric field. This causes droplets, which initially repel one another, to rotate into a position where a force of attraction exists between them. Such forces are important in the formation of pearl chains. As the separation of the droplets reduces, until they contact one another, the limiting angle, between zones of repulsion and attraction, increases from 54.7° to 75.1°.

44. If the applied electric field strength is sufficiently large, Brownian motion cannot prevent the formation of pearl chains in a W/O emulsion.

45. Electrophoretic forces arise as the result of an electric field acting on a charged object, and are polarity dependent. Dielectrophoretic forces, however, are due to the polarisation of neutral matter, in a non-uniform electric field, and are independent of field polarity. Dielectrophoretic forces are usually weak in comparison with electrophoretic ones, though at short range they can become enormous.

46. If the dispersed phase of an emulsion cannot be regarded as a perfect conductor, interfacial polarization arises, which can lead to changes in the dipole moment of a dispersed phase droplet. Forces which depend on the dipole moment, such as the interactive force between polarised droplets, may therefore be affected.

Chapter 6

47. The final stages in the coalescence of a pair of droplets, or of a droplet with the bulk phase at a plane interface, may be considered using film drainage theory. It is necessary to know the driving force which, for example, may be gravitational or electrostatic in nature. The geometry of the opposed liquid surfaces is of importance since this controls film drainage. Deformable droplets are likely to flatten off which leads to a reduced rate of drainage of the intervening film.

48. The film drainage equations may be used to calculate the rate of film thinning, for deformable and undeformable droplets, assuming an electrostatic driving force. These equations may be integrated to determine the time taken by the droplets in approaching one another. For undeformable droplets, the time reduces with droplet size whereas the reverse is true for deformable droplets. This suggests that small droplets coalesce readily but that once they become larger, a longer time elapses

before coalescence can occur. This is in agreement with the experimental findings that larger droplets are more stable than smaller ones.

49. The rest time of two droplets in close proximity, before they coalesce, is roughly Gaussian in nature. In water/oil systems, the mean rest time generally increases with the addition of surfactant, decrease in temperature and increase in droplet size; it decreases when electrolytes are added to the water phase.

Chapter 7

50. The phase-separation efficiency of an electro-coalescer increases, as the applied electric field strength is increased, until dispersion processes arise. As the applied electric field strength is further increased, a situation occurs where more droplets are dispersed by the field than are coalesced. Further increasing the electric field strength is counter productive.

51. Droplet dispersion occurs in an electro-coalescer when the cohesion due to interfacial tension is overcome by surface stresses instigated electrostatically. The applied electric field and the presence of charge on a droplet lead directly to electrostatic stresses at the surface of the droplet. Hydrodynamic stresses may arise indirectly due to droplets being driven electrophoretically or dielectrophoretically by the applied electric field. In general, electrostatic and hydrodynamic stresses will be present simultaneously which complicates the issue.

52. An uncharged droplet, which is not subject to hydrodynamic stresses, will disrupt when the electrostatic Weber number $W_e \geq 0.405$ (where $W_e = 2a\epsilon_c E_o^{\,2}/\gamma$).

53. When the electric field strength applied to a conducting droplet is sufficiently large a conical protrusion can develop at its end. The protrusion, known as a Taylor cone, tends to oscillate and issues a jet of charged droplets from its vertex. Under ideal conditions, the semi-angle of the cone is 49.3°.

54. Under certain conditions, the coalescence of droplets is inhibited by a mechanism called contact-separation charging. This is characterized by charge exchange between droplets which are on the point of coalescing; the charge exchange, believed to be due to an electrostatic discharge,

results in repulsion between the droplets which prevents their coalescence with one another. The critical electric field strength for the mechanism is given by the expression $E_o = 0.24\ (\gamma/a\epsilon_c)^{\frac{1}{2}}$ which is equivalent to the electrostatic Weber number $W_e \geq 0.115$.

55. Hydrodynamic dispersion may be considered in terms of various well-defined flow regimes (e.g. parallel flow, axisymmetric hyperbolic flow, Couette flow, plane hyperbolic flow, and turbulent flow). Hydrodynamic stresses can be gauged in terms of the generalised Weber group $W = \Psi d/\gamma$. When viscous forces dominate $\Psi = \eta_c S$, where S is the maximum velocity gradient in the external flow field. However, if dynamic pressure is dominant, the stress is given by $\Psi = \rho_c u^2$, where u is the continuous phase flow speed in relation to the droplet. For plane hyperbolic and Couette flows, where droplet deformation is controlled by viscous forces, the critical Weber number W_c is a function of the viscosity ratio η_d/η_c. For plane hyperbolic flow $W_c \simeq 0.2$ whereas for Couette flow $W_c \simeq 0.7$.

56. In turbulent flow, the viscous dissipation of energy occurs in small eddies of length scale $\delta \simeq 25\mu m$. For droplets of diameter $d_m \geq \delta$ it is necessary to consider the Weber number defined in terms of dynamic pressure. For droplets of diameter $d_m < \delta$, however, it is appropriate to use the viscous stress formulation. Hinze (1955), using Clay's (1940) experimental data and assuming isotropic homogeneous turbulence (where dynamic pressure dominates viscous stress), established a critical Weber number of $W_c \simeq 1.2$.

57. Hydrodynamic droplet disruption would appear to be more critical than electrostatic droplet disruption in a strong electric field.

Chapter 8

58. The energy required to create new interface vastly underestimates the energy of emulsification since it neglects the work done in setting up liquid motion.

59. Practical emulsions are generally made using mixers, colloid mills or homogenizers which give typical droplet sizes of $5\mu m$, $2\mu m$ and $1\mu m$ diameter respectively.

60. Emulsions may be prepared ultrasonically using the piezoelectric effect, magnetostriction, and the Pohlman whistle (which relies on the mechanical resonance of a blade). The underlying disruption mechanisms are believed to be cavitation and the Rayleigh–Taylor surface wave instability.

61. Emulsions may be prepared by a condensation process in which the dispersed phase vapour condenses in the continuous phase. This leads to low–concentration emulsions, though droplets as large as 20μm diameter can readily be produced.

62. Monodisperse emulsions can be produced by dispersing an aerosol of one phase in the other, continuous phase. The aerosols used for this purpose are mainly prepared by an electrostatic dispersal process or a condensation technique.

63. Emulsions can be prepared by the method of orifice mixing, in which the liquid destined to form the dispersed phase is introduced into the continuous phase through an orifice. The technique only becomes efficient when the critical flow velocity is reached.

64. Electrostatic emulsification is sometimes utilised in the desalting process to mix fresh water with oil containing brine droplets, prior to phase separation. The water must already be dispersed in the oil to a certain extent, so that the electric field can act on the droplets to disrupt them.

65. When an emulsion is being created two opposing effects arise, namely disruption and coalescence of the dispersed phase droplets. Initially, relatively few droplets are present and disruption is the dominant process. With the passage of time, however, the droplets become smaller and less susceptible to breakup, and their probability of collision increases. Equilibrium results when disruption and recombination processes balance. The time required for emulsification is generally accepted as being from 1–5 minutes.

66. The mean droplet size of an emulsion decreases as the interfacial tension is reduced and the level of agitation increased.

67. Increasing temperature usually helps emulsification since viscosity and interfacial tension are lowered. However, in the case of ultrasonic emulsification the converse may be true since a rise in temperature

militates against cavitation.

68. Four emulsification techniques were tried during the experimentation, namely: centrifugal mixing; condensation; and two ultrasonic methods, one of which relied on magnetostriction, the other on the piezoelectric effect. The method which was found to be most convenient was ultrasonic emulsification by magnetostriction. Relatively stable W/O emulsions, of known concentration, could be produced in a matter of minutes. Unfortunately the reproducibility of the technique was not always reliable (according to turbidity measurement).

Chapter 9

69. Coalescence, in its broadest sense, can be described by the following five stages: (i) Long-range flocculation, (ii) short-range flocculation (film thinning), (iii) collision, (iv) film rupture, (v) unification of droplets.

70. Coalescence is the converse of dispersion; all of the forces which produce emulsification (e.g. electrostatic, hydrodynamic, mechanical, acoustic) can also give rise to coalescence, if the intensity of the mechanism is reduced. Coalescence can also result from sedimentation and Brownian motion.

71. Dipole coalescence forces are weak except at small separations and so, in low-concentration W/O emulsions, independent processes must be relied upon to bring the droplets into close proximity (such as Brownian motion and sedimentation).

72. In migratory coalescence, for which the droplets must be charged and which relies on electrophoresis, the continous phase must be of low conductivity so that it does not conduct free charge away from the dispersed droplets at too high a rate. It should be noted that dipole coalescence always augments migratory coalescence, though the converse is not necessarily true (e.g. in high-conductivity oils or ac applied electric fields).

73. Owe Berg et al. (1963) considered coalescence to be due to the formation of intermolecular bonds between droplets, and suggested two mechanisms by which bonds may be switched from within the droplets to across their interface. One mechanism, which is favoured by energy supply (such as an electrical discharge), requires bonds to be broken and new ones formed.

In the other mechanism bonds are not broken but, rather, are gradually re–arranged.

74. The integral characteristics of an emulsion (mean size, variance, symmetry coefficient), as a function of time, may be investigated without the need to solve the coagulation kinetics of the droplet size distribution function (Volkov and Krylov, 1972a,b).

75. Sadek and Hendricks (1974), investigated the coalescence of dispersed water droplets, in low–conductivity oil, to which a dc electric field was applied. They concluded that the droplet size distribution was of the self–preserving type in that it was of fixed form when plotted as a function of normalised radius a/a_m (where a_m is the mean droplet radius as a function of time).

76. When a droplet of liquid coalesces with the bulk liquid, at a plane interface, under the influence of gravity, it is possible for the process to be incomplete. That is, a smaller secondary droplet may be produced, in a process called partial coalescence. The secondary droplet may also be subject to this phenomenon and as many as eight stages have been observed in some binary systems (Charles and Mason, 1960b). However, in the case of electrical coalescence, in strong electrostatic fields, coalescence is expected to be single staged.

77. The dispersed phase droplets in a W/O emulsion may acquire charge in a number of ways: by contacting a charged electrode, chemical ionisation, preferential adsorption, frictional contact, contact–separation charging, and droplet disruption.

78. Migratory coalescence is the name given to the coalescence of dispersed phase droplets, in a W/O emulsion, as a result of electrophoretic forces arising from an applied electric field. The droplets must possess charge which may be free, or bound as in the case of the electric double layer. For migratory coalescence to be effective, the conductivity of the continuous phase must generally be low to prevent free charge relaxing away from the droplets too quickly. Bound charge will not, of course, be able to relax away at all, no matter what the conductivity of the continuous phase is. A further requirement is that the applied electric field should be unidirectional or of very low frequency ac.

79. The velocity acquired by a water droplet in oil, after contacting a charged electrode, increases as the salinity of the droplet increases. Further, it is approximately proportional to the droplet radius and the square of the applied electric field strength (Panchenkov et al., 1970).

80. Dipole coalescence is the name given to the coalescence of dispersed phase droplets, in a W/O emulsion, as a result of the droplets being polarised in an external applied electric field. The resulting force of interaction is attractive, and independent of field polarity since it is dielectrophoretic in nature.

81. There would appear to be two basic ways of modelling coalescence in emulsions. The first is statistical in nature and considers the emulsion macroscopically. The emulsion is specified by a droplet size distribution, and coagulation kinetics equations are solved in order to describe how it changes as a function of time. The second approach is mechanistic in nature and considers the emulsion microscopically, that is in terms of a single pair of droplets.

82. Before phase separation, the increase in size of a water droplet, in a W/O emulsion subjected to an electric field, increases exponentially with time and the square of the applied electric field strength.

83. Using turbidimetric techniques, it is possible to monitor the water content of a W/O emulsion, and hence to establish its resolution time. Although simplifying assumptions must be made, with regard to droplet size distribution and spatial arrangement, it is possible to predict the manner in which emulsion resolution time decreases, with increasing electric field strength, in an experimental system. The theory can be extended to account for the steady upward flow of emulsion in an electro-coalescer, rather than the stationary situation considered above.

84. The water content of relatively low concentration W/O emulsions ($\varphi < 0.1\%$) may be monitored using a nephelometer to measure turbidity. The turbidity is found to be roughly proportional to the volume fraction φ of dispersed water. The nephelometer is capable of measuring down to 1NTU which is approximately equivalent to 1ppm by volume of water. One proviso is that the continuous oil phase should be transparent, which rules out the technique so far as fuel oils and crudes are concerned.

85. Nephelometric experiments, performed on 750ppm W/O emulsions, showed that phase separation was more efficient for dc than ac applied electric fields. For example, an excitation of 150V dc gave a faster phase separation than 500V RMS ac, when applied between the electrodes (which is probably a reflection of how small dipole coalescence forces are in low-concentration W/O emulsions). The same findings were obtained for emulsions in which the oil had been doped with ASA-3 to increase its conductivity. Initialy this seems somewhat surprising since migratory coalescence is generally regarded as being ineffective in the case of emulsions having high-conductivity continuous oil phases. However, when it is remembered that the water concentration is low, which gives rise to small dipole coalescence forces (the mean droplet separation being large), and that there is probably migratory coalescence due to double layer charge (which cannot relax away from droplets in the high-conductivity, continuous oil phase), the result does not seem unreasonable.

86. Some experiments were performed in a closed-loop emulsification system in which a centrifugal pump was used to create a W/O emulsion and an electro-coalescer to resolve it. The electrodes were insulated from the emulsion using perspex and it was found necessary to use a time-varying excitation in order to induce effective coalescence of water droplets in the emulsion. If the emulsion flow was stopped, it was possible to obtain substantial phase separation in a matter of seconds. If the flow was slowed down sufficiently, it was possible to obtain effective phase separation within the body-length of the electro-coalescer.

87. The size distribution of dispersed water droplets in a W/O emulsion, subjected to a dc electric field, and how it changes in time can be determined using a laser light scattering technique. The coalescence effects of Brownian motion and sedimentation are found to be small in comparison with the coalescence caused by strong electric fields (dipole and migratory coalescence). Ultrasonically-prepared W/O emulsions (of distilled water in silicone oil) are found to have bimodal size distributions initially. With the passage of time, and the application of an electric field, the size distributions become unimodal. The volume median diameter is found to increase with time and the fractional obscuration (like turbidity) to reduce.

88. When an electric field is applied to certain types of suspension (including W/O emulsions), the formation of particle chains can occur which align themselves with the local electric lines of force.

89. Pearce (1954) found that conducting particles formed chains whereas insulating ones did not, and concluded that it was the conductivity of the particle and not just its permittivity which was of importance.

90. Brownian motion cannot prevent the formation of pearl chains, in W/O emulsions, if the electric field strength is sufficiently large.

91. Hydrodynamic disturbance, such as fast speed of flow, tends to inhibit the formation of pearl chains in W/O emulsions. In the absence of such disturbance, pearl chains can bridge the gap between uninsulated electrodes and short circuit the power supply.

92. The forces concerned with pearl-chain formation are dielectrophoretic in nature and arise due to droplet polarisation in the applied electric field. For large separations of the particles, the radial and transverse components of the interactive force are proportional to the volumes of the particles, the square of the applied electric field strength, and inversely to the fourth power of the separation. They also depend on the angle θ which the line of centres makes with the applied electric field. For $\theta < 54.7^\circ$ or $125.3^\circ < \theta < 180^\circ$, the radial force is attractive, otherwise it is repulsive. The transverse force generates torque which tends to align the line of centres with the field direction. Even if the particles are oriented such that the radial force is repulsive, the transverse force eventually alters their orientation until it is attractive. Thus pairs of particles attract one another and align themselves with the electric field. At small separations, the dipole approximation becomes invalid and other force expressions pertain. The angle defining the zones of attraction and repulsion increases, and when the particles contact one another the radial force is attractive for $\theta < 75.1^\circ$ or $104.9^\circ < \theta < 180^\circ$ and repulsive otherwise. It is not difficult to imagine how further particles are attracted to form a chain aligned with the applied electric field.

93. The formation of pearl chains is more complicated than that of particle chains, in that droplet stability must be considered. Thus, droplets either

coalesce or just flocculate. The coalescence of emulsion droplets, at a rate which reduces to zero as the droplets approach a limiting size and approximately uniform size distribution, has been termed limited coalescence (Wiley, 1954). The phenomenon is believed to be associated with the presence of surface active agents.

94. By using a small electrode system, it is possible to observe chain formation in suspensions, microscopically, at a relatively low potential difference; levels between 100 and 300V were found suitable for an electrode separation of 5mm.

95. Tiny water droplets, in a W/O emulsion, appear to coalesce readily in an applied electric field. However, as the size of dispersed phase droplets increases, the droplets become more stable and start to form pearl chains which align themselves with the applied field. Droplets of larger diameter (typically 15–45μm) do not readily coalesce with one another even though they appear to be in contact. This may be attributed to limited coalescence.

96. Pearl chains and sometimes trees form in the inter–electrode space and at the negative electrode. Very few, sometimes none at all, are found at the positive electrode, which suggests that the droplets possess a net positive charge. If the electric field strength is sufficiently large, pearl chains are forced off the electrodes.

97. The behaviour of pearl chains in a W/O emulsion, subjected to an applied electric field, is complex. Sometimes a free pearl chain joins another attached to an electrode, so elongating it. A pearl chain can also bounce off an electrode or a droplet or pearl chain attached to the electrode. It is possible for a droplet or pearl chain to oscillate between a pearl chain attached to an electrode and another in the inter–electrode space, which sometimes leads to coalescence of some of the droplets. On occasion, multiple pearl chains can link up and bridge the gap between the electrodes. Such droplet bridges are relatively stable and may attract free pearl chains laterally.

98. The insulation of electrodes from one another can be advantageous in the electrical separation of W/O emulsions of high water content. In the absence of such insulation, pearl chains can form low-impedance droplet bridges between the electrodes which may short-circuit the power supply. The probability of this happening increases as the electrode separation and emulsion flow speed reduce. The use of current limiters, to overcome this problem in uninsulated systems, reduces separation efficiency since the electric field strength must be reduced and time wasted in waiting for droplet bridges to disperse.

99. The use of electrode insulation is a practised separation technique, according to the patent literature, as is the almost-equivalent process of energizing electrodes via a capacitor.

100. If the electrodes of an electro-coalescer are insulated from one another, it is necessary for a time-varying voltage to be applied between them, otherwise a strong electric field cannot be established across the emulsion (due to the build-up of free charge at insulator/emulsion interfaces caused by interfacial polarisation).

101. The use of an applied voltage waveform of zero mean value is recommended, since otherwise the presence of free charge at the interface (of non-zero mean value) would act to reduce the electric field strength within the W/O emulsion.

102. The simplest time-varying excitation, which can be applied to a pair of electrodes, is one of periodic nature; especially a sinusoid since then only a transformer is necessary to obtain a suitable voltage level from the local supply.

103. There are three ways of increasing the electric field in an emulsion, which is generated by the application of a voltage via insulated electrodes: (i) by increasing the frequency of the applied waveform, (ii) by increasing the conductivity of the insulating dielectric (within reason), (iii) by reducing the width of the insulating dielectric (as constrained by electrical breakdown conditions). All of these measures increase the current drawn by the electro-coalescer and require that the supply be sufficiently powerful.

104. The voltage waveform appearing across a W/O emulsion differs from that applied between the electrodes, if they are insulated from the emulsion, the transfer function being frequency dependent. The amplitude of the voltage dropped across an emulsion increases with frequency, so long as the power supply can provide the necessary current.

105. The upper frequency limit, for electro-coalescer operation, is determined by the power supply and its load. In practice it is difficult to obtain high voltage at high frequency since this requires the generation of large currents and hence power. Thus the output voltage of a power supply will reduce as the frequency of operation increases.

106. When modelling the effect of applying a periodic voltage waveform to an emulsion, via insulated electrodes, it is necessary to consider the effects of interfacial polarisation at the water/oil interface of the emulsion, and at the emulsion/insulator interface of the electro-coalescer. For W/O emulsions, the effective dielectric constant and conductivity may be taken as the low-frequency limits (K_ℓ and σ_ℓ respectively) since the characteristic frequency, associated with the water/oil interface, is usually much greater than the excitation frequency of the supply. Thus the emulsion may be specified by dielectric constant $K_2 = K_\ell$ and conductivity $\sigma_2 = \sigma_\ell$, where K_ℓ and σ_ℓ are both functions of the conductivities and dielectric constants of the emulsion phases (σ_c, σ_d, K_c and K_d); the insulator is simply specified by its dielectric constant K_1 and conductivity σ_1. The capacitances and conductances (C_1, C_2, G_1 and G_2) of the insulator/emulsion system may then be determined from its geometry. The system capacitance C_L, at any power supply excitation frequency ω, may then be determined from C_1, C_2, G_1, G_2 and ω. This may be used to determine the system operating frequency $\omega_o = 1/(R_\ell C_L)$ where R_ℓ is the current-limiting resistance of the power supply. In order to obtain a large potential difference across the emulsion, in relation to that applied between the electrodes, it is necessary for the excitation frequency to be greater than the system operating frequency ($\omega > \omega_o$).

107. For W/O emulsions, in which there is little probability of droplet bridges short-circuiting the power supply (i.e. those having a low water content), it is preferable not to use insulated electrodes since, otherwise, some of the applied voltage is bound to be dropped across the insulation (which reduces the electric field within the emulsion). The use of a dc electric field is then possible which is known to provide better separation efficiency

than an ac field, in the case of low-conductivity emulsions.

108. The mean square electric field strength is of primary importance in determining coalescence effectiveness, in an electro-coalescer, according to the consensus of scientific opinion.

109. The instability (change of interfacial area and associated effect on interfacial tension) induced at the surface of a droplet during rapid changes in the applied electric field (due, for example, to the application of a pulsed waveform) may promote dispersed phase droplet coalescence.

110. The cheapest and most convenient way of powering the electrodes in an electro-coalescer is to use a high-voltage transformer, preferably at the frequency of the local mains supply. Extra equipment is necessary if it is required to use a dc or pulsed electric field, which increases the complexity and cost of the power supply.

Miscellaneous

111. In order to obtain optimum phase separation in an electro-coalescer, its electrodes and their energization should be tailored to the dispersed phase droplet size distribution, which may vary in time and from one place to another during operation. This may necessitate the use of multiple electrodes, so that electric fields of the appropriate strength can be generated in the various regions of the electro-coalescer. Thus, in slowly-flowing systems, where the larger droplets settle out and the smaller ones rise in the upwardly-flowing emulsion, it would be appropriate to use a strong electric field in the upper regions and a weaker field in the lower regions. The electric field strength, in each case, should not be so large that it leads to droplet dispersion. In batch systems, where the emulsion does not flow, it may be appropriate to reduce the field strength temporally, as the droplet size increases due to coalescence. It may be necessary to account for sedimentation during batch processing, since there is the tendency for larger droplets to fall to the lower regions.

FUTURE DEVELOPMENTS

Over the years, the techniques of electrical separation have improved and are now very efficient. Nevertheless, there is still a requirement to improve the efficiency of electro-coalescers, for the following reasons:

(i) Secondary recovery techniques will be used more commonly in future, as oil supplies dwindle, and so it is likely that the produced oil will be more heavily contaminated than was previously the case.

(ii) User fuel specifications are likely to be more stringent in future as efforts are made to save time and money in relation to the problems associated with corrosion (especially in the case of gas turbines), scaling, coking, plugging and the like.

(iii) The complexity of refinery operations is likely to increase, with the introduction of new processes, as is their sensitivity to contaminants in the crude oil charge.

(iv) Benefits may be obtained in terms of increasing oil throughput or saving space (particularly important in the case of ships and off-shore applications).

It is feasible to improve the efficiency of electro-coalescers by considering, carefully, the design of electrodes and their energization, as well as other factors such as the addition of chemical demulsifiers, operating temperature and emulsion flow rate.

The use of feedback control, which does not seem to have attracted much attention in the literature, would improve the efficiency of electro-coalescers by allowing them to respond, automatically, to changing conditions, such as variation in water content or droplet size distribution. This, perhaps, could be achieved by monitoring the water content of the treated oil, using a capacitance probe†, conductivity probe, or light-scattering technique (in the case of transparent oils). The derived signal could be used to control electrode energisation (e.g. voltage levels). It should then be possible to work at the greatest electric field strength consistent with not adversely dispersing water droplets. This would maximise the coalescence of dispersed phase water droplets and phase separation in a W/O emulsion.

---

† Commercial capacitance probes, for use as BS & W monitors, include the following CE (Combustion Engineering) Invalco models: 400, 2000, 1728 and 1864; it is claimed that water concentrations in the range of 0.1-100% can be measured.

REFERENCES

Albers W and Overbeek J T G, 1959, J. Colliod Sci., Vol. 14, 501, 510.

Alexander A E, 1941, Nature, Vol. 148, 752.

Alexander A E and Johnson P, 1949, Colloid Sci., Oxford University Press, London.

Allan R S and Mason S G, 1961, Effects of Electric Fields on Coalescence in Liquid + Liquid Systems, Trans. Faraday Soc., Vol. 57, 2027–2040.

Allan R S and Mason S G, 1962, Coalescence of Liquid Drops in Electric and Shear Fields, J. Colloid Sci., Vol. 17, 383–408.

Anisimov B F and Emel'yanchenko V G, 1976, Coalescence Criterion of Reversed Emulsion Drops in Uniform Electric Field, Kollodnyi Zhurn., Vol. 39, 528–534.

Bailes P J and Larkai S K L, 1981, An Experimental Investigation into the Use of High Voltage DC Fields for Liquid Phase Separation, Trans. I. Chem. E., Vol. 59, 229–237.

Bailes P J and Larkai S K L, 1982, Liquid Phase Separation in Pulsed DC Fields, Trans. I. Chem. E., Vol. 60, 115–121.

Bailes P J and Larkai S K L, 1984, Influence of the Phase Ratio on Electrostatic Coalescence of Water–in–Oil Dispersions, Chem. Eng. Res. Des., Vol. 62, 33–38.

Bancroft W D, 1926, Applied Colloid Chemistry, 2nd edn., McGraw–Hill Book Co., New York.

Bartok W and Mason S G, 1959, J. Colloid Sci., Vol. 14, 13.

Batchelor G K, 1951, Proc. Cambridge Phil. Soc., Vol. 47, 359.

Batchelor G K, 1970, An Introduction to Fluid Dynamics, Cambridge University Press.

Becher P, 1977, Emulsions: Theory and Practice, 2nd edn., Krieger, New York.

Benguigui L and Lin I J, 1981, More About the Dielectrophoretic Force, J. Appl. Phys., Vol. 53, 2, 1141–1143.

Bhatnagar S S, 1920, J. Chem. Soc., Vol. 117, 542.

Böttcher C J F, 1952, Theory of Electric Polarization, Elsevier Publishing Co., New York.

de Brey J H C, 1926, patent US 1570209.

Briggs T L, 1914, J. Phys. Chem., Vol. 18, 34.

Briggs T R, 1920, J. Phys. Chem., Vol. 24, 120–126.

Brown A H and Hanson C, 1965, Effect of Oscillating Electric Fields on Coalescence in Liquid + Liquid Systems, Trans. Faraday Soc., Vol. 61, 1754–1760.

Bruggeman D A G, 1935, Annln. Phys., Vol. 24, 636.

Buchholz H, 1957, Elektrische und Magnetische Potentialfelder, Springer–Verlag, Berlin.

Chapman D, 1913, Phil. Mag., Vol. 25, 475.

Chappelear D C, 1961, J. Colloid Sci., Vol. 16, 186.

Charles G E and Mason S G, 1960a, The Coalescence of Liquid Drops with Flat Liquid/Liquid Interfaces, J. Colloid Sci., Vol. 15, 236–267.

Charles G E and Mason S G, 1960b, The Mechanism of Partial Coalescence of Liquid Drops at Liquid/Liquid Interfaces, J. Colliod Sci., Vol. 15, 105–122.

Cheesman D F and King A, 1940, Trans. Faraday Soc., Vol. 36, 1241.

Cho A Y H, 1964, Contact Charging of Micron–Sized Particles in Intense Electric Fields, J. Appl. Phys., Vol. 35, 9, 2561–2564.

Clay P H, 1940, Proc. Roy. Acad. Sci. (Amsterdam), Vol. 43, 852, 979.

Clayton W, 1943, The Theory of Emulsions and Their Technical Treatment, 4th edn., Churchill Ltd., London.

Clift R, Grace J R and Weber M E, 1978, Bubbles, Drops and Particles, Academic Press.

Cobb R M K, 1946, Emulsion Technology, Chemical Publishing Co., Brooklyn, 7–32.

Cockbain E G and McRoberts T S, 1953, J. Colloid Sci., Vol. 8, 440.

Coehn A, 1898, Ann. Physik, Vol. 66, 217.

Conway B E and Dobry–Duclaux A, 1960, Rheology, Theory and Applications, ed. Eirich F, Vol. 3, New York and London.

Davies J T, 1961, J. Soc. Cosmetic Chemists, Vol. 12, 193.

Davis, Jones and Neilson, 1938, Oil and Gas Journal, Vol. 37, 2, 62.

Davis M H, 1961, The Forces Between Conducting Spheres in a Uniform Electric Field, The RAND Corporation, Paper RM–2607.

Debye P and Prins W, 1958, J. Colloid Sci., Vol. 13, 86.

Denegri G B, Liberti G, Molinari G and Viviani A, 1977, Field–Enhanced Motion of Impurity Particles in Fluid Dielectrics Under Linear Conditions, IEEE Trans. Elect. Insul., Vol. EI–12, 2, 114–125.

Derjaguin B V and Kussakov M, 1939, Acta Physicochim, URSS, Vol. 10, 25.

Dupré A, 1869, Théorie Méchanique de la Chaleur, Gauthier–Villars, Paris.

Dvoretskaya R M, 1949, Kolloidn. Zhur., Vol. 11, 311.

Einstein A, 1906, Ann. Physik, Vol. 19, 4, 289.

Elton G A H and Picknett R G, 1957, Proc. Intern. Congr. Surface Activity, 2nd, London, Vol. 1, 288–294.

Eötvös R, 1886, Ann. Physik, Vol. 27, 448.

Ewers W E and Sutherland K L, 1952, Aust. J. Scient. Res., Vol. 45, 697.

Exner S, 1900, Ann. Physik, Vol. 2, 843.

Feat G R and Levine S, 1976, The Double-Layer Interaction of Two Charged Colliodal Spherical Particles of a Concentrated Dispersion in a Medium of Low Dielectric Constant, J. Colloid and Interface Sci., Vol. 54, 1, 34-44.

Ferguson, 1915, Science Progress, Vol. 9, 445.

Findeisen W, 1932, Gerland Beitr., Vol. 35, 295.

Fisher L E, Hall G C and Stenzel R W, 1962, Crude Oil Desalting, Materials Protection, Vol. 1, 5, 8-11, 14-17.

Fowkes F M, 1962, J. Phys. Chem., Vol. 66, 382.

Fradkina E M, 1950, Zhur. Eksptl. Teoret. Fiz., Vol. 20, 1011.

Frankel S P and Mysels K J, 1962, J. Phys. Chem., Vol. 66, 190.

Frenkel Y I, 1948, Kolloid. Zhur., Vol. 10, 148.

Fricke H and Curtis H J, 1937, J. Phys. Chem., Vol. 41, 729.

Friedlander S K and Wang C S, 1966, The Self-Preserving Size Distribution for Coagulation by Brownian Motion, J. Colloid and Interface Sci., Vol. 22, 126-132.

Frumpkin A N and Levich V G, 1947, Zhur. Fiz. Khim., Vol. 21, 1183.

Fuchs N A, 1964, The Mechanics of Aerosols, Pergamon Press, London.

Galvin C P, 1984, Design Principles for Electrical Coalescers, Extraction '84, I. Chem. E. Symposium Series No. 88.

General Electric publication, c. 1973.

Gibbs J W, 1876, Trans. Conn. Acad. Sci., Vol. 3, 391.

Gillespie T and Rideal E K, 1956, Trans. Faraday Soc., Vol. 53, 173.

Girifalco L A and Good R J, 1957, J. Phys., Chem., Vol. 61, 904.

Gopal E S R, 1963, Rheology of Emulsions, ed. Sherman P, Pergamon Press, Oxford, 15–26.

Gouy G, 1910, J. Phys. Radium, Vol. 9, 457.

Greenlee R W and Lucas R N, 1972, Electrical Purification of Gas Turbine Fuels, Presented at Symposium: Gas Turbine Fuel Handling and Quality Control, ASTM 75th Annual Meeting and Exposition, Los Angeles, 3–23.

Griffin W C, 1949, J. Soc., Cosmetic Chemists, Vol. 1, 311.

Guillien R, 1941, Ann. Phys., Vol. 16, 205.

Hadamard J, 1911, Compt Rend., Vol. 154, 1735.

Hanai T, 1960, Kolloidzeitschrift, Vol. 171, 23.

Hanai T, 1961, Kolloidzeitschrift, Vol. 177, 57.

Hanai T, Koizumi N and Gotoh R, 1962, Kolloidzeitschrift, Vol. 184, 143.

Hanai T, Koizumi N, Sugano T and Gotoh R, 1960, Kolloidzeitschrift, Vol. 171, 20.

Hatschek E, 1911, Kolloidzeitschrift, Vol. 8, 34.

Hinze J O, 1955, Fundamentals of the Hydrodynamic Mechanism of Splitting in Dispersion Processes, A. I. Ch. E. Journal, Vol. 1, 3, 289–295.

Hollmann H E, 1950, J. Applied Phys., Vol. 21, 402.

Janovsky W and Pohlman R, 1948, Z. Angew. Phys., Vol. 1, 222–228.

Jones T B, 1979, Dielectric Measurements on Packed Beds, Report No. 79CRD131, Corporate Research and Development, Schenectady, New York.

Jones T B and Kallio G A, 1979, J. Electrostatics, Vol. 6, 207.

Joos F M and Snaddon R W L, 1985, On the Frequency Dependence of Electrically Enhanced Emulsion Separation, Chem. Eng. Res. Des., Vol. 63, 305–311.

Joos F M, Snaddon R W L and Johnson N A, 1984, Electrostatic Droplet Growth in a Neutrally Buoyant Emulsion, IEEE–IAS–84 Annual Meeting, Chicago, Conf. Rec. IAS, No. 14.

Klinkenberg A and van der Minne J L, 1958, Electrostatics in the Petroleum Industry, Elsevier.

Kolmogoroff A N, 1949, Dokl. Akad. Nauk SSSR, Vol. 66, 825–828.

Krasny–Ergen W, 1936, Zwei Leitende, Isolierte Kugeln im Homogenen Elektrischen Feld, Ann. Phys., Vol. 27, 459–471.

Krishnan R S, Venkatasubramanian V S and Raja Gopal E S, 1959, Brit. J. Appl. Phys., Vol. 10, 250.

Kubo M and Nakamura S, 1953, Bull. Chem. Soc. Japan, Vol. 26, 318.

Kuczynski T, 1929, Przem. Chem., Vol. 13, 161–167.

Landau L D and Lifshitz E M, 1960, Electrodynamics of Continuous Media, Art. 9, Pergamon, Oxford.

Langmuir I, 1948, J. Meteor., Vol. 5, 175.

Lebedev N N and Skal'skaya I P, 1962, Sov. Phys.–Tech. Phys., Vol. 2, 268–270.

Lewis W C M, 1934, Trans. Faraday Soc., Vol. 30, 958.

Lichtenecker K, 1926, Phys. Z., Vol. 27, 115.

Lorentz H A, 1880, Wied. Ann., Vol. 11, 70.

Lorenz L, 1880, Wied. Ann., Vol. 9, 641.

Macky W A, 1931, Some Investigations on the Deformation and Breaking of Water Drops in Strong Electric Fields, Proc. Roy. Soc., Vol. A133, 565.

Maxwell J C, 1881, A Treatise on Electricity and Magnetism, 2nd edn., Clarendon Press, Oxford.

Maxwell J C, 1892, Electricity and Magnetism, Vol. 1, Clarendon Press, Oxford.

McBain J W, 1944, Colloid Chemistry, ed. Alexander J, Vol. 5, 102–103, Reinhold Publishing Corp., New York.

McBain J W, Ford T F and Wilson D A, 1937, Kolloid-Z., Vol. 78, 1.

McBain J W and Woo T, 1937, Proc. Roy. Soc., Vol. A163, 182–188.

McKibben, 1919, Patent US 1299589.

Meredith R E and Tobias C W, 1960a, J. Appl. Phys., Vol. 31, 1270.

Meredith R E and Tobias C W, 1960b, J. Electrochem. Soc., Vol. 108, 286.

Molinari G and Viviani A, 1978, Analytical Evaluation of the Electro–Dielectrophoretic Forces Acting on Spherical Impurity Particles in Dielectric Fluids, J. Electrostatics, Vol. 5, 343–354.

Monk G W, 1952, J. Appl. Phys., Vol. 23, 288.

Morse P M and Feshbach H, 1953, Methods of Theoretical Physics, Vol. 2, McGraw–Hill Book Co., Inc., New York.

Muth E, 1927, Kolloid-Zeitschrift, Vol. 41, 97–102.

Nawab M A and Mason S G, 1958a, J. Colloid Sci., Vol. 13, 179–187.

Nawab M A and Mason S G, 1958b, Trans. Faraday Soc., Vol. 54, 1712.

Neduzhii S A, 1965, Nature of the Disturbances Giving Rise to Formation of the Disperse Phase of an Emulsion in an Acoustic Field, Soviet Phys. Acoustics, Vol. 10, 4, 390–397.

Newmann F, 1914, J. Phys. Chem., Vol. 18, 34.

Nolan J J, 1926, Proc. Roy. Irish Acad., Vol. 37, 28.

Ohnesorge W, 1936, Z. Angew. Math. u. Mech., Vol. 16, 355.

Oliver D R and Ward S G, 1953, Nature, Vol. 171, 396.

Ostwald W, 1910, Kolloid-Z., Vol. 6, 103.

Owe Berg T G, Fernish G C and Gaukler T A, 1963, The Mechanism of Coalescence of Liquid Drops, J. Atmospheric Sci., Vol. 20, 153–158.

Panchenkov G M and Tsabek L K, 1968a, Strength of Electric Field Between Two Spherical Droplets of an Emulsion in a Quasi-Constant External Homogeneous Electric Field, Russian J. of Phys. Chem., Vol. 42, 5, 649–651.

Panchenkov G M and Tsabek L K, 1968b, Critical Strength of Quasi-Constant External Homogeneous Electric Field for Disruption of an Emulsion Droplet, Russian J. of Phys. Chem., Vol. 42, 5, 651–652.

Panchenkov G M, Vinogradov V M and Papko V V, 1970, The Motion of Charged Water Drops in a Uniform Constant Electric Field, Chem. and Tech. of Fuels and Oils, Vol. 15, 2, 120–122.

Panofsky W K H and Phillips M, 1978, Classical Electricity and Magnetism, 2nd edn., Addison-Wesley Publishing Co.

Parts A, 1945, Nature, Lond., Vol. 155, 236.

Pearce C A R, 1954, The Mechanism of the Resolution of Water-in-Oil Emulsions by Electrical Treatment, Brit. J. Appl. Phys., Vol. 5, 136–143.

Pearce C A R, 1955, Brit. J. Appl. Phys., Vol. 6, 113.

Pohl H A, 1978, Dielectrophoresis, Cambridge University Press, London, New York and Melbourne.

Princen H M, 1963, J. Colloid Sci., Vol. 18, 178.

Putilova I N, Gindin L G and Moros L M, 1950, Dokl. Akad. Nauk SSSR, Vol. 74, 81.

Raja Gopal E S, 1959, Kolloidzeitschrift, Vol. 167, 17–23.

Raja Gopal E S, 1960, Z. Phys. Chem., Vol. 23, 342.

Ramsay R and Shields J, 1893, Trans. Roy. Soc. (London), Vol. A184, 647.

Lord Rayleigh, 1879, Proc. Lond. Math. Soc., Vol. 10, 4.

Lord Rayleigh, 1882, On the Equilibrium of Liquid Conducting Masses Charged with Electricity, Phil. Mag. Series 5, Vol. 14, 184–186.

Lord Rayleigh, 1892, Phil. Mag., Vol. 34, 481.

Richardson E G, 1950, J. Colloid Sci., Vol. 5, 404.

Robertson T B, 1910, Kolloid–Z., Vol. 7, 7.

Rodger W A, Trice V G and Rushton J H, 1956, Chem. Eng. Prog., Vol. 52, 515–520.

Rosenkilde C E, 1969, Proc. Roy. Soc., Vol. A312, 473.

Roth W, 1956, J. Soc. Cosmetic Chemists, Vol. 7, 565.

de la Rue R E and Tobias C W, 1959, J. Electrochem Soc., Vol. 106, 827.

Runge I, 1925, Z. Tech. Phys., Vol. 6, 61.

Rybczynski W, 1911, Bull. Acad. Sci. Cracovie, 40.

Sadek S E and Hendricks C D, 1974, Electrical Coalescence of Water Droplets in Low–Conductivity Oils, Ind. Eng. Chem. Fundam., Vol. 13, 2, 139–142.

Saito M and Schwan H P, 1961, The Time Constants of Pearl–Chain Formation, Proc. 4th Tri–Service Conf. on the Biological Effects of Microwave Radiation, Vol. 1, ed. Peyton M F, Plenum Press, New York.

Sartor D, 1954, A Laboratory Investigation of Collison Efficiencies, Coalescence and Electrical Charging of Simulated Cloud Droplets, J. Meteorology, Vol. 11, 91–103.

Schmidt K, 1976, Patent DD 95899.

Shaw D J, 1980, Introduction to Colloid and Surface Chemistry, 3rd edn., Butterworths, London.

Sherman P, 1955, Research (London), Vol. 8, 396.

Sherman P, 1968, Emulsion Science, Academic Press, London and New York.

Shinnar R, 1961, J. Fluid Mech., Vol. 10, 259–275.

Shvetsov Y U N, Yunusov A A and Mukhametzy A K, 1984, Patent SU 119255.

Signer R and Berneis K, 1957, Z. Naturforsch, Vol. 12b, 261.

Sirotyuk M G, 1963, Soviet Phys. Acoust., Vol. 8, 201–213.

von Smoluchowski M, 1916, Phys. Z., Vol. 17, 557, 585.

Smythe W R, 1968, Static and Dynamic Electricity, 3rd edn., McGraw–Hill Book Co., Inc., New York.

Speed B, 1919, An Appreciation of Dr Cottrell, J. of Ind. and Eng. Chem., Vol. 11, 153–154.

Stern O, 1924, Z. Electrochem., Vol. 30, 508.

Stokes G G, 1851, Trans. Cambridge Phil. Soc., Vol. 9.

Subramanyam S V and Raja Gopal E S, 1966, Kolloidzeitschrift u. Z. Polymere, Vol. 210, 80–81.

Sumner C G, 1933, On the Formation, Size and Stability of Emulsion Particles, J. Phys. Chem., Vol. 37, 3, 279–302.

Sutheim G M, 1946, Introduction to Emulsions, Chemical Publishing Co., Inc., New York.

Sutherland K L, 1951, Rev. Pure Appl. Chem. (Aust.), Vol. 1, 35–50.

Swithenbank J, Beer J M, Taylor D S, Abbot D and McCreath G C, 1976, A Laser Diagnostic Technique for the Measurement of Droplet and Particle Size Distribution, Paper 76–69 presented at AIAA Aerospace Science Meeting.

Taylor G I, 1932, Proc. Roy. Soc. (London), Vol. A138, 41.

Taylor G I, 1934, Proc. Roy. Soc., Vol. A132, 302.

Taylor Sir G, 1964, Disintegration of Water Drops in an Electric Field, Proc. Roy. Soc., Vol. A280, 383–397.

Tomotika S, 1935, Proc. Roy. Soc., Vol. A150, 322.

Voet A, 1947, J. Phys. Colloid Chem., Vol. 51, 1037.

Volkov V N and Krylov I A, 1972a, Calculation of the Coagulation Kinetics of a Polydisperse Emulsion in an Electrostatic Field, Fluid Mech. – Soviet Research, Vol. 1, 3, 28–34.

Volkov V N and Krylov I A, 1972b, Investigation of Coagulation of a Concentrated Emulsion in a Strong Electric Field, Izvestiya AN SSSR Energetika i Transport, Vol. 5, 70–75.

Vygovski V P, Mansurov K I, Sidurin Y V and Shutova Z M, 1980, Influence of Charge Relaxation on Movement of Water Drops in Weakly Conducting Media, Khimiya i Technologiya Topliv i Masel, No. 8, 18–20.

Wachtel R E and La Mer V K, 1962, J. Colloid Sci., Vol. 17, 531–564.

Wagner K W, 1914, Arch. Elektrotech, Vol. 2, 378.

Wang C S and Friedlander S K, 1967, The Self-Preserving Size Distribution for Coagulation by Brownian Motion, J. Colloid and Interface Sci., Vol. 24, 170–179.

Warren K W and Prestridge F L, 1980, Patent US 4204934.

Waterman L C, 1965a, Crude Desalting: Why and How, Hydrocarbon Processing, Vol. 44, 2, 133–138.

Waterman L C, 1965b, Electrical Coalescers: Coalescence, Chem. Eng. Prog., Vol. 61, 10, 51–57.

Waterman L C and Pettefer R L, 1969, Surface Ops. in Petr. Prodn.: Oil Field Emulsions and Their Electrical Resolution, ed. Chilingar G V and Beeson C M, Elsevier Publishing Co., New York.

Weber C, 1931, Z. Angew. Math. Mech., Vol. 11, 136.

Wellman V E and Tartar H V, 1930, J. Phys. Chem., Vol. 34, 379.

Wiener O, 1912, Abh. Sächs. Akad. Wiss., Math.–Phys. Kl, Vol. 32, 509.

Wiley R M, 1954, J. Colloid Sci., Vol. 9, 427.

Williams T J and Bailey A G, 1983, The Resolution Times of Water–in–Oil Emulsions Subjected to External Electric Fields, Inst. Phys. Conf. Ser. No. 66, Electrostatics '83, Oxford.

Williams T J and Bailey A G, 1984, Changes in the Size Distribution of Water–in–Oil Emulsions due to Electric Field Induced Coalescence, IEEE–IAS–84 Annual Meeting, Chicago, Conf. Rec. IAS, No. 14, 1162. (IEEE Trans. Ind. Appl. 1986, IA–22(3), 536–541.)

Wilson C T R and Taylor G I, 1925, Proc. Camb. Phil. Soc., Vol. 22, 728.

Wilten H N, 1962, Pet. Refiner, Vol. 41, 1–22.

Winslow W M, 1949, J. Appl. Phys., Vol. 20, 1137.

Zaky A A and Hawley R, 1973, Conduction and Breakdown in Mineral Oil, Peter Peregrinus Ltd. on behalf of the Institute of Electrical Engineers.

Zeef E and Visser H P, 1987, Electrostatic Crude Oil Dehydration, International Conference on Offshore Separation Processes, Edinburgh.

Zeleny J, 1917, Phys. Rev. Vol. 10, 1.

APPENDIX A

BISPHERICAL CO-ORDINATE SYSTEM

Bispherical co-ordinates are suitable for mathematically describing physical systems involving two spheres (see Figure A.1). The variables used μ, η and λ relate to the cartesian variables x, y and z as follows:

$$x = \frac{c \sin\eta \cos\lambda}{(\cosh\mu - \cos\eta)}, \quad y = \frac{c \sin\eta \sin\lambda}{(\cosh\mu - \cos\eta)}, \quad z = \frac{c \sinh\mu}{(\cosh\mu - \cos\eta)}$$

In these equations, the constant $c = a \sinh|\mu_0|$ where a is the radius of a spherical surface defined by $\mu = \mu_0$. The above equations can be algebraically manipulated to give the inverse relations shown below.

$$x^2 + y^2 + (z - c \coth\mu)^2 = (c \operatorname{cosech}\mu)^2$$

This shows that the μ-variable specifies a spherical surface with centre at the point $c \coth\mu$, on the z-axis, and of radius $c \operatorname{cosech}|\mu|$ (see Figure A.1).

$$(r - c \cot\eta)^2 + z^2 = (c \operatorname{cosec}\eta)^2, \quad r^2 = x^2 + y^2$$

This is the equation of a circle with centre displaced from the origin (normal to the z-axis) by a distance of $c \cot\eta$, and of radius $c \operatorname{cosec}\eta$. All such circles pass through the two poles of the system $z = \pm c$. The surface generated by rotating such a circle (truncated at the poles) about the z-axis corresponds to the η variable (see Figure A.1).

$$y = x \tan\lambda, \text{ for any value of } z$$

This shows that the λ co-ordinate specifies a plane, passing through the z-axis, whose intersection with the x,y-plane is at an angle λ to the x-axis (see Figure A.1). The spherical surface defined by $\mu = \mu_0$ has its centre on the z-axis at the point $z = b = c \coth\mu_0$. Now since $c = a \sinh|\mu_0|$, as mentioned previously, it follows that $b = \text{sgn}(\mu_0)\cosh\mu_0$ (i.e. if $\mu_0 > 0$ then $b = \cosh\mu_0$ and if $\mu_0 < 0$ then $b = -\cosh\mu_0$)

The μ-variable ranges from $-\infty$ to ∞. The value $\mu = 0$ corresponds to the median plane whereas $\mu = \pm\infty$ corresponds to the poles of the system (0, 0, $\pm$ c). An intermediate value of μ defines a spherical surface with centre at (0, 0, $c \coth\mu$) and of radius $c \operatorname{cosech}|\mu|$. The spherical surfaces corresponding to $\mu > 0$

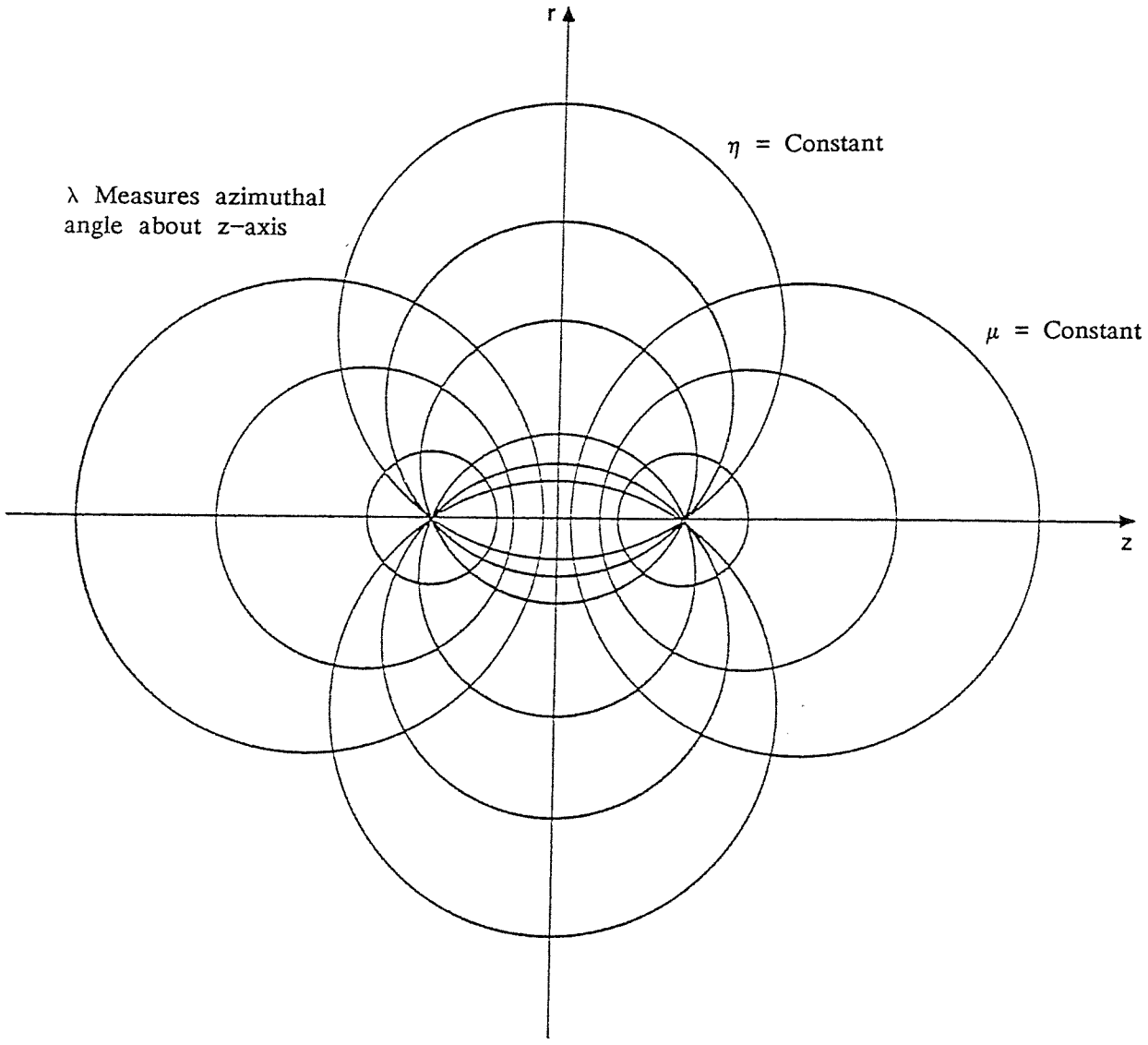

FIGURE A.1 Bispherical co–ordinate system.

lie in the region where $z > 0$ and those corresponding to $\mu < 0$ lie in the region where $z < 0$.

The η-variable ranges from 0 to π. The value $\eta = 0$ corresponds to the z-axis for $|z| > c$ (i.e. outside the poles). The value $\eta = \pi$ corresponds to the z-axis for $|z| < c$ (i.e. at or within the poles). An intermediate value of η corresponds to the surface of revolution, about the z-axis, of the appropriate circle which terminates at the poles.

The λ-variable varies from 0 to 2π and corresponds to a semi-infinite plane which intersects the z-axis and which is at an angle λ to the x-axis.

The Lamé coefficients for the bispherical co-ordinate system are as follows:

$$h_\mu = h_\eta = \frac{c}{(\cosh\mu - \cos\eta)} \quad , \quad h_\lambda = \frac{c \sin\eta}{(\cosh\mu - \cos\eta)}$$

Lamé coefficients are important since they occur in differential equations involving the operator $\underline{\nabla}$ (e.g. $\underline{E} = -\underline{\nabla}V$ relating electric field $\underline{E}$ to potential V, and Poisson's equation $\nabla^2 V = -\rho/\epsilon$). They also occur in line, surface and volume integrals (e.g. the elemental surface area of a spherical surface, in bispherical co-ordinates, is $dS = (h_\eta d\eta)(h_\lambda d\lambda) = h_\eta h_\lambda d\eta d\lambda$).

The operator $\underline{\nabla}$, in orthogonal curvilinear co-ordinates, is:

$$\underline{\nabla} = \left[\frac{1}{h_\mu}\frac{\partial}{\partial\mu}, \frac{1}{h_\eta}\frac{\partial}{\partial\eta}, \frac{1}{h_\lambda}\frac{\partial}{\partial\lambda}\right]$$

The electric field $\underline{E}$ and potential V are related by:

$$\underline{E} = -\underline{\nabla}V = -\left[\frac{1}{h_\mu}\frac{\partial V}{\partial\mu}, \frac{1}{h_\eta}\frac{\partial V}{\partial\eta}, \frac{1}{h_\lambda}\frac{\partial V}{\partial\lambda}\right]$$

The components in the above vector are the electric field components in the μ, η and λ directions.

Poisson's equation in orthogonal curvilinear co-ordinates is:

$$\nabla^2 V = \frac{1}{h_\mu h_\eta h_\lambda}\left[\frac{\partial}{\partial\mu}\left[\frac{h_\eta h_\lambda}{h_\mu}\frac{\partial V}{\partial\mu}\right] + \frac{\partial}{\partial\eta}\left[\frac{h_\mu h_\lambda}{h_\eta}\frac{\partial V}{\partial\eta}\right] + \frac{\partial}{\partial\lambda}\left[\frac{h_\mu h_\eta}{h_\lambda}\frac{\partial V}{\partial\lambda}\right]\right] = \frac{-\rho}{\epsilon}$$

Laplace's equation is obtained by letting the charge density ρ be zero in Poisson's equation.

For further information on bispherical co-ordinates see the following references: Davis (1961), Morse and Feshbach (1953), Buchholz (1957), Panchenkov and Tsabek (1968), Feat and Levine (1975), Smythe (1968).

APPENDIX B – List of patents held before computer searches were performed

Number	Date	Abstract	Company or Inventor
GB 941129	6.11.63	Process and apparatus for electrically resolving oil continuous dispersion.	Petrolite Corp.
GB 950748	26. 2.64	Process for reducing sulphate content in stock feed.	Howe-Baker Eng.
GB 953841	2. 4.64	Electric Treater.	Petrolite Corp.
GB 977124	2.12.64	Method and apparatus for electrically treating emulsions.	Howe-Baker Eng.
GB 1047507	2.11.66	Separating gas and water from oil-continuous emulsions.	Petrolite Corp.
GB 1120579	17. 7.68	A distributor for fluids.	Petrolite Corp.
GB 1201457	5. 8.70	Electric treatment of conductive dispersions.	Petrolite Corp.
GB 1204206	3. 9.70	Apparatus for treating emulsions.	Howe-Baker Eng.
GB 1247500	22. 9.71	Electric treater for emulsions.	Petrolite Corp.
GB 1297447	22.11.72	Electric treater for treating jet fuel and other dispersions.	Petrolite Corp.
GB 1312742	4. 4.73	Separator with vessel-length phase separating sections.	Petrolite Corp.
GB 1327991	22. 8.73	Phase separator for immiscible fluids.	Petrolite Corp.
GB 1354641	30. 5.74	Electric treater with gravity-liquid heat barrier.	Petrolite Corp.
GB 1368522	25. 9.74	Electrical treater system for producing combustible fuel.	Petrolite Corp.
GB 1378260	27.12.74	Shipboard electrical treater.	Petrolite Corp.

All patents listed here are the British equivalents of basic American patents.

APPENDIX C – List of patents found by computer searches (1979/80)

Number	Date	Abstract	Company or Inventor
US 4100068 (759202**)	12. 1.77	System for the dielectrophoretic separation of particulate and granular materials.	C E Jordan C P Weaver
US ------- (589179**)	6. 4.73	Generating periodic non-uniform electric field and removing polarizable particulate material from fluid, using ferroelectric apparatus.	Carborundum Co.
US 3930982	6. 2.73	Ferroelectric apparatus for dielectrophoretic particle extraction.	Carborundum Co.
GB 1358695	5. 8.70	Dielectrophoretic separation process for waxy petroleum feedstocks.	Esso Research and Engineering Co.
SU 578977 -A38	–	Oil contaminated water purifier – with electrical field treatment section between stationary centrifugal flow separator and filter.	Y I Karpinskii
US 4049535 -Y39	–	Resolving a water-in-oil emulsion by treatment with a combination AC and DC electric field.	Petrolite Corp.
US 3905891 -W39	–	Electric treater for oil well emulsions – with heater element located at oil water interface and in series with primary of treater power transformer.	Combustion Engineering
US 3855103 -W01	–	Electrical treater system for producing combustible fuels – desalts crude oil and residium to provide fuel for gas turbines.	Petrolite Corp.
US 3849285 -V48	–	Oil field emulsion electric treater – with detection of emulsion conductivity in electric field to guide operator or control separated water level.	Combustion Engineering

Number	Date	Abstract	Company or Inventor
US 3839176 -V41	-	Electric emulsion treater especially for fuels - with fuzzy hydrophilic layer on ground electrode to promote coalescence.	North American Rockwell
US 3812027 -V22	-	Dispersed water/oil separator - including an electric treating zone and an inlet baffle arrangement which removes large water volumes.	Petrolite Corp.
US 3808795 -V20 GB 1407173 -W39	-	Pollution free gas turbine operation - by mixing untreated oil containing alkali metal salt with water then separating oil using electric field.	Petrolite Corp.
CA 849507 -R34	-	Electric treater for resolving emulsion of oil and water.	Combustion Engineering Inc.
SU 648267 -B44	1. 6.76	Electro-hydrodynamic separator for liquids with dielectric properties - has parallel rows of rod electrodes connected to successive phases of multiphase high voltage source.	V N Novikov
US 4169037 -B40	6.10.78	Entrance bushing system for electrically resolving emulsions - has spring loading for establishing high pressure fluid-tight seal.	Petrolite Corp.
US 4161439 -B31	3. 4.78	Apparatus for applying electrostatic fields to mixing and separating - especially for removal of salt from crude oil via mixing with water.	Combustion Engineering
US 4120769 -A43	27. 7.77	Selective extraction of metal, especially copper, from aqueous leach solution by ion exchange with separation of aqueous and organic phases by electrostatic coagulation before cyclone.	Combustion Engineering

Number	Date	Abstract	Company or Inventor
US 4116790 -A40	18. 7.77	Two fluid mixture separation by passing mixture through electric field and centrifuge in sequence.	Combustion Engineering
SU 572440 -A28	22. 8.75	Removal of colloidally dispersed polymer from waste by electrolytic treatment to coagulate the polymer and electro-flotation, with reduced electrical consumption.	Khark Vodgeo
US 4066526 -A03 GB 1527103 -A40	19. 8.74	Device for electrostatic separation of charged material dispersed in fluids - which produces a dense, uniform corona discharge to form a fluid portion with low particle concentration and one with higher concentration.	G C Yeh
SU 549177 -A01	8.12.75	Solid phase separation from drilling fluid - controlled automatically by installation containing electrical sensors.	C Asia Natural Gas
US4122382 -A44	20. 4.77	Load responsive control for electrical power supply - is used in liquid emulsion separation system and senses and stores peak current values.	Combustion Engineering
US4056451 -Y45	29. 3.76	Oil field electrical emulsion treater - with serial trays containing electrodes connected respectively to AC and pulsed DC power.	Malone-Crawford TA
DL 125506 -Y25	12. 8.74	Separating electrostatically broken water-in-oil emulsion in horizontal tank with lower and upper separating zones.	K Schmidt
SU 514632 -Y17	24. 5.74	Condensing liquid dispersed system - by subjecting to orthogonal electric and magnetic fields using ultrasonic standing waves and separating.	V M Fomchenkov
SU 517621 -Y07	28. 1.74	Electrical treatment of petroleum emulsion - using high voltage pulsed field to reduce residual salt and water content.	Ryzan Petro Autom

Number	Date	Abstract	Company or Inventor
SU 517323 -Y06	4. 7.73	Hydrocyclone for purifying contaminated water - using tangential feed, electric field and pressurised gas to separate the phases.	Y I Karpinskii
FR 2326689 -Y27	30. 9.75	Localisation of phase separation level - between two fluids having different electrical conductivities using vertical array of electrodes.	Commiss. Energie Atomique
SU 474723 -X13	4. 6.73	Dispersed particle separator - with chamber and ribbon/ needle electrodes producing non-uniform electric field for electrophoretic mobility.	As. USSR Biolog. Phys.
SU 452349 -X05	9. 7.73	Electrostatic separator - to separate poorly-conducting liquids from colloidal muds and emulsifying impurities.	M G Granovski
US 3929625 -X02	2. 8.74	Removal of inorganic solid contaminants from shale oil by electrically resolving aqueous dispersion of oil containing a polyoxalkylene-derived nonionic polymeric surfactant.	Petrolite Corp.
US 3926774 -W52 GB 1487279 -Y39	13.11.74	Electric treater for resolving emulsions - has pressure balanced bushing.	Petrolite Corp.
J 49079963 -W16	8.12.72	Treatment of ash from fuel oil combustion - using electrostatic precipitator for recovery of vanadium and nickel values.	Balcock - Hitachi KK
US 3898537 -W33	7. 6.74	Modular high voltage DC power supply with removable component rack - for use with electric field heater for resolution of dispersions.	Petrolite Corp.
GB 1372844 -V45	24. 9.70	Electrostatic precipitator - detecting relative phase change for separate indications of sparking and arcing.	Westinghouse Brake and Sig.

Number	Date	Abstract	Company or Inventor
DL 120590 -X32	18.12.72	Purifying industrial waste waters containing oils & fats - as emulsions or dispersions, by treatment with electrostatic filter ash to break emulsion and bind oils and fats.	Institut fur Energetik
US 3806437 -V18	22. 3.73	Naphthenic acids removal from heavy distillates - from naphthenic based crude oils, by alkali washing and electric treatment of emulsions.	Petrolite Corp.
US 3794578 -V10	26.12.72	Electric emulsion treater - with central and offset electrodes energized from three-phase transformer.	Petrolite Corp.
GB 1444434 -X31 to GB 1444436 -X31	15.11.72	Electrostatic oil/water separator - has electrode pair in solvent layer, with overflow separation of floating foreign particles and water.	T Tokumoto
US 3772180 -U47	10.11.71	Electrical emulsion treater - with electrodes connected to pulsed DC source.	Combustion Engineering Inc.
US 3707458 -U01	22. 2.71	Electric emulsion treater - with cooled external insulator housings.	Petrolite Corp.
US 3701723 -T46	22. 2.71	Electric treatment of dispersions - to coalesce water by flow through unidirectional electric field.	Petrolite Corp.
US 3674677 -T29	2. 6.70	Electric emulsion treater - with interleaved part cylindrical high voltage and ground electrodes.	R Roberts
US 3661746 -T22	19. 1.71	Electric emulsion treater - with spaced constant potential planes normal to flow.	Petrolite Corp.
CA 896016 -T14	26. 3.68	Crude emulsion electric treater - with adjustably spaced charged and earthed grids.	F L Murdock
US 3582527 -S23	15. 5.69	Resolving dispersions with uniform electric fields.	Petrolite Corp.

Number	Date	Abstract	Company or Inventor
CA 865718 -S11	26. 3.68	Horizontal electric emulsion treater for crude oil.	F L Murdock
CA 859122 -S05	19. 2.68	Electric emulsion treater for crude oil.	F L Murdock
DT 1907880 -R28	11.11.68	Electrostatic separation and sorting of finely dispersed particles.	Dtsche Akad der Wissench
CA 843429 -R28 GB 1208067 -R39	30.10.67	Energization of electric emulsion treaters.	Petrolite Corp.
DT 1804060 -R35 GB1224950 -S09	19.10.68	Separation of phases accelerated by electric field.	Metallgesell-schaft A G

PATENT NUMBER IDENTIFICATION

SU – Soviet Union
US – United States
CA – Canada
GB – Great Britain
DL – Germany
FR – France
J – Japan
** – Application Number

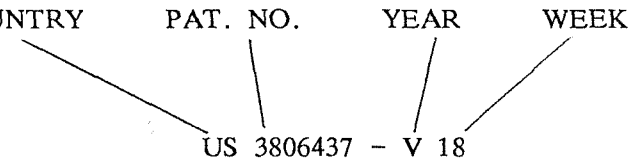

R 1970
S 1971
T 1972
U 1973
V 1974
W 1975
X 1976
Y 1977
A 1978
B 1979
C 1980

APPENDIX D - List of patents found by computer searches (1985/86)

APIPAT - AMERICAN PETROLEUM INSTITUTE (PATENTS)

1. DD 154445
2. US 3258421

CHEMICAL ABSTRACTS

1. JP 83222187

PATSEARCH

1. US 4419200
2. US 4415426 (like US 4419200)
3. US 4409078 (like US 4391698)
4. US 4406793
5. US 4399041
6. US 4374724
7. US 4372837
8. US 4370236
9. US 4349430
10. US 4305797
11. US 4302310
12. US 4140609

WORLD PATENTS INDEX (1963-1980)

1. SU 724168
2. SU 725707 (Triboelectric charging)
3. SU 724201
4. SU 722554
5. US 4226690
6. US 4226689
7. US 4224124 (Interesting electrodes)
8. SU 716569
9. SU 711099 (Aerating emulsion)
10. US 4209374
11. SU 700163
12. US 4204934

13. SU 689732
14. US 4200516 (Like US 4224124 - Interesting treating zones)
15. SU 2597099
16. JP 80012303
17. JP 55028747
18. SU 674756
19. SU 671829
20. SU 2569097
21. SU 2560640 (Flat emulsion jet)
22. SU 662574 (Pulsed magnetic separation)
23. US 4182672
24. SU 648267 (Like US 4204934 - Electro-hydrodynamic)
25. US 4161439
26. SU 625741
27. SU 617046 (Cyclone with electrodes)
28. SU 617045 (Corrugated perforated electrode and filter)
29. SU 617044
30. SU 613771
31. SU 613770
32. US 4149958
33. SU 608537 (Spherical tank, velocity less in middle)
34. SU 599821
35. SU 585856
36. US 4126537
37. SU 589003
38. SU 584870
39. US 4116790
40. SU 578978
41. SU 573169
42. SU 555125
43. SU 5550163
44. SU 5557804
45. US 4056451
46. US 4049535
47. SU 529204
48. SU 539586
49. US 4033851
50. US 4031007
51. SU 517621
52. SU 517323 (Hydrocyclone + electric field for resolving W/O emulsions on ship)

53. SU 497030
54. SU 432170 (Electrical resolution & passage of emulsion through fluoroplastic–corona discharge)
55. US 3926774
56. SU 462858
57. US 3905891 (Heater element at O/W interface)
58. US 3898152
59. SU 427044
60. GB 139359
61. JP 49074666
62. SU 417462
63. US 3855103
64. US 3847775
65. SU 411118
66. US 3839176
67. US 3813328
68. US 3812027
69. US 3799856 (Dissolve salt water in fuel then pass through electrofilter)
70. US 3799855 (Like US 3799856 above)
71. US 3794578
72. US 3891537, GB 1444434/5/6
73. US 3772180
74. DE 2319737
75. SU 362044
76. US 3736245, GB 1378260
77. DE 2253507
78. DE 2248298 (Electrostatic Micro–filter, glass beads)
79. DD 95899
80. DE 147068
81. NL 7208713
82. US 3701723, JP 48072755
83. DE 1420894 (Petrolite)
84. US 3674677
85. US 3661746 (dc preferred to ac for economy)
86. FR 2095132 (Magnetic particles added and magnetic field applied)
87. US 3649516, GB 1312742
88. US 3620959
89. DE 2122045 (Magnetic separation using ferromagnetic particles)
90. US 3616460 (Downward flow into bed of porous material)
91. US 3597346

92. SU 277991
93. US 3592756
94. US 3592752 (Petrolite)
95. US 3582489
96. US 3574085
97. US 3567619 (Charged emitting screen electrode & fibrous collecting bed)
98. US 3531393
99. US 3505194
100. SU 578977
101. SU 275282 (Bipolar pulses, thyristor switching circuit)
102. SU 268385
103. CA 859122 (F C Murdock)

WORLD PATENTS INDEX LATEST (1981+)

1. JP 60222114 (Fuel oil purification using water or oil-based ferromagnetic liquid for water or sludge removal)
2. JP 60220110
3. SU 1158212
4. EP 159909 (ESSO, for removal of particulates and water droplets, charge injection method for dehazing fuel oil)
5. SU 1151258
6. SU 1144725 (Treating space filled with flexible organic fibre)
7. SU 1144712 (Electrode mechanically vibrated to prevent deposition, wire bundles and metal chips)
8. JP 60156512
9. SU 1127895
10. SU 1127613 (Treater has perforated dielectric diaphragm with semiconducting rods)
11. JP 60081289
12. SU 1125003 (Has dielectric partitions)
13. FR 2550545
14. GB 2143157 (UK Electricity Council, C P Galvin)
15. SU 1101255
16. EP 130118
17. SU 1082794
18. SU 1080829 (Dielectric tank, fibres connected to lower electrode)
19. SU 1079267 (Top electrode has vertical plates bottom electrode has needles)
20. SU 219731

21. GB 2136323 (Surfactant-treated percolating membrane electrode)
22. SU 1065027
23. SU 1058576
24. SU 283470 (Insulating tank)
25. SU 1033155
26. SU 678743
27. SU 623281
28. SU 1017362
29. JP 5901274
30. SU 990260
31. SU 1007696 (Treater has corona discharge electrodes)
32. GB 2123716 (Electrodes made from directionally solidified eutectic, D Graham)
33. SU 1005819 (Electrode pairs in mutually perpendicular positions)
34. SU 1003870 (Has inner electrode with dielectric rings)
35. SU 1001962
36. EP 96739 (Conductivity of electrode material varies in predetermined direction)
37. SU 995848 (Has dielectric body)
38. SU 993976 (Has metallized sphere which moves between electrodes; rate of separation increased by 2-2.5)
39. SU 988313
40. JP 58156309
41. GB 2117370 (Breaking emulsions using microwaves, λ = 0.1-30cm)
42. SU 978889 (Electrically insulating body with spiral strip electrodes)
43. US 4469582, JP 58170508 (Inclined plate separator)
44. CA 1152019
45. US 4400253
46. SU 971426 (Has dielectric disc with internal ribbing opposed to electrode ribs)
47. SU 971406
48. SU 971405 (Cylindrical cell with alternate metallic and insulating materials)
49. EP 85842
50. DE 3203842 (Separation using curved venturi gap - electric field helps - can be part of a cyclone)
51. US 4391698
52. US 4252631
53. SU 950417 (Coalescence helped by having electric fields in different directions)
54. SU 948394

55. EP 80618
56. SU 943267 (Electric coagulator with dielectric washers - has electrodes in the form of alternating discs with apertures at periphery and centre)
57. EP 72628 (Uses insulated electrode with hydrophobic surface)
58. SU 912204 (Has mesh electrodes, vertical screen at sides and earthed impeller shaft)
59. SU 912203 (Has conical insert which permits infinitely variable emulsion flow)
60. SU 891112 (Increased perforation size in lower electrode)
61. SU 889036 (Has internal baffle with slits)
62. SU 889035 (Positive electrode made from container with metal turnings)
63. SU 889034 (Has mixer with deflecting plates)
64. SU 874747 (Uses high frequency electric field generator)
65. SU 860806 (Electrodes form channel and are connected via capacitors to a current source)
66. SU 865325 (Outer ring electrode has dielectric lining, inner electrode is inverted, truncated cone grounded by capacitors)
67. SU 850122 (Has coaxial electrodes separated by ferromagnetic particles)
68. SU 850121 (The high-voltage electrode exhibits pins, coaxial electrodes)
69. EP 51463 (Has insulated electrode and unidirectional pulsed supply 1-30Hz)
70. US 4326954
71. SU 839844 (Cyclone chamber and charged electrical grids - O/W)
72. GB 2083838 (Has side distributor and hydraulically independent flow channels)
73. SU 829656 (Water/Tar emulsions)
74. SU 829130 (Positively charged particles in peripheral zone, negative in central zone, mixed by dielectric swirlers)
75. SU 827112
76. SU 827111 (Has perforated dielectric screen between electrodes)
77. WO 8204202 (Centrifuge/electrostatic separator for cleaning waste oil)
78. US 4308127
79. SU 810755 (Electrostatic separator for coal tar)
80. SU 802357
81. SU 770547 (Coagulation and precipitation of aviation fuel impurities: uses rotating discs of different metal surfaces to generate charge by tribo-electrification)
82. SU 770513 (Has two perforated baffle plates at side)
83. BE 886503 (Separation using surfactant of particular hydrophilic-lipophobic equilibrium index)

84. SU 765341 (Petroleum desalinated using petroleum W/O emulsion; mixture agitated and coalesced electrostatically)
85. SU 764699 (Electrodes are hollow truncated half-cones, stepped sides and perforated partitions)
86. US 4257895 (Uses separator screens and baffles)
87. SU 749399 (Has hollow electrode containing waveguide linked to UHF generator)
88. SU 743692
89. JP 58137406
90. US 4396404, CA 1184132

APPENDIX E

THE DERIVATION OF DROPLET SIZE DISTRIBUTION FROM EMULSION SETTLING RATE

If the turbidity of a W/O emulsion is measured as a function of volume fraction of water then a straight line results (approximately):

$$KT = \varphi \qquad \text{(E1)}$$

T = Turbidity in NTU (Nephelometric Turbidity Unit)
φ = Volume fraction of dispersed water in emulsion
K = Constant of proportionality.

Consider the turbidity of a W/O emulsion, in the nephelometer cuvette, a distance d below the emulsion surface. The largest droplet at this level, after time t, is given by Stokes' Law:

$$\frac{d}{t} = \frac{2(\rho_d - \rho_c)\ g\ r^2}{9\eta_c} = \alpha r^2 \qquad \text{(E2)}$$

Re-arranging eqn. (E2) gives:

$$r = \left[\frac{d}{\alpha t}\right]^{\frac{1}{2}} \qquad \text{(E3)}$$

ρ_d = density of water
ρ_c = density of oil
g = acceleration due to gravity
η_c = viscosity of oil

Suppose, initially, that the emulsion is homogeneous in so far as the droplet volume fraction distribution is independent of location. As time goes by, the volume fraction distribution is truncated (see Figure E.1) at the droplet radius specified by the previous equation.

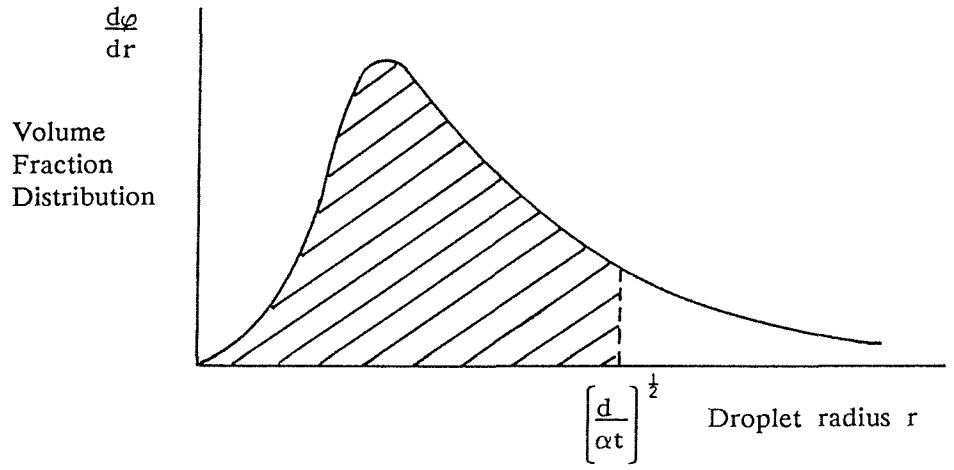

FIGURE E.1 Truncated volume fraction distribution of dispersed phase water droplets.

At time t, the volume fraction, according to the previous theory, can be found by integration as shown below:

$$\varphi = \int_{r=0}^{r=(d/\alpha t)^{\frac{1}{2}}} \left[\frac{d\varphi}{dr}\right] dr \qquad \text{(E4)}$$

Using eqn. (E1):

$$\varphi = KT = \int_{0}^{r} \left[\frac{d\varphi}{dr}\right] dr \qquad \text{(E5)}$$

This may be differentiated by considering the following identity:

$$\frac{d}{dt}\int_{g(t)}^{h(t)} F(r,t)dr = \frac{dh}{dt}F(h,t) - \frac{dg}{dt}F(g,t) + \int_{g(t)}^{h(t)} \frac{\partial}{\partial t}F(r,t)dr$$

Differentiating eqn. (E5) therefore gives:

$$\frac{d\varphi}{dt} = K\frac{dT}{dt} = \frac{dr}{dt}\left[\frac{d\varphi}{dr}\right]$$

which may be re-arranged to obtain $d\varphi/dr$:

$$\left[\frac{d\varphi}{dr}\right] = K\frac{dT}{dt} \Big/ \frac{dr}{dt} \qquad \text{(E6)}$$

Eqn. (E3) may be re-arranged to give:

$$r^2 t = \frac{d}{\alpha}$$

Differentiation leads to:

$$2rt\,\frac{dr}{dt} + r^2 = 0$$

which yields:

$$\frac{dr}{dt} = -\frac{r}{2t} = \frac{-\alpha r^3}{2d} \qquad \text{(E7)}$$

Combining eqns. (E6) and (E7) gives:

$$\left[\frac{d\varphi}{dr}\right] = -\frac{2dK}{\alpha r^3}\,\frac{dT}{dt}$$

To obtain the volume fraction distribution it is necessary to express the rate of change of turbidity dT/dt as a function of r. Suppose that the logarithm of the turbidity decreases linearly with time. This is approximately true for the initial settling rate of an emulsion under gravity. If the departure from linearity is attributed to coalescence then the initial settling rate may be assumed appropriate for calculating volume fraction distribution.

$$\ell n\ T = -\frac{t}{t_o} + \ell n\ T_o \qquad \text{(E8)}$$

$\frac{-1}{t_o}$ = gradient of straight line graph

$\ell n\ T_o$ = intercept of straight line graph

Eqn. (E8) may be re-arranged to give:

$$T = T_o \exp(-t/t_o) \qquad \text{(E9)}$$

This corresponds to an emulsion of initial turbidity T_o settling at a rate determined by the time constant t_o. Differentiating eqn. (E9) gives:

$$\frac{dT}{dt} = \frac{-T_o}{t_o} \exp(-t/t_o)$$

This may be expressed as a function of r by replacing t by $d/\alpha r^2$ using eqn. (E3):

$$\frac{dT}{dt} = \frac{-T_o}{t_o} \exp\left[\frac{-d}{\alpha t_o r^2}\right] \qquad \text{(E10)}$$

Consequently the volume fraction distribution is given by the following:

$$\left[\frac{d\varphi}{dr}\right] = \frac{2dKT_o}{\alpha t_o r^3} \exp\left[\frac{-d}{\alpha t_o r^2}\right] \qquad \text{(E11)}$$

Let $\beta = \frac{2dKT_o}{\alpha t_o}$ and $\chi = \frac{d}{\alpha t_o}$ then:

$$\left[\frac{d\varphi}{dr}\right] = \frac{\beta}{r^3} \exp(-\chi/r^2) \qquad \text{(E12)}$$

$$\alpha = \frac{2(\rho_d - \rho_c)g}{9\eta_c}$$

$$\beta = \frac{2dKT_o}{\alpha t_o} \quad \text{where } K = \frac{\varphi_o}{T_o}$$

$$\chi = \frac{d}{\alpha t_o}$$

$\rho_d = 1000 kgm^{-3}$, $\rho_c = 830 kgm^{-3}$, $g = 9.81 ms^{-2}$.

$\eta_c = 3.2 \times 10^{-3} Pas$, $d = 0.03m$, $t_o = 238 \times 60s$,

$T_o = 1033$ NTU, $\varphi_o = 909 \times 10^{-6}$.

Here φ_o is the initial volume fraction and T_o is the initial turbidity. The above values give the following results for α, β, χ and K.

$\alpha = 1.158 \times 10^5 m^{-1} s^{-1}$, $\beta = 3.3 \times 10^{-14} m^2$,

$\chi = 1.81 \times 10^{-11} m^2$, $K = 8.8 \times 10^{-7}$ NTU^{-1}.

The number density distribution can be derived from the volume fraction distribution by dividing by $(4/3)\pi r^3$ as follows:

$$\left[\frac{dN}{dr}\right] = \frac{3}{4\pi r^3}\left[\frac{d\varphi}{dr}\right] = \frac{3\beta}{4\pi r^6}\exp(-\chi/r^2) \qquad \text{(E13)}$$

The initial number density of droplets N_o may be found by integrating as follows:

$$N_o = \int_o^\infty \left[\frac{dN}{dr}\right] dr$$

Substituting in for dN/dr using eqn. (E13) gives:

$$N_o = \frac{3\beta}{4\pi}\int_o^\infty \frac{e^{-(\chi/r^2)}}{r^2} dr \qquad \text{(E14)}$$

$$N_o = \frac{9\beta}{32\pi^{\frac{1}{2}}\chi^{5/2}} = 3.76 \times 10^{12} m^{-3} \qquad \text{(E15)}$$